Applicability of Undermatched Welds for High Strength Steel Structures

by

Nikolaos K. Kafetsis

B.S. in Marine Engineering
Hellenic Naval Academy, 1985

Submitted to the Departments of Ocean Engineering
and Materials Science and Engineering
in partial fulfillment of the requirements for the degrees of

Naval Engineer

and

Master of Science in Materials Science

at the

MASSACHUSETTS INSTITUTE OF TECHNOLOGY

June 1995

Author .....
Department of Ocean Engineering
May 12, 1995

Certified by .....
Koichi Masubuchi, Kawasaki Professor of Engineering
Thesis Supervisor, Department of Ocean Engineering

Certified by .....
Frederick J. McGarry, Professor of Civil Engineering and Polymer
Thesis Reader, Department of Materials Science and Engineering

Accepted by .....
A. Douglas Carmichael, Professor of Power Engineering
Chair, Departmental Committee on Graduate Students

Accepted by .....
Carl V. Thompson II, Professor of Electronic Materials
Chair, Departmental Committee on Graduate Students

Applicability of Undermatched Welds for High Strength Steel Structures

by

Nikolaos K. Kafetsis

Submitted to the Departments Ocean Engineering
and Materials Science and Engineering
on May 12, 1995, in partial fulfillment of the
requirements for the degrees of
Naval Engineer
and
Master of Science in Materials Science

Abstract

This study presents experimental and numerical results for the strength of welded joints, made on high strength steels with different degrees of strength matching. The steels involved are the HY-100 and HY-130 U.S. Navy, quenched and tempered steels. The test methods are the self restraint cracking test, the tensile test and the fatigue test. The investigated parameters are the strength of the weld metal and the preheat temperature.

The self restraint cracking test does not show clearly the expected results, that the required preheat temperature to avoid cold cracking can be reduced by applying undermatched welds at the root of the welding. This conclusion was reached in a similar experiment that was performed on HT-80 high strength steel.

The tensile test and the numerical analysis show that the strength properties of the undermatched weld are not the typical properties of the unrestrained weld material. They are greatly elevated due to the restraint effect provided by both the base metal and the stronger surrounding weld metal.

Results from the fatigue test show that the degree of strength undermatching, does not affect significantly the crack propagation rate at the joint.

Thesis Supervisor: Koichi Masubuchi
Title: Kawasaki Professor of Engineering

Acknowledgments

I would like to express my gratitude to my advisor Professor Koichi Masubuchi for his guidance and support. I am also grateful to Professor F. McGarry for his advice.

Special thanks to Akira Umekuni for his involvement and suggestions throughout this thesis. His help was invaluable.

I would also like to thank D. Fitzerald and F. Gaudette for their assistance during the tests, Juliana Atmadja and Platon Velonias for their help with the ADINA program, Spyros Maragos for his advice and comments on writing and presenting this thesis, and Muriel Bernier for proof-reading the text.

Finally, I would like to thank my wife Athena for her continuous support and understanding throughout my studies.

Contents

List of Figures

List of Tables

Chapter 1

Indroduction

Without a doubt, the most important challenge in today's technology is that most structural applications should be designed and constructed having the smallest possible size and weight in order to satisfy the demand for improved efficiency. To achieve this goal many types of high strength steels have been developed and used in numerous applications, such as the construction of warships and submarines.

The performance of these steels has reached an outstanding level not only due to their increased strength, but also due to other improved properties such as ductility and toughness. Welding these steels, however, is not free from problems, which become even more difficult to solve as loading requirements of structures are increased. One of the most serious problems of all is the occurrence of cold cracking. To avoid this phenomenon, these structural steels should be preheated to temperatures that may exceed 100°C. In an actual structure such as a ship, this procedure is extremely difficult, and results not only in a significant increase of fabrication cost but also in the reduction of productivity.

By using undermatched welds at the root of the bevel, where cracking is most likely to occur, the requirement for preheating can be reduced. This method provides the following advantages:

- the residual stresses at that area are reduced
- the fracture toughness can be increased and can reach values similar to those

of the base metal

- the heat of the first pass can serve as a preheating source for subsequent passes applied after a predetermined period of time.

The next passes of welding can be made by an evenmatched weld material, which increases the strength of the joint, shields the soft metal from excessive stresses and plastic deformation, and elevates the strength properties of the soft metal due to the restraint effect.

It has been estimated that the elimination of preheat for HY steels in thickness 0.5" or less can provide savings in excess of one million dollars per ship (1981 dollars). The economic advantages are related to the possible elimination of preheat requirements for weldments, to the relaxed inspection requirements, and to the greater use of higher deposition rates.

Chapter 2

Background

2.1 Past studies on high strength steel welding

Welded joint heterogeneity

In welding high strength steels, it is increasingly difficult to obtain welded joints that match the strength and the toughness of the base metal. This is especially true in the case of quenched and tempered steels, such as HY80, HY100 or HY130, whose strength and fatigue toughness are obtained through heat treatment.

Some reasons for weakness in the welded joints that make them vulnerable to failure are as follows [1, 2]:

- the existence of metallurgical and geometrical defects
- the presence of stress raisers
- the deformation level in the vicinity of the crack tip which is mainly controlled by the fracture toughness
- the existence of residual stresses
- the embrittlement in the HAZ and weld metal due to metallurgical changes
- and the heterogeneous properties of the material in the joint

The heterogeneity of the material is not only due to the degree of strength mismatching, but also due to the microstructural changes during the weld thermal cycles. It changes the mechanical properties of the joints, such as yield strength, ultimate strength, strain hardenability, and elongation, affecting both the static ductility test and the the fracture behavior of the welded joints.

Surface cracks and notches can also affect the tensile properties and fracture behavior of welded structures under tensile stress. They result in concentration of stress and strain, local yielding and development and growth of cracks, which make joints the prime location for fatigue failure. They can also reduce both the tensile strength and the tensile ductility. The strength and ductility reduction become worse by weld undermatching and increased crack size [3].

The most important region in a welded joint is the HAZ because it is the region with the lowest fracture toughness [4], resulting in a large possibility for crack initiation. The metallurgical and physical properties of the HAZ depend on the base metal composition, the peak temperature during welding, the heat input and the cooling rate. The latter depends on the plate thickness, preheat and interpass temperatures [5].

Behavior of weld joint due to strength matching

There are two approaches to overcome the problem coming from the heterogeneous properties of the material in the welded joints. One is to accept weld metals that are slightly undermatched in fracture toughness but make certain that they are overmatched in strength. The other approach is to accept weld metals that are slightly undermatched in strength but have adequate fracture toughness.

The first approach prevents strain concentration and subsequent fracture in the weld zone. It has been tested by explosion bulge tests (Masubuchi 1966, Pellini 1976) and has been used by the U.S. Navy in the construction of submarine hulls with HY-80 and HY-100. In the second approach the lower strength of the weld metal may permit a reduction in preheating temperatures. Also, the stress concentration in hard spots can be reduced by allowing local plastic deformation.

In a welded joint loaded perpendicular to the welding direction [2, 5], the acting strain in each cross section is not the same. In an overmatched weld, plastic strains occur essentially in the base metal while the weld metal and the HAZ remain elastically strained, receiving protection against small surface cracks. In the undermatched case the plastic strain accumulation is mainly concentrated in both the weld metal and the HAZ. Due to the strain concentration, at the lower strength weld metal, the driving force of crack propagation increases. To compensate the loss of strength and to allow for high level strain deformation it is essential that the weld metal should have high strain hardening and high fracture toughness [6].

Many investigators believe that the driving force for fracture is inversely proportional to the yield strength of the material at the defective region. Since it is extremely

difficult to achieve high toughness level in fabrication welds, undermatching should be avoided and the weld metal overmatching should be ensured in a weldment [5]. Thus weld metal cracks, especially small ones, will be protected from severe plastic strains. However, increased weld metal strength can only be achieved with electrodes having increased alloy content. As the yield strength increases the choice of weld electrodes with adequate toughness becomes limited, and the tendency for weld metal cracking increases.

The idea of evenmatching or undermatching started recently. It is believed that evenmatching or undermatching can not only provide the benefit of improved toughness, but can also reduce the required preheat temperature, improving both the fracture performance and the fabrication cost [2]. In most cases the fracture toughness is more important than the degree of overmatching, especially when the upper value of the base metal yield strength is not required at the weld metal.

Evaluation of fracture tendency

To evaluate the tendency for fracture, two methods are available. The J-integral and the crack tip opening displacement (CTOD). The J-integral depends on the degree of strength matching and on the crack size [3]. For small cracks in overmatched joints, the J values are significant smaller than those from evenmatched or undermatched joints. Thus overmatched welds shield small cracks from plastic strains. However, large cracks have large J values in all welding conditions.

The fracture toughness of the HAZ can also be evaluated in terms of the crack tip opening displacement (CTOD), which is determined by the local brittle zone. Although the CTOD is similar to the J-integral method, it was proved [4] that the degree of strength matching does not affect the CTOD value at brittle crack initiation obtained by the three-point bent test and the through-thickness notched wide plate tensile tests. The CTOD value in this case is only a function of material toughness at the crack tip. Only in the ductile mode, the degree of strength matching influences the overall performance of welded joints.

During fatigue test, the results are not significantly affected by the degree of

strength matching. Although the crack propagates faster in the overmatched case, it propagates toward the base metal. In the evenmatched case it propagates straight forward and in the undermatched case it propagates toward the weld metal [4]. From experiments made by Satoh and Nagai (1969), it was found that the hard interlayer had no effect on the fatigue strength, however the thickness of the soft interlayer affects significantly the fatigue limit. As the thickness of the soft interlayer increases, the fatigue limit decreases drastically.

Eliminating preheating

When welding high strength steels, the risk of cold crack becomes even higher as the degree of restraint of the welding or the yield strength of the base material increases. Although modern steels and low hydrogen electrodes have been developed, the cold crack can only be avoided with the use of preheating. According to some investigators [7], the need for preheating can be eliminated with the use of electrodes of low yield strength at the root of the weldment during the first pass. The rest of the bevel is filled with matching electrodes. This method reduces the risk of cold crack initiation and also results in a less expensive technique. It can be used when welding thick constructional steels, high strength steels or during repair welding with severe restraint conditions. The reduction of the preheat temperature depends on the hydrogen content of the electrode and on the base metal carbon equivalent. For hydrogen content less than 3 ml/100 gr, on a 50 mm thick FeE355 steel with CE less than 0.11, no preheat is required, while in many other cases the reduction in the preheat temperature can be approximately 50 to 75 ^{o}C.

Similar results were obtained from weld cracking tests on 50 mm, HT80 steel with E11016 and JISD5816 electrodes [8]. The use of an undermatched electrode with lower NTS can prevent root cracking along the fusion line even if the preheat temperature is 25 ^{o}C lower than that required at the case of E11016 type electrode, under the same hydrogen level.

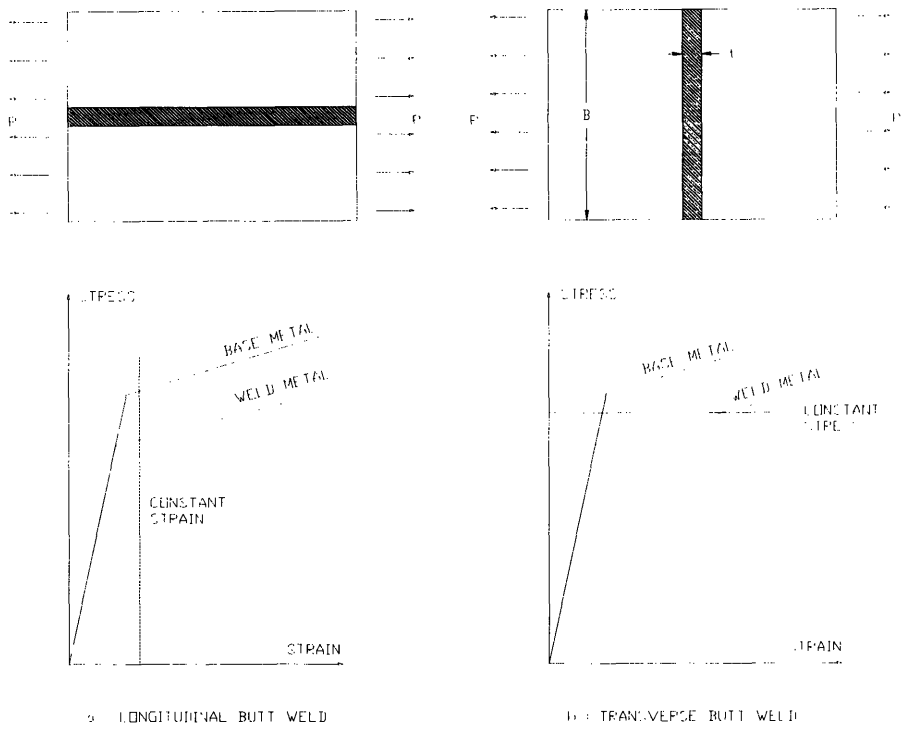

Figure 2-1: Butt welds subjected to tensile loading

Behavior of soft welded joints

There are many factors that affect the mechanical behavior of a soft welded joint. Some of those are the type of the joint, the size of the weldment, the degree of strength reduction, the width of the soft inderlayer and the loading direction.

Referring to Figure 2-1, we note that when a tensile load is applied parallel to the welding direction of a butt weld, the joint is under constant strain and the effect of the lower yield strength material is very small as long as the zone has enough ductility. When the applied tensile load is perpendicular to the welding direction, the joint is under constant stress. If the applied stress exceeds the yield strength of the soft zone, strain concentration occurs in the weld metal, resulting in fracture.

However, the strength of a weld metal does not behave as the soft metal itself. It has been confirmed that it is much elevated due to the restraint effect provided by the surrounding stronger metal. From quantitative evaluation of the tensile strength using a model consisting only of the base metal and the soft interlayer (Figure 2-2), it

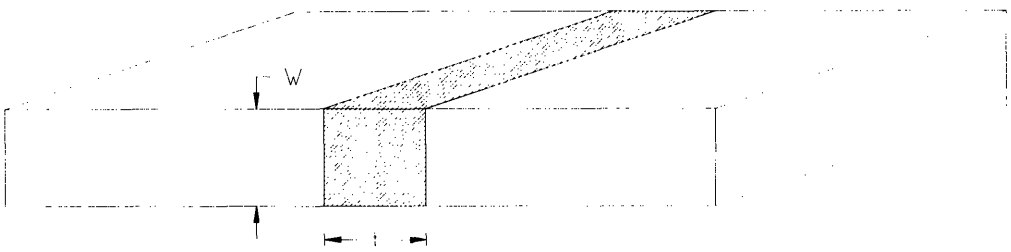

Figure 2-2: Welded plate including a soft interlayer

resulted that the static strength of welded joints depended upon the relative thickness of the soft interlayer [9, 10]. In the case of a plate, the relative thickness X is the ratio of the width of the interlayer t over the thickness of the plate W. The strength of the soft interlayer is elevated as the relative thickness X decreases. For $X \leq 1/5$ the joint strength becomes almost the same as that of the base metal.

The ductility of the welded joint also depends on the value of the relative thickness X and the ratio k which is the tensile strength of the base metal divided by that of the soft interlayer.

2.2 High-strength low-alloy quenched and tempered steels

High-strength low-alloy quenched and tempered steels (HSLA Q&T) contain less than 0.25% C and less than 5% alloy. They combine high yield and tensile strength with good ductility, notch toughness, atmospheric corrosion resistance and weldability. They are strengthened by quenching and tempering to produce microstructures that contain martensite, bainite and in some compositions, ferrite. However, as the strength level of these steels increases they tend to become more difficult to weld without crack and other defects. The most common of these steels are HY-80, HY-100 and HY-130.

The HY-80 and HY-100 are quenched and tempered with high strength, good notch toughness and good weldability. Quenching is conducted to avoid the transformation of the high temperature austenite phase into undesirable microstructures which are a normal result of the slow cooling. The austenitizing temperature is 900 ^{o}C. The quenching medium is water. Tempering involves reheating for one to several hours at 650 ^{o}C [11]. HY-80 and HY-100 are made under the specification of MIL-S-16216 and are used principally for naval ships. Welding these steels is not easy since it is extremely difficult to produce weld metal with properties the same as those of the base metal.

The austenitizing temperature of HY-130 is 815 ^{o}C, the quenching medium is water and the tempering temperature is 540 ^{o}C. The increased strength level of HY-130 makes the welding very difficult. Since it is hard to obtain weld metals having both strength and toughness comparable to those of the base metal, it is essential to use weld wire of a high metallurgical quality and then to protect the weld metal pool by the use of inert gas shielding. As a result the Gas Tungsten Arc method (GTA) is recommended while the shielded metal arc (SMA) should be avoided since it provides poor protection from atmospheric gases.

2.3 Weldability of quenched and tempered steels

Q&T steels are normally furnished in heat-treated conditions that involve austenitizing and quenching and tempering to obtain high strength properties. The HAZ (Heat Affected Zone) of the Q&T steels consists of microstructures of low carbon martensite and bainite. This type of as-welded HAZ microstructure has desirable mechanical properties that are close to those of the base metal. Consequently, these materials generally do not require postweld heat treatment or stress relief treatment.

Unlike other hardenable low alloy steels, Q&T steels require a rapid cooling rate in the HAZ to ensure the reformation of martensite and bainite microstructures [11]. A slow HAZ cooling rate must be avoided because it causes the austenitized HAZ to transform into ferrite and a mixture of hard and brittle bainite and martensite. This mixed microstructure of ferrite, bainite and martensite leads to embrittlement of the coarse-grained HAZ. When welding thinner or less hardenable material, an even faster critical cooling rate (less heat input) is required to avoid transformation of brittle mixed microstructure. Limitations on maximum welding heat input for HY 80 and HY 130 are specified in NAVSHIPS 0900-000-1000. For plate thickness less than 0.5 in the maximum allowable heat input should be 45000 joule/in, while for thickness more than 0.5 in the maximum allowable heat input should be 55000 joule/in.

Another concern when welding Q&T steels is the strict requirement of low hydrogen during welding in order to prevent underbead cold cracking. Preheating is one of the most effective ways of reducing the tendency for cold cracking, however it also reduces significantly the cooling rate in the HAZ. Consequently, it should be applied in such a way that a satisfactorily fast cooling rate can be achieved in the HAZ. As the strength level of Q&T steels becomes higher the tendency for hydrogen cracking to occur in the weld metal increases. For steels with yield strength about 690 MPa (100 ksi) the limit of the moisture content is 0.4% of weight.

The multipass welding can also help avoid regions of high hardness and low toughness in the HAZ. The advantages of the multipass welding compared to the single-pass

are that:

- the reheat thermal cycle of each subsequent welding pass normalizes and refines portions of the microstructure in the previous welding pass
- subsequent weld runs temper the previous weld metal and reduce residual stresses from previous runs
- the total energy input is reduced, resulting in a faster cooling rate which is helpful in limiting the amount of grain growth.

Although this method dissipates the hydrogen in the weld metal, it has the disadvantage of decreased productivity.

2.4 Weldability test

Weldability tests have been developed to evaluate the susceptibility of base and weld metal in cracking. The purpose of these tests is to reduce or eliminate the formation of defects during fabrication.

There are many tests available to evaluate weldability. One of them is the self-restraint test which utilizes the restraint or stress within the specimen to cause base or weld metal cracking. The Takken specimen, is a self-restraint test specimen developed in Japan [11, 12]. It is a Y sloped joint which provides more restraint than the U or double U joint. In the test the welding parameters, which are the preheating and the material properties, are varied to alter the stress state. This type of test is used to evaluate HAZ cracking and underbead root cracks.

2.5 Hot and cold cracking

Hot cracks are intergranular and can be found in both the weld metal and the HAZ. They usually occur during the solidification process at the stage where the developed solid crystals restrict the movement of the liquid. Hot cracking can also occur in the HAZ, next to the fusion line due to partial melting of the grain boundaries. In order for theses cracks to form, tensile stresses are required which are provided by the contraction of the weldment during cooling. These cracks are intergranular, small in size and usually remain stable. However, it is possible for them to extend due to hydrogen embrittlement. In that case they become transgranular.

Hot cracking is greatly affected by the chemical composition of both weld and base metal [13]. It can be prevented if $S < 0.035\%$, $Ni < 1.0\%$, $Mn > 0.8\%$, $C < 0.15\%$, $Mn/S > 35$, or if $HCS < 4$, where:

$$HCS = \frac{C[S + P + \frac{Si}{25} + \frac{Ni}{100}]10^3}{3Mn + Cr + Mo + V} \tag{2.1}$$

Cold cracks are generally transgranular and occur below 200 °C. They initiate during cooling to room temperature, after welding or long after the end of the welding. The hydrogen embrittlement is responsible for cold cracking. The hydrogen results in a decrease of ductility and tensile strength of the specimen. Cold cracking is also known as hydrogen-induced cracking or delayed cracking. It can occur without warning in the HAZ at the weld toe, the weld root or in an underbead position. As the alloy content of the base and weld metal increases cracking can occur in the weld metal.

In order for hydrogen-induced cracking to occur, the following conditions should be present at the same time. Hydrogen should be present, the weld should be under tensile stress, a susceptible microstructure should be present similar to those that exist in the HAZ, and a low temperature should be reached (-100 °C to 200 °C) [14]. Hydrogen cracking can occur without any external loading if high residual stresses are present. As the strength level of the steel increases the weldments become more susceptible to hydrogen cracking.

Hydrogen is produced from many sources such as moisture in the flux of the electrodes. It is absorbed by the weld pool and it is transfered to the HAZ by diffusion. In high strength steels, cracking can occur if the hydrogen content is more than 1 ppm. Cracking is also influenced by the welding heat input and the chemical composition of the base metal. For carbon equivalent (CE) more than 40% underbead cracking is possible to occur. CE is given by:

$$CE = C + \frac{Mn}{6} + \frac{Ni}{20} + \frac{Cr}{10} + \frac{Cu}{40} - \frac{Mo}{50} - \frac{V}{10} \tag{2.2}$$

To prevent cold cracking when welding high strength steels, low hydrogen electrodes should be used. These electrodes have a very low moisture content, which is the main source of hydrogen. Preheating can also prevent cold cracking by reducing the fast cooling that occurs in the HAZ during welding. The reduced cooling rate results in softer structure in the HAZ. Also, by keeping the temperature in the HAZ above the critical level for a longer period, the hydrogen diffusion of the HAZ is higher. Therefore the critical concentration of hydrogen at nucleation cites is avoided and the possibility of hydrogen cracking is reduced. As the CE increases, the required preheat temperature to avoid cracking increases. Unfortunately the cooling rate of the HY-100 and HY-130 must be controlled to obtain the required microstructure. Excessive preheat will allow carbides to agglomerate, reducing strength.

By increasing the reaction stresses in a joint, the distortion decreases and cold cracking is more likely to occur. So if we know the CE of the base metal, the hydrogen content of the weld metal, and the intensity of restraint of a joint, the critical cooling time can be determined.

2.6 Residual stresses

Residual stresses are those stresses that exist in a body if all external loads are removed. They can result in brittle fracture, fatigue fracture, stress corrosion fracture, cracking and buckling. Residual stresses in welds can be measured by many techniques, such as stress relaxation, x-ray diffraction, cracking and techniques that make use of stress sensitive properties. In most of these cases, strain gauges are used to measure strain release. Strain gauges are usually mounted on both surfaces of the plate to study the effect of bending stresses.

In two dimensional plane stress conditions, the fundamental relationships are:

$$\epsilon_x = \epsilon_x^{'} + \epsilon_x^{''} \qquad \epsilon_y = \epsilon_y^{'} + \epsilon_y^{''} \qquad \gamma_{xy} = \gamma_{xy}^{'} + \gamma_{xy}^{''} \tag{2.3}$$

Hook's law:

$$\epsilon_x^{'} = \frac{1}{E}(\sigma_x - \nu\sigma_y) \qquad \epsilon_y^{'} = \frac{1}{E}(\sigma_y - \nu\sigma_x) \qquad \gamma_{xy}^{'} = \frac{1}{G}\tau_{xy} \tag{2.4}$$

Equilibrium conditions:

$$\frac{\vartheta\sigma_x}{\vartheta x} + \frac{\vartheta\tau_{xy}}{\vartheta y} = 0 \qquad \frac{\vartheta\tau_{xy}}{\vartheta x} + \frac{\vartheta\sigma_y}{\vartheta y} = 0 \tag{2.5}$$

Condition of compatibility:

$$(\frac{\vartheta^2\epsilon_x^{'}}{\vartheta y^2} + \frac{\vartheta^2\epsilon_y^{'}}{\vartheta x^2} - \frac{\vartheta^2\gamma_{xy}^{'}}{\vartheta x\vartheta y}) + (\frac{\vartheta^2\epsilon_x^{''}}{\vartheta y^2} + \frac{\vartheta^2\epsilon_y^{''}}{\vartheta x^2} - \frac{\vartheta^2\gamma_{xy}^{''}}{\vartheta x\vartheta y}) = 0 \tag{2.6}$$

In the case of thermal stress: $\epsilon_x^{''} = \epsilon_y^{''} = \alpha\Delta T$ and $\gamma_{xy}^{''} = 0$ where $\epsilon_x^{'}$, $\epsilon_y^{'}$ and $\gamma_{xy}^{'}$ are components of elastic strain, $\epsilon_x^{''}$, $\epsilon_y^{''}$ and $\gamma_{xy}^{''}$ are components of plastic strain, α is the coefficient of linear thermal expansion and ΔT is the change of temperature [13].

Equation 2.6 indicates that in order for residual stresses to exist, the second parenthesis which contains the non elastic strains should not be zero. The two dimensional plane stress condition is not valid if the plate is over 1" thick, because the residual stresses in the thickness direction become significant and cannot be ignored.

Residual stresses are produced by uneven distribution of non elastic strains such as plastic strains during welding. If a material is heated uniformly, it expands uniformly and thermal stresses are not produced. But during the welding cycle, the weldment is heated locally by the welding heat source. The temperature distribution is not uniform and changes as the welding progresses. This uneven heating produces thermal stresses. After the completion of the welding, high tensile longitudinal stresses σ_x exist in regions near the weld, and compressive stresses exist in regions away from the weld. The tensile residual stresses indicate the region where the metal was melted and plastic deformation occurred during the welding thermal cycle. The region with the compressive stresses remains elastic during the entire welding thermal cycle.

The transverse residual stresses σ_y, are tensile stresses of relatively low magnitude in the middle part of the joint and compressive stresses at the ends of the joints. They are affected significantly by the reaction stresses of the external constraint which are distributed uniformly along the weld. The external constraint has little effect on the σ_x residual stresses .

Experimental and analytical results show that the maximum value of the residual stresses on low carbon steels is in the middle of the weld and can be as high as the yield stress of the material (35 to 50 ksi). However, in high strength steel such as HY 130, the residual stresses are widely scattered. Most regions have relatively low tensile stresses (50 to 80 ksi) and only small regions in the center of the weld have high tensile stresses.

From experiments on thermal stresses in weldments of an HY-130 steel, it was concluded that multiple passes produce cumulative plastic strain effects, especially during the first few passes. Little or no accumulation is noted in later passes. It was also observed that the maximum mechanical strain decreases as the base plate yield strength increases.

2.7 Degree of restraint

Residual stresses are closely related to distortion. During the welding cycle, the elastic and plastic thermal strains that are produced in the weld metal and the base metal near the weld, produce internal forces that cause bending, buckling and rotation.

In order to determine analytically the distortion caused by the transverse shrinkage of a restrained weld during the welding cycle, Kihara and Masubuchi [13] developed a formula that gives the degree of restraint on a slit weld type, having a lengthwise straight cut of length L. The geometry of the specimen is shown in Figure 2-3. If the length of the welding l covers the whole length of the slit L, $l = L$ and $F = (\frac{\pi}{2})^2$. The degree of restraint k_s is then:

$$k_s = \frac{\pi E l}{2L^2 F} = \frac{2E}{\pi L} \tag{2.7}$$

Assuming uniform stress σ_0 along the slit, the mean value of the displacement $[u]$ is then:

$$\sigma_0 = k_s[u]$$

For given σ_0 as the degree of restraint k_s increases the transverse shrinkage decreases. For this type of specimen k_s is usually between 60 to 140 $kgr/mm^2/mm$, and the ratio of the (transverse) shrinkage in a free weld to the shrinkage in a restrained weld is between 0.25 to 0.15.

In a slit weld the degree of restraint k_s is not uniform along the length of the slit. Its highest value is at the ends, and as a result the transverse shrinkage is large at the center and very small near the ends.

The major portion of transverse shrinkage of a butt weld is due to the contraction of the base plate. During the welding, the heat of the weld metal is transmitted into the base metal. This causes the base metal to expand. When the weld metal solidifies the expanded base metal starts shrinking. This shrinking is the major part of the transverse shrinkage. The shrinkage of the weld metal is about 10% of the total shrinkage. The longitudinal shrinkage is much less than the transverse shrinkage. An

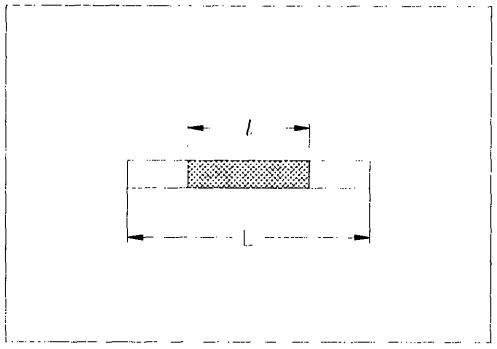

Figure 2-3: Slit type specimen

estimation for the longitudinal shrinkage in butt welds is that $\Delta L = 0.001L$.

Several techniques have been developed to reduce residual stresses and therefore distortion. The transverse shrinkage can be reduced using larger diameter electrodes, increasing the k_s or using an appropriate welding sequence. For example, the block welding causes less shrinkage that the multi layer sequences. Many techniques are also available to relax residual stresses that exist after the end of the welding. One method is the application of a uniform tensile load parallel to the direction of the residual stress. Considering the case of longitudinal stresses in a butt weld, as the external load increases there are certain regions that reach yielding, which in this case is the center of the weldment. The residual stresses that remain after the release of the tensile stress are much smaller and depend on the external load. As the level of applied stress increases, the residual stresses decrease, and become negligible if the applied stress becomes equal to the yield strength of the weld.

In general, the residual stresses affect only those phenomena that occur under a low applied stress, such as brittle fracture and stress corrosion cracking. As the level of applied stress increases, the residual stresses decrease and become negligible if the applied stress increases beyond yielding. Residual stresses and distortion affect very much the buckling phenomenon by significantly reducing the buckling strength of the structure.

2.8 Fracture toughness

Toughness is the ability of the material to absorb energy during fracture. It can be evaluated with impact toughness testing (the Charpy test) and fracture mechanics testing [11].

The Charpy test is used to measure the amount of energy absorbed during fracture of a notched specimen. It is also used to determine the transition temperature at which the material changes its fracture behavior from ductile to brittle mode.

The fracture mechanic testing is used to determine the fracture toughness K_{IC}, which is a material property. The fracture toughness in welding is usually expressed using the crack tip opening displacement.

Types of fracture

The fracture can be either transgranular, which severs the grains, or intergranular which propagate in the grain boundaries. The ductile, brittle and fatigue fracture are transgranular while the stress corrosion cracking, creep fracture and hot tearing are intergranular. Parts failing by ductile fracture (shear mode) are gray and silky, and are characterized by the "equiaxed dimples." Parts failing by brittle fracture (cleavage mode) are bright and granular and in the microscope can be characterized by a "river pattern." The fatigue fracture is characterized by "striations" [13].

Brittle fracture of steels

The appearance of a brittle fracture is granular and the plane of the fracture is perpendicular to the plate surface. The thickness reduction is negligible (less than 3%) even for ductile materials. A brittle fracture requires relatively low temperatures and can happen even if the stresses are well below yielding. The origins in most cases are small defects that cause stress concentration. In steel structures, the fracture usually propagate in the base metal and rarely in the weld metal or HAZ.

The sensitivity of the material to notch brittleness is called notch sensitivity. Notch brittleness is the phenomenon in which steel plate with a sharp notch exhibits

brittle fracture in low temperature. The temperature at which the mode of fracture changes from shear to cleavage is called transition temperature. To avoid brittle fracture in a welded structure, the material used should have adequate notch toughness, should not be notch sensitive, and the transition temperature should be lower than the minimum expected temperature during service.

To initiate a crack in a steel plate, the stress should be as high as the yield stress. Even if the applied stress is lower, the existence of a defect can increase the stresses at values close to yield strength, initiating the crack. After this, the crack can propagate at low stress. If the length of the crack becomes longer than the critical length, catastrophic fracture may occur.

One of the most important factors that affect the mechanical properties, such as notch toughness and weldability of steels, is the chemical composition. Elements used in steel manufacturing are C, Mn, Si, P, S, Al, Cr, Ni, Mo. Among those, carbon is the most important alloy. As the content of carbon increases, the ultimate strength and yield strength increases. However the elongation, the notch toughness, and the weldability decreases and the susceptibility to hot and cold cracking increases. The carbon content for a weldable steel should be less than 0.25%

To avoid brittle fracture when welding high strength, quenched and tempered steels, the weld metal should have notch toughness similar to the base metal. However as shown in the following table, this is not possible. The notch toughness requirement of some base metals and electrodes are:

	Minimum energy absorption	Temperature	notes
HY80, HY100, HY130	60 ft-lb	-120 F	thickness $\leq$ 2 in
E8018 C2	20 ft-lb	-100 F	
E8018 C1	20 ft-lb	-75 F	
E9018 M, E10018 M, E11018 M, E12018 M	20 ft-lb	-60 F	

As the yield strength of the material of the base plate increases, high quality welding processes such as GTA and GMA should be used.

2.9 Fracture mechanics theory

In the fracture mechanics theory there are three types of cracking modes. The opening mode (mode I) which is caused by stress normal to the plane of the crack, the sliding mode (mode II) which is caused by in-plane shear stresses and the tearing mode (mode III) which is caused by out of plane stresses. Although all three modes of cracks exist in a general case, the mode I is the most important.

The stresses around the tip of a mode I crack with length $2a$, in an infinite plate, under uniform tensile stress σ are:

$$\sigma_y = \frac{K}{\sqrt{2\pi r}} \cos\frac{\theta}{2}(1 + \sin\frac{\theta}{2}\sin\frac{3\theta}{2})$$

$$\sigma_x = \frac{K}{\sqrt{2\pi r}} \cos\frac{\theta}{2}(1 - \sin\frac{\theta}{2}\sin\frac{3\theta}{2}) \tag{2.8}$$

$$\tau_{xy} = \frac{K}{\sqrt{2\pi r}} \sin\frac{\theta}{2}\cos\frac{\theta}{2}\cos\frac{3\theta}{2})$$

$$K = \beta\sigma\sqrt{\pi a} \tag{2.9}$$

where K is the stress intensity factor, and β depends on the geometry and the location of the crack. If $2a$ is much smaller than the plate width w, $\beta \cong 1$. As $2a$ increases β increases and finally for $2a = w$, $\beta = 4$. Along the x axis and for $\theta = 0$

$$\sigma_y = \sigma_x = \frac{K}{\sqrt{2\pi r}} \qquad and \qquad \tau_{xy} = 0$$

Fracture will occur as K reaches the critical value K_C which is called "critical stress intensity factor" or "fracture toughness." The K_C depends on the material but also on the state of stress applied at the crack tip. For the plane strain case, the K_C gets its lower value K_{IC} which can be considered as a material constant. To obtain plane strain state of stress around a crack tip, the thickness of the plate should be $B \geq 2.5(\frac{K_{IC}}{\sigma_{ys}})^2$ [15]. The K_{IC} value of different steels decreases drastically as the yield strength of the material increases.

In a mode I crack having length $2a$, the displacement of the crack edges is given

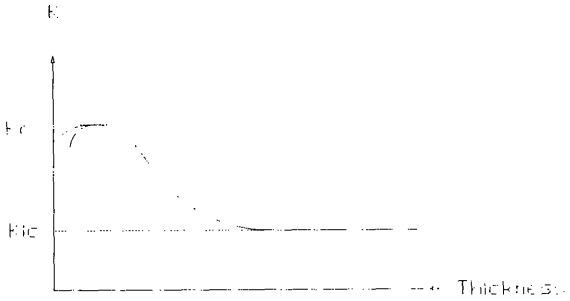

Figure 2-4: Fracture toughness against thickness.

by the crack opening displacement (COD):

$$COD = \frac{4\sigma}{E}\sqrt{a^2 - x^2} \tag{2.10}$$

where at $x = 0$ is the center of the crack and at $x = a$ is the tip of the crack. At $x = a$ the crack tip opening displacement (CTOD) is given by:

$$CTOD = \frac{K^2(1-\nu^2)}{E \cdot \lambda \cdot \sigma_{ys}} \tag{2.11}$$

or for the case of plane stress:

$$CTOD = \frac{K^2}{E \cdot \lambda \cdot \sigma_{ys}} \tag{2.12}$$

where $\lambda \cong \frac{\pi}{4} \cong 1$. Also at $x = 0$ the COD is:

$$COD = \frac{4\sigma}{E}\sqrt{a^2 + \frac{E^2}{16\sigma^2(CTOD)^2}} \tag{2.13}$$

Although a brittle fracture requires that the length of the crack should be larger than the critical length, it has been observed that brittle fracture can occur at cracks having smaller size. This can happen if there is enough energy from residual stresses during fatigue or under stress corrosion cracking.

Equation 2.11 can be used to determine the K_{IC} from a CTOD measurement on a small, three-point bent specimen with small crack.

2.10 Fatigue fracture

Under a given value of maximum applied stress, the material will fracture after a number of cycles. If the applied load is lower, more number of cycles are required for fracture. In some materials, and especially ferrous metals, the life of the structure becomes infinite if the stress is equal or less to a certain value. This value is called endurance limit. It is affected by the material strength, the stress concentration and the environment. As the material strength increases, the endurance increases by a factor of 0.5. The endurance limit is affected by the surface polishing. Cracks, notches and discontinuities such as weld reinforcement cause stress concentration which reduce the fatigue life of the structure.

There are two types of fatigue. The low cycle and the high cycle. A high cycle fatigue requires more than 10^5 cycles and the deformations of the metal are within the elastic region. A low cycle fatigue requires less than 10^5 cycles and the applied stress is above yielding.

During a fatigue test the effect of the residual stresses is not always important. As a repeated load is applied, not only the magnitude but also the direction of the stress distribution around the crack changes. For example the high tensile stresses at the tip of a crack can become compressive after a tensile load has been applied once. When this load is released, the whole specimen unloads elastically leaving compressive stresses at the tips. The magnitude of the compressive stresses depend on the tensile load. A repeated alternative load of the same magnitude will cause changes on the stresses around the crack but the stresses will remain compressive.

During the service life of a structure, a defect or a flaw may form a small crack. The crack usually initiates from the surface of the specimen; it is much smaller than the critical length and cannot cause fracture. However, it can grow until it reaches the critical size. At that time catastrophic fracture will occur.

As the crack grows the stress intensity factor K increases. During a fatigue cycle K change from $K_{max} = S_{max}\sqrt{\pi a}$ to $K_{min} = S_{min}\sqrt{\pi a}$. The rate of fatigue crack

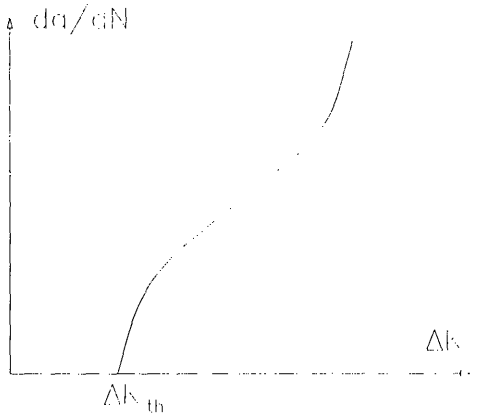

Figure 2-5: Rate of fatigue crack propagation against range of stress intensity factor.

propagation per cycle $\frac{da}{dN}$ is a function of the $\Delta K = K_{max} - K_{min}$.

$$\frac{da}{dN} = C(\Delta K)^n \tag{2.14}$$

where C and n are constants, S_{max} is the maximum applied stress, S_{min} is the minimum applied stress, $S_m = \frac{S_{max}+S_{min}}{2}$ is the mean stress and $S_r = S_{max} - S_{min}$ is the stress range.

Fatigue crack starts to grow when ΔK reaches a threshold value ΔK_{th} (Figure 2-5). The lower part of the curve represents the initiation of the crack, the middle part the stable crack growth, and the upper part the unstable fracture. Total fracture occurs during the cycle where the stress intensity reaches K_{IC} [15].

Chapter 3

Experimental Description and Results

3.1 Steel properties and electrode selection

The materials used as base metals in this study were the high strength low alloy quenched and tempered steels (HSLA $Q\&T$) HY-100 and HY-130. The consumables were selected according to the required degree of strength mismatch, the need for electrodes with the smallest possible value of carbon equivalent (CE), and the availability of those electrodes in the market. The electrodes that have the required degree of strength matching are the E80XX and the E110XX.

Carbon equivalent

The maximum and minimum values of the chemical composition for the HY-100, HY-130 and electrodes are shown in Table 3.1 [11, 16]. When only one value is shown, it is the maximum value.

The CE for each material was calculated using the following formula:

$$CE = C + \frac{Mn}{6} + \frac{Ni}{20} + \frac{Cr}{10} + \frac{Cu}{40} - \frac{Mo}{50} - \frac{V}{10}$$

For each electrode two values were calculated. One based on the average value of chemical composition and one based on the minimum values from Table 3.1.

The electrodes with the smallest carbon equivalent value were the E8018 C3, the E11018 M and the E8018 B2L. The carbon equivalent of each electrode appears in Table 3.2. Although the E8018 C3 provides better resistance to hydrogen induced cracking, the E8018 B2L was used instead.

Degree of strength mismatch

Typical mechanical properties of the materials used and the ASW specifications of those materials are shown in Tables 3.3 and 3.4. By combining these materials we can obtain joints with different degrees of strength matching. The degree of strength

matching of each joint is given by

$$DM = \frac{\sigma_{YS(weld)} - \sigma_{YS(plate)}}{\sigma_{YS(plate)}}$$

The E11018 M results in evenmatching and the E8018 in a 20% strength undermatching at the HY-100 base metal. The E11018 and the E8018 cause 40% and 25% undermatching at the HY-130 respectively.

Tensile test of base metals

To verify the properties of the HY-100 and HY-130, a tensile test was performed. A round tensile specimen was made from the plate of each material (Figure 3-3). The total length was 180 mm, the middle section length was 44 mm (1.7") and the middle section diameter was 5.08 mm (0.2").

The yield strength at 0.2% offset of the HY-100 was 724 MPa (105 ksi), the ultimate strength was 806.7 MPa (117 ksi) and the modulus of elasticity was 227.5 GPa (33 E03 ksi).

The HY-130 had both yield strength (0.2% offset) and ultimate strength at 986.0 MPa (143 ksi). The modulus of elasticity was 213.7 GPa (31 E03 ksi). Results from the tensile tests appear in Figure 3-1 and 3-2.

Plane strain effect

To evaluate the stress required to cause yielding of a homogeneous material, the plate shown in Figure 3-4 is examined analytically [17, 18]. The plate is loaded along the x_1 direction with the stress σ_1. The width W of the plate is much larger than the thickness of the plate t, so it can be assumed that the plate is under plane strain condition. Consequently $\epsilon_3 = 0$ and:

$$\epsilon_3 = \frac{1}{E}(\sigma_3 - \nu(\sigma_2 + \sigma_1)) = 0 \qquad \Rightarrow \qquad \sigma_3 = \nu(\sigma_2 + \sigma_1)$$

Since the thickness is small we can also assume that $\sigma_2 = 0$ so $\sigma_3 = \nu\sigma_1$.

Substituting in the Von Mises yield criterion:

$$(\sigma_1 - \sigma_2)^2 + (\sigma_2 - \sigma_3)^2 + (\sigma_3 - \sigma_1)^2 = 2\sigma_Y^2$$

which concludes that in order to bring the material at yield condition:

$$\sigma_1^2 = \frac{\sigma_Y^2}{1 - \nu + \nu^2}$$

For steels $\nu = 0.3$ so:

$$\sigma_1 = 1.125\sigma_Y$$

The yield strength of the material under plane strain is about 10% elevated from its original value, due to the restraint effect caused by the plane stress condition.

	HY130	HY100	E11018M	E80I8C3	E80I8B2L
C	0.12	0.12-0.20	0.1	0.12	0.1
Mn	0.60-0.90	0.10-0.40	1.30-1.8	0.40-1.1	1.3-1.8
P	0.01	0.025	0.03	0.03	0.03
S	0.015	0.025	0.03	0.03	0.03
Si	0.15-0.35	0.15-0.35	0.6	0.8	0.6
Cr	0.4-0.7	1.0-1.8	0.4	0.15	0.4
Ni	4.75-5.25	2.25-3.5	1.25-2.5	0.8-1.1	1.25-2.5
Mo	0.30-0.65	0.20-0.6	0.30-0.55	0.35	0.25-0.5
Cu		0.25			
V	0.05-0.10	0.03	0.05	0.05	0.05
Ti		0.02			

Table 3.1: Chemical composition of base and weld metals

Electrode	average CE	minimum CE
E11018 M	0.5770	0.4832
E8018/16 C3	0.2955	0.2297
E8018 B2L	0.4771	0.4092

Table 3.2: Carbon equivalent of electrodes

	HY100	HY130	E8018B2L	E11018M
yield stress (0.2% offset)	724.0 MPa 105 ksi	944.6 MPa 137 ksi	573.6 MPa 83.2 ksi	703.3 MPa 102.3 ksi
ultimate strength	813.6 MPa 118 ksi	986.0 MPa 143 ksi	673.6 MPa 97.7 ksi	774.3 MPa 112.3 ksi
elongation % in 2"			24	22
area reduction			72.6	63
charpy V notch -20 F -40 F -60 F			46 ft lbs 30 ft lbs	 65 ft lbs

Table 3.3: Typical mechanical properties of base and weld metals used in this study

	HY100	HY130	E8018B2L	E11018M
yield stress	100 ksi	130 ksi	67 ksi	98-110 ksi
ultimate strength			80 ksi	110 ksi
elongation % in 2"	17	24	19	20
area reduction longitudinally % transversely %	 55 50	 55 53		
charpy V notch -60 F -120 F 0 F	 50 ft lbs	 60 ft lbs		20 ft lbs

Table 3.4: ASW specified mechanical properties of base and weld metals used in this study

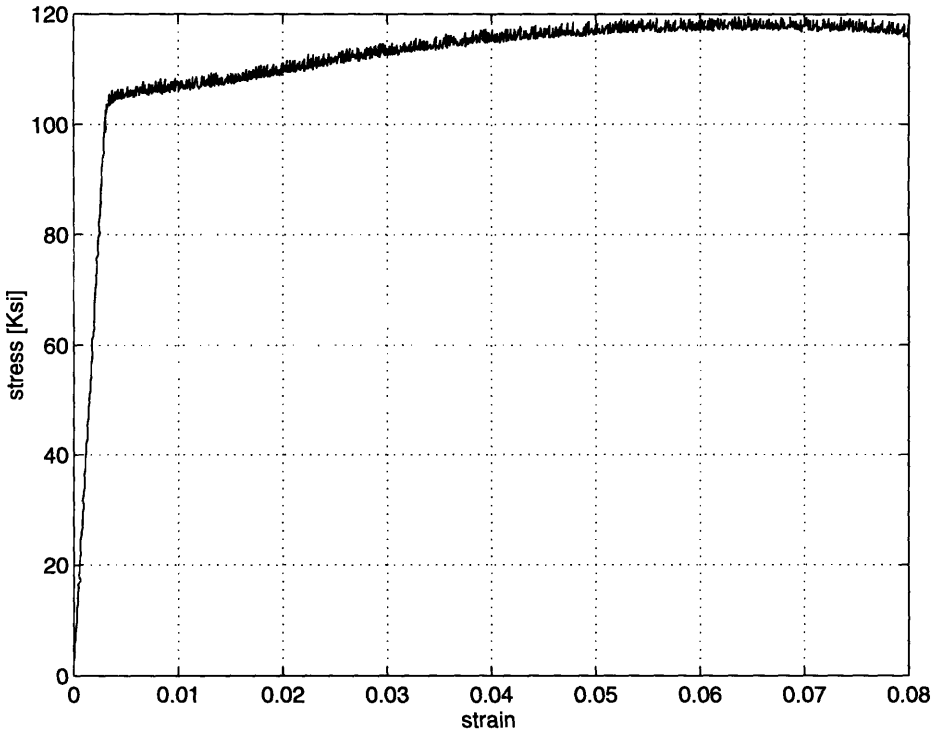

Figure 3-1: Stress strain curve from tensile test of the HY-100.

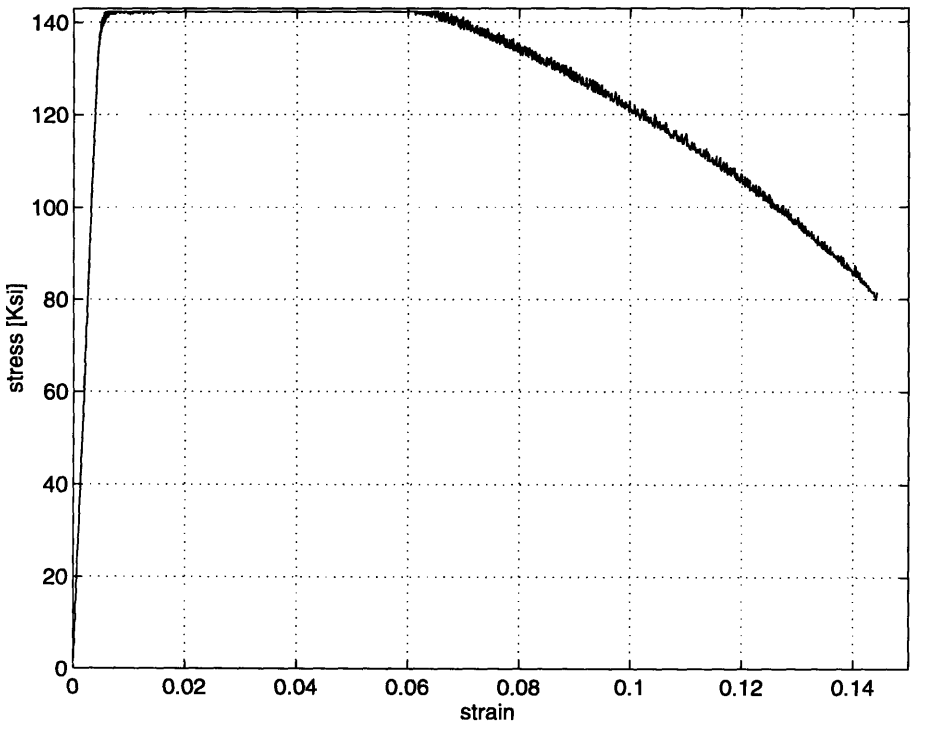

Figure 3-2: Stress strain curve from tensile test of the HY-130.

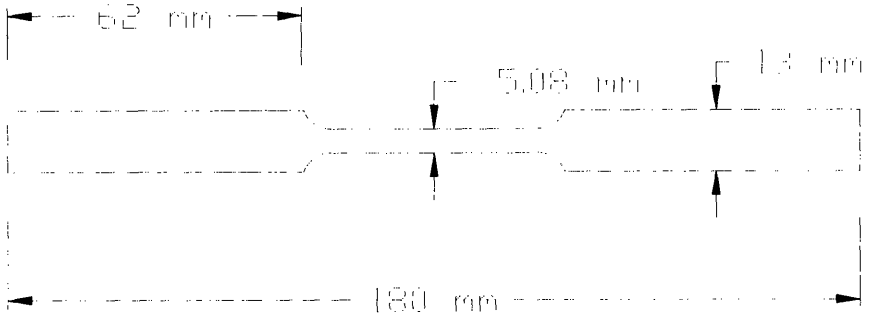

Figure 3-3: Base metal specimen for the tensile test.

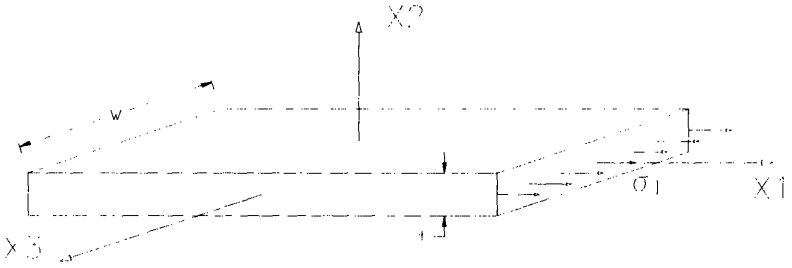

Figure 3-4: Plate subjected to tensile stress under plane strain condition.

3.2 Experimental results

The test methods used for the experimental evaluation of the strength of welded joint, were the self restraint crack test, the fatigue test, and the tensile test. The self restraint crack test was performed on HY-100 and HY-130, U.S. Navy Q&T steel specimens, welded by E8018 B2L and E11018 M electrodes.

After the welding of the first and last pass, and during the fatigue test, the specimens were observed for cracks using an optical and a helium-neon confocal laser microscope [19].

3.2.1 Self-restraint cracking test

The restraint crack test was performed to observe the effects of joint strength matching on HY-100 and HY-130 high strength steels.

During the restraint crack test, two parameters were investigated. The first parameter was the strength of the weld metal. Each base metal was welded with the two available electrodes to form different degrees of strength mismatch. Welding was performed in three passes. The second and the third passes were made with the same electrode, which was not necessarily the same as the first pass. The second parameter was the preheat temperature. Before the welding, the plates were preheated at either 20 ^oC or 50 ^oC. The preheating was done with a gas flame.

The combinations that were performed among steels plates, electrodes, and preheat temperatures are shown in Table 3.5 and 3.6. The electrode diameter was 2.6 mm. All the electrodes were in sealed tins and they were baked for more than an hour just before welding.

The F and I specimens represent 20% strength undermatching and the H and K represent evenmatching. The G and J represent the application of undermatching in the root pass of the weldment, while the rest of the groove was filled with evenmatched electrode. At the HY-130 the L specimens represent 40% undermatching, the M represent undermatching with softer material at the root pass of the weldment, and the N represent 25% undermatching.

Specimen	Preheating	first pass	next passes
F 20	20^oC	E8018	E8018
F 50	50^oC	E8018	E8018
G 20	20^oC	E8018	E11018
G 50	50^oC	E8018	E11018
H 20	20^oC	E11018	E11018
H 50	50^oC	E11018	E11018
I 20	20^oC	E8018	E8018
I 50	50^oC	E8018	E8018
J 20	20^oC	E8018	E11018
J 50	50^oC	E8018	E11018
K 20	20^oC	E11018	E11018
K 50	50^oC	E11018	E11018

Table 3.5: HY-100 welding specimens

Specimen	Preheating	first pass	next passes
L 20	20^oC	E8018	E8018
L 50	50^oC	E8018	E8018
M 20	20^oC	E8018	E11018
M 50	50^oC	E8018	E11018
N 20	20^oC	E11018	E11018
N 50	50^oC	E11018	E11018

Table 3.6: HY-130 welding specimens

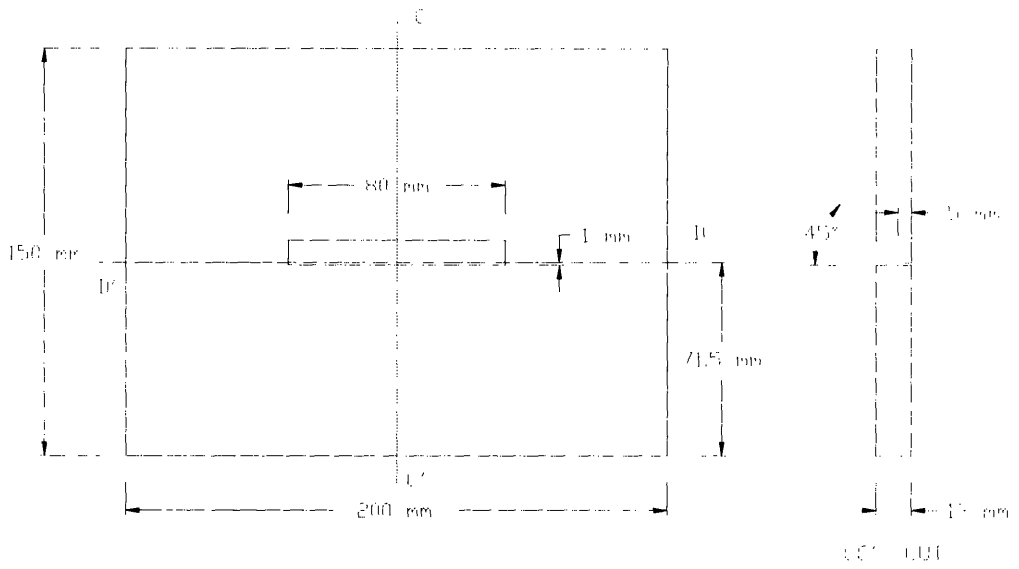

Figure 3-5: Geometry of the specimens.

Welding conditions

The welding process used for the welding was the Shielded Metal Arc welding (SMA). The welding voltage was $E = 36$ Volts, the current was $I = 100$ Amperes and the welding speed was $S = 4mm/sec = 10in/min$. The heat input is given by the formula:

$$H = \frac{E \cdot I \cdot 60}{S \cdot 1000} = 23KJ/in$$

From reference [11] (page 667, Table 7), the maximum allowed heat input for 12.7 mm plate thickness and preheat temperature 20^oC is 70 KJ/in, while for preheat temperature 50^oC is 65 KJ/in.

Test specimen description

The shape of the restraint cracking specimen is shown in Figure 3-5. The thickness of the plate was 13 mm. The notch was 1 mm thick and the angle of the groove was 45^o.

To construct the specimen, the plate in Figure 3-5 was cut along the DD' line. After the fabrication of the 1 mm notch and the 45^o groove, the two pieces were welded together along the same line to form the original specimen.

The degree of restraint for that geometry can be calculated using equation 2.7.

$$k_s = \frac{2E}{\pi L}$$

For $E = 207GPa$ and $L = 0.08m$ the degree of restraint is

$$k_s = 1.647E12\frac{N/m^2}{m} = 168\frac{kg/mm^2}{mm}$$

According to Masubuchi [13] the expected value for a slit type specimen is

$$k_s = 60 \ \ to \ \ 140\frac{kg/mm^2}{mm}$$

As a result, the transverse shrinkage is expected to be small, resulting in a high cracking possibility.

Experimental procedure

The restraint crack test was performed by welding the first pass under the conditions shown in Table 3.5 and 3.6. Twenty-four hours after the end of the first pass, the residual stresses and the transverse shrinkage of the plate were measured. The specimen was then cut along the CC' line for crack observation. After the observation, the two parts were clamped together to form the original specimen and to perform the remaining passes of the welding. When the specimens were cooled down, they were cut again along the CC', LL' and RR' line (Figure 3-8) for crack observation.

Residual stresses results

The residual stresses perpendicular to the welding direction were measured using strain gauges at two HY-100 specimens, the F20 and the H20. The strain gauges were placed at the points T1 and T3 on the upper surface of the specimen, and T2 and T4 on the lower surface. The location of these points appears in Figure 3-6. The strain gauges were placed on the base metal to prevent the welding heat from damaging them. The residual stresses at the top and bottom surfaces were averaged

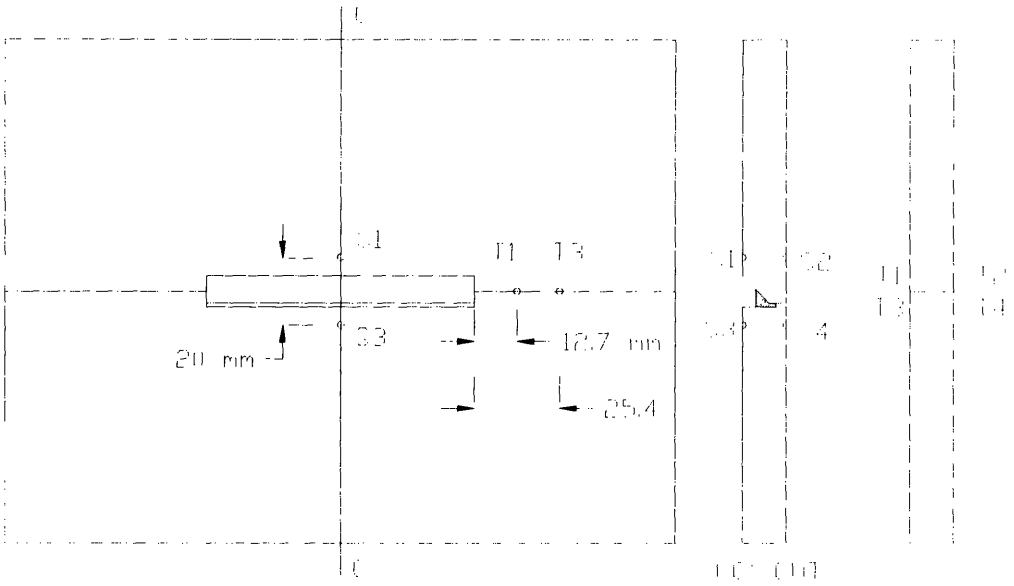

Figure 3-6: Restraint cracking specimen.

to avoid the influence of bending.

The strain gauge output voltage was measured before and after the welding of the first pass. The difference of those measurements was converted into strain using the gauge conversion factor. The conversion factor of the strain gauges is 2.09E06 V^{-1}. Assuming only elastic strain in that region of the base plate, the residual stresses in a direction perpendicular to the welding direction were obtained by multiplying the measured strains with the modulus of elasticity.

The detailed results appear in Tables 3.7 and 3.8. An estimation of the transverse residual stress distribution in the base metal, along the welding direction, is shown in Fig 3-7. From the results it is obvious that the residual stresses of undermatched welds are lower than those caused by evenmatched welds, reducing the potential of crack initiation.

	units	strain gages 1,2	strain gages 3,4
Initial strain	Volts	278.3030 E-06	91.7057 E-06
After 1st pass	Volts	-437.4000 E-06	-329.2670 E-06
Residual strain	Volts	-715.703 E-06	-420.9727 E-06
Residual strain	ϵ	-1495.8193 E-06	-879.8329 E-06
Residual stress		-31.4122 kg/mm^2	-18.4765 kg/mm^2

Table 3.7: Residual stresses at HY-100, caused by the E8018 during the first pass

	units	strain gages 1,2	strain gages 3,4
Initial strain	Volts	576.657 E-06	-179.673 E-06
After 1st pass	Volts	-347.3870 E-06	-397.137 E-06
Residual strain	Volts	-924.044 E-06	-217.464 E-06
Residual strain	ϵ	-1931.252 E-06	-454.4998 E-06
Residual stress		-40.5563 kg/mm^2	-9.5445 kg/mm^2

Table 3.8: Residual stresses at HY-100, caused by the E11018 during the first pass

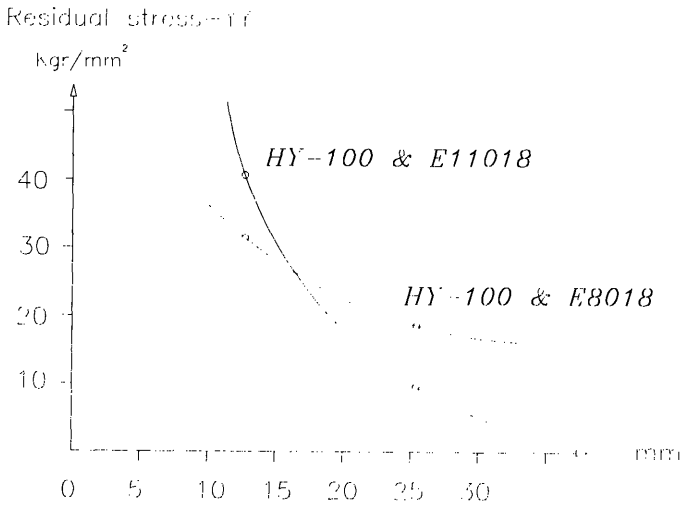

Figure 3-7: Residual stress-YY along the welding direction on the base metal.

Transverse shrinkage results

To measure the transverse shrinkage, two depressions had been formed on each side of the specimen along the line CC', at the points S1, S2, S3 and S4 (Figure 3-6). The distance between the two points was measured before and after the first pass and the difference between those two measurements was calculated for the upper and lower part of the specimen.

Due to geometry, the location of the first pass was almost at the center of the thickness of the plate. By ignoring the bending effect, the maximum transverse shrinkage u is given by:

$$u = 0.5 \cdot \frac{(u_{13} - u_{13W}) + (u_{24} - u_{24W})}{2}$$

where u_{13} is the distance between S1 and S3 measured at the upper surface before the welding, u_{13W} is the same distance measured after the welding. u_{24} is the distance between S2 and S4 measured at the upper surface before the welding and u_{24W} is the same distance measured after the welding. Detailed results are given in Table 3.9.

The mean value of the distortion is then $[u] \approx 0.85u$, and the uniform stress σ_y is given by $\sigma_y = k_s[u]$. From these calculation the uniform transverse stress σ_y can be estimated, assuming that at the base plate only elastic strains exist and that the state of stress is the same at points symmetrically placed around the welding direction.

Specimen	Surface	Initial mm	After mm	Difference mm	Average difference	Transverse shrinkage
F 20	top	21.32	21.08	0.24	0.140	0.070
	bottom	20.07	20.03	0.04		
F 50	top	20.76	20.63	0.13	0.165	0.083
	bottom	21.15	20.95	0.20		
G 20	top	21.30	21.10	0.20	0.120	0.060
	bottom	19.99	19.95	0.04		
G 50	top	21.61	21.44	0.17	0.290	0.145
	bottom	19.65	19.24	0.41		
H 20	top	21.31	21.16	0.15	0.075	0.038
	bottom	20.32	20.32	0.00		
H 50	top	20.42	20.29	0.13	0.055	0.028
	bottom	19.98	20.00	-0.02		
I 20	top	21.30	21.18	0.12	0.070	0.035
	bottom	20.20	20.18	0.02		
I 50	top	20.93	20.75	0.18	0.185	0.093
	bottom	19.72	19.53	0.19		
J 20	top	21.13	21.06	0.07	0.150	0.075
	bottom	21.05	20.82	0.23		
J 50	top	20.81	20.75	0.06	0.155	0.078
	bottom	20.44	20.19	0.25		
K 20	top	21.24	20.77	0.47	0.375	0.188
	bottom	21.56	21.28	0.28		
K 50	top	21.45	21.42	0.03	0.13	0.065
	bottom	20.58	20.35	0.23		
L 20	top	21.44	21.24	0.20	0.305	0.153
	bottom	20.03	19.62	0.41		
L 50	top	20.08	19.51	0.57	0.380	0.190
	bottom	21.09	20.90	0.19		
M 20	top	22.20	22.01	0.19	0.255	0.128
	bottom	20.15	19.83	0.32		
M 50	top	21.11	20.87	0.24	0.135	0.068
	bottom	21.49	21.46	0.03		
N 20	top	21.49	21.31	0.18	0.055	0.028
	bottom	20.41	20.48	-0.07		
N 50	top	21.24	21.14	0.10	0.04	0.020
	bottom	20.80	20.82	-0.02		

Table 3.9: Transverse shrinkage caused by the first pass of welding

Results from crack observation

After the first pass of welding, the specimens were cut along the CC' line in order to examine the left and right surface (CL and CR) of this cross section for cracks. The examination was repeated after the completion of the last pass and having cut the original specimen along the LL', RR' and CC'. The surfaces that were examined were the L surface and R surface. These surfaces are shown in Figure 3-8.

Figure 3-9 shows a typical cross section observed after the first pass. The unwelded groove size was measured after the first pass along the thickness direction. This value is the thickness of the second and last pass. Since all of the cracks were initiated from the root of the weldment, this information can be used to determine the contribution of the first pass on the joint strength.

Detail results from the crack observation are in Table 3.10. The fifth column of the table gives the crack size after the first pass, measured at the CL and CR surface. The last column gives the crack size after the last pass, measured at the L and R surface. No crack was found at the surface of the weld, except from the G20, I20 and J20 at which the fracture was complete. All the cracks were measured along the thickness direction.

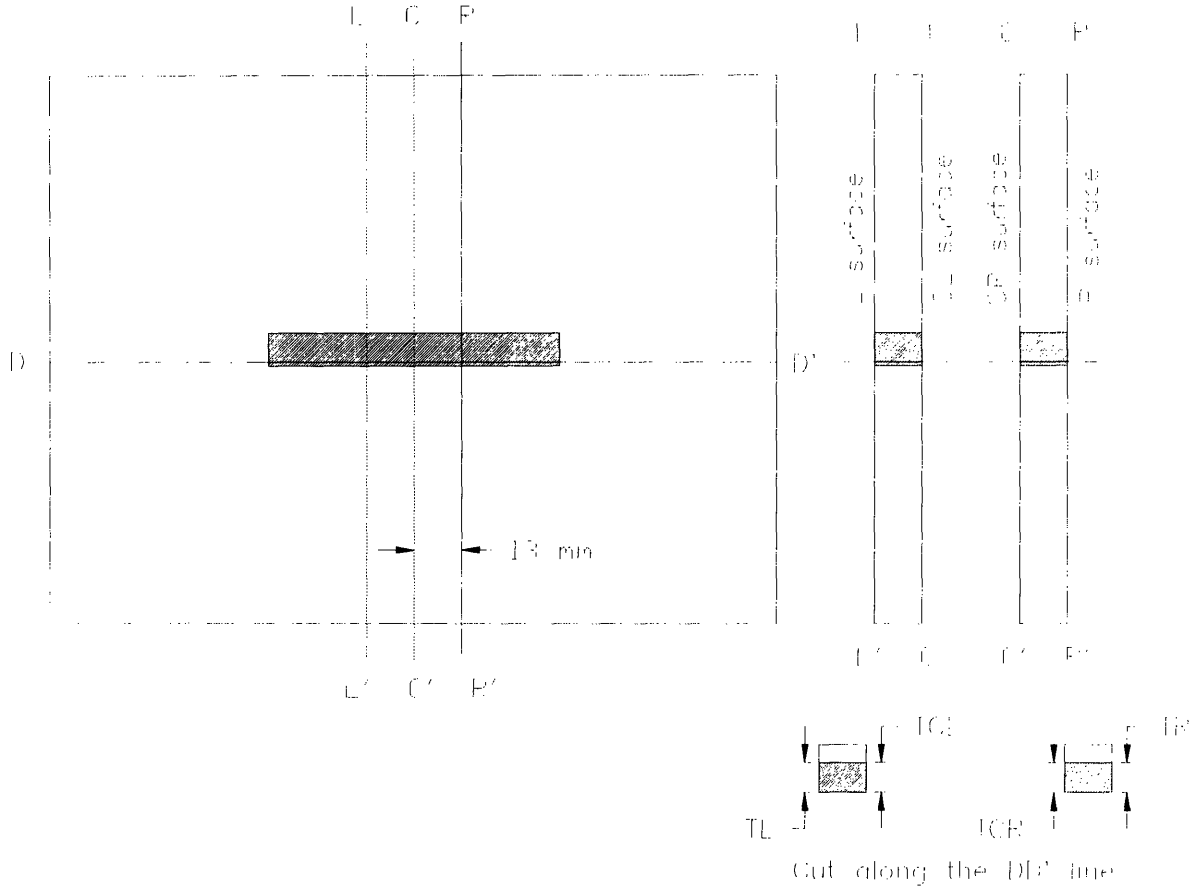

Figure 3-8: Crack observation.

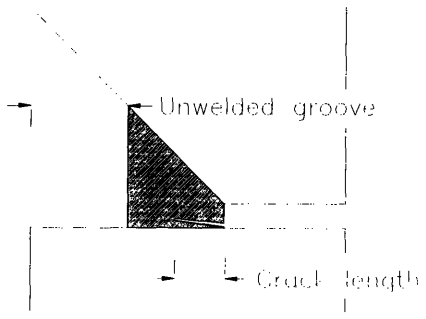

Figure 3-9: Weld observation at the cut surfaces.

Specimen	First pass	unwelded groove mm	Next passes	Crack size after first pass CL/CR mm/mm	Crack size after last pass L/R mm/mm
F 20	E8018	3.95	E8018	1.35/0.70	2.56/0.2
F 50	E8018	4.19	E8018	2.0**/ 0	0 / 0
G 20	E8018	3.17	E11018	2.7*/3.5*	3.0/1.3
G 50	E8018	3.77	E11018	1.25/1.35	3.77/1.0
H 20	E11018	4.56	E11018	1.3/1.3	2.14/1.0
H 50	E11018	4.68	E11018	0 / 0	0 / 0
I 20	E8018	3.39	E8018	3.5*/3.0*	2.0/2.2
I 50	E8018	4.88	E8018	0 / 0	0 / 0
J 20	E8018	3.62	E11018	3.0*/3.0*	2.2/3.2
J 50	E8018	4.82	E11018	0 / 0	0 / 0
K 20	E11018	4.26	E11018	0.16/0.16	0.4/ 0
K 50	E11018	4.79	E11018	0.15/0.14	0 / 0
L 20	E8018	4.09	E8018	2.85/2.00	1.21/1.35
L 50	E8018	3.69	E8018	0.12/ 0	0 / 0
M 20	E8018	4.02	E11018	0 / 0	0.2/ 0
M 50	E8018	4.01	E11018	0.32/ 0	0.5/0.5
N 20	E11018	4.04	E11018	0 / 0	0.15/0.15
N 50	E11018	4.49	E11018	0 / 0	0 / 0

$*$: complete fracture after the first pass of welding
$**$: defect at the root of the weld

Table 3.10: Crack size on HY-100 and HY-130 specimens

Specimen	TL mm	TR mm	TCL mm	TCR mm	Average mm
F 20	5.44	6.77	6.64	7.37	6.56
F 50	2.72	6.46	6.30	5.02	5.13
G 20	5.10	6.10	5.60	6.65	5.86
G 50	5.05	5.86	5.66	5.46	5.51
H 20	6.45	6.70	6.80	6.88	6.71
H 50	7.18	6.90	7.58	7.64	7.32
I 20	5.84	5.88	5.47	5.87	5.77
I 50	7.20	6.60	7.10	7.35	7.06
J 20	6.25	6.08	6.24	6.37	6.24
J 50	7.30	7.40	7.40	7.41	7.38
K 20	7.57	6.90	8.00	7.99	7.62
K 50	7.30	7.00	6.90	7.27	7.12
L 20	6.64	6.26	6.60	6.40	6.48
L 50	6.85	6.90	6.30	6.46	6.63
M 20	6.61	6.57	6.20	6.30	6.42
M 50	6.30	6.30	7.30	6.60	6.63
N 20	7.00	6.05	6.35	6.30	6.43
N 50	7.10	7.20	7.00	6.65	6.99

Table 3.11: Average thickness of the weldment on HY-100 and HY-130 specimens

Joint thickness

The specimens were also examined in order to measure the exact value of the joint thickness. Even though the geometry before the welding was the same on all the specimens, the actual thickness of the welding was different because the penetration of the first pass of the welding was not the same. The joint thickness was determined by measuring the thickness of the weldment at the L, R, CL and CR surfaces. The measured values of thickness are the TL, TR, TCL and TCR (Figure 3-8) and they appear in Table 3.11. Their average value represents the joint thickness of each specimen.

Summary of the results

The measurements from the crack observation are summarized in Table 3.12. The first column is the average thickness of the weldment from Table 3.11. The second column is the average crack length from Table 3.10. It was obtained from the crack measurements after the first and last pass. The third column is the non-cracked weld metal and was obtained by subtracting the average crack length from the average thickness of the weldment. The fourth column includes both the length of the crack and the notch. The summation of the non-cracked weld metal with the length of the crack and notch equals the thickness of the plate, which is $13.0mm$. All the measurements were done along the thickness direction. The non-cracked weld metal will be used to estimate the effective cross sectional area. Thus the normalized stress in that cross sectional area can be determined more accurately.

The average transverse shrinkage observed at the center of the groove along the CC line (Table 3.9), and the average crack length, are shown in Table 3.13. The average crack length includes the measurements after the first pass only. Large values of crack length result in small and not accurate values of transverse shrinkage. So the specimens F20, G20, G50, H20, I20 and J20 can be ignored.

Table 3.14 demonstrates the effect of electrode strength and preheat temperature.

Spec.	Weldment mm	Crack mm	Non cracked weld metal mm	Crack & notch mm
F 20	6.56	1.2	5.36	7.64
F 50	5.13	0	5.13	7.87
G 20	5.86	3.1	2.76	10.24
G 50	5.51	1.8	3.67	9.33
H 20	6.71	1.4	5.27	7.73
H 50	7.32	0	7.32	5.68
I 20	5.77	2.7	3.09	9.91
I 50	7.06	0	7.06	5.94
J 20	6.24	2.8	3.44	9.56
J 50	7.38	0	7.38	5.62
K 20	7.62	0.2	7.42	5.58
K 50	7.12	0.1	7.02	5.98
L 20	6.48	1.9	4.58	8.42
L 50	6.63	0	6.63	6.37
M 20	6.42	0	6.42	6.58
M 50	6.63	0.2	6.43	6.52
N 20	6.43	0	6.43	6.57
N 50	6.99	0	6.99	6.01

Table 3.12: Average size of cracked, and non-cracked weld metal after the last pass

Specimen	First pass	Average cracking mm	Transverse shrinkage mm
F 20	E8018	1.0	0.070
F 50	E8018	0	0.083
G 20	E8018	failed	0.060
G 50	E8018	1.3	0.145
H 20	E11018	1.3	0.038
H 50	E11018	0	0.028
I 20	E8018	failed	0.035
I 50	E8018	0	0.093
J 20	E8018	failed	0.075
J 50	E8018	0	0.078
K 20	E11018	0.1	0.188
K 50	E11018	0.1	0.065
L 20	E8018	failed	0.153
L 50	E8018	0	0.190
M 20	E8018	0	0.128
M 50	E8018	0.3	0.068
N 20	E11018	0	0.028
N 50	E11018	0	0.020

Table 3.13: Transverse shrinkage after the first pass

Base metal	First pass	Preheating ^oC	Distortion mm	Average shrinkage	Specimen
HY-100	E8018	20		??	
		50	0.085		F50, I50, J50
	E11018	20	0.188	0.12	K20
		50	0.047		H50, K50
HY-130	E8018	20	0.128	0.13	M20
		50	0.129		M50, L50
	E11018	20	0.028	0.02	N20
		50	0.002		N50

Table 3.14: Average transverse shrinkage after the first pass

3.2.2 Fatigue test

When a partial penetration groove joint is used for the fatigue test, the stresses at the root are much higher than those at the surface due to the joint bending. In order to reproduce the actual stresses distribution of the joints used in steel building, a symmetric specimen was used. The specimen was extracted from the restraint cracking specimens after cutting along the LL' RR' and CC' line. The two pieces were welded together to form one symmetric notched specimen as is shown in Figure 3-10. The reinforcement of the weld was removed.

The specimens tested were the K20, I50 and J50. They were selected because their initial crack size was almost zero. The K20 represents the evenmatched welding on the HY-100, the I50 the undermatched, and the J50 the application of undermatching only at the root of the weldment.

The fatigue test was performed by an INSTRON fatigue test machine. The loading was cyclic, the amplitude of the load was 20 KN, and the mean value was zero. The frequency of the test was 7 cycles per second. The load amplitude was determined from empirical data [20, 21] for joints with evenmatched welds. The specimens were expected to fail between 20,000 to 100,000 cycles.

Experimental results

During the fatigue test, the crack propagation was measured only along the L and R surface (Figure 3-10). The values of the left CL and right CR surface were estimated after the complete fracture of the specimen, by observing the striations lines. Thus the average value of the crack propagation is more accurate.

The average crack is the crack size along the thickness direction, and it was measured from the tip of the notch. The total crack length α was obtained by adding the length of the notch to the length of the average cracking. The results from the fatigue test are in Tables 3.15, 3.16 and 3.17. The results can be summarized in plot 3-12.

The I50 specimen failed at 93,000 cycles and the J50 at 121,000 cycles. For the

first 25,000 cycles the J50 behaved similar to the I50 but during the 25,000 and 60,000 cycles the crack growth rate of the J50 decreased. The K20 did not fail after 300,000 cycles.

Stress intensity factor

To calculate the stress intensity factor the following formula was used:

$$K_I = \sigma\sqrt{\pi\alpha} \cdot F(\frac{\alpha}{b})$$

where σ is the nominal stress applied at the end of the specimen, 2α is the size of crack and notch, and $2b$ is the width of the specimen, which is twice the thickness of the base plate $w = 13.00mm$. The $F(\frac{\alpha}{b})$ is a factor given by the empirical formula:

$$F(\frac{\alpha}{b}) = \frac{1 - 0.5(\alpha/b) + 0.370(\alpha/b)^2 - 0.044(\alpha/b)^3}{\sqrt{1-(\alpha/b)}}$$

The error using this formula is less than 0.3% for any (α/b). This formula is a modification of Koiter's formula [22].

Having thickness of the fatigue specimen $t = 12.85mm$, $b = 13.00mm$, and maximum load 20 KN, the nominal stress away from the notch is $\sigma = 59.86N/mm^2$. The different values of α are the notch size plus the average values of crack propagation taken from Tables 3.15, 3.16 and 3.17. Since the applied stress was alternating, the ΔK_I is twice the value of the K_I.

The results from the fatigue test are in Tables 3.18, 3.19 and 3.20. The results can be summarized in plots 3-14 and 3-15

In Figure 3-14, one straight line was drawn to fit the points from each specimen in a least-square sense. Obviously the straight lines from the I50 and J50 are almost identical and represent the stable crack growth part during the fatigue test.

The K20 specimen appears to have a totally different behavior. However, due to the fact that its joint thickness is very high, it never reached the stress intensity factor of the other two specimens. As a result, it remained in a stage where the range of

the stress intensity factor was lower than the theoretical threshold value ΔK_{th}.

Assuming that the K20 also behaves similar to the other two specimens, a third order polynomial line was drawn to fit all the points as is shown in Figure 3-15.

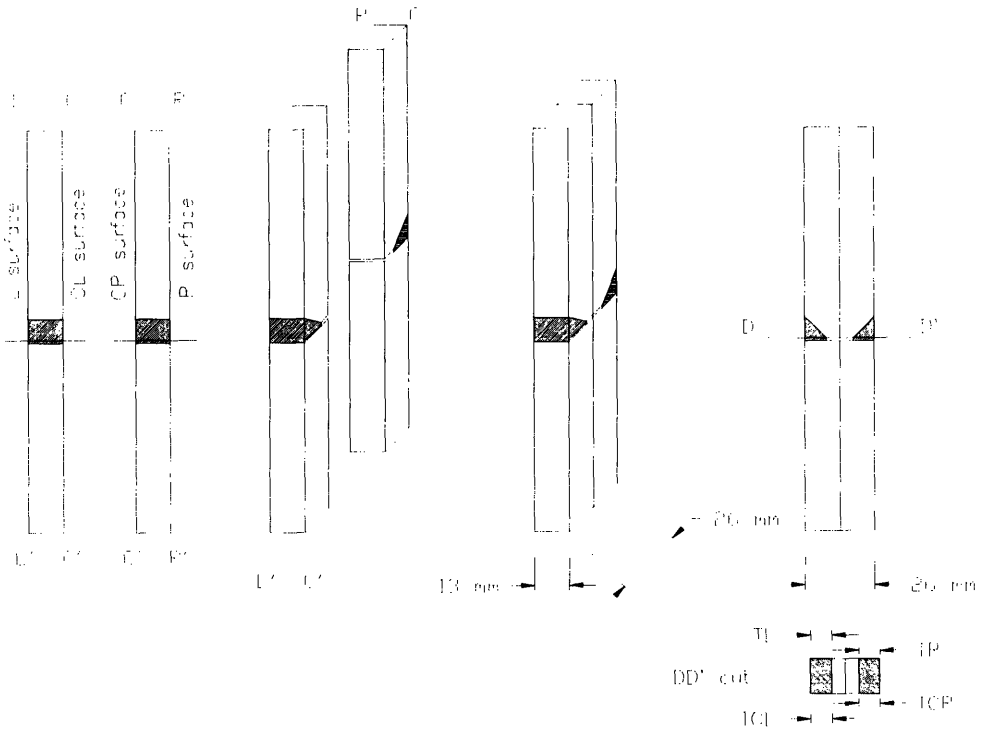

Figure 3-10: Fatigue test specimen.

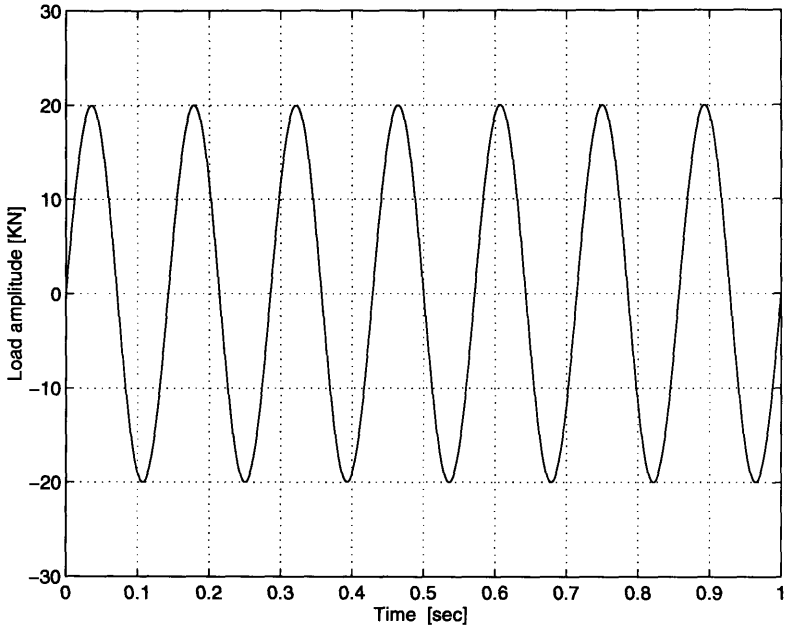

Figure 3-11: Applied load during fatigue test. The frequency is 7 Hz.

Cycles	TL mm	TR mm	TCL mm	TCR mm	Average mm
0	0	0	0	0	0
6,000	0	0	0	0	0
15,000	0.26	0.35	0	0	0.15
25,000	0.51	0.75	0.2	0.3	0.44
35,000	0.58	1.65	0.3	1.0	0.88
45,000	0.58	2.75	0.4	1.8	1.38
55,000	0.64	3.28	0.5	2.3	1.68
85,000	3.17	4.92	2.5	3.5	3.52
93,000					7.06

Table 3.15: Crack propagation on I-50 specimen

Cycles	TL mm	TR mm	TCL mm	TCR mm	Average mm
0	0	0	0	0	0
5,000	0.55	0.27	0	0.5	0.33
15,000	0.67	0.54	0	1.04	0.56
25,000	1.19	0.58	0.2	1.12	0.77
35,000	1.25	0.61	0.3	1.18	0.84
45,000	1.29	0.63	0.4	1.22	0.89
65,000	1.63	0.63	0.7	1.22	1.05
80,000	2.27	0.63	1.4	1.22	1.38
85,000	2.99	0.63	2.3	1.22	1.79
105,000	3.20	1.81	2.5	3.5	2.75
121,500					7.38

Table 3.16: Crack propagation on J-50 specimen.

Cycles	TL mm	TR mm	TCL mm	TCR mm	Average mm
0	0.40	0	0	0	0.10
25,000	0.40	0.12	0	0.12	0.16
50,000	0.40	0.14	0.2	0.14	0.22
100,000	0.40	0.24	0.4	0.25	0.32
250,000	0.45	0.28	0.72	0.30	0.44

Table 3.17: Crack propagation on K-20 specimen

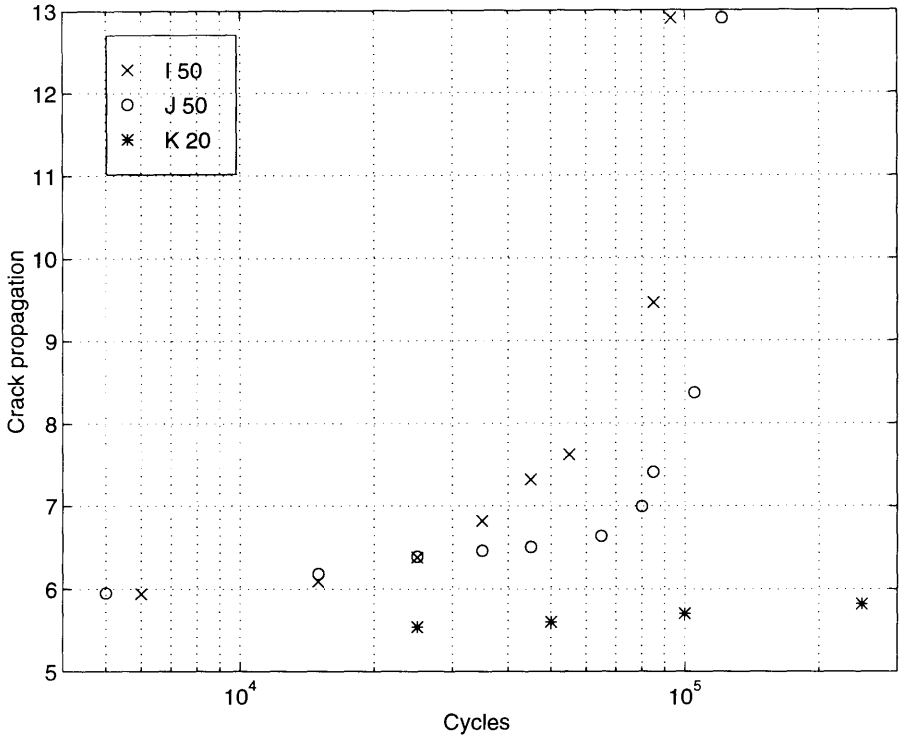

Figure 3-12: Crack propagation.

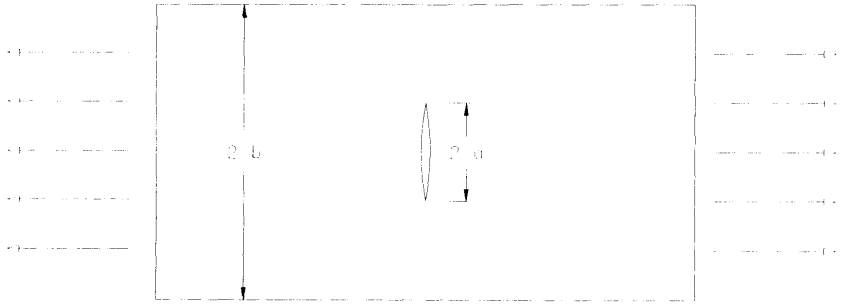

Figure 3-13: Geometry of a plate with width $2b$ and crack length 2α, under tensile load.

Cycles	α mm	$F(\frac{\alpha}{b})$	ΔK_I $\frac{N\sqrt{mm}}{mm^2}$	$\frac{d\alpha}{dN}$ $\frac{mm}{cycle}$
0	5.94	1.1461	592.7	
6,000	5.94	1.1461	592.7	0
15,000	6.09	1.1555	605.1	17E-06
25,000	6.38	1.1751	629.8	29E-06
35,000	6.82	1.2084	669.7	44E-06
45,000	7.32	1.2525	719.1	50E-06
55,000	7.62	1.2827	751.4	30E-06
85,000	9.46	1.5621	1019.5	61E-06
93,000	12.9	9.4	7171	430E-06

Table 3.18: Stress intensity factor and rate of crack propagation on I-50 specimen

Cycles	α mm	$F(\frac{\alpha}{b})$	ΔK_I $\frac{N\sqrt{mm}}{mm^2}$	$\frac{d\alpha}{dN}$ $\frac{mm}{cycle}$
0	5.62	1.1274	567.2	
5,000	5.95	1.1467	593.6	66E-06
15,000	6.18	1.1614	612.7	23E-06
25,000	6.39	1.1758	630.7	21E-06
35,000	6.46	1.1808	636.9	7E-06
45,000	6.51	1.1844	641.3	5E-06
65,000	6.64	1.1942	653.0	6.5E-06
80,000	7.00	1.2235	686.9	24E-06
85,000	7.41	1.2613	728.6	82E-06
105,000	8.37	1.3735	843.3	48E-06
121,500	12.9	9.4	7171	275E-06

Table 3.19: Stress intensity factor and rate of crack propagation on J-50 specimen

Cycles	α mm	$F(\frac{\alpha}{b})$	ΔK_I $\frac{N\sqrt{mm}}{mm^2}$	$\frac{d\alpha}{dN}$ $\frac{mm}{cycle}$
0	5.48	1.1198	556.3	
25,000	5.54	1.1230	560.9	24E-06
50,000	5.60	1.1263	565.6	24E-06
100,000	5.70	1.1319	573.5	20E-06
250,000	5.82	1.1389	583.0	8E-06

Table 3.20: Stress intensity factor and rate of crack propagation on K-20 specimen

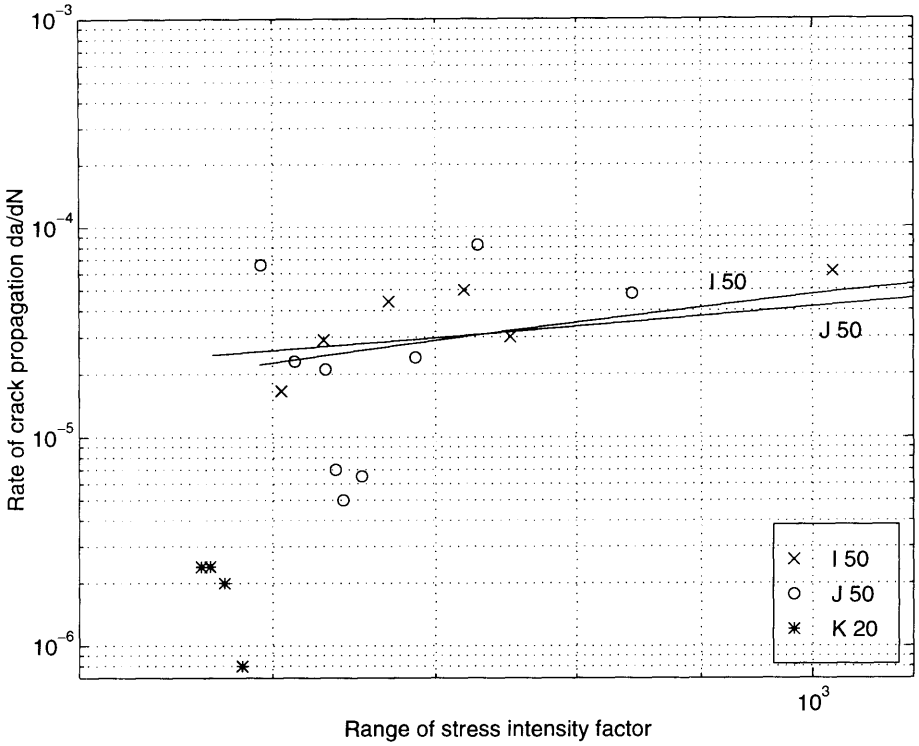

Figure 3-14: Stress intensity factor vs. rate of crack propagation.

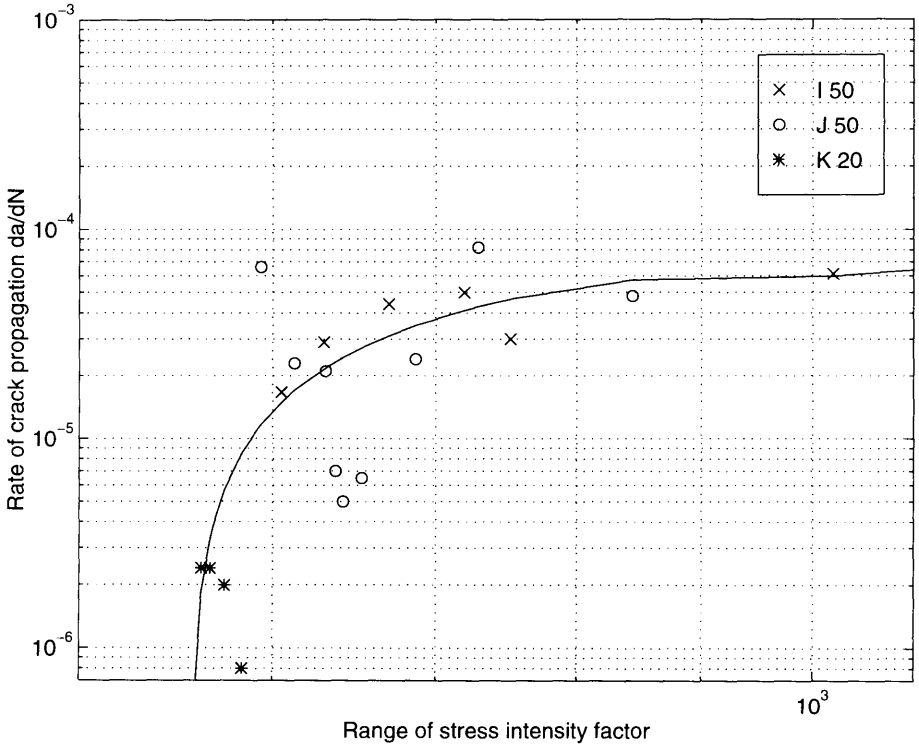

Figure 3-15: Stress intensity factor vs. rate of crack propagation.

3.2.3 Tensile test

The specimens that were subjected to tensile test were identical to those tested in the fatigue test. They were extracted from the restraint cracking specimens after cutting along the LL' RR' and CC' line. The two pieces were welded together to form one symmetric notched specimen as is shown in Figure 3-10.

The ultimate load of each joint is shown in Table 3.21. In order to obtain the ultimate stress, the load was divided by the cross sectional area of the welding, which equals the length of the non-cracked weld metal multiplied by the width of the specimen. The non-cracked weld metal was taken from Table 3.12 and the thickness of the tensile specimen was measured to be $t = 12.85mm$. The ultimate stress is calculated in Table 3.21. The results can be summarized in Table 3.22.

From the results the increase of the joint strength due to the restraint effect became evident. The restraint effect was either due to base metal alone or due to a combination of base metal and the stronger last passes of weld metal.

Spec.	Weld metal	Ultimate force N	Non cracked weld metal mm	Ultimate stress MPa
F 20	E8018 & E8018	106570	5.36	774
F 50	E8018 & E8018	115405	5.13	875
G 20	E8018 & E11018	53766	2.76	758
G 50	E8018 & E11018	73823	3.67	783
H 20	E11018 & E11018	118443	5.27	875
I 20	E8018 & E8018	58218	3.09	733
J 20	E8018 & E11018	87279	3.44	987
K 50	E11018 & E11018	164371	7.02	911
L 20	E8018 & E8018	108363	4.58	921
M 20	E8018 & E11018	153735	6.42	932
M 50	E8018 & E11018	162867	6.43	986
N 20	E11018 & E11018	168062	6.43	1017

Table 3.21: Ultimate load and ultimate stress

Base metal	Weld metal	Spec	Ultimate force N	Non cracked weld metal mm	Ultimate stress MPa	Average ultimate stress
HY-100	E8018 & E8018	F 20	106570	5.36	774	794
		F 50	115405	5.13	875	
		I 20	58218	3.09	733	
	E8018 & E11018	G 20	53766	2.76	758	843
		G 50	73823	3.67	783	
		J 20	87279	3.44	987	
	E11018 & E11018	H 20	118443	5.27	875	893
		K 50	164371	7.02	911	
HY-130	E8018 & E8018	L 20	108363	4.58	921	921
	E8018 & E11018	M 20	153735	6.42	932	960
		M 50	162867	6.43	986	
	E11018 & E11018	N 20	168062	6.43	1017	1017

Table 3.22: Ultimate load and ultimate stress

Chapter 4

Numerical Analysis

4.1 Strength of plate with soft interlayer

The properties of welded plates and round bars including a soft interlayer were first evaluated in an extensive research program in Japan, in the late 1960's. Results from the tensile tests suggested that the strength of the joint approaches that of the base metal, when the thickness of the soft interlayer to the diameter of the bar is sufficiently small [23]. Although these results have been verified both analytically and experimentally, an attempt was made in this study to confirm them using the finite element program ADINA [24].

The materials were modeled as elastic plastic with a liner strain hardening. Their properties are the typical mechanical properties and they are shown in Figure 4-1 and Table 4.1. The ultimate strength value of each material was not incorporated into the model. The stress strain curve does not end at the ultimate strength, but it continues beyond this point. To avoid exceeding this value, the stress on each node of the mesh was examined at the ADINA's output file. Once the equivalent stress at any node was higher than the ultimate strength, it was assumed that the material had failed.

The specimen, which was 150 mm long and 12 mm thick, was simulated by a two dimensional mesh under plane strain condition. Due to symmetry, only one quarter of the cross sectional area of the plate was modeled having length 75 mm and thickness 6 mm. The geometry of the mesh is shown in Fig 4-2 and 4-3. The mesh was subjected to a tensile stress applied at the end of the specimen. This externally applied stress was increased and the displacement at the end of the plate was measured for each loading. The difference of the displacement before and after the load application, divided by one half of the total length (75 mm), represents the overall engineering strain. The externally applied stress and the overall engineering strain was then plotted. The intersection of that stress strain curve, with a 0.2% offset line, gives the joint yield strength.

The value of the overall engineering strain depends on the ratio of the length of the base metal to the length of the weld metal. Consequently, the value of the

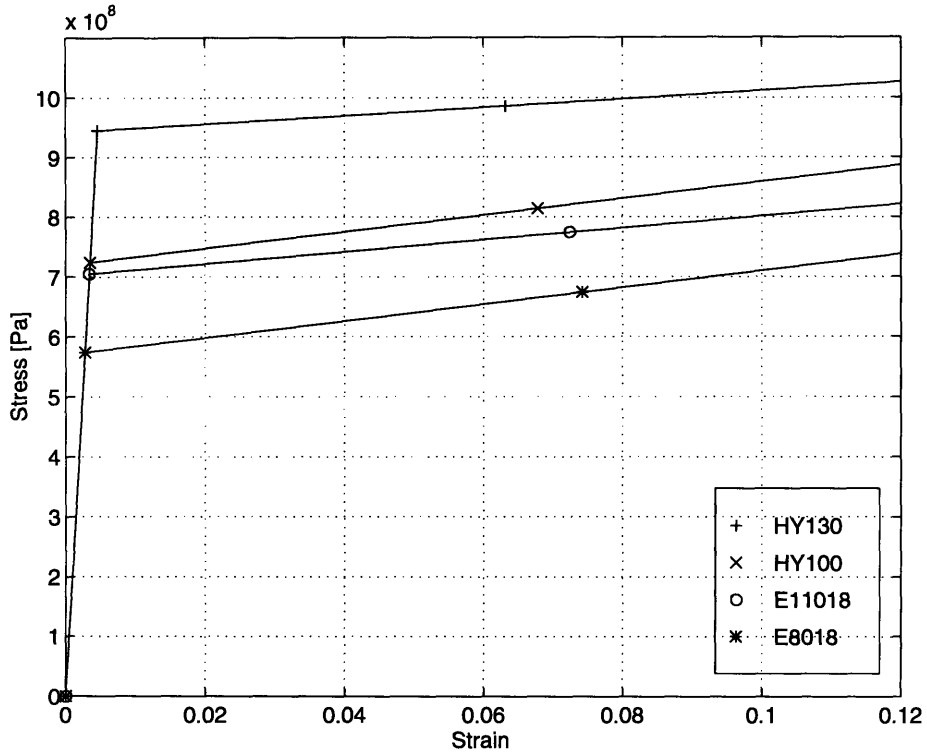

Figure 4-1: Mechanical properties of the materials used in ADINA.

	HY100	HY130	E8018	E110I8
yield stress (0.2% offset)	724 MPa 105 ksi	945 MPa 137 ksi	574 MPa 83.2 ksi	705 MPa 102.3 ksi
ultimate strength	814 MPa 118 ksi	986 MPa 143 ksi	674 MPa 97.7 ksi	774 MPa 112.3 ksi
E	207E9 Pa	207E9 Pa	207E9 Pa	207E9 Pa
Et	1.4E9 Pa	0.7E9 Pa	1.4E9 Pa	1.0E9 Pa

Table 4.1: Mechanical properties used in ADINA

yield strength of the joint also depends on the specimen geometry. However since the purpose of this study is a comparison of different degree of strength matching and joint relative thickness, this method is acceptable.

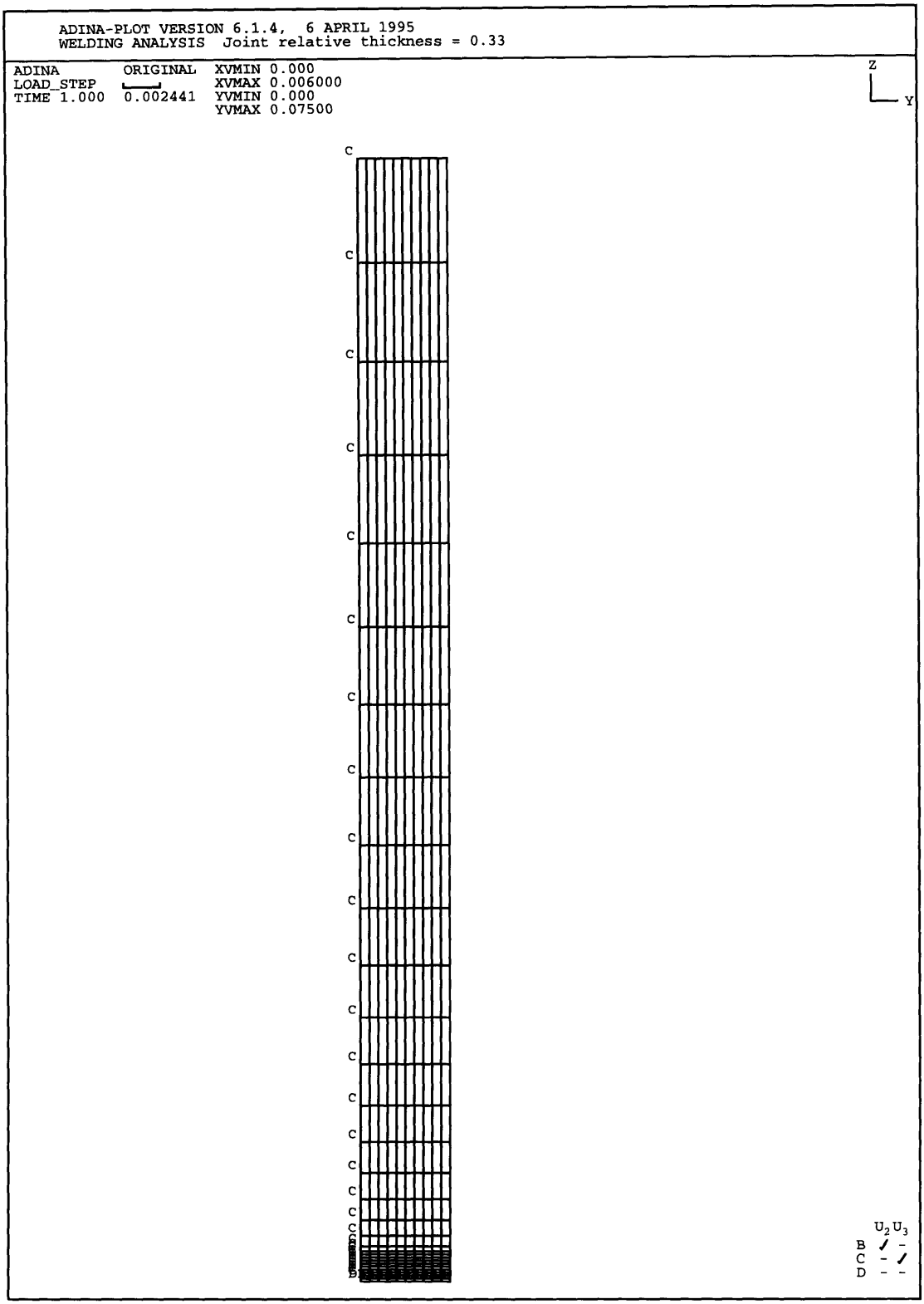

Figure 4-2: Mesh of base metal and soft interlayer. The relative thickness is RT=0.33.

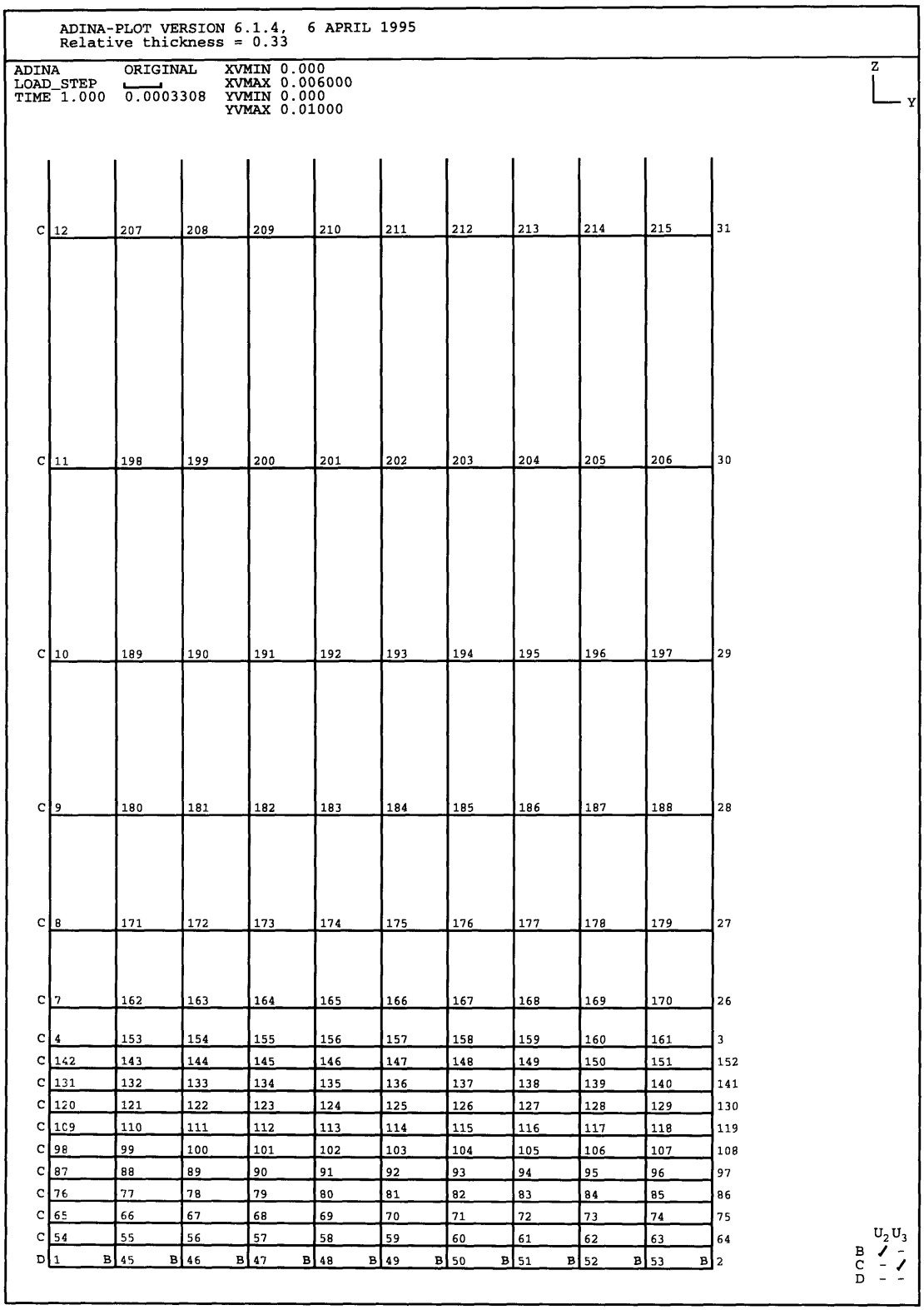

Figure 4-3: Mesh and nodes on base metal and soft interlayer. The relative thickness is RT=0.33.

Numerical procedure and results

To examine different degrees of strength mismatch, the following combinations were performed:

Base metal	Weld metal	Degree of undermatching
HY-100	E8018	20%
HY-130	E8018	40%
HY-130	E11018	25%

In each case, the relative thickness of the joint was changed, which resulted in a different stress strain curve. Results are shown in Figure 4-4, 4-5 and 4-6. Detailed results are given in Appendix B.

After each run of the ADINA program, the mesh was examined in order to determine the value and the location of the maximum equivalent effective stress. This was done on two cross sections. The first was in the middle of the soft interlayer along the line from node 1 to node 2 (Figure 4-3), and the other was in the base metal, next to the soft interlayer, along the line from node 3 to node 4. In the ADINA program this cross section has ten elements. Each element was examined to determine if the deformation was elastic or plastic.

As the load was increased, the equivalent effective stress on each element was increased. The first element that reached yielding was the element in the center of the soft metal. Even when the total section along the line from node 1 to node 2 had reached yielding, the specimen continued to deform almost elastically, especially if the joint thickness was small. From Figures 4-4, 4-5 and 4-6 it is obvious that for very small joint thickness, the yielding is delayed until the base metal reaches yielding. As the joint thickness increases, this delayed phenomenon is not so intense, but still the soft metal starts to deform plastically at values of equivalent effective stress well above its yield strength. This phenomenon is due to the restrain effect that the strong base metal provides on the soft weld metal.

To evaluate the effect of the strength matching, these curves were compared to the stress strain curve of a specimen having base metal the same material as the weld metal. In that case the specimen was homogeneous and there was no restraint effect.

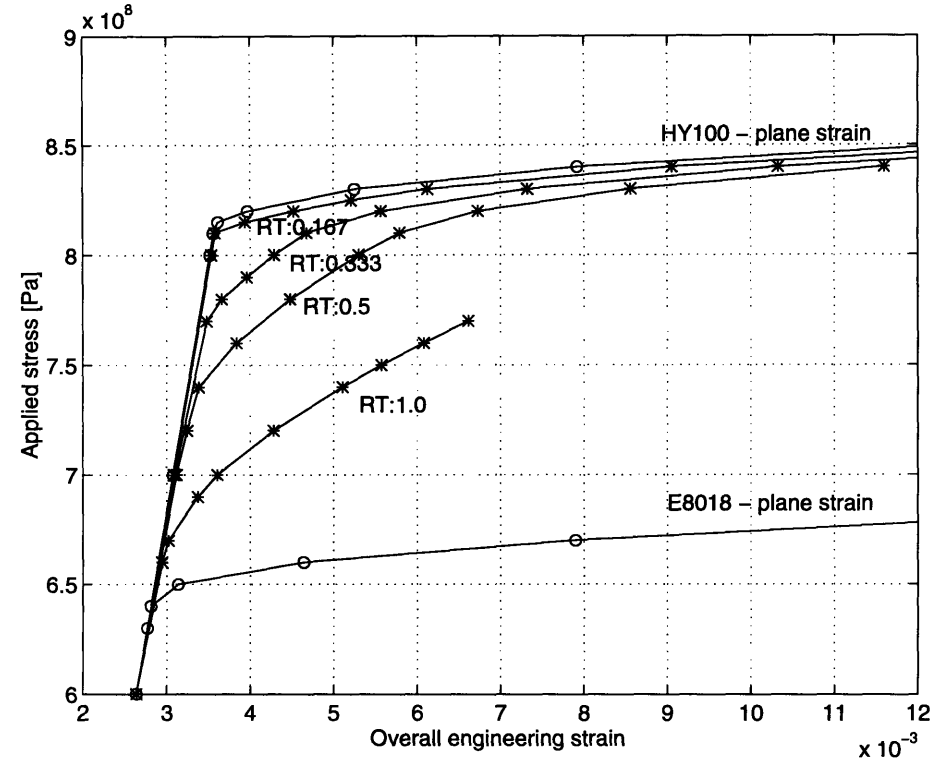

Figure 4-4: Stress strain behavior of a joint on HY-100 base metal as a function of the relative thickness of the soft interlayer E8018.

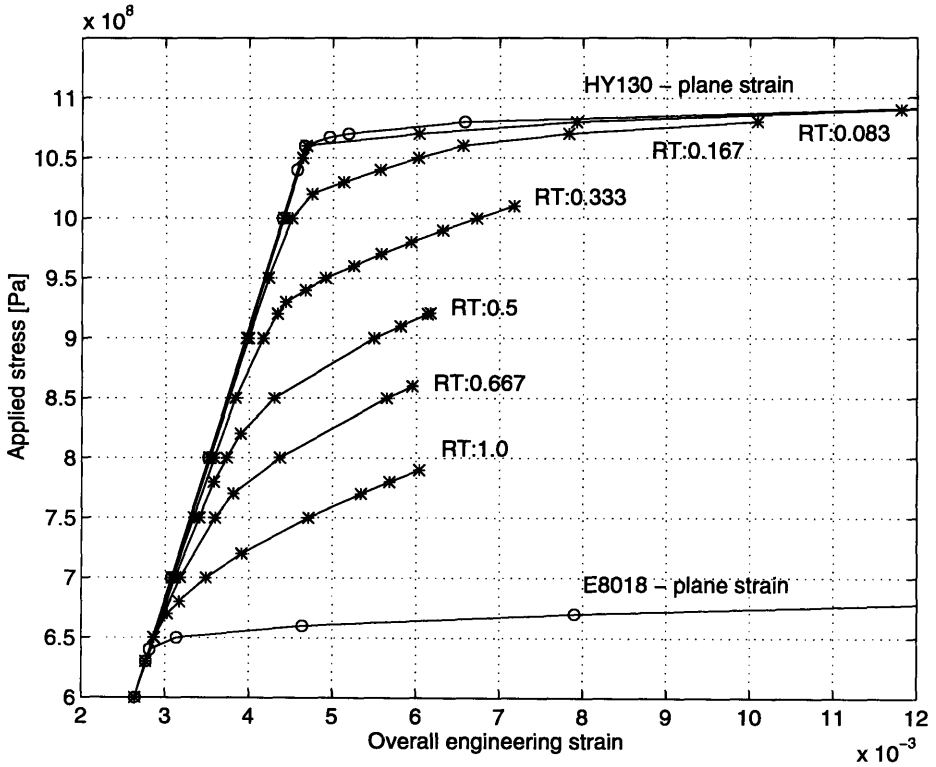

Figure 4-5: Stress strain behavior of a joint on HY-130 base metal as a function of the relative thickness of the soft interlayer E8018.

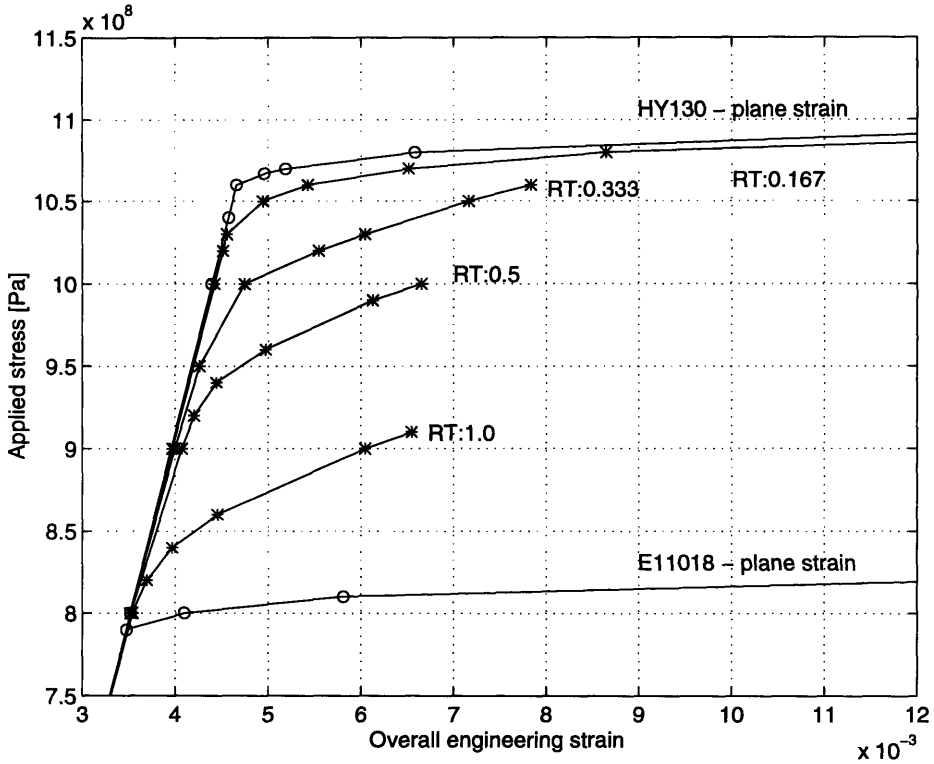

Figure 4-6: Stress strain behavior of a joint on HY-130 base metal as a function of the relative thickness of the soft interlayer E11018.

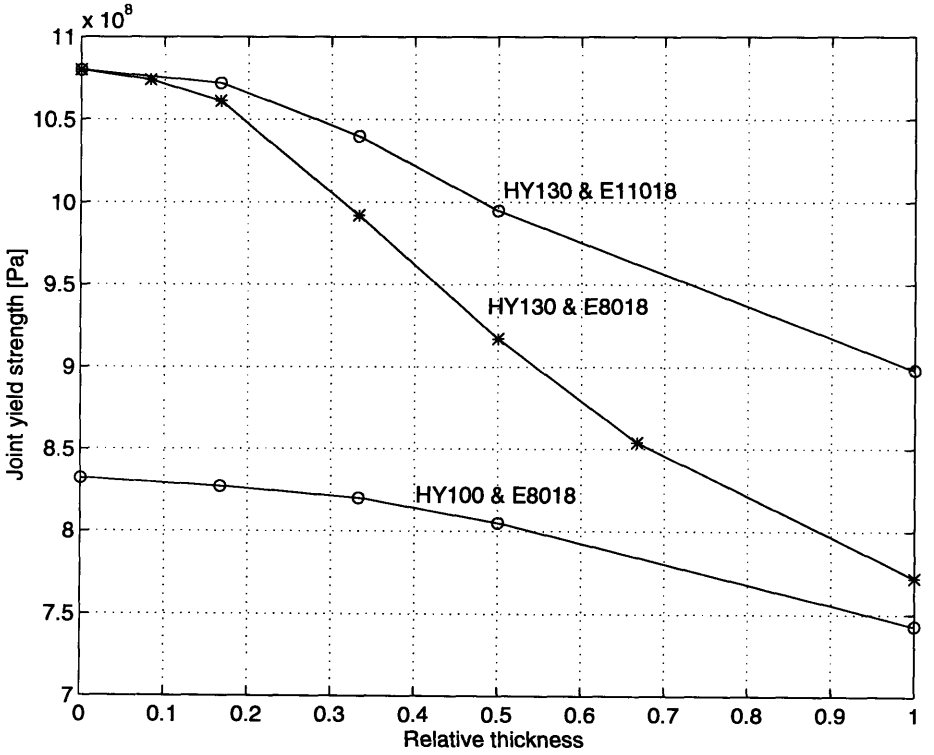

Figure 4-7: Joint tensile strength as a function of the relative thickness of the soft interlayer.

Relative thickness	Joint yield strength [MPa]	Strength elevation
∞	661	1.00
1.0	743	1.12
0.5	805	1.22
0.33	820	1.24
0.17	827	1.25
0	832	1.26

Table 4.2: Joint yield strength and the joint strength elevation of the E8018 weld metal due to HY-100 base metal

Relative thickness	Joint yield strength [MPa]	Strength elevation
∞	661	1.00
1.0	772	1.17
0.67	854	1.29
0.5	917	1.39
0.33	992	1.50
0.17	1061	1.60
0.08	1074	1.62
0	1080	1.63

Table 4.3: Joint yield strength and the joint strength elevation of the E8018 weld metal due to HY-130 base metal

These curves are the E8018 and E11018 under plane strain condition and they are shown in Figures 4-4, 4-5 and 4-6. They represent a very large relative thickness.

As the relative thickness decreases, the strength of the joint increases and finally gets its maximum value when the relative thickness is zero. This is shown by the curve of HY-100 and HY-130 under plane strain.

By drawing a 0.2% offset line on Figures 4-4, 4-5 and 4-6, we get the joint yield strength. The results are in Figure 4-7 and in Tables 4.2, 4.3 and 4.4. Figure 4-7 demonstrates that as the relative thickness becomes smaller, the tensile properties of the material become similar to those of the base metal.

Relative thickness	Joint yield strength	Strength elevation
∞	809	1.00
1.0	898	1.11
0.5	995	1.23
0.33	1040	1.29
0.17	1072	1.32
0	1080	1.33

Table 4.4: Joint yield strength and the joint strength elevation of the E11018 weld metal due to HY-130 base metal

Material	Yield strength MPa	Plane strain yield strength MPa	Joint yield strength from ADINA MPa
HY-100	724	815	832
HY-130	945	1064	1080
E8018	574	645	661
E11018	705	793	809

Table 4.5: Comparison of yield strength and the joint strength of HY-100, HY-130, E8018 and E11018 alone, under plane strain

To verify these results, the yield strength of each metal under plane strain was compared to its joint yield strength calculated by ADINA. For example, the yield strength of the E8018 is given in Table 4.1 as 574 MPa. Due to the plane strain effect the material will yield at $574 * 1.125 = 646$ MPa, which is very close to the joint yield strength at very large joint thickness 661 MPa (Table 4.2). Also the yield strength of the HY-100 is given in Table 4.1 as 724 MPa, and under plane strain condition it yields at $724 * 1.125 = 815$ MPa. This agrees with the joint yield strength at zero joint thickness which is 832 MPa. The comparison is in Table 4.5.

ADINA input files, quantitatively results and plots of the original and deformed models on each case are in appendix B.

4.2 Strength of restraint cracking test specimen

The same procedure applied at the previous section was used to examine the behavior of a joint having the geometry of the self restraint specimen after the welding. The examined specimen consisted of two cross sections of the test specimen. The boundary conditions imposed on the mesh (Figures 4-8 and 4-9) denote that the other cross section is the mirror image of the first. Together they form a 10 mm notch in the middle of the specimen.

Another assumption made was that no bending existed after the welding and that the only heterogeneity was due to the degree of strength matching. Only one mesh geometry was examined; therefore, the relative thickness of the material was held constant.

The material was modeled as elastic plastic with linear strain hardening up to the ultimate strength, and totally plastic with no hardening after that point (Figure 4-10).

To examine different degrees of strength mismatch, the following combinations were performed:

Base metal	Weld metal	Degree of undermatching
HY-100	E8018	20%
HY-130	E8018	40%
HY-130	E11018	25%

The mesh was subjected to a tensile stress applied at its end. The difference of the displacement, measured at the end of the plate before and after the load application, divided by the total length of both weld and base metal (150 mm), is the overall engineering strain. The externally applied load and the overall engineering strain was then plotted. The intersection of that stress strain curve with a 0.2% offset line gives the yield strength of the joint. The equivalent plastic strain is the accumulative effective plastic strain and it is given by:

$$AEPS = \int_0^t d\bar{\varepsilon}^p$$

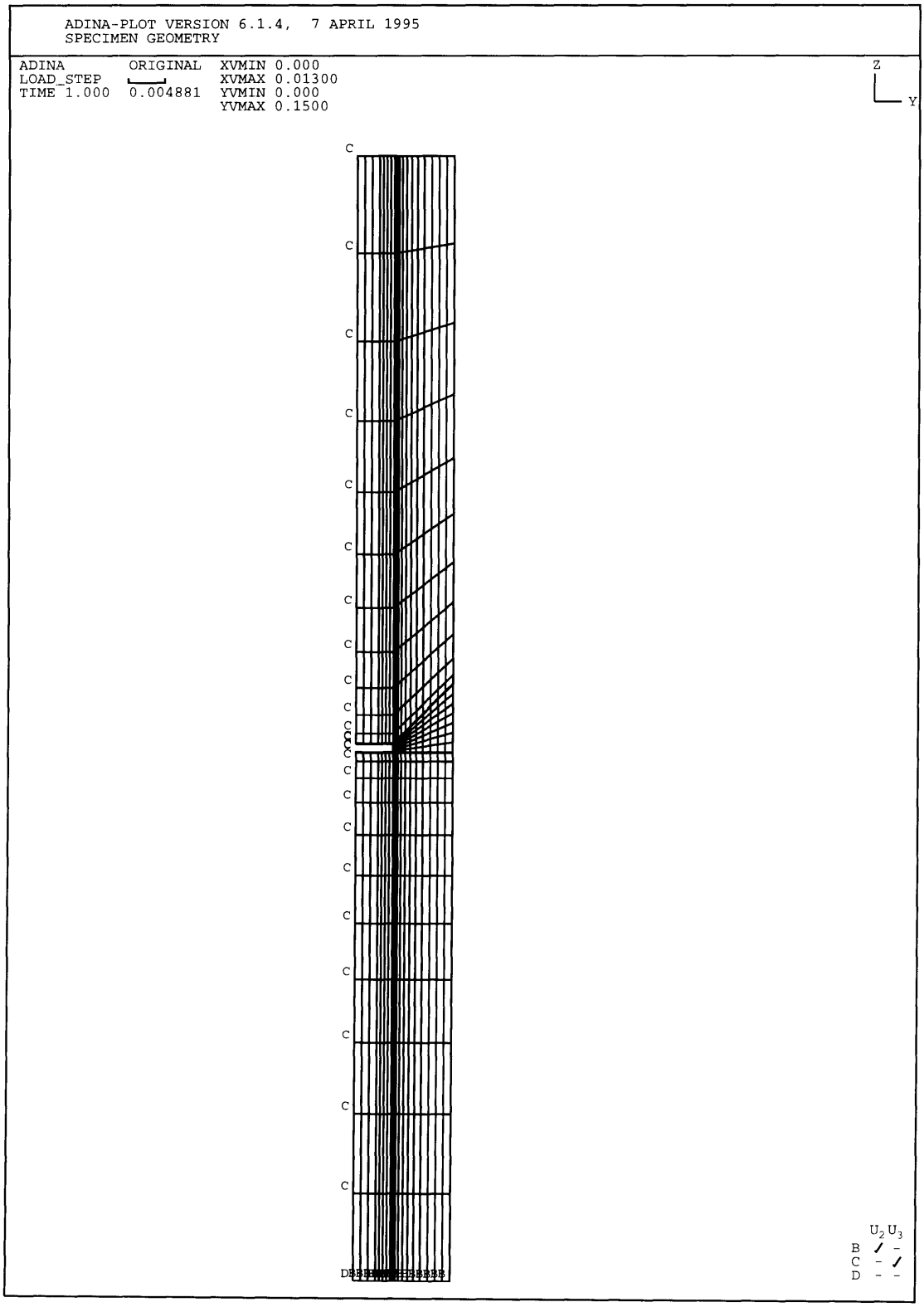

Figure 4-8: Mesh of the specimen

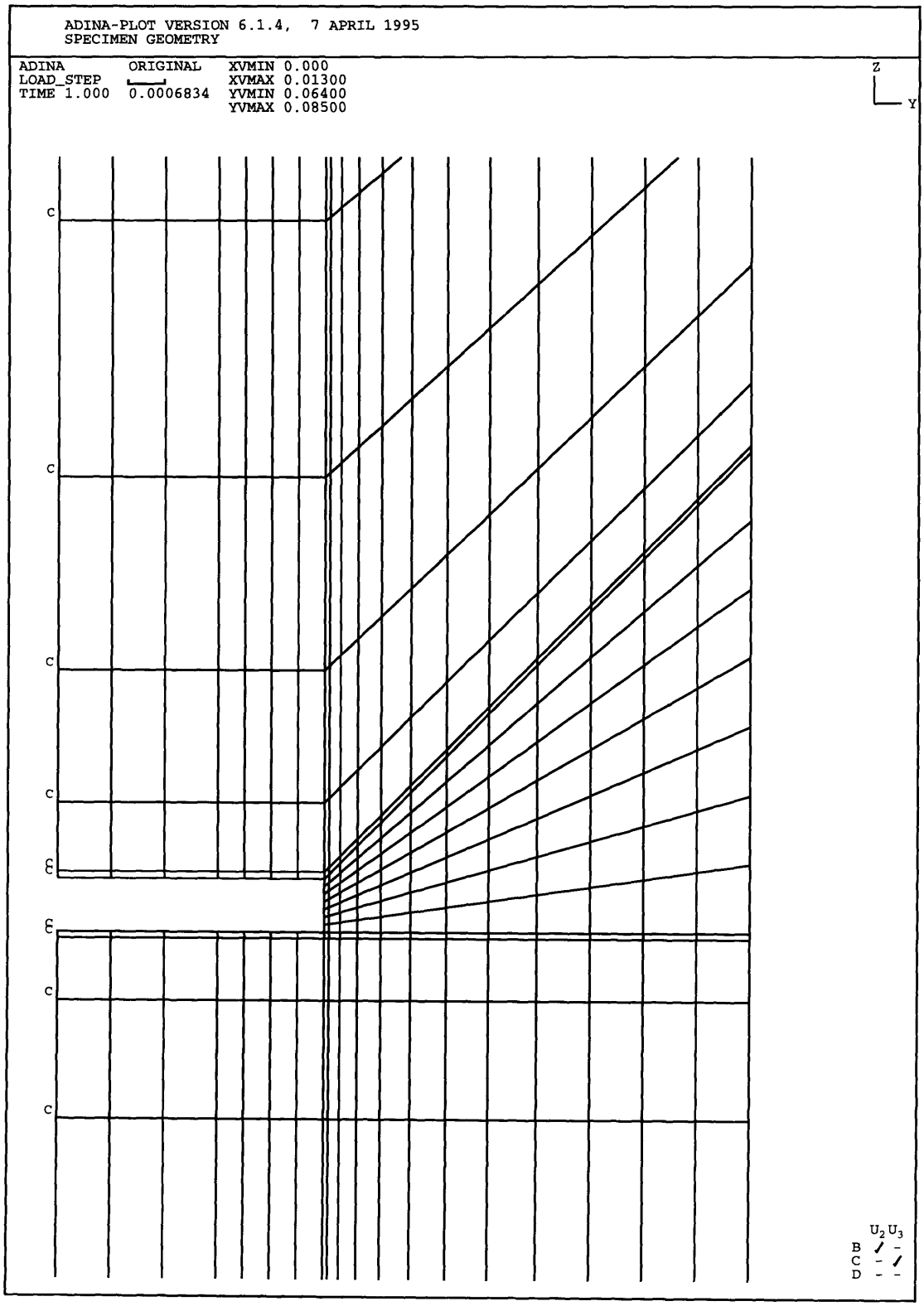

Figure 4-9: Mesh of the specimen around the notch

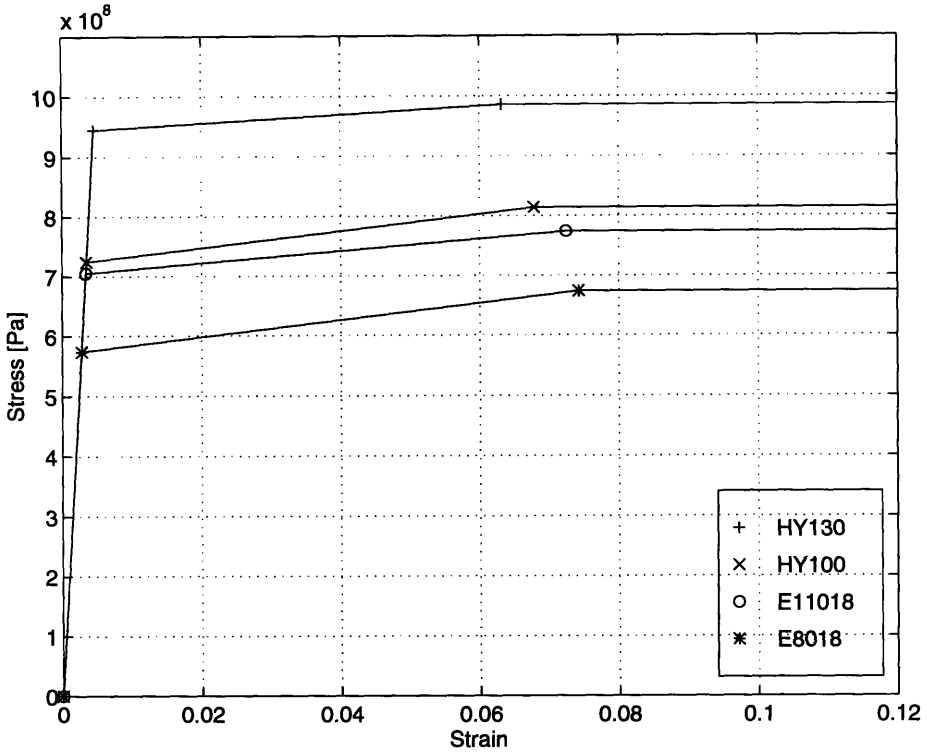

Figure 4-10: Mechanical properties of the materials used in ADINA.

where

$$d\bar{e}^p = \sqrt{\frac{2}{3} d\bar{e}^p_{ij} d\bar{e}^p_{ij}}$$

The equivalent stress σ_e is the von Mises effective stress:

$$\sigma_e = \sqrt{\frac{1}{2}\{(\sigma_x - \sigma_y)^2 + (\sigma_y - \sigma_z)^2 + (\sigma_z - \sigma_x)^2 + 6({\sigma_{xy}}^2 + {\sigma_{yz}}^2 + {\sigma_{xz}}^2)\}}$$

Results

The tip of the notch is the area that demonstrates high stress concentration, early yielding and elevated strains. However, by using the material model shown in Figure 4-10, the equivalent stress at the tip of the notch cannot exceed the ultimate strength of the material. So the only concern is the plastic strain.

To determine the behavior of the joint, the overall engineering strain and the accumulative effective plastic strain was recorded for each applied load. Figures 4-11 and 4-13 show the overall engineering strain versus the applied stress. The maximum value of the accumulative effective plastic strain was observed at the tip of the notch. This value is plotted against the applied stress in Figures 4-12 and 4-14.

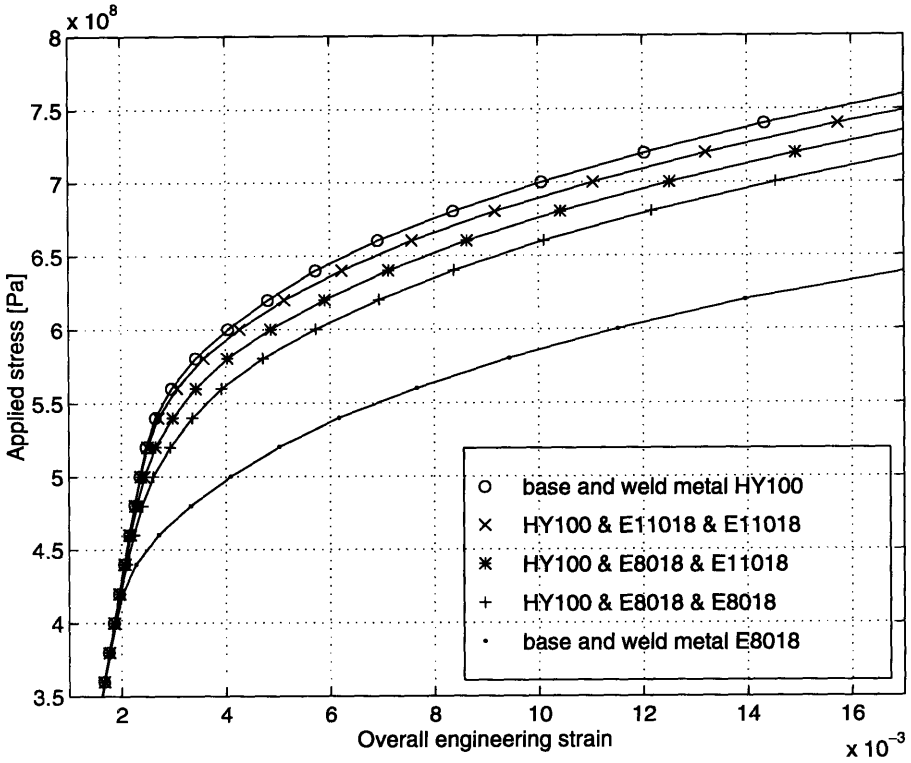

Figure 4-11: Stress strain behavior of a notched joint on HY-100 base metal as a function of the material of the weldment.

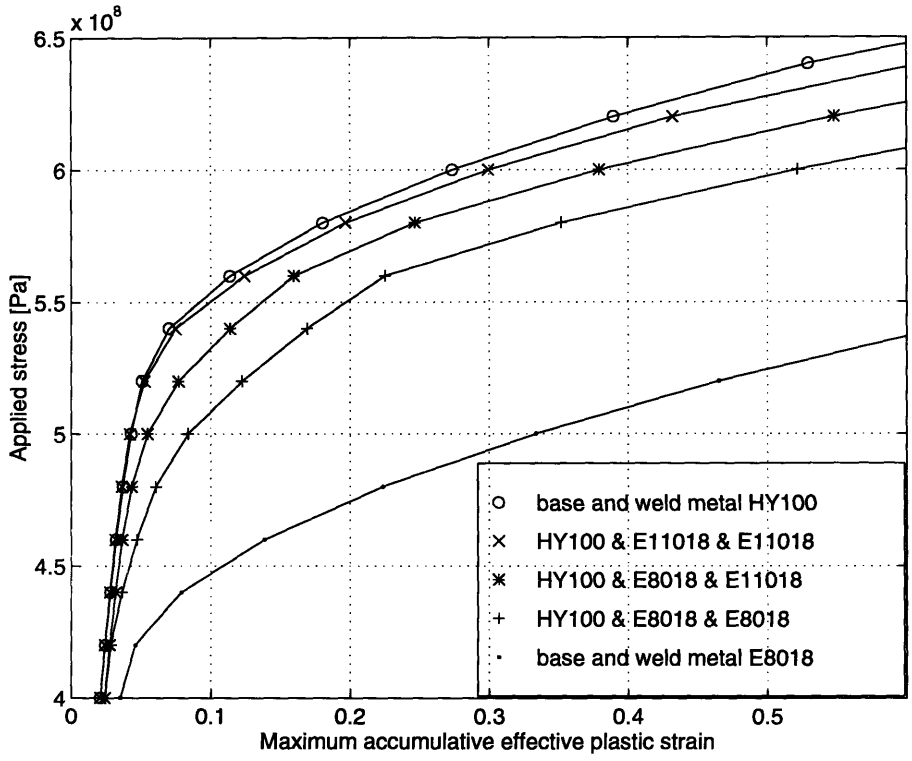

Figure 4-12: Accumulative effective plastic strain against applied load.

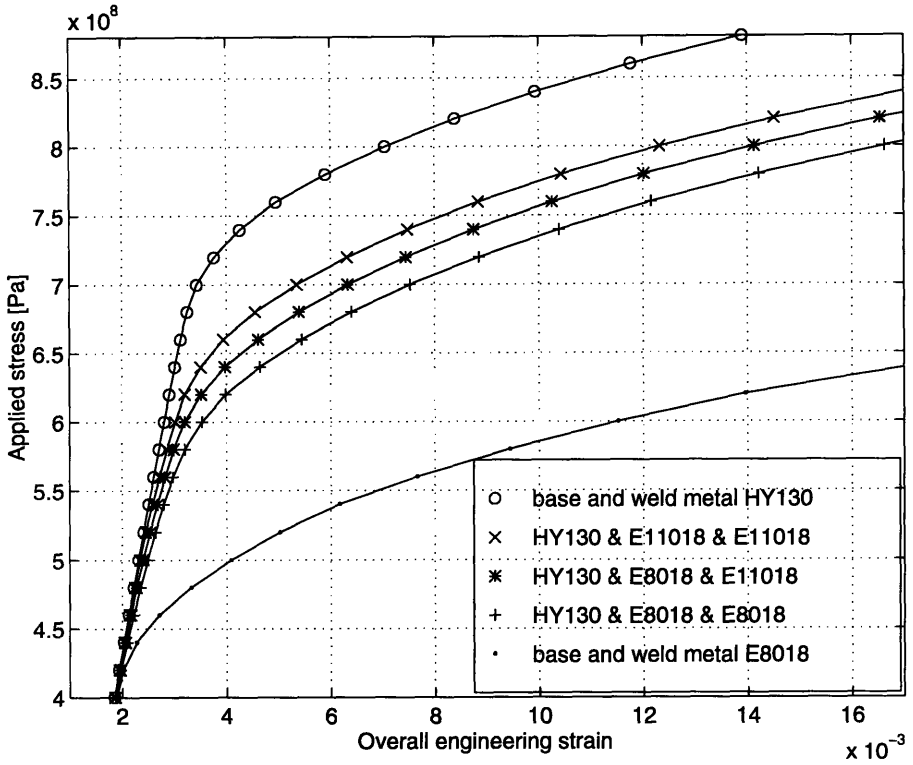

Figure 4-13: Stress strain behavior of a notched joint on HY-130 base metal as a function of the material of the weldment.

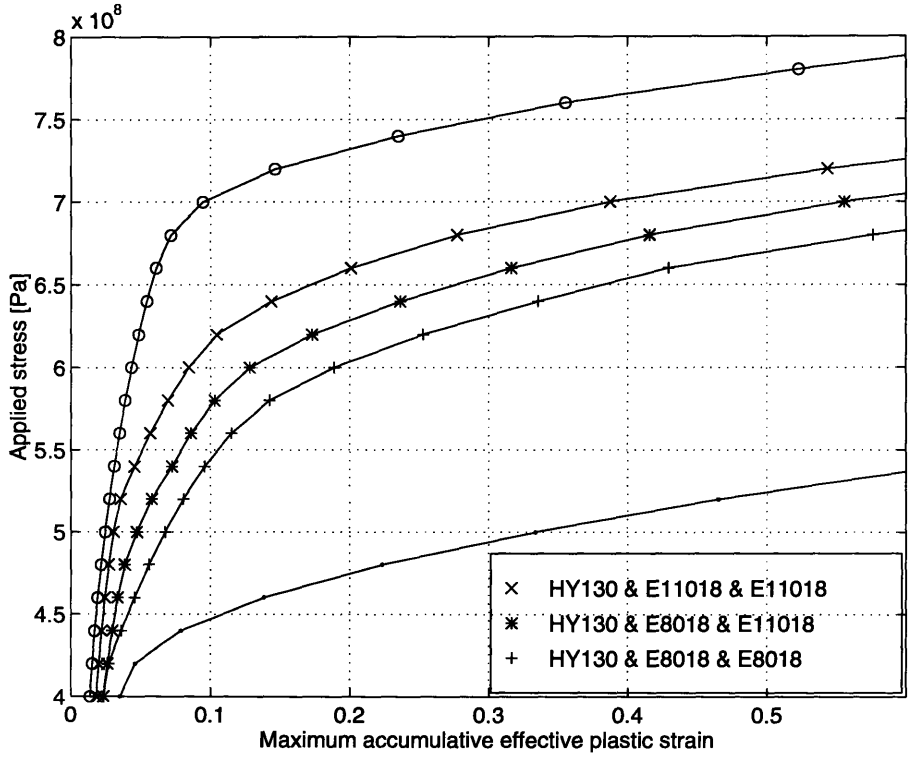

Figure 4-14: Accumulative effective plastic strain against applied load.

The joint yield strength was obtained from the intersection of the curves from Figures 4-11 and 4-13 with the 0.2% offset line. The effective plastic strain at the tip of the notch was between 0.35 and 0.46 and was obtained from Figures 4-12 and 4-14 using the joint yield strength. Results are in Table 4.6. That method resulted in large values of effective plastic strain. For more reasonable results, it was assumed that the specimen will collapse once the equivalent plastic strain at any element at the tip of the notch reaches the maximum elongation that the material located at the root of the notch can withstand. The elongation of the E8018 was taken 0.24, of the E11018 0.22, of the HY-130 0.25 [25] and of the HY-100 was assumed to be 0.25.

Imposing these values at the tip of the notch, the applied stress was found from Figures 4-12 and 4-14. This value is the the ultimate stress of the joint. The results are in Table 4.7. The joint ultimate stress was then normalized at the notched cross section area, assuming uniform stress distribution. The thickness of the specimen was $13mm$ while the thickness at the notch was $8mm$.

Stress distribution

To observe the distribution of the equivalent stress and the effective plastic strain on the specimen, the mesh was subjected to its joint ultimate stress (Table 4.7). The plots are in Appendix B.

As expected, the distribution of the effective plastic strain on all those plots is similar, having the maximum value at the tip of the notch. This maximum value is the elongation that the material located at the root of the notch can withstand. By examining the stress distribution around the notch, it is clear that the softer material has reduced stresses. For similar distribution of plastic deformations, the E11018 shields the soft E8018 that is located at the root, by reducing its stresses. Thus the stress concentration at the tip of the notch is also reduced.

Although the applied stresses were not equal, the difference in the stress between an evenmatched weld and an evenmatched having a softer material at the root of the weld is very small. Thus it can be assumed that the strength reduction is not significant.

Base and weld metal	Joint yield strength [MPa]	Effective plastic strain	Normalized strength [MPa]
HY-100	622	0.46	1011
HY-100&E11018&E11018	614	0.37	998
HY-100&E8018&E11018	598	0.38	972
HY-100&E8018&E8018	580	0.38	943
E8018	506	0.37	822
HY-130	773	0.40	1256
HY-130&E11018&E11018	697	0.39	1133
HY-130&E8018&E11018	673	0.37	1094
HY-130&E8018&E8018	650	0.35	1056
E8018	506	0.37	822

Table 4.6: Joint yield strength, effective plastic strain and normalized strength of the joint using the 0.2% offset line

Base and weld metal	Effective plastic strain	Joint ultimate strength [MPa]	Normalized ultimate strength [MPa]
HY-100	0.25	595	967
HY-100&E11018&E11018	0.22	584	949
HY-100&E8018&E11018	0.24	579	941
HY-100&E8018&E8018	0.24	562	913
E8018	0.24	484	787
HY-130	0.25	743	1207
HY-130&E11018&E11018	0.22	665	1081
HY-130&E8018&E11018	0.24	641	1042
HY-130&E8018&E8018	0.24	616	1001
E8018	0.24	484	787

Table 4.7: Ultimate strength of the joint

4.3 Degree of restraint of the cracking test specimen

The degree of restraint of the self restraint specimen was examined using ADINA. The mesh used is shown in Figure 4-15. The load was applied at the notch perpendicular to the welding direction. One quarter of the specimen was modeled due to symmetry and ignoring the groove geometry. Only a 9 mm gap was considered.

The maximum displacement was measured at the middle of the groove at the node 8 (Figure 4-16) , and its value was plotted versus the applied load (Figure 4-17).

From the experimental results in this study, no specimen was found having maximum displacement at the node 8 higher than 0.2 mm. Up to that value, the curve is linear and the degree of restrain is constant. The degree of restrain k_s is equal to the ratio of the uniform applied stress divided by the the mean value of the displacement $[u]$. Since $[u] \approx 0.85u$

$$k_s = 1.61E12\frac{N/m^2}{m}$$

This result verifies the analytical result from equation 2.7 where

$$k_s = 1.647E12\frac{N/m^2}{m} = 168\frac{kg/mm^2}{mm}$$

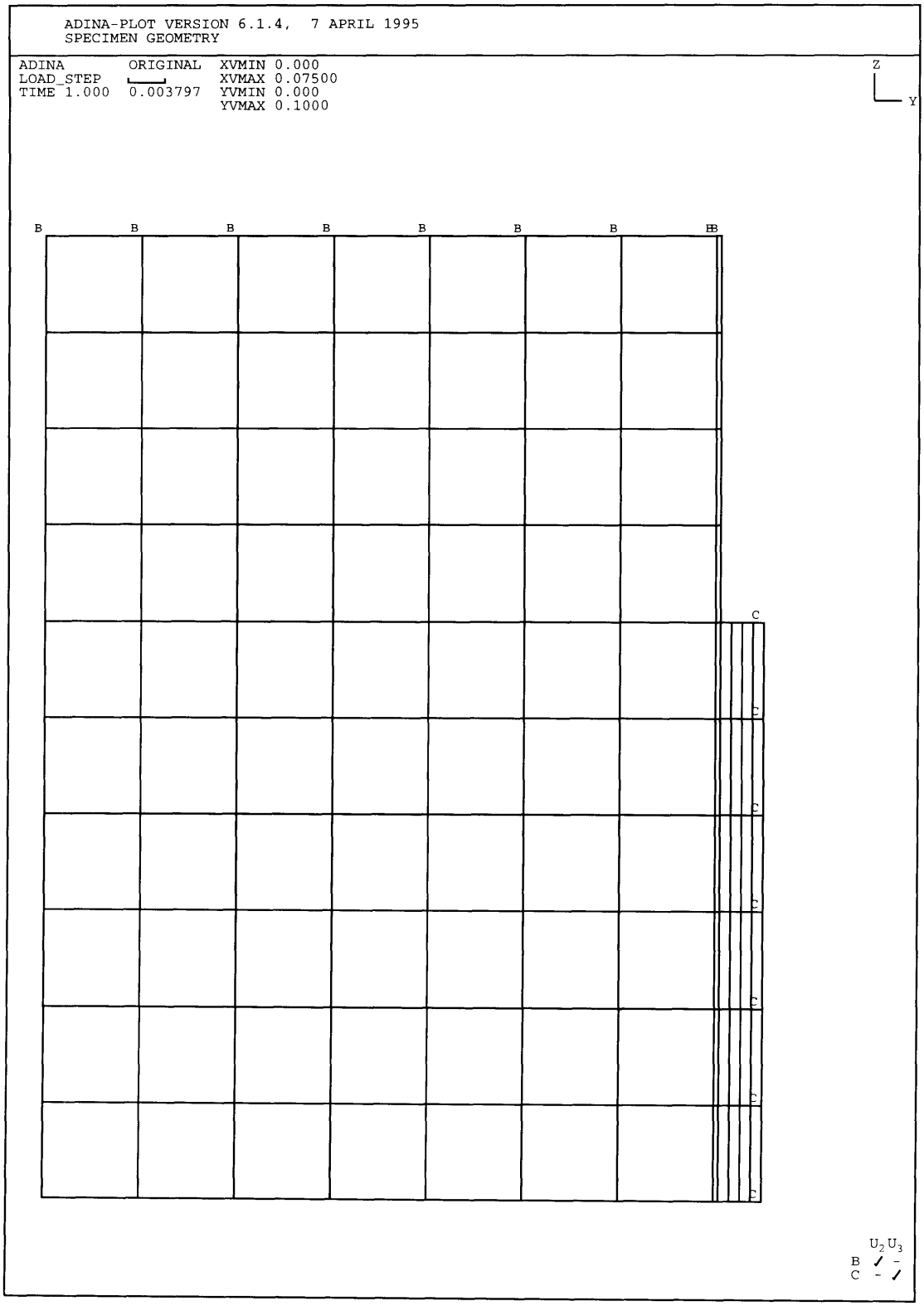

Figure 4-15: Mesh of the specimen for the k_s calculation

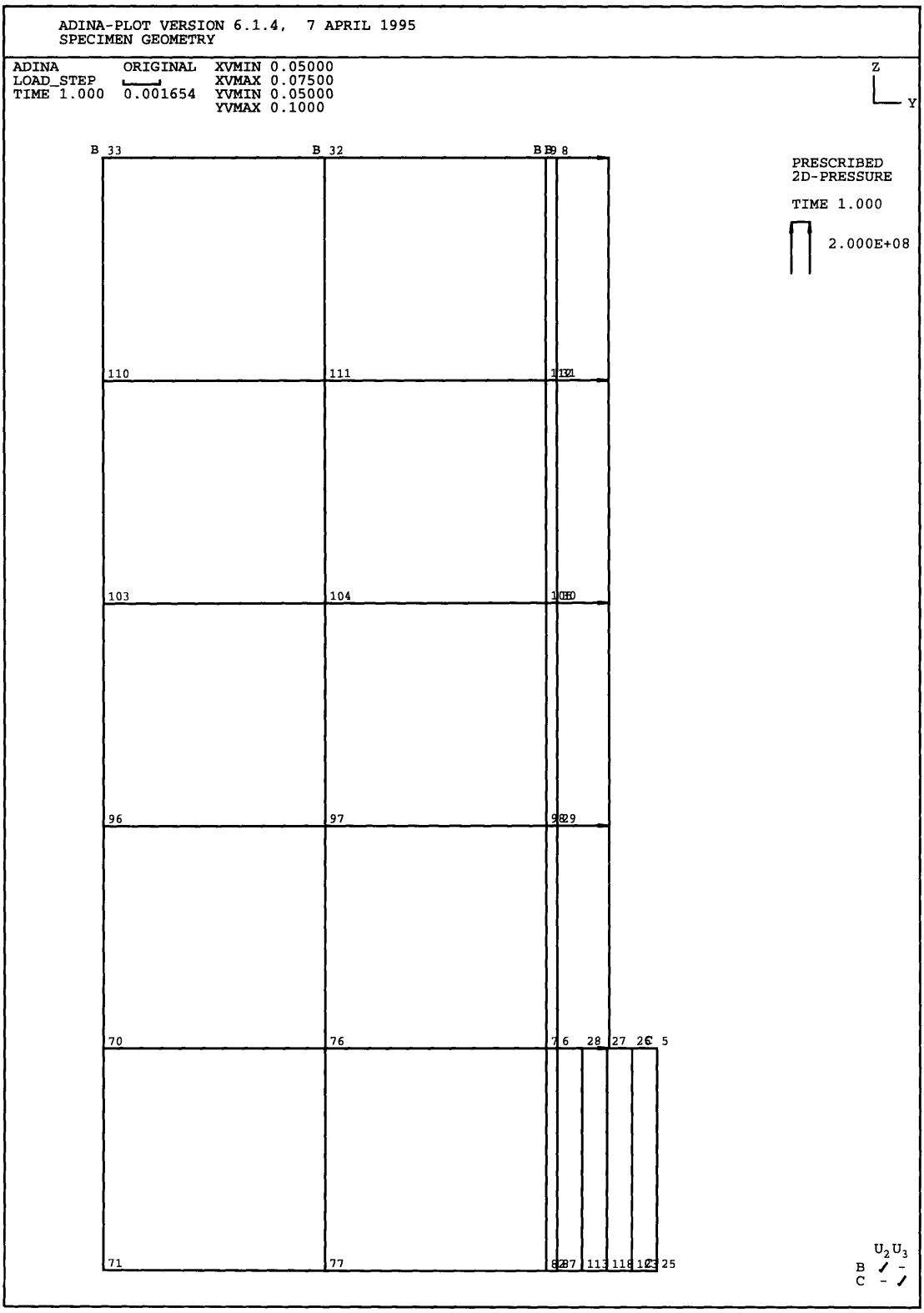

Figure 4-16: Mesh and nodes of the specimen for the k_s calculation

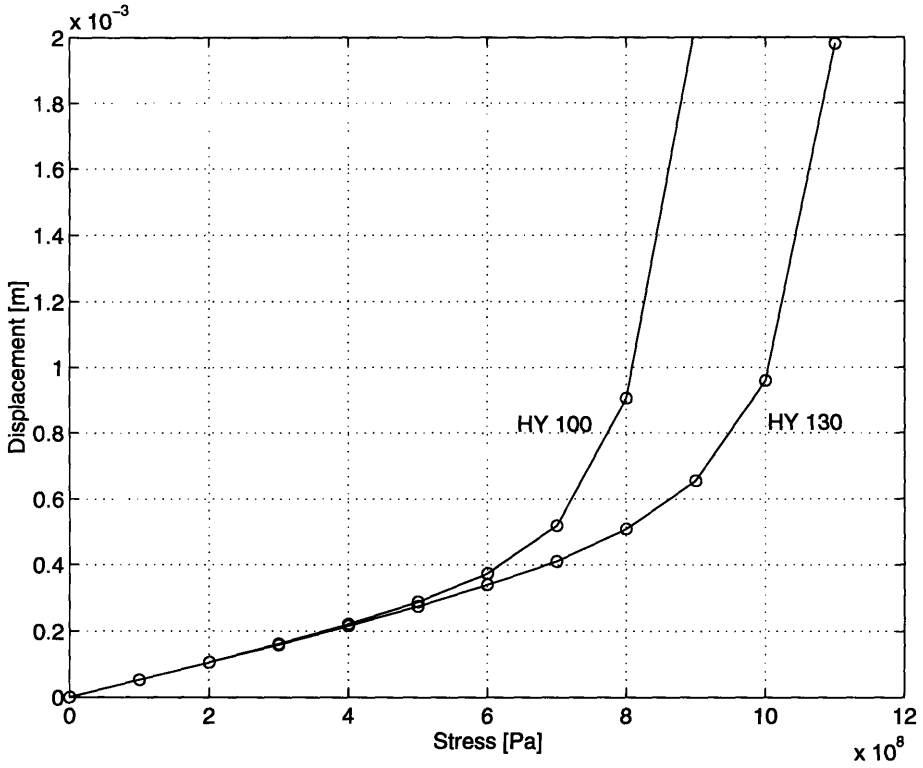

Figure 4-17: Degree of restraint of the self restraint cracking specimen.

Chapter 5

Discussion and Conclusions

The effect of undermatched welds on cold cracking

One of the expected results from the restraint cracking test is that the minimum required preheat temperature to avoid cold cracking can be reduced by applying undermatched weld at the root of the welding. However, these results were not observed in this study. The main reason is that the E8018B2L covered electrode does not have the improved fracture toughness as it was expected, considering its lower strength. As a result, the joint did not have the ability to allow the large plastic deformations required to compensate the lower yield strength.

The expected results were confirmed by another experiment made on HT-80 steel and welded by ER70S-G, ER80S-G and ER110S-G [26]. The welding process was Gas Metal Arc and the shielding gas was CO_2. The diameter of the solid welding wire was 1.2 mm. The specimen was similar to those used in this study, with a single bevel groove. The thickness of the specimen was 32 mm. The preheating temperature was 20 ^{o}C, 50 ^{o}C and 100 ^{o}C. In that experiment, no crack was initiated at the root of the undermatched weld after the first pass, making clear that preheating is not necessary to prevent crack initiation. The evenmatched welds applied at the root of the weld required a preheat temperature of more than 100 ^{o}C to prevent cold cracking. It is known that the HT-80 steel has a minimum preheat temperature of 125 ^{o}C. Therefore, the minimum preheat temperature required to prevent crack initiation at the root of

the first pass for undermatched welds was at least 95 °C lower than that required for evenmatched welds.

Increase of the weld strength due to restraint effect

The increase of the weld strength was confirmed by both the tensile strength experiment, and the numerical analysis and the results can be summarized in the following table. The stresses are normalized on the notched cross section of the weld, assuming uniform distribution.

Base metal	Weld metal	Numerical analysis [MPa]	Experimental analysis [MPa]
HY-100	E8018&E8018	913	794
	E8018&E11018	941	843
	E11018&E11018	949	893
HY-130	E8018&E8018	1001	921
	E8018&E11018	1042	960
	E11018&E11018	1081	1017

Although the results are not exactly the same for each case, they demonstrate the same behavior. The soft weld joint does not behave as the unrestrained weld metal. Its strength properties are much elevated and depend on the restraint of the base metal and the surrounding weld metal. As the relative thickness of the joint decreases, the restraint effect increases, and therefore the strength properties of the joint increase. For a very small relative thickness, the soft weld metal has similar properties to the base metal.

Effect of undermatched welds on stress distribution

By examining the stress and strain distribution plots from the numerical analysis, it is clear that for similar distribution of plastic deformations, the E11018 shield the soft first pass made with E8018 by reducing its stresses. Thus the stress concentration at the tip of the notch is also reduced.

Effect of undermatched welds on fatigue strength

All the data from the fatigue test are concentrated on one typical fatigue curve. Therefore undermatched welds have the same fatigue characteristics as the evenmatched welds. The discrepancy among the three specimens were due to the fact that the weld penetration at the root of the weld was not the same. If all the specimens had exactly the same dimensions the fatigue life of all of them was expected to be almost the same.

Conclusion

The following conclusions can be made from this study:

- The required preheat temperature to avoid cold cracking at high strength steels can be reduced by applying undermatched welds at the root of the welding. The strength performance of the joint does not decrease significantly, given that the softer material has adequate fracture toughness to compensate the large plastic deformations.

- The soft weld joint does not behave as the weld metal alone. Its strength properties are much elevated due to the restraint effect of both the base metal and the stronger surrounding weld metal. These results were confirmed by both experimental and numerical analysis.

- When a evenmatched joint with soft first pass is subjected to its ultimate load, it exhibits stresses that are lower at the tip of the notch, than those exhibited at an evenmatched weld joint without the soft pass, under its ultimate load. Thus the tendency for crack initiation is reduced.

- The crack propagation rate during fatigue test does not depend on the strength of the material at the crack tip.

Appendix A

Crack observation

After the first and last pass of welding and during the fatigue test the specimens were observed for cracks, using an optical microscope and a helium-neon confocal laser microscope. The pictures from this observation are in the following pages.

To scale the size of the cracks, the following table gives the vertical and horizontal length of each photograph taken with the laser microscope according to the magnification of the lens.

Magnification	Horizontal length	Vertical length
	mm	mm
X 5	0.900	0.650
X 10	0.450	0.325
X 20	0.225	0.165
X 40	0.115	0.082

A.1 Crack observation after the first pass of welding

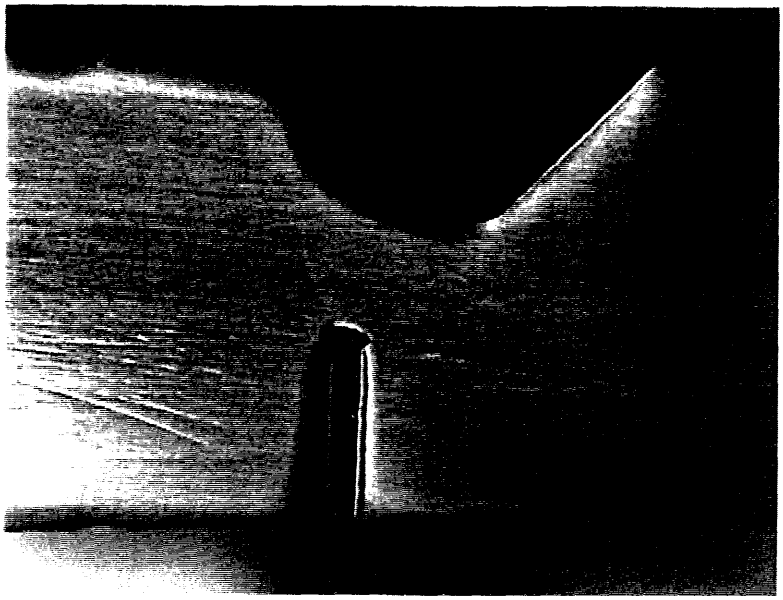

HY-100 F20, CL side, 1.35 mm root crack.

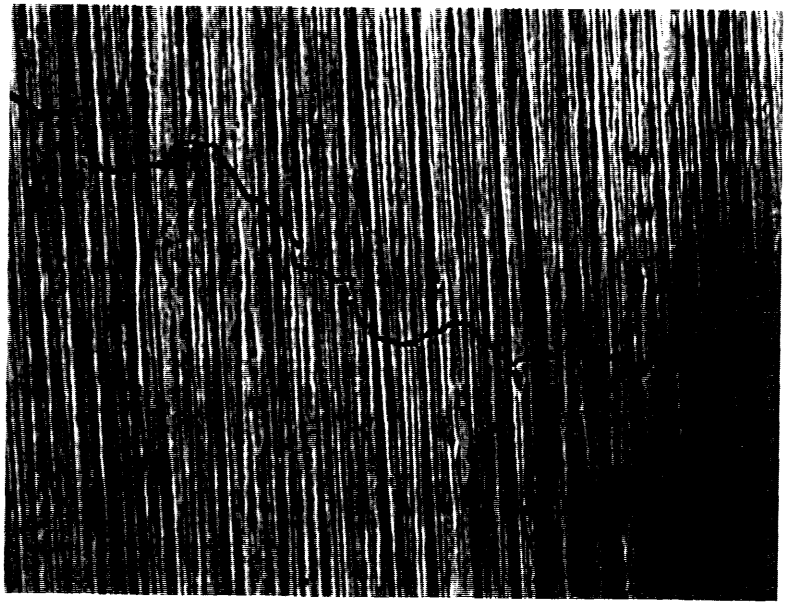

HY-100 F20, CL side, 1.35 mm root crack, x 20

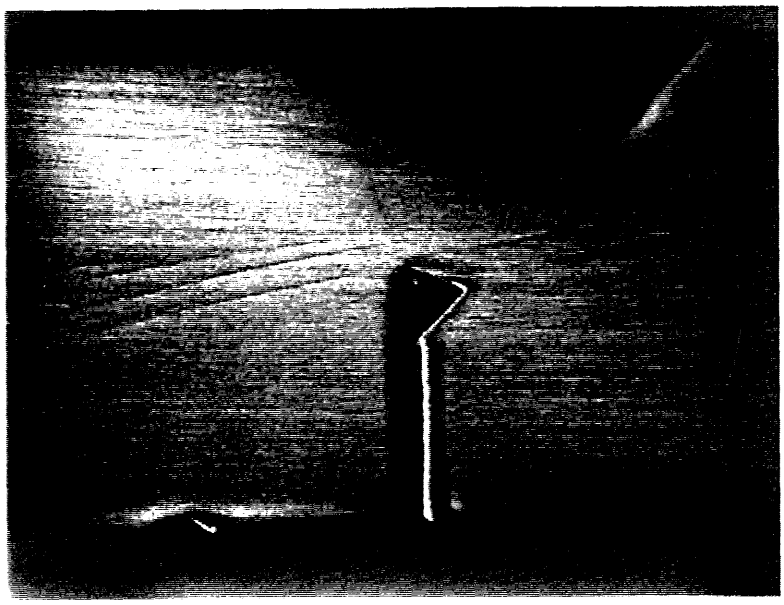

HY-100 F50, CL side, 2.00 mm root defect.

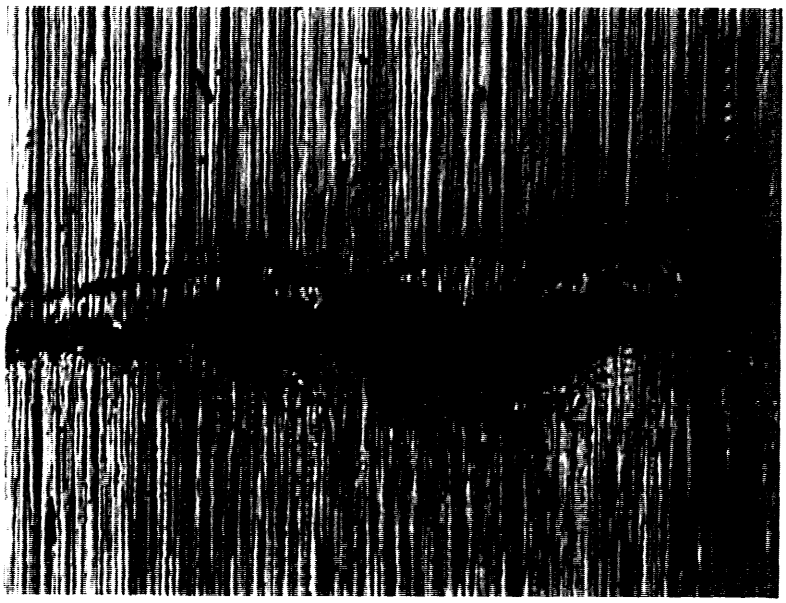

HY-100 F50, CL side, 2.00 mm root defect, x 5

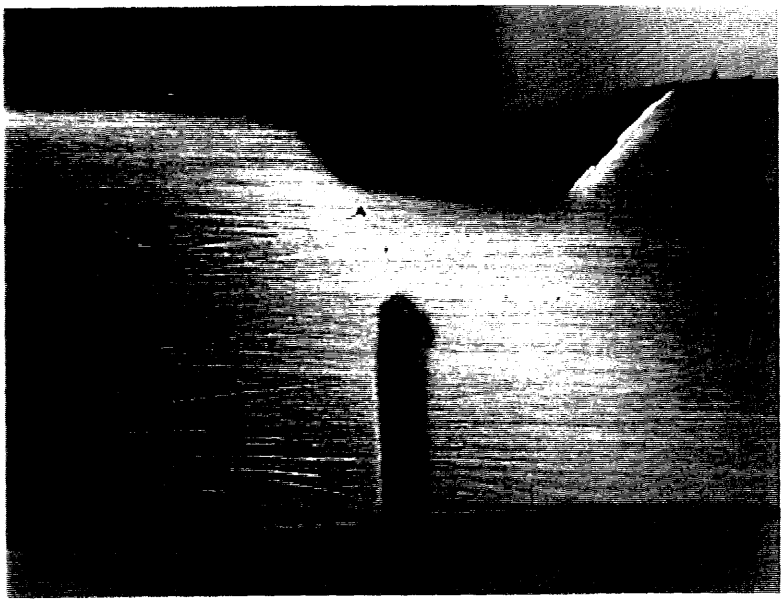

HY-100 G20, CL side, complete fracture.

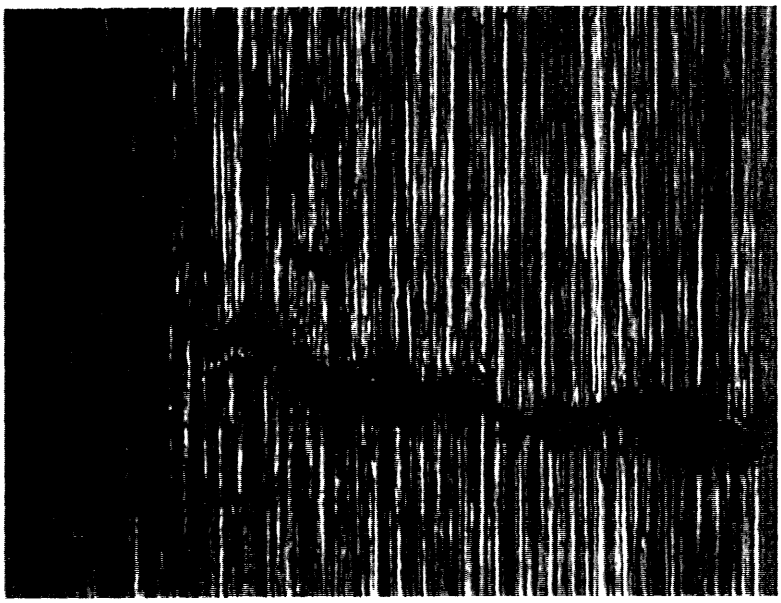

HY-100 G20, CL side, complete fracture, x 5

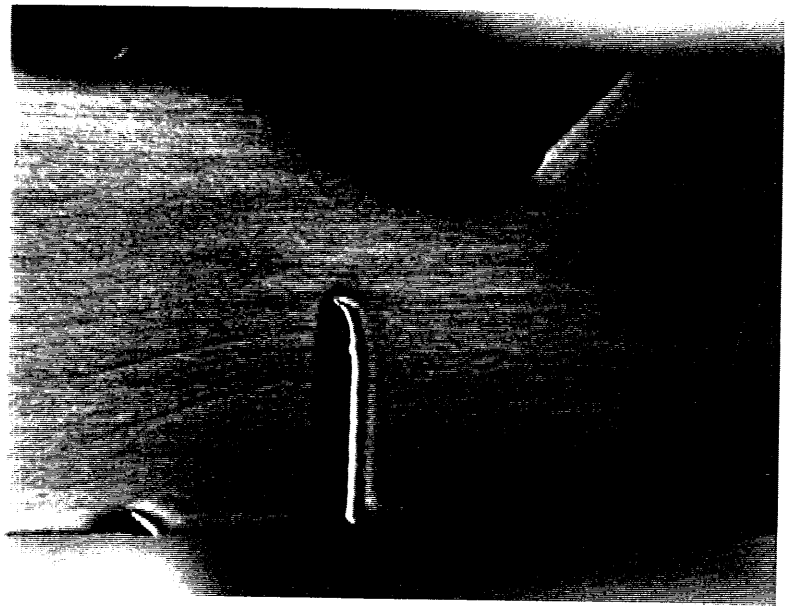

HY-100 G50, CL side, 1.25 mm root crack.

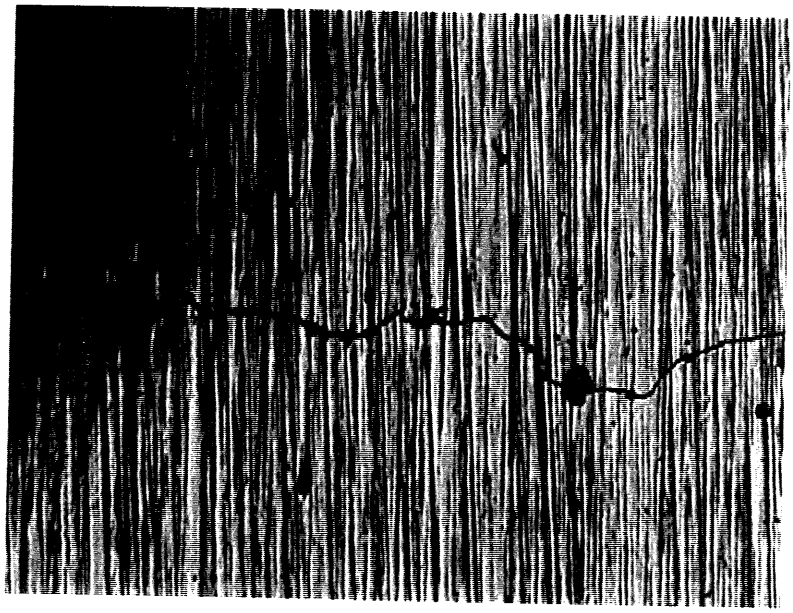

HY-100 G50, CL side, 1.25 mm root crack, x 5

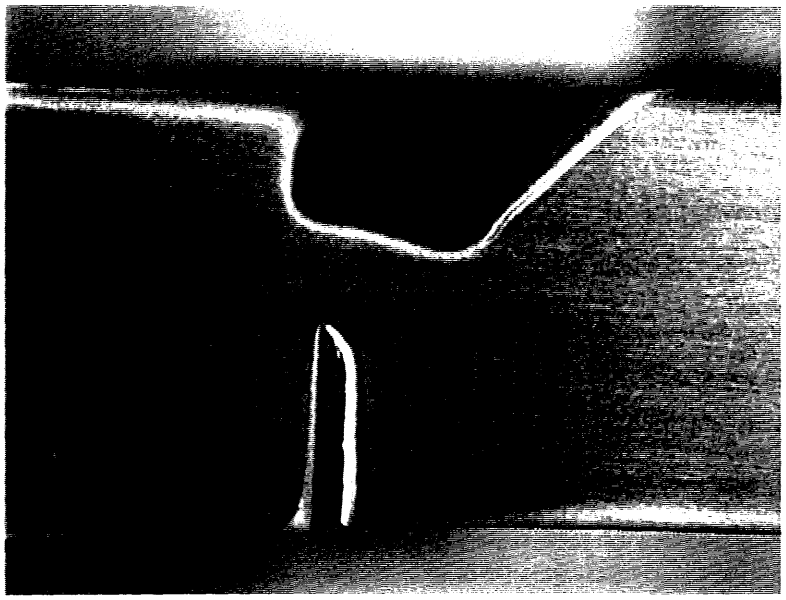

HY-100 H20, CL side, 1.3 mm root crack.

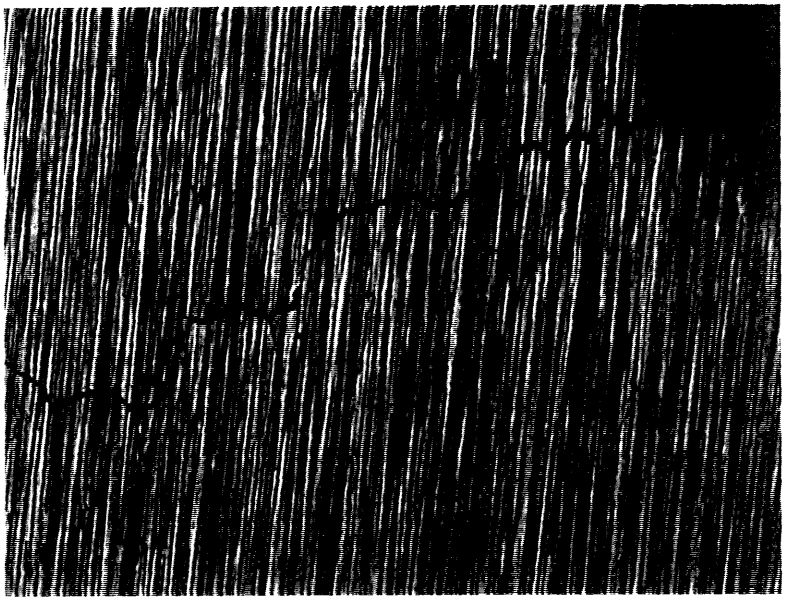

HY-100 H20, CL side, 1.3 mm root crack, x 5

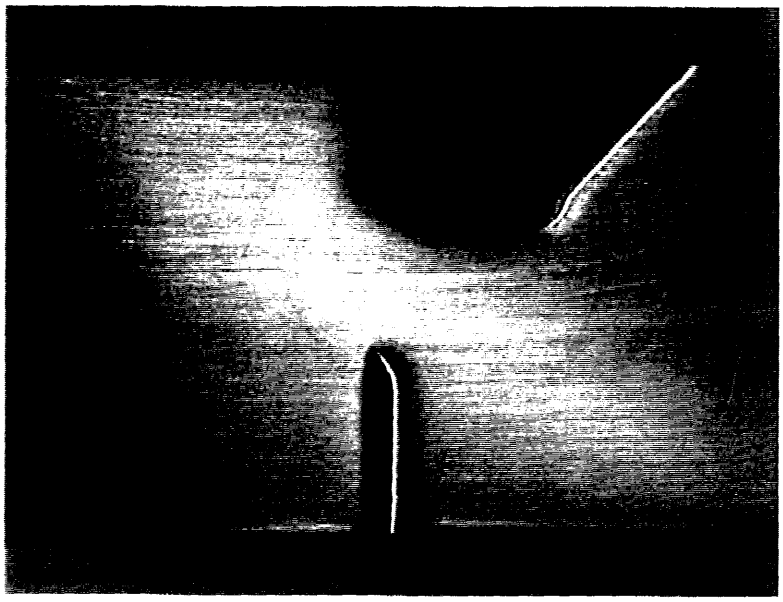

HY-100 H50, CL side, no crack.

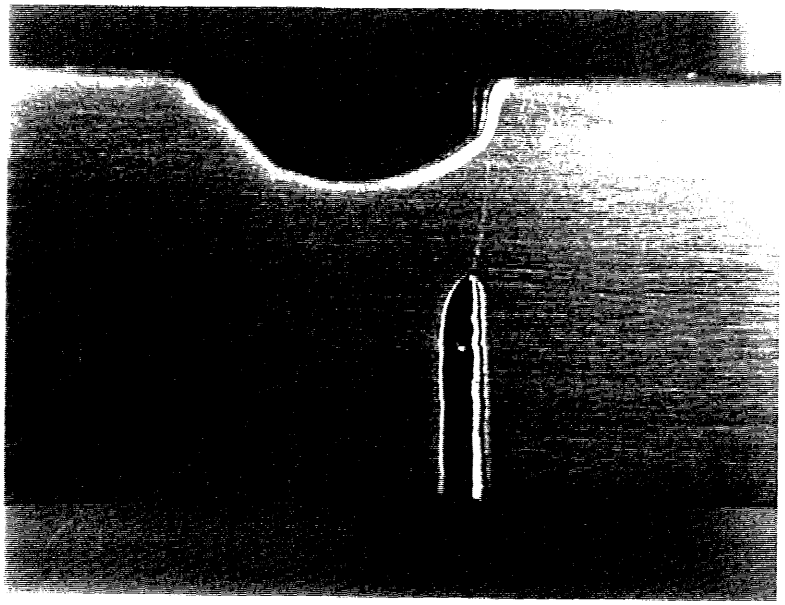

HY-100 I20, CR side, complete fracture.

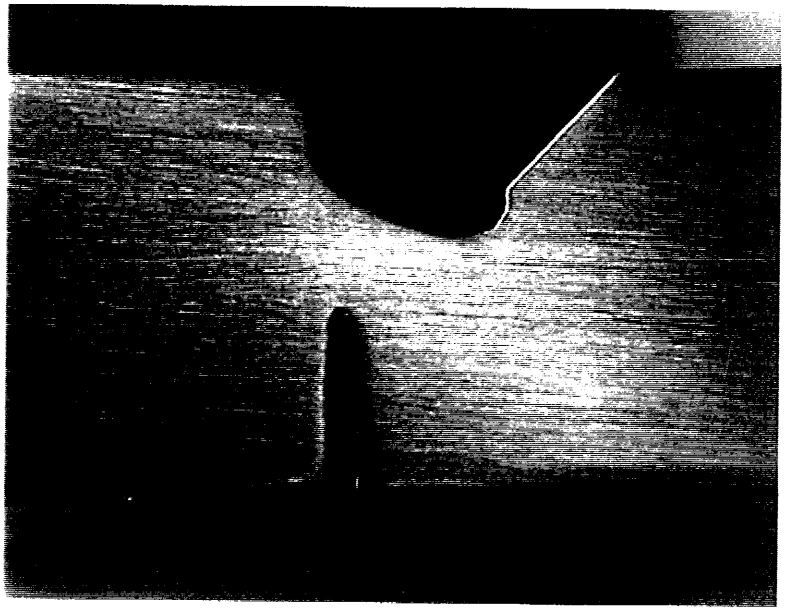

HY-100 I50, CL side, no crack.

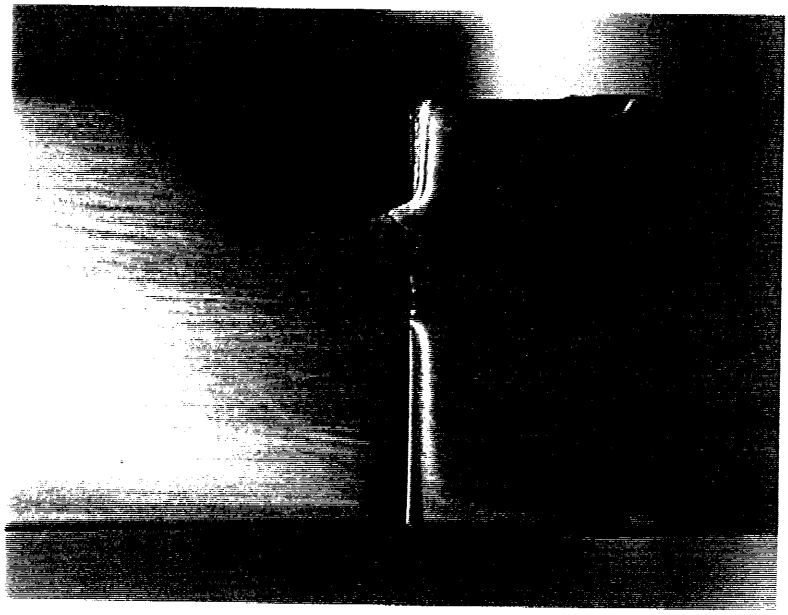

HY-100 J20, CR side, complete fracture.

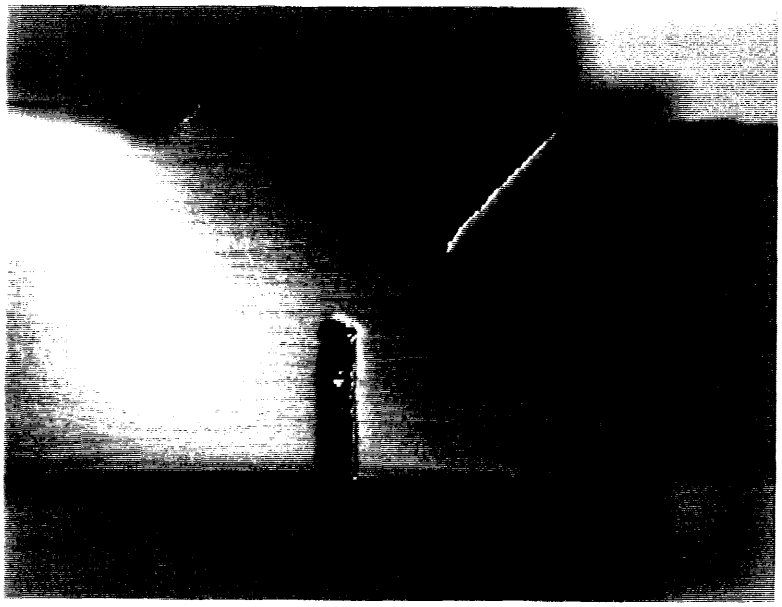

HY-100 J50, CL side, no crack.

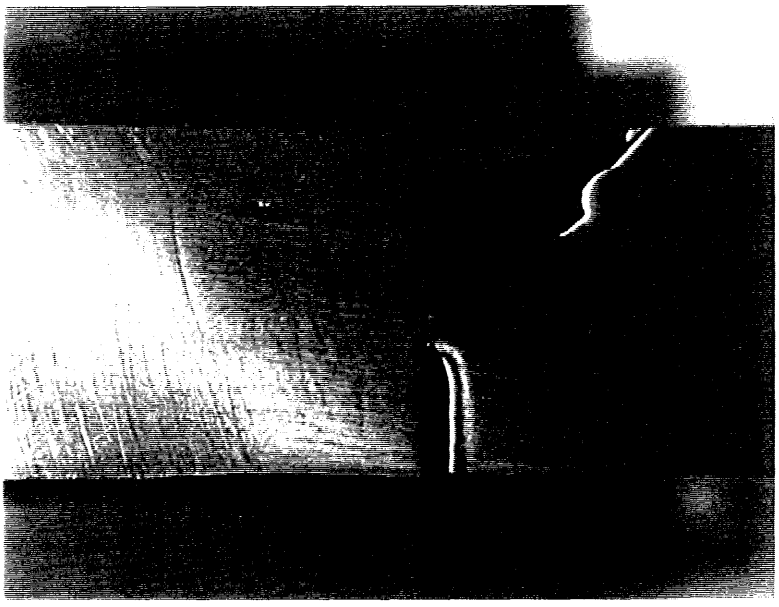

HY-100 K20, CL side, 0.16 mm root crack.

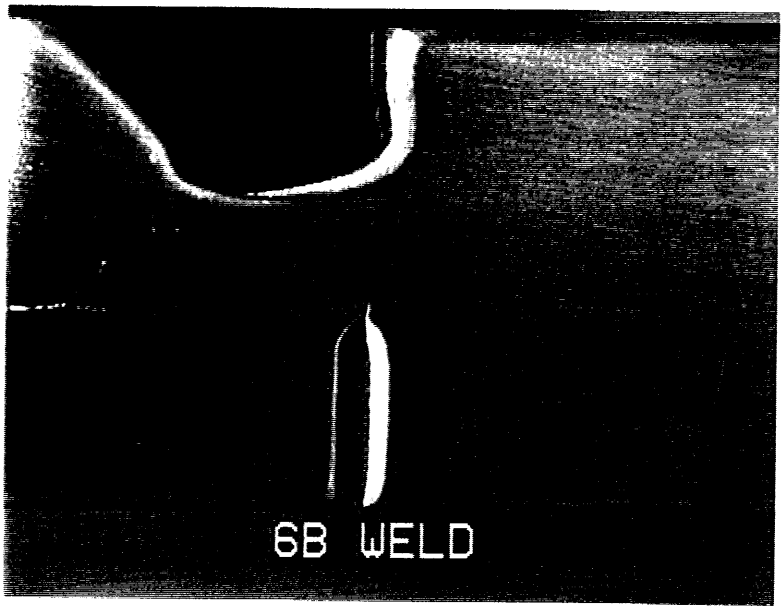

HY-100 K50, CR side, 0.14 mm root crack.

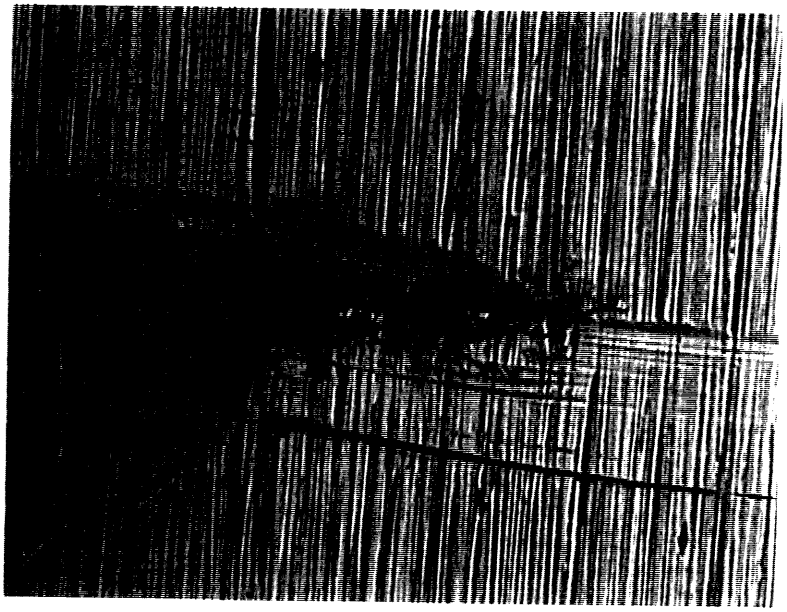

HY-100 K50, CR side, 0.14 mm root crack, x 10

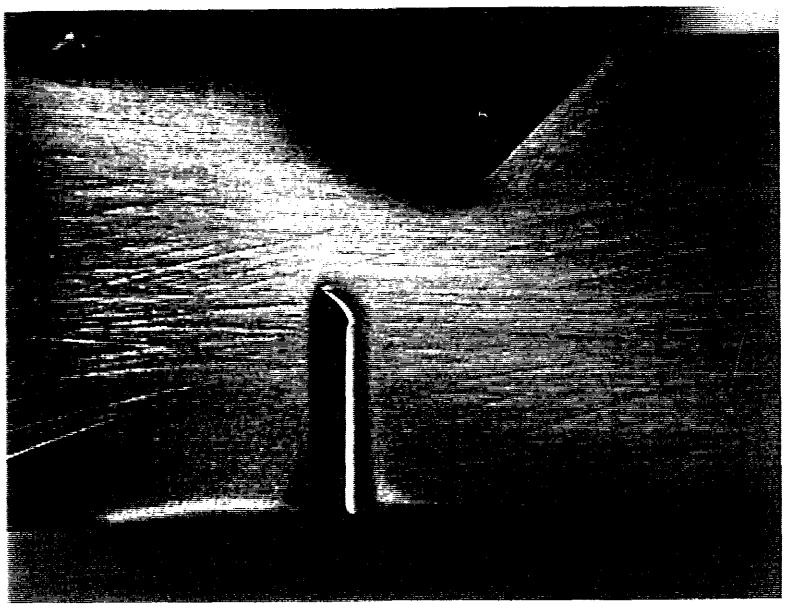

HY-130 L20, CL side, 2.85 mm root crack.

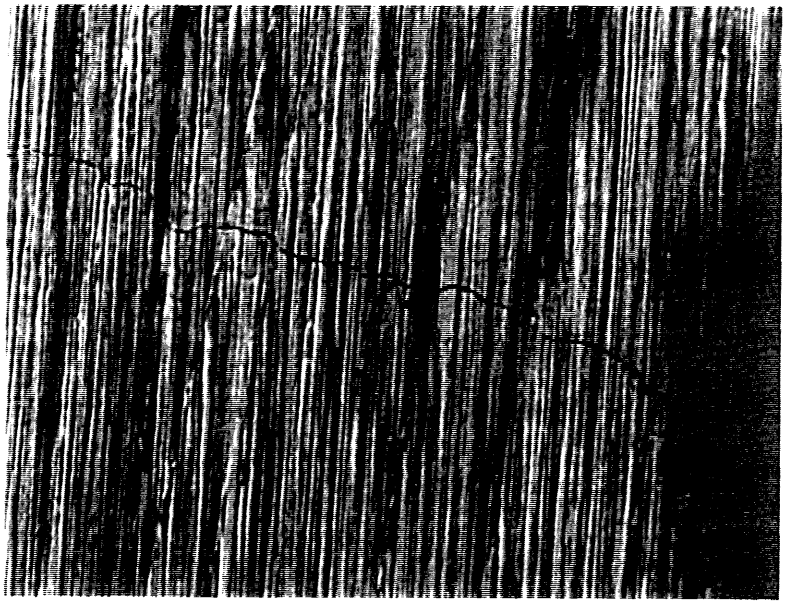

HY-130 L20, CL side, 2.85 mm root crack, x 5

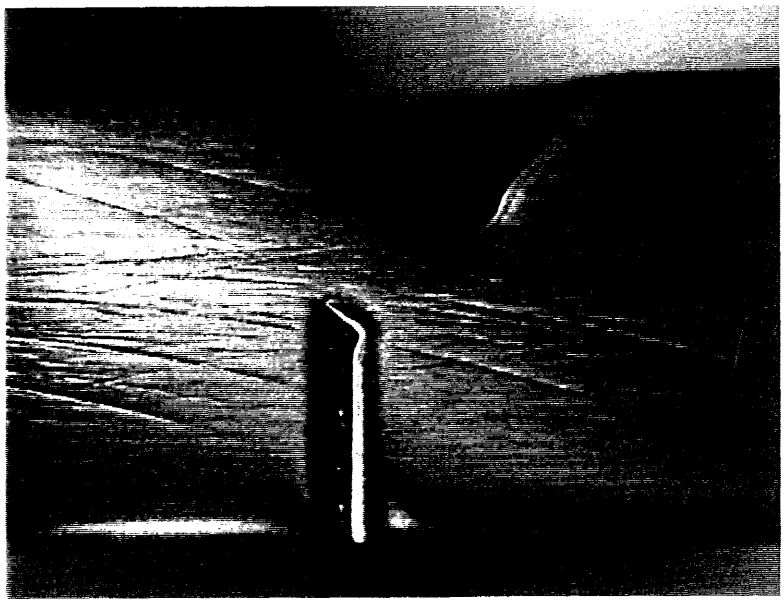

HY-130 L50, CL side, no crack.

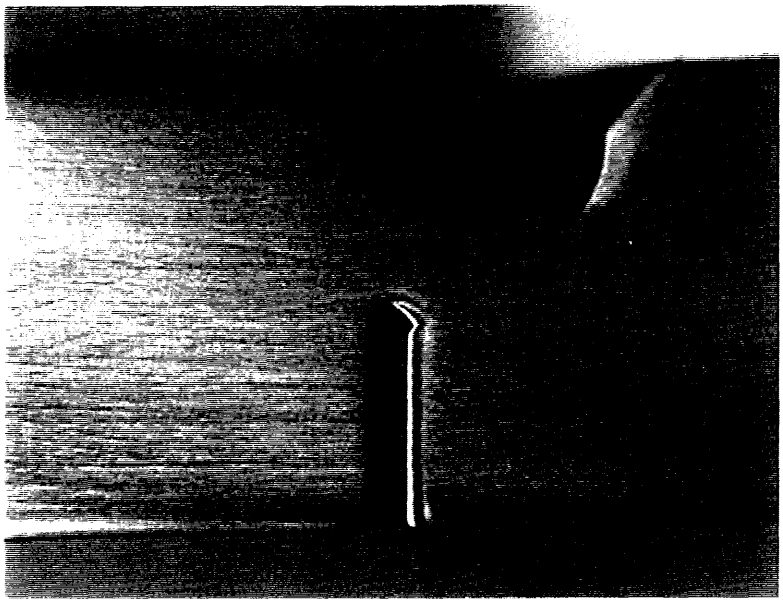

HY-130 M20, CL side, no crack.

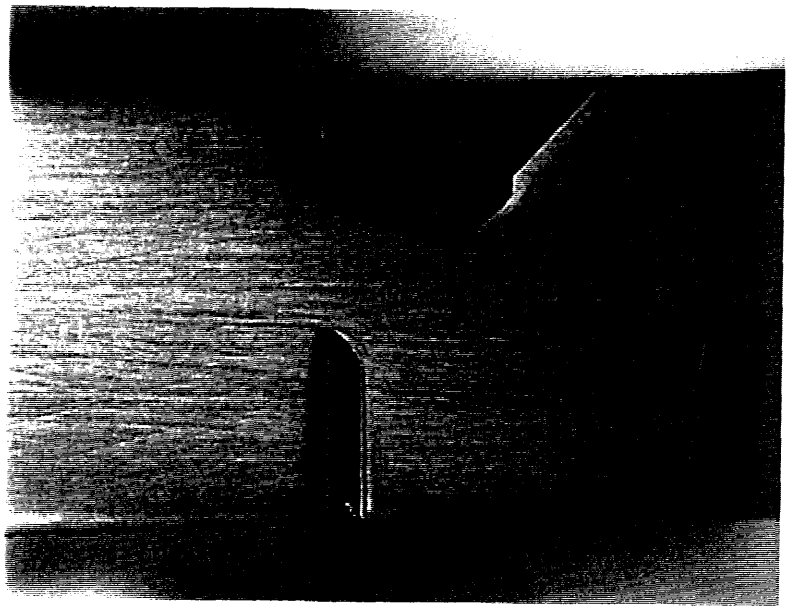

HY-130 M50, CL side, no crack.

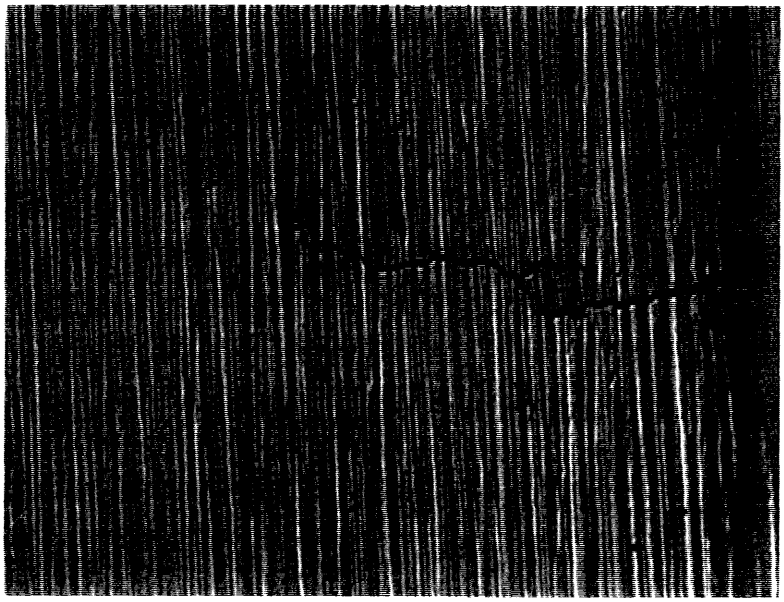

HY-130 M50, CL side, no crack, x 10

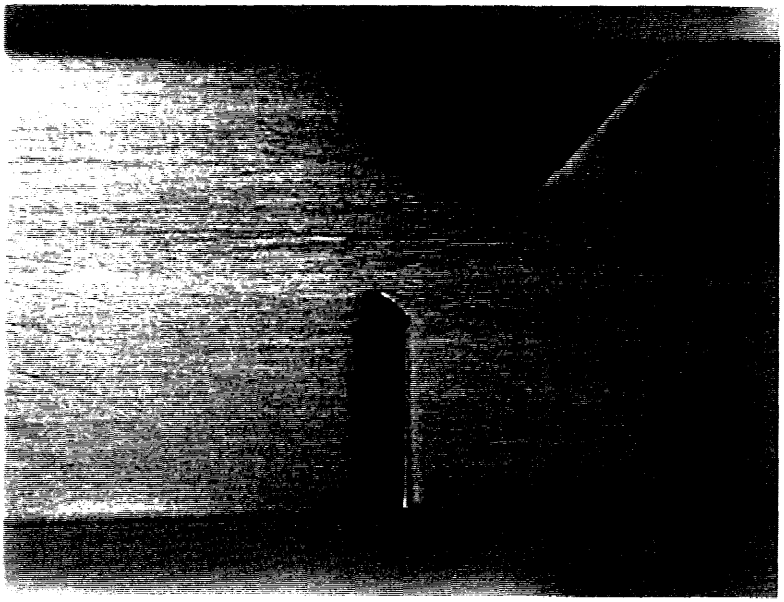

HY-130 N20, CL side, no crack.

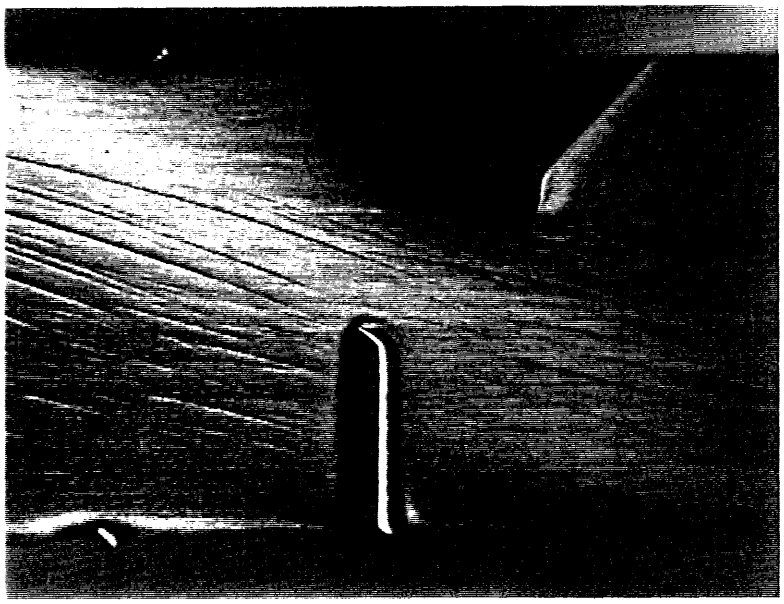

HY-130 N50, CL side, no crack.

A.2 Crack observation after the last pass of welding

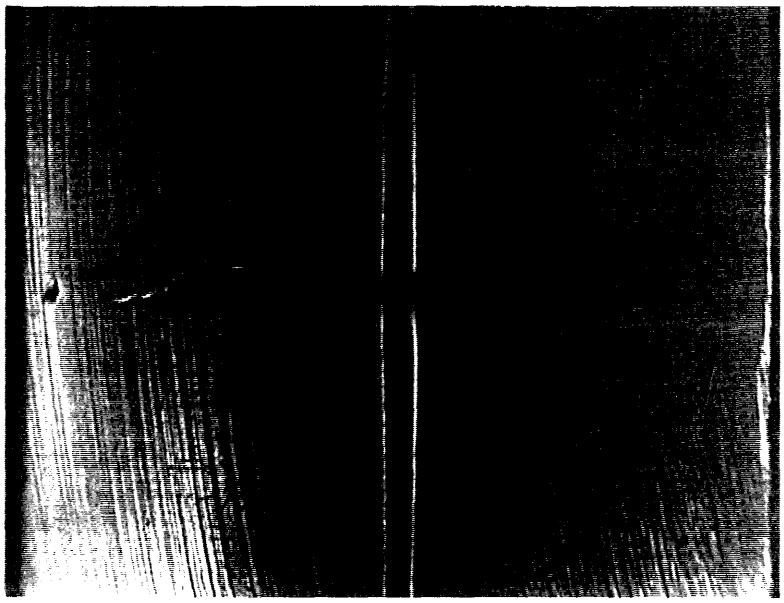

HY-100 F20, 2.56/0.2 mm root crack.

HY-100 F20, L side, 2.56 mm root crack, x 5

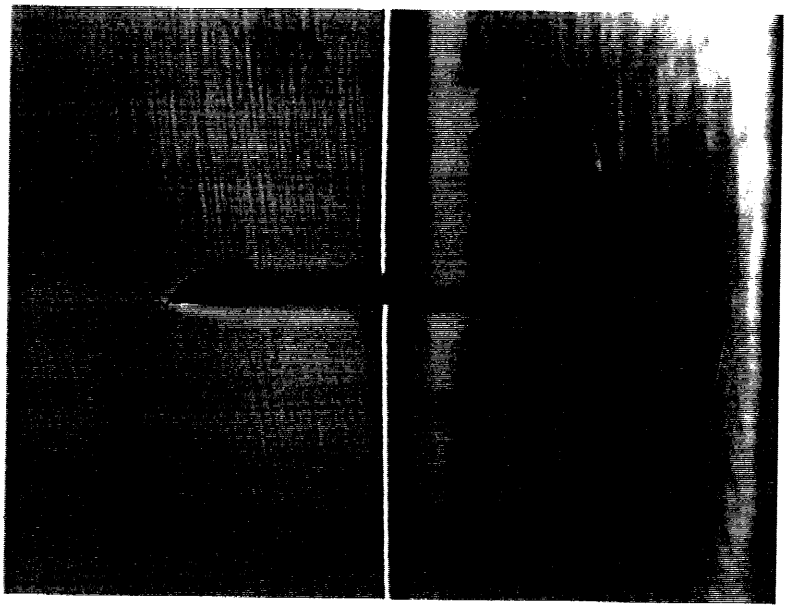

HY-100 G20, 3.0/1.3 mm root crack.

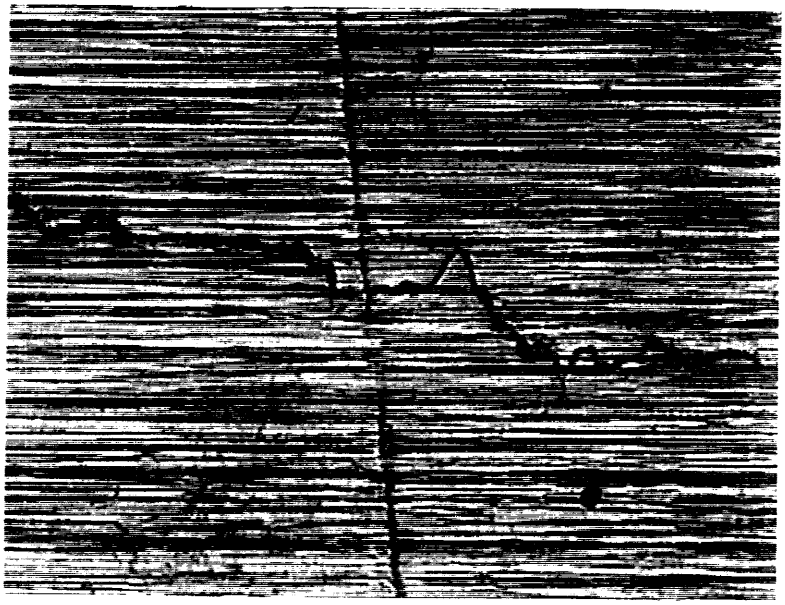

HY-100 F20, R side. 1.3 mm root crack, x 5

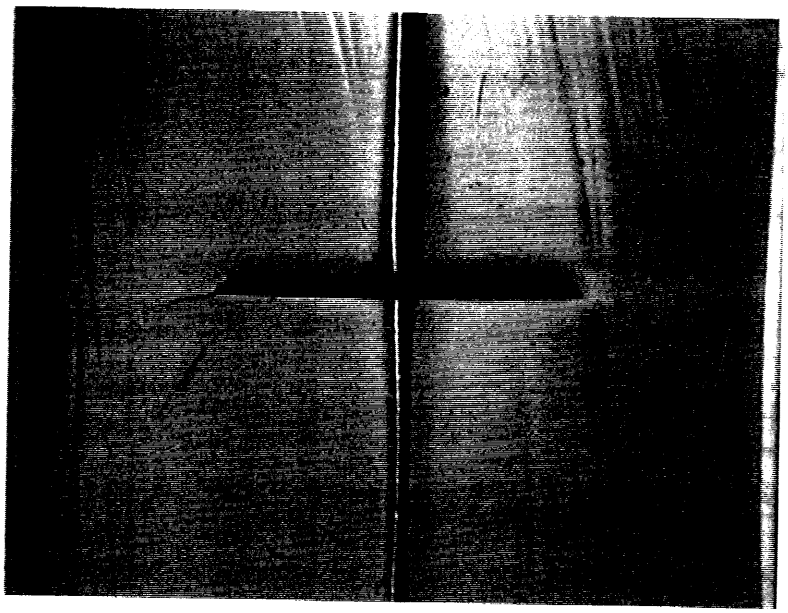

HY-100 H20, 2.14/1.0 mm root crack.

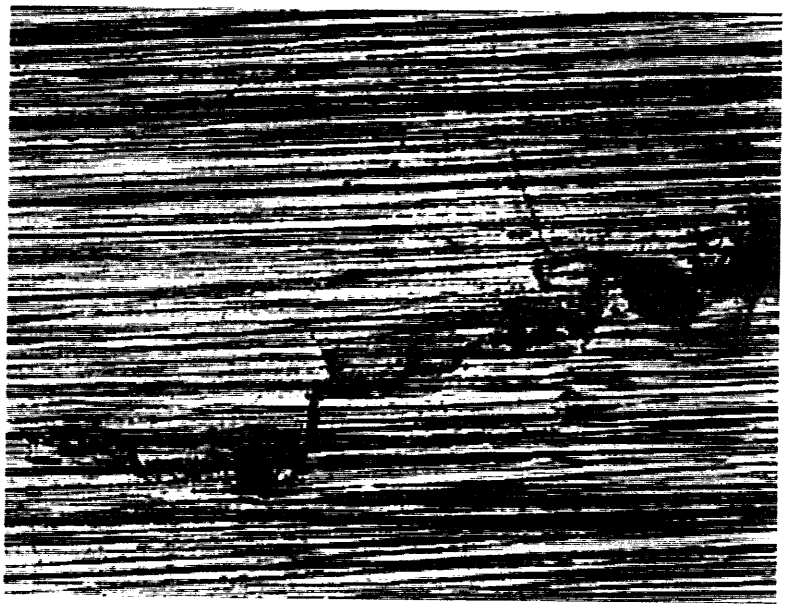

HY-100 F20, L side, 2.14 mm root crack, x 10

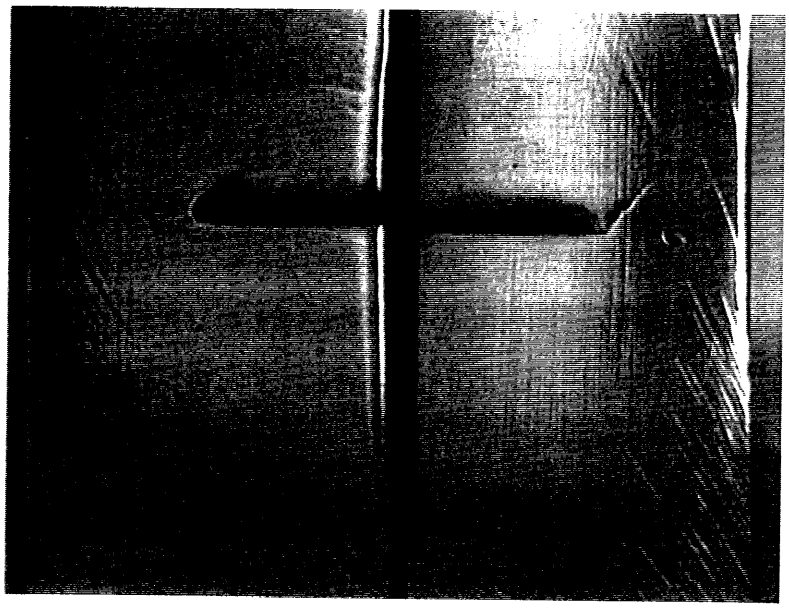

HY-100 I20, 2.0/2.2 mm root crack.

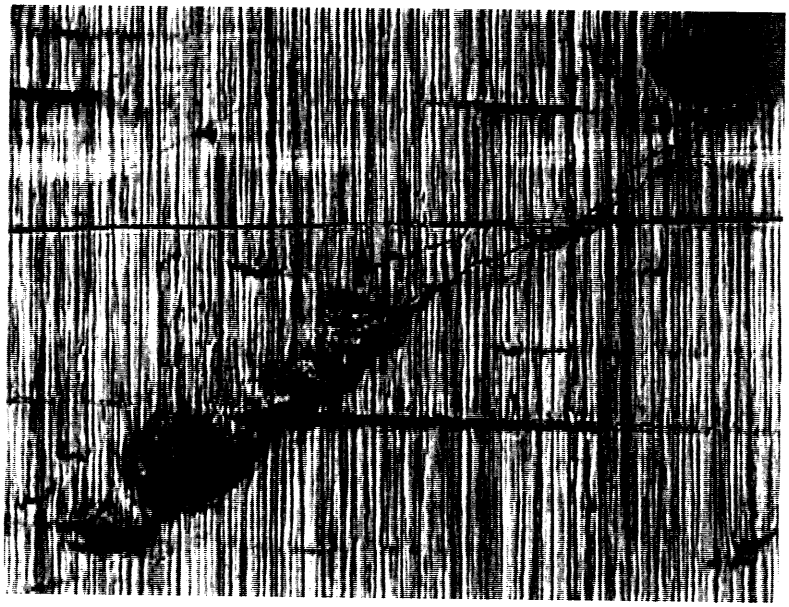

HY-100 I20, L side, 2.0 mm root crack, x 5

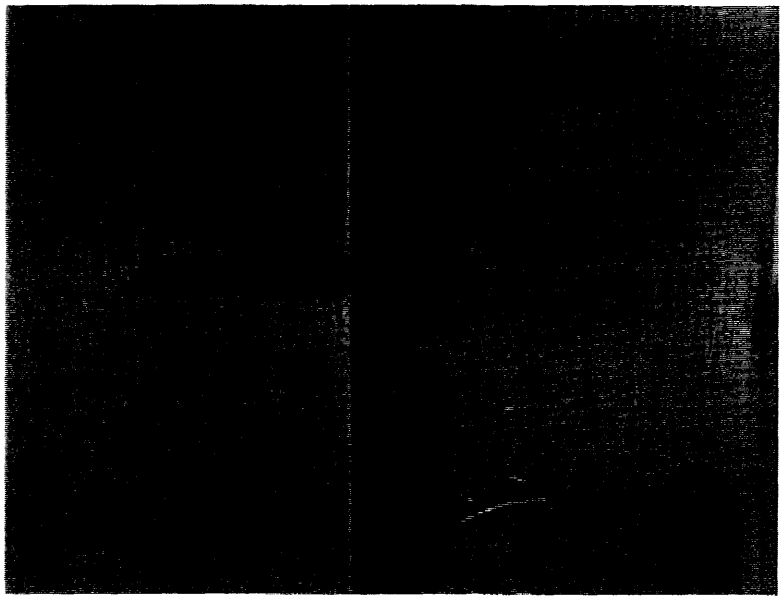

HY-100 J20. 2.2/3.2 mm root crack.

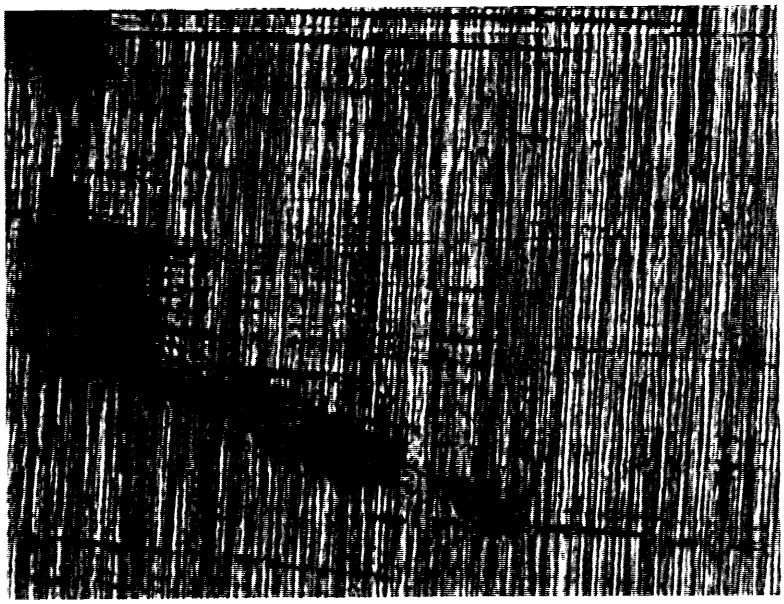

HY-100 J20, R side, 3.2 mm root crack, x 5

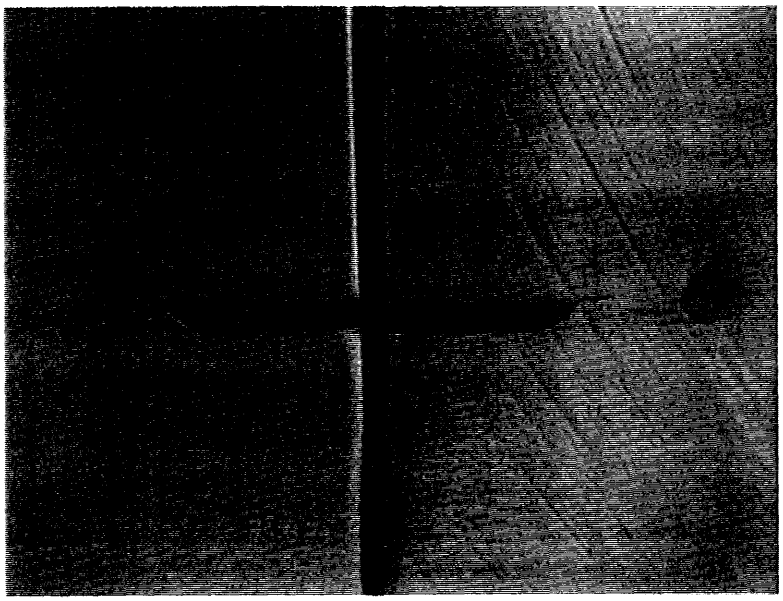

HY-100 L20, 1.21/1.35 mm root crack.

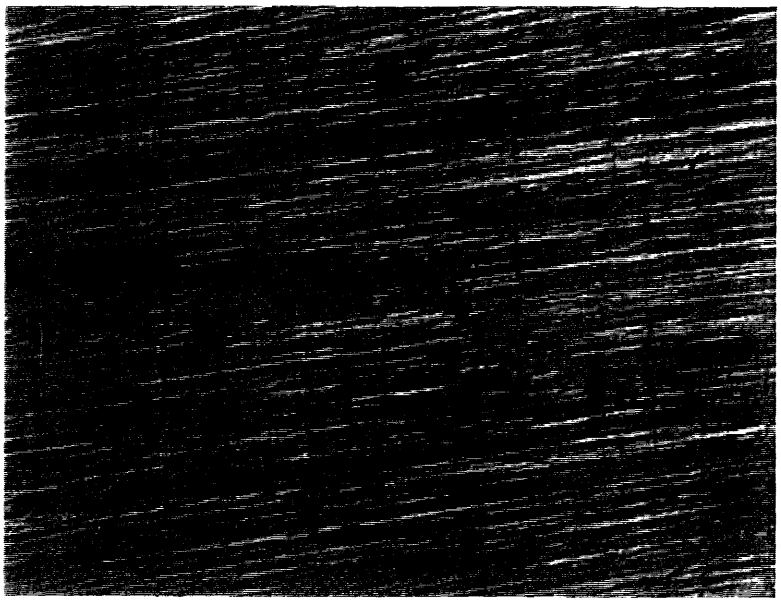

HY-100 L20, R side, 1.35 mm root crack, x 5

A.3 Crack observation during the fatigue test

HY-100 I50, L side, 0.58 mm root crack, 45,000 cycles, x 20

HY-100 I50, R side, 2.75 mm root crack, 45,000 cycles, x 10

HY-100 J50. L side, 1.29 mm root crack, 45,000 cycles, x 20

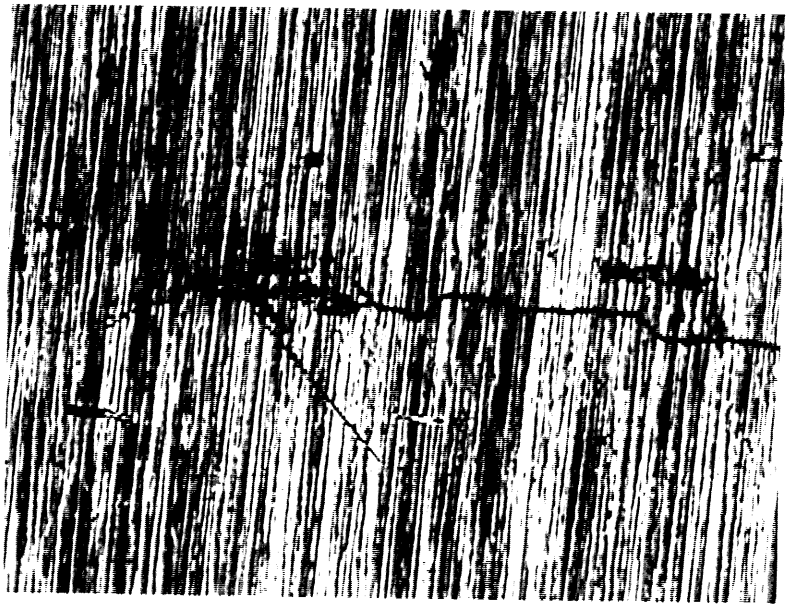

HY-100 J50. L side, 3.20 mm root crack, 105,000 cycles, x 5

HY-100 J50, R side, 0.63 mm root crack, 45,000 cycles, x 20

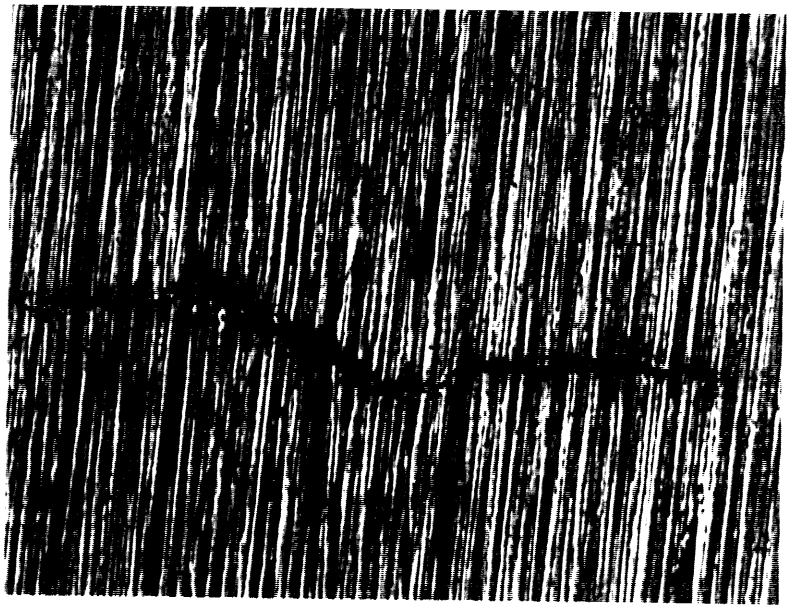

HY-100 J50, R side, 1.81 mm root crack, 105,000 cycles, x 5

HY-100 K20. L side, 0.4 mm root crack, 45,000 cycles. x 20

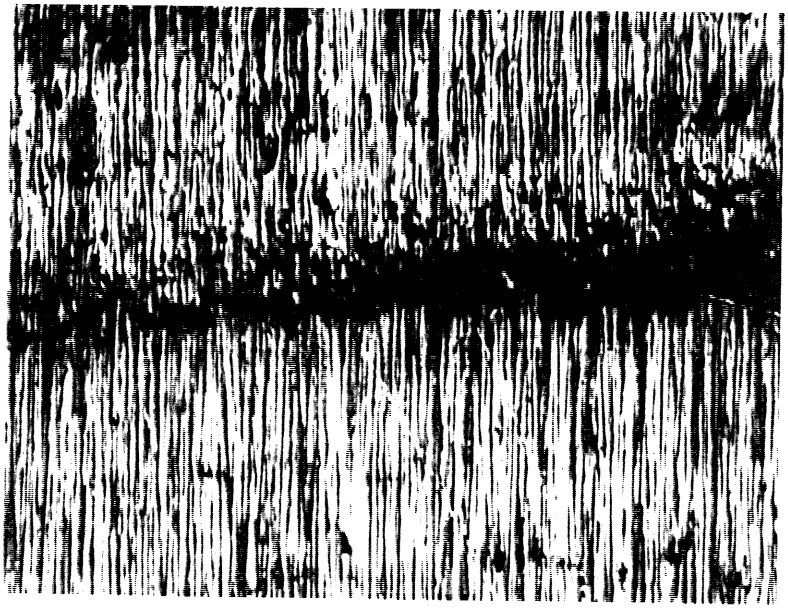

HY-100 K20. L side, 0.4 mm root crack, 150,000 cycles. x 5

HY-100 K20. R side, 0.14 mm root crack, 45,000 cycles, x 20

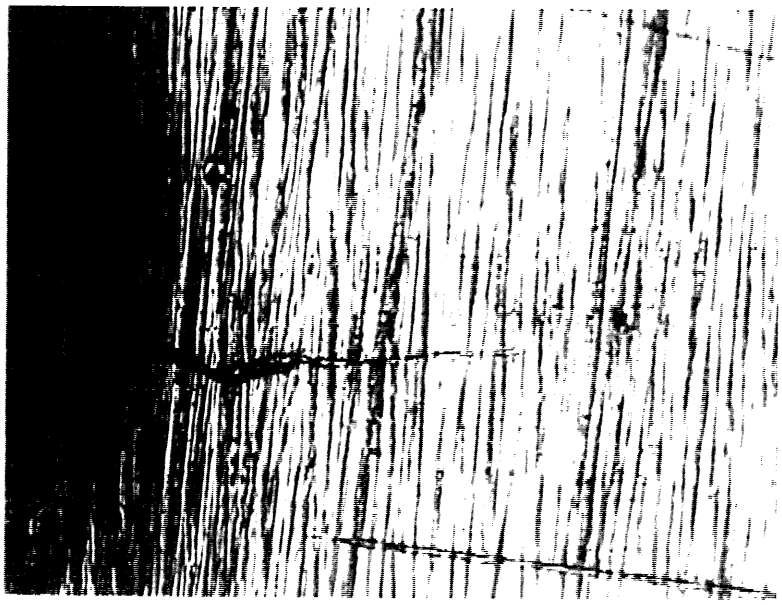

HY-100 K20. R side, 0.24 mm root crack, 150,000 cycles, x 10

Appendix B

Detailed results from numerical analysis

This appendix contains the following data:

- Input and plot files used in the numerical analysis
- Results from the output files that appear in figures 4-4 4-5 4-6 and in figures 4-11 4-12 4-13 4-14 The results contain the applied stress, the translation at the end of the mesh, the maximum value of the effective stress and the the maximum value of the effective plastic strain.
- Plot that show the distribution of the equivalent stress and the effective plastic strain of each specimen due to the applied stress. The value of the applied stress is the joint ultimate strength as it appears in table 4.7. The header of each plot contains the base metal, the material of the first pass, the material of the last pass, the relative thickness and the stress applied at the end of the mesh.

B.1 ADINA input and plot files

```
*
*       ADINA INPUT FILE - PLATE WITH SOFT INTERLAYER
*
* Welding Analysis
*
WORKSTATION SYS=12 COLOR=RGB
*
FILEUNITS LIST=8 LOG=7 ECHO=7
FCONTROL HEADING=UPPER ORIGIN=UPPER
CONTROL HEIGHT=1.5
DATABASE CREATE
*
HEAD 'WELDING ANALYSIS'
*
MASTER IDOF=100111 REACTION=YES
PRINTOUT VOLUME=MAXIMUM IPRIC=0 IPRIT=0 IPDATA=3 CARDIMAGE=NO
PORTHOLE FORMATTED=YES
*
COORDINATES
ENTRIES       NODE      Z        Y
                1       0        0
                2       0        0.006
                3       0.002    0.006
                4       0.002    0
                5       0.075    0.006
                6       0.075    0
*
LINE STRAIGHT   4       6        20       RATIO=20
LINE STRAIGHT   3       5        20       RATIO=20
*
MAT 1  PLASTIC  HARD=ISO  E=207E9    NU=0.3  YIELD=945E6  ET=0.7E9  D=7800
MAT 2  PLASTIC  HARD=ISO  E=207E9    NU=0.3  YIELD=724E6  ET=1.4E9  D=7800
MAT 3  PLASTIC  HARD=ISO  E=207E9    NU=0.3  YIELD=705E6  ET=1.0E9  D=7800
MAT 4  PLASTIC  HARD=ISO  E=207E9    NU=0.3  YIELD=574E6  ET=1.4E9  D=7800
*
*MAT 1  HY130   E=30000 ksi=207E9 Pa  YIELD=137 ksi=945E6 Pa ULT=143=986E6 Pa
*MAT 2  HY100   E=30000 ksi=207E9 Pa  YIELD=105 ksi=724E6 Pa ULT=118=814E6 Pa
*MAT 3  E11018  E=         =207E9 Pa  YIELD=102 ksi=705E6 Pa ULT=112=774E6 Pa
*MAT 4  E 8018  E=         =207E9 Pa  YIELD= 83 ksi=574E6 Pa ULT= 98=674E6 Pa
*
EGROUP 1        TWODSOLID       SUBTYPE=STRAIN  DISP=SMALL       MAT=3
GSURFACE        1       2       3       4       10      10      node=4
EDATA   1 1
*
EGROUP 2        TWODSOLID       SUBTYPE=STRAIN  DISP=SMALL       MAT=1
GSURFACE        4       3       5       6       10      20      node=4
EDATA   2 1
*
*ANALYSIS MASSMATRIX=CONSISTENT
*
FIXBOUNDARIES   3       TYPE=LINES
        1       2
FIXBOUNDARIES   2       TYPE=LINES
        1       4
        4       6
*
LOAD PRESSURE LINE
        6       5       1       10.4E8  10.4E8
*
ADINA
*
END
```

```
*
*       ADINA PLOT FILE - PLATE WITH SOFT INTERLAYER
*
DATABASE CREATE FORMATTED=YES
FCONTROL HEADING=UPPER ORIGIN=UPPERLEFT
CONTROL HEIGHT=1.5
FILEU LIST=8 LOG=7
*ECHO=7

*WORKSTATION 12 1 1 0 COLOR=RGB BACK=BLACK PENW=0.01 LINEW=0.025,
*SIZE=DIRECT  XSMIN=2.5  XSMAX=25.5  YSMIN=2.5  YSMAX=18.5
*
HEAD 'HY130 - E8018   RT:0.083 '
*
ALIAS SYY STRESS-YY
ALIAS SZZ STRESS-ZZ
ALIAS SYZ STRESS-YZ
*RESULTANT VONMISES, 'SQRT(0.5*(SYY**2+(SYY-SZZ)**2+SZZ**2+6*SYZ*SYZ))'
ALIAS SXX STRESS-XX
RESULTANT VM1, '(  ((SXX-SYY)**2) + ((SYY-SZZ)**2) + ((SZZ-SXX)**2) )'
RESULTANT VONMISES, 'SQRT(0.5*(VM1 + 6*SYZ*SYZ))'
*
**VIEW 1                  1 0  0  R=180
FRAME H=U
WINDOW   1      0       0.006   0       0.010
MESH WINDOW=1 ORIGINAL=2 DEFORMED=1 MARGIN=YES BCODE=ALL
*SMOOTHING TYPE=AVERAGE
BAND VAR=ACCUM_EFF_PLASTIC_STRAIN TLENGTH=65
*BAND VAR=VONMISES TLENGTH=65
*BAND VAR=STRESS-ZZ TLENGTH=65
*LVECTOR VAR=P2DPRESSURE
**TEXT XP=81 YP=60 STRING='MAX'
*COLORS DEFORMED=WHITE
*
END
```

```
*
*       ADINA INPUT FILE - RESTRAINT CRACKING TEST SPECIMEN
*
* Welding Analysis
*
WORKSTATION SYS=12 COLOR=RGB
*
FILEUNITS LIST=8 LOG=7 ECHO=7
FCONTROL HEADING=UPPER ORIGIN=UPPER
CONTROL HEIGHT=1.5
DATABASE CREATE
*
HEAD 'WELDING ANALYSIS'
*
MASTER IDOF=100111 REACTION=YES
PRINTOUT VOLUME=MAXIMUM IPRIC=0 IPRIT=0 IPDATA=3 CARDIMAGE=NO
PORTHOLE FORMATTED=YES
*
COORDINATES
ENTRIES       NODE      Z         Y
                1       0         0
                2       0         0.003
                3       0         0.005
                4       0         0.009
                5       0         0.013
                6       0.0705    0
                7       0.0705    0.003
                8       0.0705    0.005
                9       0.0705    0.009
                10      0.0705    0.013
                11      0.0715    0
                12      0.0715    0.003
                13      0.0715    0.005
                14      0.0755    0.009
                15      0.0795    0.013
                16      0.150     0
                17      0.150     0.003
                18      0.150     0.005
                19      0.150     0.009
                20      0.150     0.013
*
LINE STRAIGHT   1       6       12      RATIO=0.01
LINE STRAIGHT   2       7       12      RATIO=0.01
LINE STRAIGHT   3       8       12      RATIO=0.01
LINE STRAIGHT   4       9       12      RATIO=0.01
LINE STRAIGHT   5       10      12      RATIO=0.01
*
LINE STRAIGHT   11      16      12      RATIO=100
LINE STRAIGHT   12      17      12      RATIO=100
LINE STRAIGHT   13      18      12      RATIO=100
LINE STRAIGHT   14      19      12      RATIO=100
LINE STRAIGHT   15      20      12      RATIO=100
*
LINE STRAIGHT   6       7       3       RATIO=1
LINE STRAIGHT   7       8       4       RATIO=1
LINE STRAIGHT   8       9       8       RATIO=10
LINE STRAIGHT   9       10      4       RATIO=1
*
LINE STRAIGHT   11      12      3       RATIO=1
LINE STRAIGHT   12      13      4       RATIO=1
LINE STRAIGHT   13      14      8       RATIO=10
LINE STRAIGHT   14      15      4       RATIO=1
*
LINE STRAIGHT   3       4       8       RATIO=10
LINE STRAIGHT   18      19      8       RATIO=10
*
```

```
*LINE STRAIGHT   6       10
*LINE STRAIGHT   11      13
*LINE STRAIGHT   13      15

MAT 1 PLASTIC-M HARD=ISO E=207E9 NU=0.3 D=7800
        0.004567        945E6
        0.06467         986E6
        250             986E6
MAT 2 PLASTIC-M HARD=ISO E=207E9 NU=0.3 D=7800
        0.003500        724E6
        0.06850         814E6
        250             814E6
MAT 3 PLASTIC-M HARD=ISO E=207E9 NU=0.3 D=7800
        0.003410        705E6
        0.07008         774E6
        250             774E6
MAT 4 PLASTIC-M HARD=ISO E=207E9 NU=0.3 D=7800
        0.002773        574E6
        0.07527         674E6
        250             674E6
*
*MAT 1  PLASTIC  HARD=ISO  E=207E9    NU=0.3  YIELD=945E6  ET=0.7E9  D=7800
*MAT 2  PLASTIC  HARD=ISO  E=207E9    NU=0.3  YIELD=724E6  ET=1.4E9  D=7800
*MAT 3  PLASTIC  HARD=ISO  E=207E9    NU=0.3  YIELD=705E6  ET=1.0E9  D=7800
*MAT 4  PLASTIC  HARD=ISO  E=207E9    NU=0.3  YIELD=574E6  ET=1.4E9  D=7800
*
*MAT 1  HY130   E=30000 ksi=207E9 Pa  YIELD=137 ksi=945E6 Pa ULT=143=986E6 Pa
*MAT 2  HY100   E=30000 ksi=207E9 Pa  YIELD=105 ksi=724E6 Pa ULT=118=814E6 Pa
*MAT 3  E11018  E=         =207E9 Pa  YIELD=102 ksi=705E6 Pa ULT=112=774E6 Pa
*MAT 4  E 8018  E=         =207E9 Pa  YIELD= 83 ksi=574E6 Pa ULT= 98=674E6 Pa
*
EGROUP 1        TWODSOLID       SUBTYPE=STRAIN  DISP=SMALL       MAT=1
GSURFACE        1       2       7       6       3       12      node=4
GSURFACE        2       3       8       7       4       12      node=4
GSURFACE        3       4       9       8       8       12      node=4
GSURFACE        4       5       10      9       4       12      node=4
EDATA   1 1
*
EGROUP 2        TWODSOLID       SUBTYPE=STRAIN  DISP=SMALL       MAT=3
*GSURFACE       7       8       13      12      4       7       node=4
GSURFACE        8       9       14      13      8       7       node=4
EDATA   2 1
*
EGROUP 3        TWODSOLID       SUBTYPE=STRAIN  DISP=SMALL       MAT=3
GSURFACE        9       10      15      14      4       7       node=4
EDATA   3 1
*
EGROUP 4        TWODSOLID       SUBTYPE=STRAIN  DISP=SMALL       MAT=1
GSURFACE        11      12      17      16      3       12      node=4
GSURFACE        12      13      18      17      4       12      node=4
GSURFACE        13      14      19      18      8       12      node=4
GSURFACE        14      15      20      19      4       12      node=4
EDATA   4 1
*
*ANALYSIS MASSMATRIX=CONSISTENT
*
FIXBOUNDARIES   3       TYPE=LINES
        1       2
        2       3
        3       4
        4       5
FIXBOUNDARIES   2       TYPE=LINES
        1       6
        11      16
*
```

```
LOAD PRESSURE LINE
        16      17      1       6.65E8  6.65E8
        17      18      1       6.65E8  6.65E8
        18      19      1       6.65E8  6.65E8
        19      20      1       6.65E8  6.65E8
*
ADINA
*
END
```

```
*
*       ADINA PLOT FILE - RESTRAINT CRACKING TEST SPECIMEN
*
DATABASE CREATE FORMATTED=YES
FCONTROL HEADING=UPPER ORIGIN=UPPERLEFT
CONTROL HEIGHT=1.5
FILEU LIST=8 LOG=7
*ECHO=7
*
**WORKSTATION SYS=12 COLORS=RGB BACKGROUND=WHITE
*COLORS ORI=INVERSE EL=INVERSE BC=INVERSE XYA=INVERSE XYL=INVERSE VE=INVERSE
*
**WORKSTATION 12 1 1 0 COLOR=RGB BACK=WHITE PENW=0.01 LINEW=0.025,
*      SIZE=DIRECT  XSMIN=2.5  XSMAX=25.5  YSMIN=2.5  YSMAX=18.5
*
HEAD 'HY100'
*
ALIAS SYY STRESS-YY
ALIAS SZZ STRESS-ZZ
ALIAS SYZ STRESS-YZ
*RESULTANT VONMISES, 'SQRT(0.5*(SYY**2+(SYY-SZZ)**2+SZZ**2+6*SYZ*SYZ))'
ALIAS SXX STRESS-XX
RESULTANT VM1, '(  ((SXX-SYY)**2) + ((SYY-SZZ)**2) + ((SZZ-SXX)**2) )'
RESULTANT VONMISES, 'SQRT(0.5*(VM1 + 6*SYZ*SYZ))'
*
ALIAS AEPS ACCUM_EFF_PLASTIC_STRAIN
ALIAS PEZZ PLASTIC_STRAIN-ZZ
ALIAS EZZ  STRAIN-ZZ
*
FRAME H=U
WINDOW   1      0       0.013   0.069   0.09
*WINDOW  1      0.004   0.006   0.07    0.073
MESH WINDOW=1 ORIGINAL=1 DEFORMED=2 MARGIN=YES BCODE=ALL
SMOOTHING TYPE=AVERAGE
BAND VAR=ACCUM_EFF_PLASTIC_STRAIN TLENGTH=65
*BAND VAR=VONMISES TLENGTH=65
*BAND VAR=STRESS-ZZ TLENGTH=65
*BAND VAR=STRAIN-ZZ TLENGTH=65
*
NPOINT NAME=CENT  NODE=18
PLIST POINTNAME=CENT  VARIABLES=Z-DISPLACEMENT
*
BZONE   NOTCH   YMIN=0.005 YMAX=0.006  ZMIN=0.07 ZMAX=0.073
ZLIST   NOTCH   VAR=AEPS  PEZZ  EZZ
*
END
*
```

```
*
*       ADINA INPUT FILE - DEGREE OF RESTRAINT OF TEST SPECIMEN
*
* Welding Analysis
*
WORKSTATION SYS=12 COLOR=RGB
*
FILEUNITS LIST=8 LOG=7 ECHO=7
FCONTROL HEADING=UPPER ORIGIN=UPPER
CONTROL HEIGHT=1.5
DATABASE CREATE
*
HEAD 'WELDING ANALYSIS BASE METAL:HY130'
*
MASTER IDOF=100111 REACTION=YES
PRINTOUT VOLUME=MAXIMUM IPRIC=0 IPRIT=0 IPDATA=3 CARDIMAGE=NO
PORTHOLE FORMATTED=YES
*
COORDINATES
ENTRIES        NODE      Z         Y
                 1       0         0
                 2       0         0.07
                 3       0         0.0705
                 4       0         0.075
                 5       0.06      0.075
                 6       0.06      0.0705
                 7       0.06      0.07
                 8       0.10      0.0705
                 9       0.10      0.07
                 10      0.10      0
                 11      0.06      0
*
LINE STRAIGHT    1       2         7         RATIO=1
LINE STRAIGHT    2       3         1         RATIO=1
LINE STRAIGHT    3       4         4         RATIO=1
LINE STRAIGHT    4       5         6         RATIO=1
LINE STRAIGHT    5       6         4         RATIO=1
LINE STRAIGHT    6       8         4         RATIO=1
LINE STRAIGHT    8       9         1         RATIO=1
LINE STRAIGHT    9       10        7         RATIO=1
LINE STRAIGHT    1       11        6         RATIO=1
LINE STRAIGHT    11      10        4         RATIO=1
*
MAT 1 PLASTIC-M HARD=ISO E=207E9 NU=0.3 D=7800
        0.004567         945E6
        0.06467          986E6
        250              986E6
MAT 2 PLASTIC-M HARD=ISO E=207E9 NU=0.3 D=7800
        0.003500         724E6
        0.06850          814E6
        250              814E6
*
EGROUP 1         TWODSOLID        SUBTYPE=STRAIN          MAT=2
GSURFACE         11      1        2        7       6      7       node=4
GSURFACE         7       2        3        6       6      1       node=4
GSURFACE         11      7        9        10      7      4       node=4
GSURFACE         7       6        8        9       1      4       node=4
GSURFACE         6       3        4        5       6      4       node=4
EDATA    1  1
*
FIXBOUNDARIES    3       TYPE=LINES
        10       9
        9        8
FIXBOUNDARIES    2       TYPE=LINES
        4        5
*
```

```
LOAD PRESSURE LINE
        8       6       1       2E8     2E8
*
*FRAME  XF=17   YF=1.4
*FRAME H=U
*WINDOW  1      0       1.3     6.5     8
*MESH   WINDOW=1        BCODE=ALL
*MESH   BCODE=ALL
*LVECTOR VAR=P2DPRESSURE
*
ADINA
*
END
```

```
*
*       ADINA PLOT FILE - DEGREE OF RESTRAINT OF TEST SPECIMEN
*
DATABASE CREATE FORMATTED=YES
FCONTROL HEADING=UPPER ORIGIN=UPPERLEFT
CONTROL HEIGHT=1.5
FILEU LIST=8 LOG=7
*ECHO=7
*
**WORKSTATION SYS=12 COLORS=RGB BACKGROUND=WHITE
*COLORS ORI=INVERSE EL=INVERSE BC=INVERSE XYA=INVERSE XYL=INVERSE VE=INVERSE
*
**WORKSTATION 12 1 1 0 COLOR=RGB BACK=WHITE PENW=0.01 LINEW=0.025,
*      SIZE=DIRECT  XSMIN=2.5  XSMAX=25.5  YSMIN=2.5  YSMAX=18.5
*
HEAD 'HY100 '
*
ALIAS SYY STRESS-YY
ALIAS SZZ STRESS-ZZ
ALIAS SYZ STRESS-YZ
*RESULTANT VONMISES, 'SQRT(0.5*(SYY**2+(SYY-SZZ)**2+SZZ**2+6*SYZ*SYZ))'
ALIAS SXX STRESS-XX
RESULTANT VM1, '(  ((SXX-SYY)**2) + ((SYY-SZZ)**2) + ((SZZ-SXX)**2) )'
RESULTANT VONMISES, 'SQRT(0.5*(VM1 + 6*SYZ*SYZ))'
*
FRAME H=U
WINDOW    1       0.05     0.075    0.05     0.10
MESH WINDOW=1 ORIGINAL=0 DEFORMED=2 MARGIN=YES BCODE=ALL
SMOOTHING TYPE=AVERAGE
*BAND VAR=VONMISES TLENGTH=65
*BAND VAR=STRESS-ZZ TLENGTH=65
*BAND VAR=STRAIN-ZZ TLENGTH=65
BAND VAR=ACCUM_EFF_PLASTIC_STRAIN TLENGTH=65

NPOINT NAME=TIP NODE=8
PLIST POINTNAME=TIP VARIABLES=Y-DISPLACEMENT
*
END
```

B.2 Detailed results from numerical analysis

HY130 - E11018

relat thick	applied stress	Z-TRANSLATION NODE: 5, 6	ELEM	EFFECTIVE STRESS weld E11018 Yield=0.705E+09 Pa ult =0.774E+09 Pa		base HY130 =0.945E+09 Pa =0.986E+09 Pa
mm/mm	MPa			MPa		MPa
1/6	1E8	0.329710E-04		0.88882E+08		
	2E8	0.659420E-04		0.17776E+09		
	3E8	0.989130E-04		0.26665E+09		
	4E8	0.131884E-03		0.35553E+09		
	5E8	0.164855E-03		0.44441E+09		
	6E8	0.197826E-03		0.53329E+09		
	7E8	0.230797E-03		0.62217E+09		
	8E8	0.263831E-03		0.70506E+09*T	6	0.71504E+09
	9E8	0.297730E-03	8	0.70669E+09*T	6	0.86364E+09
	10E8	0.331644E-03	8	0.70833E+09*T	6	0.94520E+09*T
	10.2E8	0.338428E-03				
	10.3E8	0.341820E-03				
	10.5E8	0.370757E-03				
	10.6E8	0.407154E-03				
	10.7E8	0.488530E-03				
	10.8E8	0.648364E-03				
	11E8	0.149884E-02	8	0.76288E+09*T	3	0.98020E+09*T

HY130 - E11018

relat thick	applied stress	Z-TRANSLATION NODE: 5, 6	ELEM	EFFECTIVE STRESS weld E11018 Yield=0.705E+09 Pa ult =0.774E+09 Pa		base HY130 =0.945E+09 Pa =0.986E+09 Pa
mm/mm	MPa			MPa		MPa
2/6	1E8	0.329710E-04		0.88882E+08		
	2E8	0.659420E-04		0.17776E+09		
	3E8	0.989130E-04		0.26665E+09		
	4E8	0.131884E-03		0.35553E+09		
	5E8	0.164855E-03		0.44441E+09		
	6E8	0.197826E-03		0.53329E+09		
	7E8	0.230797E-03		0.62217E+09		
	8E8	0.263957E-03	7	0.70515E+09*T	1	0.71957E+09
	9E8	0.299752E-03	7	0.70741E+09*T	1	0.93551E+09
	9.5E8	0.319663E-03				
	10E8	0.355886E-03	6	0.71728E+09*T	1	0.94947E+09*
	10.2E8	0.415782E-03				
	10.3E8	0.453557E-03				
	10.5E8	0.537221E-03	3	0.75878E+09*T	1	0.97351E+09*T
	10.6E8	0.587655E-03	3	0.76809E+09*T	1	0.97905E+09*T
	10.7E8	0.687758E-03	4	0.77770E+09*FR	1	0.98497E+09*T

HY130 - E11018

relat thick	applied stress	Z-TRANSLATION NODE: 5, 6	ELEM	EFFECTIVE STRESS weld E11018 Yield=0.705E+09 Pa ult =0.774E+09 Pa		base HY130 =0.945E+09 Pa =0.986E+09 Pa
mm/mm	MPa			MPa		MPa
3/6	1E8	0.329710E-04		0.88882E+08		
	2E8	0.659420E-04		0.17776E+09		
	3E8	0.989130E-04		0.26665E+09		
	4E8	0.131884E-03		0.35553E+09		
	5E8	0.164855E-03		0.44441E+09		
	6E8	0.197826E-03		0.53329E+09		
	7E8	0.230797E-03		0.62217E+09		
	8E8	0.264175E-03	5	0.70522E+09*	1	0.72337E+09
	9E8	0.305335E-03	5	0.70996E+09*	10	0.94567E+09*T
	9.2E8	0.315292E-03				
	9.4E8	0.333258E-03				
	9.6E8	0.372848E-03				
	9.9E8	0.459450E-03				
	10E8	0.498953E-03	1	0.76680E+09*T	10	0.96537E+09*T
	10.1E8	0.538138E-03	1	0.77652E+09*FR	8	0.96884E+09*T

HY130 - E11018

relat thick	applied stress	Z-TRANSLATION NODE: 5, 6	ELEM	EFFECTIVE STRESS weld E11018 Yield=0.705E+09 Pa ult =0.774E+09 Pa		base HY130 =0.945E+09 Pa =0.986E+09 Pa
mm/mm	MPa			MPa		MPa
6/6	1E8	0.329710E-04		0.88882E+08		
	2E8	0.659420E-04		0.17776E+09		
	3E8	0.989130E-04		0.26665E+09		
	4E8	0.131884E-03		0.35553E+09		
	5E8	0.164855E-03		0.44441E+09		
	6E8	0.197826E-03		0.53329E+09		
	7E8	0.230797E-03				
	8E8	0.265456E-03				
	8.2E8	0.277086E-03				
	8.4E8	0.297621E-03				
	8.6E8	0.334276E-03				
	9E8	0.453412E-03	1	0.76078E+09*T	10	0.96339E+09
	9.1E8	0.491063E-03	1	0.77031E+09*T	10	0.96673E+09*T

E11018 ONLY

relat thick	applied stress	Z-TRANSLATION NODE: 5, 6	ELEM	EFFECTIVE STRESS weld E11018 Yield=0.705E+09 Pa ult =0.774E+09 Pa	
mm/mm	MPa			MPa	
inf/6	1E8	0.329710E-04		0.88882E+08	
	2E8	0.659420E-04		0.17776E+09	
	3E8	0.989130E-04		0.26665E+09	
	4E8	0.131884E-03		0.35553E+09	
	5E8	0.164855E-03		0.44441E+09	
	6E8	0.197826E-03		0.53329E+09	
	7E8	0.230797E-03		0.62217E+09	
	7.9E8	0.260471E-03		0.70217E+09	
	8E8	0.307393E-03		0.70566E+09	P
	8.1E8	0.435708E-03		0.70755E+09	
	8.9E8	0.455993E-02		0.77082E+09	P
	9E8	0.512255E-02		0.77947E+09	FAIL

HY130 ONLY

relat thick	applied stress	Z-TRANSLATION NODE: 5, 6	ELEM	EFFECTIVE STRESS HY130 Yield=0.945E+09 Pa ult =0.986E+09 Pa	
mm/mm	MPa			MPa	MPa
inf/6	1E8	0.329710E-04		0.88882E+08	
	2E8	0.659420E-04		0.17776E+09	
	3E8	0.989130E-04		0.26665E+09	
	4E8	0.131884E-03		0.35553E+09	
	5E8	0.164855E-03		0.44441E+09	
	6E8	0.197826E-03		0.53329E+09	
	7E8	0.230797E-03		0.62217E+09	
	8E8	0.263768E-03		0.71106E+09	
	10E8	0.329710E-03		0.88882E+09	
	10.2E8	0.336304E-03		0.90660E+09	
	10.4E8	0.342899E-03		0.92437E+09	
	10.5E8	0.346196E-03		0.93326E+09	
	10.6E8	0.349493E-03		0.94215E+09	
	10.67E8	0.371946E-03		0.94521E+09	
	10.7E8	0.388950E-03		0.94538E+09	P
	10.8E8	0.493551E-03		0.94645E+09	P
	11E8	0.123224E-02		0.95429E+09	P
	11.2E8	0.272139E-02		0.97029E+09	P
	11.3E8	0.351402E-02		0.97882E+09	P
	11.4E8	0.431247E-02		0.98741E+09	FR

HY130 - E8018

relat thick	applied stress	Z-TRANSLATION NODE: 5, 6	ELEM	EFFECTIVE STRESS weld E8018 Yield=0.574E+09 Pa ult =0.674E+09 Pa		base HY130 =0.945E+09 Pa =0.986E+09 Pa
mm/mm	MPa			MPa		MPa
0.5/6	1E8	0.329710E-04		0.88882E+08		
	2E8	0.659420E-04		0.17776E+09		
	3E8	0.989130E-04		0.26665E+09		
	4E8	0.131884E-03		0.35553E+09		
	5E8	0.164855E-03		0.44441E+09		
	6E8	0.197826E-03		0.53329E+09		
	7E8	0.230991E-03	9	0.57495E+09*T	7	0.64167E+09
	8E8	0.264323E-03	9	0.57676E+09*T	7	0.76688E+09
	9E8	0.297658E-03	9	0.57864E+09*T	8	0.89314E+09
	10E8	0.330996E-03	9	0.58057E+09*T	8	0.94522E+09*90%
	10.5E8	0.347666E-03	9	0.58156E+09*T	8	0.94541E+09*T
	10.6E8	0.351000E-03				
	10.7E8	0.452561E-03				
	10.8E8	0.594183E-03				
	10.9E8	0.885495E-03				
	11E8	0.143039E-02	9	0.64564E+09*T	6	0.97326E+09*T
	11.1E8	0.215418E-02	9	0.66511E+09*T	6	0.98173E+09*T
	11.2E8	0.292764E-02	9	0.68439E+09*FR	6	0.99029E+09*FR

HY130 - E8018

relat thick	applied stress	Z-TRANSLATION NODE: 5, 6	ELEM	EFFECTIVE STRESS weld E8018 Yield=0.574E+09 Pa ult =0.674E+09 Pa		base HY130 =0.945E+09 Pa =0.986E+09 Pa
mm/mm	MPa			MPa		MPa
1/6	1E8	0.329710E-04		0.88882E+08		
	2E8	0.659420E-04		0.17776E+09		
	3E8	0.989130E-04		0.26665E+09		
	4E8	0.131884E-03		0.35553E+09		
	5E8	0.164855E-03		0.44441E+09		
	6E8	0.197826E-03		0.53329E+09		
	7E8	0.231296E-03		0.57512E+09*T	6	0.65410E+09
	8E8	0.265201E-03		0.57745E+09*T	6	0.80357E+09
	9E8	0.299324E-03	8	0.58073E+09*T	6	0.94508E+09*30%
	9.5E8	0.317235E-03	8	0.58314E+09*T	6	0.94571E+09*T
	10E8	0.338062E-03	8	0.58838E+09*T	6	0.94715E+09*T
	10.2E8	0.355867E-03				
	10.3E8	0.384599E-03				
	10.4E8	0.417529E-03				
	10.5E8	0.451672E-03	7	0.62121E+09*T	3	0.96237E+09*T
	10.6E8	0.491612E-03				
	10.7E8	0.587088E-03				
	10.8E8	0.756721E-03	7	0.65845E+09*T	3	0.97884E+09*T

* Effective stress is equal or higher to yield strength.
The deformation is plastic.

HY130 - E8018

relat thick	applied stress	Z-TRANSLATION NODE:5, 6	ELEM	EFFECTIVE STRESS weld E8018 Yield=0.574E+09 Pa ult =0.674E+09 Pa		base HY130 =0.945E+09 Pa =0.986E+09 Pa
mm/mm	MPa			MPa		MPa
2/6	1E8	0.329710E-04		0.88882E+08		
	2E8	0.659420E-04		0.17776E+09		
	3E8	0.989130E-04		0.26665E+09		
	4E8	0.131884E-03		0.35553E+09		
	5E8	0.164855E-03		0.44441E+09		
	6E8	0.197826E-03		0.53329E+09		
	7E8	0.232304E-03	7	0.57568E+09*T	1	0.69006E+09
	7.5E8	0.250523E-03	6	0.57766E+09*T	1	0.80448E+09
	8E8	0.268818E-03	7	0.57987E+09*T	1	0.91913E+09*
	8.5E8	0.287887E-03	7	0.58281E+09*T	1	0.94568E+09*90%
	9E8	0.312456E-03	6	0.59015E+09*T	10	0.94759E+09*T
	9.2E8	0.325557E-03				
	9.3E8	0.332771E-03				
	9.4E8	0.350332E-03				
	9.5E8	0.368428E-03	5	0.60955E+09*T	1	0.95375E+09*T
	9.6E8	0.393847E-03				
	9.7E8	0.418358E-03				
	9.8E8	0.445127E-03				
	9.9E8	0.473590E-03				
	10E8	0.504234E-03	3	0.65966E+09*T	1	0.97241E+09*T
	10.1E8	0.537553E-03	3	0.67045E+09*T	1	0.97669E+09*T
	10.2E8	0.574585E-03	3	0.68137E+09*FR	1	0.98117E+09*FR

HY130 - E8018

relat thick	applied stress	Z-TRANSLATION NODE:5, 6	ELEM	MAX EFFECTIVE STRESS weld E8018 Yield=0.574E+09 Pa ult =0.674E+09 Pa		base HY130 =0.945E+09 Pa =0.986E+09 Pa
mm/mm	MPa			MPa		MPa
3/6	1E8	0.329710E-04	1	0.88882E+08	1	0.88882E+08
	2E8	0.659420E-04	1	0.17776E+09	1	0.17776E+09
	3E8	0.989130E-04	1	0.26665E+09	1	0.26665E+09
	4E8	0.131884E-03	1	0.35553E+09	1	0.35553E+09
	5E8	0.164855E-03	1	0.44441E+09	1	0.44441E+09
	6E8	0.197826E-03	1	0.53329E+09	1	0.53329E+09
	7E8	0.234053E-03	6	0.57640E+09*T	1	0.72124E+09
	7.5E8	0.255417E-03	5	0.58057E+09*T	10	0.91350E+09
	7.8E8	0.268432E-03	5	0.58318E+09*T	10	0.94544E+09*40%
	8E8	0.280057E-03	4	0.58689E+09*T	1	0.94717E+09*T
	8.2E8	0.292304E-03				
	8.5E8	0.322637E-03	1	0.60623E+09*T	10	0.95375E+09*T
	9E8	0.411821E-03	1	0.65223E+09*T	10	0.96459E+09*T
	9.1E8	0.435836E-03				
	9.2E8	0.460204E-03	1	0.67332E+09*T	10	0.96929E+09*T
	9.21E8	0.462753E-03	1	0.67436E+09*T	10	0.96952E+09*T
	9.3E8	0.486403E-03	1	0.68380E+09*FR	10	0.97165E+09*T

* Effective stress is equal or higher to yield strength.
The deformation is plastic.

HY130 - E8018

relat thick	applied stress	Z-TRANSLATION NODE: 5, 6	ELEM	MAX EFFECTIVE STRESS weld E8018 Yield=0.574E+09 Pa ult =0.674E+09 Pa		base HY130 =0.945E+09 Pa =0.986E+09 Pa
mm/mm	MPa			MPa		MPa
4/6	1E8	0.329710E-04	1	0.88882E+08	1	0.88882E+08
	2E8	0.659420E-04	1	0.17776E+09	1	0.17776E+09
	3E8	0.989130E-04	1	0.26665E+09	1	0.26665E+09
	4E8	0.131884E-03	1	0.35553E+09	1	0.35553E+09
	5E8	0.164855E-03	1	0.44441E+09	1	0.44441E+09
	6E8	0.197826E-03	1	0.53329E+09	1	0.53329E+09
	6.3E8	0.207717E-03	1	0.55996E+09	1	0.55996E+09
	6.5E8	0.214756E-03	1	0.57425E+09*T	10	0.58738E+09
	7E8	0.238546E-03	4	0.57881E+09*T	10	0.82034E+09
	7.5E8	0.269546E-03	1	0.58938E+09*T	10	0.94752E+09*30%
	7.7E8	0.286052E-03	1	0.59725E+09*T	10	0.95012E+09*T
	8E8	0.327637E-03	1	0.62069E+09*T	10	0.95704E+09*T
	8.5E8	0.423338E-03	1	0.66702E+09*T	10	0.96905E+09*T
	8.6E8	0.446386E-03	1	0.67707E+09*FR	10	0.97150E+09*T

HY130 - E8018

relat thick	applied stress	Z-TRANSLATION NODE:5, 6	ELEM	MAX EFFECTIVE STRESS weld E8018 Yield=0.574E+09 Pa ult =0.674E+09 Pa		base HY130 =0.945E+09 Pa =0.986E+09 Pa
mm/mm	MPa			MPa		MPa
6/6	1E8	0.329710E-04	1	0.88882E+08	1	0.88882E+08
	2E8	0.659420E-04	1	0.17776E+09	1	0.17776E+09
	3E8	0.989130E-04	1	0.26665E+09	1	0.26665E+09
	4E8	0.131884E-03	1	0.35553E+09	1	0.35553E+09
	5E8	0.164855E-03	1	0.44441E+09	1	0.44441E+09
	6E8	0.197826E-03	1	0.53329E+09	1	0.53329E+09
	6.5E8	0.215327E-03	1	0.57449E+09*T	10	0.59434E+09
	6.7E8	0.226842E-03				
	6.8E8	0.237649E-03				
	7E8	0.261719E-03	1	0.59191E+09*T	10	0.94644E+09*10%
	7.2E8	0.293487E-03				
	7.5E8	0.353224E-03	1	0.63160E+09*T	10	0.95713E+09*60%
	7.7E8	0.400476E-03				
	7.8E8	0.425954E-03	1	0.66007E+09*T	10	0.96478E+09*T
	7.9E8	0.452605E-03	1	0.66990E+09*T	10	0.96739E+09*T
	8E8	0.480424E-03	1	0.67985E+09*FR	10	0.97000E+09*T

* Effective stress is equal or higher to yield strength.
The deformation is plastic.

E8018 - ONLY

relat thick	applied stress	Z-TRANSLATION NODE:5, 6	ELEM	MAX EFFECTIVE STRESS weld E8018 Yield=0.574E+09 Pa ult =0.674E+09 Pa
mm/mm	MPa			MPa
inf/6	1E8	0.329710E-04	1	0.88882E+08
	2E8	0.659420E-04	1	0.17776E+09
	3E8	0.989130E-04	1	0.26665E+09
	4E8	0.131884E-03	1	0.35553E+09
	5E8	0.164855E-03	1	0.44441E+09
	6E8	0.197826E-03	1	0.53329E+09
	6.3E8	0.207717E-03	1	0.55996E+09
	6.4E8	0.211014E-03	1	0.56884E+09
	6.5E8	0.235336E-03	1	0.57445E+09*T
	6.6E8	0.347985E-03	1	0.57677E+09*T
	6.7E8	0.592473E-03	1	0.58195E+09*T
	7E8	0.173340E-02	1	0.60642E+09*T
	7.5E8	0.373966E-02	1	0.64957E+09*T
	7.7E8	0.454414E-02	1	0.66688E+09*T
	7.8E8	0.494647E-02	1	0.67553E+09*FR

HY100 - E8018

relat thick	applied stress	Z-TRANSLATION NODE:5, 6	ELEM	MAX EFFECTIVE STRESS weld E8018 Yield=0.574E+09 Pa ult =0.674E+09 Pa		base HY100 =0.724E+09 Pa =0.814E+09 Pa
mm/mm	MPa			MPa		MPa
1/6	1E8	0.329710E-04	1	0.88882E+08	1	0.88882E+08
	2E8	0.659420E-04	1	0.17776E+09	1	0.17776E+09
	3E8	0.989130E-04	1	0.26665E+09	1	0.26665E+09
	4E8	0.131884E-03	1	0.35553E+09	1	0.35553E+09
	5E8	0.164855E-03	1	0.44441E+09	1	0.44441E+09
	6E8	0.197826E-03	1	0.53329E+09	1	0.53329E+09
	7E8	0.231296E-03	8	0.57519E+09*	6	0.65410E+09
	8E8	0.265201E-03	8	0.57745E+09*	6	0.72447E+09*
	8.1E8	0.268592E-03				
	8.15E8	0.295511E-03				
	8.2E8	0.339033E-03				
	8.25E8	0.390414E-03				
	8.3E8	0.459148E-03				
	8.4E8	0.679133E-03				
	8.6E8	0.137800E-02				
	9E8	0.296457E-02	8	0.66563E+09*	4	0.80471E+09*
	9.1E8	0.336559E-02	8	0.67536E+09*FR	4	0.81362E+09*

HY100 - E8018

relat thick	applied stress	Z-TRANSLATION NODE:5, 6	ELEM	MAX EFFECTIVE STRESS weld E8018 Yield=0.574E+09 Pa ult =0.674E+09 Pa		base HY100 =0.724E+09 Pa =0.814E+09 Pa
mm/mm	MPa			MPa		MPa
2/6	1E8	0.329710E-04	1	0.88882E+08	1	0.88882E+08
	2E8	0.659420E-04	1	0.17776E+09	1	0.17776E+09
	3E8	0.989130E-04	1	0.26665E+09	1	0.26665E+09
	4E8	0.131884E-03	1	0.35553E+09	1	0.35553E+09
	5E8	0.164855E-03	1	0.44441E+09	1	0.44441E+09
	6E8	0.197826E-03	1	0.53329E+09	1	0.53329E+09
	7E8	0.232304E-03	7	0.57568E+09*	1	0.69006E+09
	7.7E8	0.261135E-03				
	7.8E8	0.274646E-03				
	7.9E8	0.297313E-03				
	8E8	0.321494E-03	4	0.59892E+09*	1	0.74269E+09*
	8.1E8	0.350782E-03				
	8.2E8	0.417363E-03				
	8.3E8	0.549233E-03				
	8.4E8	0.774407E-03				
	8.6E8	0.147640E-02	5	0.65511E+09*	1	0.79223E+09*
	8.7E8	0.186690E-02	5	0.66490E+09*	1	0.80108E+09*
	8.8E8	0.226309E-02	5	0.67459E+09*FR	1	0.80991E+09*

HY100 - E8018

relat thick	applied stress	Z-TRANSLATION NODE:5, 6	ELEM	MAX EFFECTIVE STRESS weld E8018 Yield=0.574E+09 Pa ult =0.674E+09 Pa		base HY100 =0.724E+09 Pa =0.814E+09 Pa
mm/mm	MPa			MPa		MPa
3/6	1E8	0.329710E-04	1	0.88882E+08	1	0.88882E+08
	2E8	0.659420E-04	1	0.17776E+09	1	0.17776E+09
	3E8	0.989130E-04	1	0.26665E+09	1	0.26665E+09
	4E8	0.131884E-03	1	0.35553E+09	1	0.35553E+09
	5E8	0.164855E-03	1	0.44441E+09	1	0.44441E+09
	6E8	0.197826E-03	1	0.53329E+09	1	0.53329E+09
	7E8	0.234053E-03	5	0.57648E+09*	1	0.72124E+09
	7.2E8	0.243397E-03				
	7.4E8	0.253920E-03				
	7.6E8	0.287718E-03				
	7.8E8	0.335858E-03				
	8E8	0.397446E-03	1	0.63333E+09*	1	0.75515E+09*
	8.1E8	0.434427E-03				
	8.2E8	0.504735E-03				
	8.3E8	0.642009E-03				
	8.4E8	0.869675E-03	1	0.67148E+09*	1	0.78706E+09*
	8.5E8	0.119757E-02	1	0.68077E+09*FR		
	8.6E8	0.157248E-02	FRACTURE			

HY100 - E8018

relat thick	applied stress	Z-TRANSLATION NODE:5, 6	ELEM	MAX EFFECTIVE STRESS weld E8018 Yield=0.574E+09 Pa ult =0.674E+09 Pa		base HY100 =0.724E+09 Pa =0.814E+09 Pa
mm/mm	MPa			MPa		MPa
6/6	1E8	0.329710E-04	1	0.88882E+08	1	0.88882E+08
	2E8	0.659420E-04	1	0.17776E+09	1	0.17776E+09
	3E8	0.989130E-04	1	0.26665E+09	1	0.26665E+09
	4E8	0.131884E-03	1	0.35553E+09	1	0.35553E+09
	5E8	0.164855E-03	1	0.44441E+09	1	0.44441E+09
	6E8	0.197826E-03	1	0.53329E+09	1	0.53329E+09
	6.6E8	0.221067E-03				
	6.7E8	0.226842E-03				
	6.9E8	0.253147E-03				
	7E8	0.270584E-03	1	0.59629E+09*	10	0.73344E+09*
	7.2E8	0.320886E-03				
	7.4E8	0.382834E-03				
	7.5E8	0.417917E-03				
	7.6E8	0.455853E-03	1	0.65632E+09*	10	0.76327E+09*
	7.7E8	0.496158E-03	1	0.66649E+09*	10	0.76814E+09*
	7.8E8	0.537984E-03	FRACTURE			

E8018 - ONLY

relat thick	applied stress	Z-TRANSLATION NODE:5, 6	ELEM	MAX EFFECTIVE STRESS weld E8018 Yield=0.574E+09 Pa ult =0.674E+09 Pa	
mm/mm	MPa			MPa	MPa
inf/6	1E8	0.329710E-04	1	0.88882E+08	
	2E8	0.659420E-04	1	0.17776E+09	
	3E8	0.989130E-04	1	0.26665E+09	
	4E8	0.131884E-03	1	0.35553E+09	
	5E8	0.164855E-03	1	0.44441E+09	
	6E8	0.197826E-03	1	0.53329E+09	
	6.3E8	0.207717E-03	1	0.55996E+09	
	6.4E8	0.211014E-03	1	0.56884E+09	
	6.5E8	0.235336E-03	1	0.57445E+09*T	
	6.6E8	0.347985E-03	1	0.57677E+09*T	
	6.7E8	0.592473E-03	1	0.58195E+09*T	
	7E8	0.173340E-02	1	0.60642E+09*T	
	7.5E8	0.373966E-02	1	0.64957E+09*T	
	7.7E8	0.454414E-02	1	0.66688E+09*T	
	7.8E8	0.494647E-02	1	0.67553E+09*FR	

HY100 ONLY

relat thick	applied stress	Z-TRANSLATION NODE:5, 6	ELEM	MAX EFFECTIVE STRESS HY100 Yield=0.724E+09 Pa ult =0.814E+09 Pa
mm/mm	MPa			MPa
0/6	1E8	0.329710E-04	1	0.88882E+08
	2E8	0.659420E-04	1	0.17776E+09
	3E8	0.989130E-04	1	0.26665E+09
	4E8	0.131884E-03	1	0.35553E+09
	5E8	0.164855E-03	1	0.44441E+09
	6E8	0.197826E-03	1	0.53329E+09
	7E8	0.230797E-03	1	0.62217E+09
	8E8	0.263768E-03	1	0.71106E+09
	8.1E8	0.267065E-03		
	8.15E8	0.270889E-03		
	8.2E8	0.297582E-03		
	8.3E8	0.393775E-03		
	8.4E8	0.593913E-03		
	8.6E8	0.128365E-02		
	9E8	0.286932E-02	1	0.77958E+09*
	9.3E8	0.407391E-02	1	0.80549E+09*
	9.4E8	0.447593E-02	1	0.81414E+09* FR

Joint yield strength

Relative Thickness	HY130-E8018	HY130-E11018	HY100-E8018
0	10.80E8	10.80E8	8.32E8
0.083	10.74E8		
0.167	10.61E8	10.72E8	8.27E8
0.333	9.92E8	10.40E8	8.20E8
0.5	9.17E8	9.95E8	8.05E8
0.667	8.54E8		
1.0	7.72E8	8.98E8	7.43E8

ADINA-PLOT VERSION 6.1.4, 6 APRIL 1995
Relative thickness = 0.33

ADINA ORIGINAL
LOAD_STEP
TIME 1.000 0.0003308

XVMIN 0.000
XVMAX 0.006000
YVMIN 0.000
YVMAX 0.01000

C	12	207	208	209	210	211	212	213	214	215	31
C	11	198	199	200	201	202	203	204	205	206	30
C	10	189	190	191	192	193	194	195	196	197	29
C	9	180	181	182	183	184	185	186	187	188	28
C	8	171	172	173	174	175	176	177	178	179	27
C	7	162	163	164	165	166	167	168	169	170	26
C	4	153	154	155	156	157	158	159	160	161	3
C	142	143	144	145	146	147	148	149	150	151	152
C	131	132	133	134	135	136	137	138	139	140	141
C	120	121	122	123	124	125	126	127	128	129	130
C	109	110	111	112	113	114	115	116	117	118	119
C	98	99	100	101	102	103	104	105	106	107	108
C	87	88	89	90	91	92	93	94	95	96	97
C	76	77	78	79	80	81	82	83	84	85	86
C	65	66	67	68	69	70	71	72	73	74	75
C	54	55	56	57	58	59	60	61	62	63	64
D	1 B	45 B	46 B	47 B	48 B	49 B	50 B	51 B	52 B	53 B	2

	U_2	U_3
B	/	-
C	-	/
D	-	-

RESTRAINT CRACKING TEST SPECIMEN

HY100 - 1st:E8018 - 2nd:E11018

applied stress	Z-TRANSLATION NODE: 18	NODE	EQUIVAL PLASTIC STRAIN	PLASTIC STRAIN-ZZ	TOTAL STRAIN-ZZ
Pa	m				
2E8	1.38450E-04	348	4.80925E-03	4.37663E-03	7.30773E-03
3E8	2.08416E-04	348	1.26413E-02	1.07474E-02	1.33279E-02
3.4E8	2.36844E-04	348	1.62110E-02	1.36165E-02	1.62087E-02
3.6E8	2.51267E-04	348	1.83837E-02	1.53676E-02	1.80160E-02
3.8E8	2.65895E-04	348	2.09251E-02	1.74105E-02	2.01183E-02
4E8	2.80663E-04	348	2.39954E-02	1.98624E-02	2.26325E-02
4.2E8	2.95635E-04	348	2.75897E-02	2.27129E-02	2.55566E-02
4.4E8	3.10879E-04	348	3.16545E-02	2.59137E-02	2.88445E-02
4.6E8	3.26674E-04	348	3.65596E-02	2.97422E-02	3.27810E-02
4.8E8	3.44293E-04	348	4.33536E-02	3.49922E-02	3.81849E-02
5E8	3.66270E-04	348	5.47792E-02	4.37025E-02	4.71439E-02
5.2E8	3.98684E-04	348	7.69192E-02	6.02100E-02	6.40866E-02
5.4E8	4.47679E-04	348	1.13876E-01	8.72326E-02	9.17916E-02
5.6E8	5.13987E-04	348	1.59519E-01	1.20590E-01	1.26271E-01
5.8E8	6.05224E-04	393	2.46637E-01	1.64981E-01	1.77430E-01
6E8	7.29713E-04	393	3.79117E-01	2.58678E-01	2.74695E-01
6.2E8	8.85159E-04	393	5.47840E-01	3.81931E-01	4.02030E-01
6.4E8	1.06933E-03	393	7.48477E-01	5.31194E-01	5.55647E-01
6.6E8	1.29432E-03	393	9.89942E-01	7.12756E-01	7.41991E-01
6.8E8	1.56363E-03	393	1.26918E+00	9.24418E-01	9.58880E-01
7E8	1.87749E-03	393	1.58614E+00	1.16649E+00	1.20660E+00
7.2E8	2.23936E-03	393	1.94499E+00	1.44260E+00	1.48894E+00
7.4E8	2.65428E-03	393	2.34221E+00	1.75008E+00	1.80316E+00
7.6E8	3.12404E-03	393	2.77268E+00	2.08476E+00	2.14497E+00

HY100 - 1st:E11018 - 2nd:E11018

2E8	1.38355E-04	348	3.49183E-03	3.27126E-03	6.91778E-03
3E8	2.07966E-04	348	1.02419E-02	9.02376E-03	1.23877E-02
3.4E8	2.35994E-04	348	1.36168E-02	1.18268E-02	1.51606E-02
3.6E8	2.50084E-04	393	1.55668E-02	1.25722E-02	1.71685E-02
3.8E8	2.64264E-04	393	1.80084E-02	1.43518E-02	1.90564E-02
4E8	2.78574E-04	393	2.08029E-02	1.63661E-02	2.12152E-02
4.2E8	2.93063E-04	393	2.40441E-02	1.86765E-02	2.36959E-02
4.4E8	3.07768E-04	393	2.76286E-02	2.12032E-02	2.64037E-02
4.6E8	3.22830E-04	393	3.16554E-02	2.40143E-02	2.94129E-02
4.8E8	3.38359E-04	393	3.63260E-02	2.72497E-02	3.28759E-02
5E8	3.54623E-04	393	4.20262E-02	3.11719E-02	3.70705E-02
5.2E8	3.74902E-04	393	5.24343E-02	3.82882E-02	4.46415E-02
5.4E8	4.06480E-04	393	7.46939E-02	5.35787E-02	6.08368E-02
5.6E8	4.60530E-04	393	1.24163E-01	8.70178E-02	9.60152E-02
5.8E8	5.36734E-04	393	1.96869E-01	1.35514E-01	1.46837E-01
6E8	6.39897E-04	393	2.99376E-01	2.03876E-01	2.18174E-01
6.2E8	7.69019E-04	393	4.32008E-01	2.94109E-01	3.11808E-01
6.4E8	9.34940E-04	393	6.12628E-01	4.22327E-01	4.43838E-01
6.6E8	1.13576E-03	393	8.28126E-01	5.78422E-01	6.04344E-01
6.8E8	1.37540E-03	393	1.07526E+00	7.59849E-01	7.90613E-01
7E8	1.65729E-03	393	1.35652E+00	9.68947E-01	1.00494E+00
7.2E8	1.98160E-03	393	1.67186E+00	1.20613E+00	1.24785E+00
7.4E8	2.36164E-03	393	2.03229E+00	1.48010E+00	1.52818E+00
7.6E8	2.79649E-03	393	2.42737E+00	1.78246E+00	1.83736E+00

HY100 - 1st:E8018 - 2nd:E8018

2E8	1.38450E-04	348	4.80925E-03	4.37663E-03	7.30773E-03
3E8	2.08416E-04	348	1.26413E-02	1.07474E-02	1.33279E-02
3.4E8	2.36844E-04	348	1.62110E-02	1.36165E-02	1.62087E-02
3.6E8	2.51267E-04	348	1.83837E-02	1.53676E-02	1.80160E-02
3.8E8	2.65910E-04	348	2.09291E-02	1.74143E-02	2.01234E-02
4E8	2.80913E-04	348	2.41219E-02	1.99728E-02	2.27609E-02
4.2E8	2.96616E-04	348	2.83232E-02	2.33262E-02	2.62236E-02
4.4E8	3.15642E-04	348	3.63138E-02	2.96459E-02	3.27280E-02
4.6E8	3.36383E-04	348	4.70387E-02	3.79619E-02	4.12370E-02
4.8E8	3.59470E-04	348	6.06206E-02	4.82512E-02	5.17563E-02
5E8	3.92027E-04	348	8.37878E-02	6.53328E-02	6.92218E-02
5.2E8	4.41147E-04	348	1.22518E-01	9.32723E-02	9.78876E-02
5.4E8	5.04342E-04	348	1.69173E-01	1.26773E-01	1.32515E-01
5.6E8	5.88443E-04	393	2.25085E-01	1.50545E-01	1.62484E-01
5.8E8	7.07172E-04	393	3.51978E-01	2.42804E-01	2.57921E-01
6E8	8.59185E-04	393	5.21672E-01	3.68940E-01	3.88195E-01
6.2E8	1.04170E-03	393	7.22375E-01	5.19330E-01	5.43232E-01
6.4E8	1.25676E-03	393	9.54367E-01	6.94458E-01	7.23335E-01
6.6E8	1.51583E-03	393	1.22556E+00	9.01136E-01	9.35337E-01
6.8E8	1.82545E-03	393	1.54152E+00	1.14411E+00	1.18402E+00
7E8	2.18192E-03	393	1.89856E+00	1.42020E+00	1.46634E+00
7.2E8	2.58921E-03	393	2.29827E+00	1.73096E+00	1.78391E+00
7.4E8	3.05232E-03	393	2.73205E+00	2.06964E+00	2.12979E+00
7.6E8	3.57940E-03	393	3.19931E+00	2.43621E+00	2.50389E+00

E8018 - 1st:E8018 - 2nd:E8018

2E8	1.38456E-04	348	4.81091E-03	4.38988E-03	7.34604E-03
3E8	2.08536E-04	393	1.39761E-02	1.10686E-02	1.49428E-02
3.4E8	2.37344E-04	393	2.04766E-02	1.57481E-02	1.99410E-02
3.6E8	2.52168E-04	393	2.44536E-02	1.85664E-02	2.29549E-02
3.8E8	2.67474E-04	394	1.64578E-02	1.20503E-02	1.40267E-02
4E8	2.83522E-04	393	3.51153E-02	2.60055E-02	3.09143E-02
4.2E8	3.03234E-04	393	4.58406E-02	3.34142E-02	3.88042E-02
4.4E8	3.41825E-04	393	7.87191E-02	5.61759E-02	6.30129E-02
4.6E8	4.06481E-04	393	1.38370E-01	9.61624E-02	1.05148E-01
4.8E8	4.98893E-04	393	2.23444E-01	1.51635E-01	1.63326E-01
5E8	6.14544E-04	393	3.33525E-01	2.23078E-01	2.37876E-01
5.2E8	7.53630E-04	393	4.64995E-01	3.09660E-01	3.27816E-01
5.4E8	9.25347E-04	393	6.24804E-01	4.16759E-01	4.38642E-01
5.6E8	1.14911E-03	393	8.39440E-01	5.67356E-01	5.93348E-01
5.8E8	1.41488E-03	393	1.08709E+00	7.47286E-01	7.77768E-01
6E8	1.72757E-03	393	1.36987E+00	9.57518E-01	9.93009E-01
6.2E8	2.09446E-03	393	1.69214E+00	1.20006E+00	1.24120E+00
6.4E8	2.57831E-03	393	2.07404E+00	1.49000E+00	1.53773E+00
6.6E8	3.56214E-03	393	2.53080E+00	1.83987E+00	1.89526E+00
6.8E8	5.44963E-03	393	3.07167E+00	2.25603E+00	2.32039E+00
7E8	7.74232E-03	393	3.66358E+00	2.71101E+00	2.78525E+00
7.2E8	1.02812E-02	393	4.29578E+00	3.19706E+00	3.28174E+00
7.4E8	1.31030E-02	393	4.97031E+00	3.71801E+00	3.81349E+00
7.6E8	3.61439E-02	393	7.71438E+00	5.97936E+00	6.10718E+00

HY100 - 1st:HY100 - 2nd:HY100

2E8	1.38348E-04	348	3.33163E-03	3.13156E-03	6.88486E-03
3E8	2.07939E-04	348	9.88173E-03	8.74682E-03	1.22479E-02
3.4E8	2.35937E-04	348	1.31745E-02	1.15054E-02	1.49920E-02
3.6E8	2.50007E-04	393	1.53381E-02	1.24585E-02	1.72063E-02
3.8E8	2.64167E-04	393	1.79243E-02	1.43536E-02	1.92149E-02
4E8	2.78455E-04	393	2.08594E-02	1.64791E-02	2.14910E-02
4.2E8	2.92896E-04	393	2.42355E-02	1.88970E-02	2.40868E-02
4.4E8	3.07551E-04	393	2.79510E-02	2.15288E-02	2.69048E-02
4.6E8	3.22530E-04	393	3.21731E-02	2.44939E-02	3.00820E-02
4.8E8	3.37907E-04	393	3.70408E-02	2.78894E-02	3.37202E-02
5E8	3.53860E-04	393	4.28366E-02	3.19088E-02	3.80241E-02
5.2E8	3.71496E-04	393	5.08770E-02	3.74553E-02	4.39490E-02
5.4E8	3.98104E-04	393	7.00821E-02	5.07234E-02	5.80606E-02
5.6E8	4.44772E-04	393	1.13738E-01	8.05041E-02	8.94238E-02
5.8E8	5.13341E-04	393	1.80218E-01	1.24638E-01	1.35750E-01
6E8	6.06663E-04	393	2.73315E-01	1.85620E-01	1.99475E-01
6.2E8	7.21884E-04	393	3.89424E-01	2.61583E-01	2.78588E-01
6.4E8	8.58843E-04	393	5.29354E-01	3.54705E-01	3.75091E-01
6.6E8	1.03733E-03	393	7.19204E-01	4.84832E-01	5.09152E-01
6.8E8	1.25413E-03	393	9.36623E-01	6.37441E-01	6.66119E-01
7E8	1.50901E-03	393	1.18496E+00	8.16106E-01	8.49546E-01
7.2E8	1.80539E-03	393	1.46863E+00	1.02444E+00	1.06315E+00
7.4E8	2.15017E-03	393	1.79239E+00	1.26519E+00	1.30984E+00
7.6E8	2.55387E-03	393	2.15803E+00	1.53988E+00	1.59106E+00

****

HY130 - 1st:E8018 - 2nd:E11018

2E8	1.38449E-04	348	4.81140E-03	4.37850E-03	7.30962E-03
3E8	2.08411E-04	348	1.26262E-02	1.07133E-02	1.32576E-02
3.4E8	2.36832E-04	348	1.60893E-02	1.34707E-02	1.59723E-02
3.6E8	2.51245E-04	348	1.80958E-02	1.50706E-02	1.75893E-02
3.8E8	2.65851E-04	348	2.04211E-02	1.69237E-02	1.94749E-02
4E8	2.80564E-04	348	2.31262E-02	1.90670E-02	2.16436E-02
4.2E8	2.95431E-04	348	2.62364E-02	2.15115E-02	2.41053E-02
4.4E8	3.10465E-04	348	2.96745E-02	2.41932E-02	2.68047E-02
4.6E8	3.25803E-04	348	3.36471E-02	2.72693E-02	2.99079E-02
4.8E8	3.41850E-04	348	3.86735E-02	3.11329E-02	3.38209E-02
5E8	3.60704E-04	348	4.72670E-02	3.76597E-02	4.04357E-02
5.2E8	3.80525E-04	348	5.79184E-02	4.55885E-02	4.84451E-02
5.4E8	4.01369E-04	366	7.23919E-02	6.28297E-02	6.58972E-02
5.6E8	4.23585E-04	366	8.60966E-02	7.47718E-02	7.80404E-02
5.8E8	4.48390E-04	366	1.03018E-01	8.95630E-02	9.31439E-02
6E8	4.80166E-04	366	1.28269E-01	1.11696E-01	1.15816E-01
6.2E8	5.28060E-04	366	1.72937E-01	1.51043E-01	1.56422E-01
6.4E8	5.96058E-04	366	2.36119E-01	2.06907E-01	2.14495E-01
6.6E8	6.91369E-04	366	3.16105E-01	2.77731E-01	2.88500E-01
6.8E8	8.08965E-04	375	4.15819E-01	3.50090E-01	3.65321E-01
7E8	9.49484E-04	393	5.55798E-01	3.96418E-01	4.16262E-01
7.2E8	1.11634E-03	393	7.46777E-01	5.47080E-01	5.71340E-01
7.4E8	1.31194E-03	393	9.72969E-01	7.24940E-01	7.54480E-01
7.6E8	1.53838E-03	393	1.23199E+00	9.28639E-01	9.63902E-01
7.8E8	1.80256E-03	393	1.52893E+00	1.16290E+00	1.20412E+00
8E8	2.11952E-03	393	1.87976E+00	1.43985E+00	1.48748E+00
8.2E8	2.48185E-03	393	2.27092E+00	1.74834E+00	1.80287E+00
8.4E8	2.89084E-03	393	2.69777E+00	2.08505E+00	2.14685E+00
8.6E8	3.33940E-03	393	3.15359E+00	2.44472E+00	2.51406E+00
8.8E8	3.82229E-03	393	3.63383E+00	2.82388E+00	2.90095E+00

HY130 - 1st:E11018 - 2nd:E11018

2E8	1.38354E-04	348	3.49552E-03	3.27455E-03	6.92109E-03
3E8	2.07944E-04	348	1.02212E-02	8.96454E-03	1.22472E-02
3.4E8	2.35944E-04	348	1.33109E-02	1.14873E-02	1.46466E-02
3.6E8	2.50010E-04	348	1.48231E-02	1.27061E-02	1.58179E-02
3.8E8	2.64128E-04	348	1.64553E-02	1.40109E-02	1.70906E-02
4E8	2.78324E-04	348	1.81444E-02	1.53541E-02	1.84198E-02
4.2E8	2.92626E-04	348	1.99642E-02	1.68011E-02	1.98733E-02
4.4E8	3.07046E-04	348	2.20138E-02	1.84345E-02	2.15430E-02
4.6E8	3.21655E-04	348	2.44058E-02	2.03493E-02	2.35292E-02
4.8E8	3.36503E-04	348	2.72270E-02	2.26087E-02	2.58678E-02
5E8	3.51718E-04	348	3.06255E-02	2.53204E-02	2.86533E-02
5.2E8	3.68193E-04	357	3.55443E-02	3.11565E-02	3.48887E-02
5.4E8	3.87251E-04	366	4.55761E-02	3.96909E-02	4.30280E-02
5.6E8	4.07402E-04	366	5.68757E-02	4.95008E-02	5.29808E-02
5.8E8	4.29001E-04	366	6.94944E-02	6.04891E-02	6.41738E-02
6E8	4.52818E-04	366	8.44949E-02	7.35870E-02	7.75224E-02
6.2E8	4.81099E-04	366	1.04491E-01	9.10954E-02	9.54346E-02
6.4E8	5.26256E-04	366	1.43446E-01	1.25380E-01	1.30770E-01
6.6E8	5.91025E-04	366	2.00731E-01	1.76037E-01	1.83391E-01
6.8E8	6.83162E-04	366	2.77103E-01	2.43717E-01	2.54073E-01
7E8	8.02414E-04	384	3.87474E-01	3.01548E-01	3.17500E-01
7.2E8	9.47474E-04	393	5.43777E-01	3.89958E-01	4.10125E-01
7.4E8	1.12158E-03	393	7.45490E-01	5.44800E-01	5.69683E-01
7.6E8	1.32530E-03	393	9.81003E-01	7.26131E-01	7.56242E-01
7.8E8	1.56413E-03	393	1.25327E+00	9.36339E-01	9.72135E-01
8E8	1.84790E-03	393	1.56893E+00	1.18041E+00	1.22243E+00
8.2E8	2.17740E-03	393	1.92502E+00	1.45682E+00	1.50545E+00
8.4E8	2.55300E-03	393	2.31678E+00	1.76214E+00	1.81770E+00
8.6E8	2.97371E-03	393	2.74190E+00	2.09421E+00	2.15708E+00
8.8E8	3.43167E-03	393	3.19477E+00	2.44869E+00	2.51912E+00

HY130 - 1st:E8018 - 2nd:E8018

2E8	1.38449E-04	348	4.81140E-03	4.37850E-03	7.30962E-03
3E8	2.08411E-04	348	1.26262E-02	1.07133E-02	1.32576E-02
3.4E8	2.36832E-04	348	1.60893E-02	1.34707E-02	1.59723E-02
3.6E8	2.51245E-04	348	1.80958E-02	1.50706E-02	1.75893E-02
3.8E8	2.65866E-04	348	2.04253E-02	1.69278E-02	1.94802E-02
4E8	2.80809E-04	348	2.32548E-02	1.91793E-02	2.17747E-02
4.2E8	2.96350E-04	366	2.70340E-02	2.35869E-02	2.62338E-02
4.4E8	3.14631E-04	366	3.59924E-02	3.13058E-02	3.39688E-02
4.6E8	3.33644E-04	366	4.57274E-02	3.97077E-02	4.24225E-02
4.8E8	3.53268E-04	366	5.61343E-02	4.87160E-02	5.15431E-02
5E8	3.73883E-04	366	6.75780E-02	5.86552E-02	6.16635E-02
5.2E8	3.95772E-04	366	8.05207E-02	6.99188E-02	7.31153E-02
5.4E8	4.19559E-04	366	9.57919E-02	8.32400E-02	8.66764E-02
5.6E8	4.46652E-04	366	1.14960E-01	1.00022E-01	1.03850E-01
5.8E8	4.80597E-04	366	1.42482E-01	1.24187E-01	1.28658E-01
6E8	5.29914E-04	366	1.88831E-01	1.65060E-01	1.70889E-01
6.2E8	5.98331E-04	366	2.52549E-01	2.21445E-01	2.29530E-01
6.4E8	6.96466E-04	366	3.35342E-01	2.94832E-01	3.06244E-01
6.6E8	8.17008E-04	384	4.29177E-01	3.29459E-01	3.46076E-01
6.8E8	9.60412E-04	393	5.76233E-01	4.09950E-01	4.30584E-01
7E8	1.12923E-03	393	7.69330E-01	5.63212E-01	5.88254E-01
7.2E8	1.32724E-03	393	9.99091E-01	7.45117E-01	7.75456E-01
7.4E8	1.55822E-03	393	1.26598E+00	9.56119E-01	9.92317E-01
7.6E8	1.82400E-03	393	1.56638E+00	1.19379E+00	1.23616E+00
7.8E8	2.13292E-03	393	1.90887E+00	1.46515E+00	1.51395E+00
8E8	2.49433E-03	393	2.30290E+00	1.77735E+00	1.83309E+00
8.2E8	2.90169E-03	393	2.73546E+00	2.12004E+00	2.18314E+00
8.4E8	3.35424E-03	393	3.20044E+00	2.48833E+00	2.55910E+00
8.6E8	3.84086E-03	393	3.69035E+00	2.87626E+00	2.95491E+00
8.8E8	4.36252E-03	393	4.20330E+00	3.28253E+00	3.36924E+00

HY130 - ONLY

2E8	1.38304E-04	348	1.28506E-03	1.27712E-03	6.26009E-03
3E8	2.07620E-04	348	6.74743E-03	6.20890E-03	1.09348E-02
3.4E8	2.35444E-04	348	9.26516E-03	8.40018E-03	1.29880E-02
3.6E8	2.49376E-04	348	1.06008E-02	9.54692E-03	1.40778E-02
3.8E8	2.63330E-04	348	1.21021E-02	1.08212E-02	1.53063E-02
4E8	2.77299E-04	348	1.36827E-02	1.21536E-02	1.66251E-02
4.2E8	2.91290E-04	348	1.52715E-02	1.34823E-02	1.79438E-02
4.4E8	3.05312E-04	348	1.70209E-02	1.49333E-02	1.93843E-02
4.6E8	3.19364E-04	393	1.91177E-02	1.57232E-02	2.17798E-02
4.8E8	3.33480E-04	393	2.17104E-02	1.76052E-02	2.37513E-02
5E8	3.47672E-04	393	2.44770E-02	1.95987E-02	2.58695E-02
5.2E8	3.61977E-04	393	2.75802E-02	2.18183E-02	2.82367E-02
5.4E8	3.76393E-04	393	3.10223E-02	2.42632E-02	3.08500E-02
5.6E8	3.90970E-04	393	3.48089E-02	2.69323E-02	3.36981E-02
5.8E8	4.05712E-04	393	3.88584E-02	2.97661E-02	3.67181E-02
6E8	4.20773E-04	393	4.33983E-02	3.29227E-02	4.00808E-02
6.2E8	4.36123E-04	393	4.84326E-02	3.64054E-02	4.37905E-02
6.4E8	4.51891E-04	393	5.42089E-02	4.03830E-02	4.80225E-02
6.6E8	4.68313E-04	393	6.09941E-02	4.50389E-02	5.29760E-02
6.8E8	4.87252E-04	393	7.15906E-02	5.22775E-02	6.06044E-02
7E8	5.15214E-04	393	9.45634E-02	6.79355E-02	7.69932E-02
7.2E8	5.64070E-04	393	1.46474E-01	1.03323E-01	1.13963E-01
7.4E8	6.39120E-04	393	2.34958E-01	1.63294E-01	1.76345E-01
7.6E8	7.42776E-04	393	3.55221E-01	2.44478E-01	2.60577E-01
7.8E8	8.84521E-04	393	5.22735E-01	3.58059E-01	3.77999E-01
8E8	1.05657E-03	393	7.15104E-01	4.89117E-01	5.13382E-01
8.2E8	1.25777E-03	393	9.34132E-01	6.40380E-01	6.69391E-01
8.4E8	1.49033E-03	393	1.18251E+00	8.15837E-01	8.49932E-01
8.6E8	1.76519E-03	393	1.46499E+00	1.01948E+00	1.05918E+00
8.8E8	2.08604E-03	393	1.78469E+00	1.25360E+00	1.29945E+00

ADINA-PLOT VERSION 6.1.4, 7 APRIL 1995
SPECIMEN GEOMETRY

ADINA ORIGINAL
LOAD_STEP
TIME 1.000 0.0001081

XVMIN 0.004500
XVMAX 0.006500
YVMIN 0.07000
YVMAX 0.07300

Z
Y

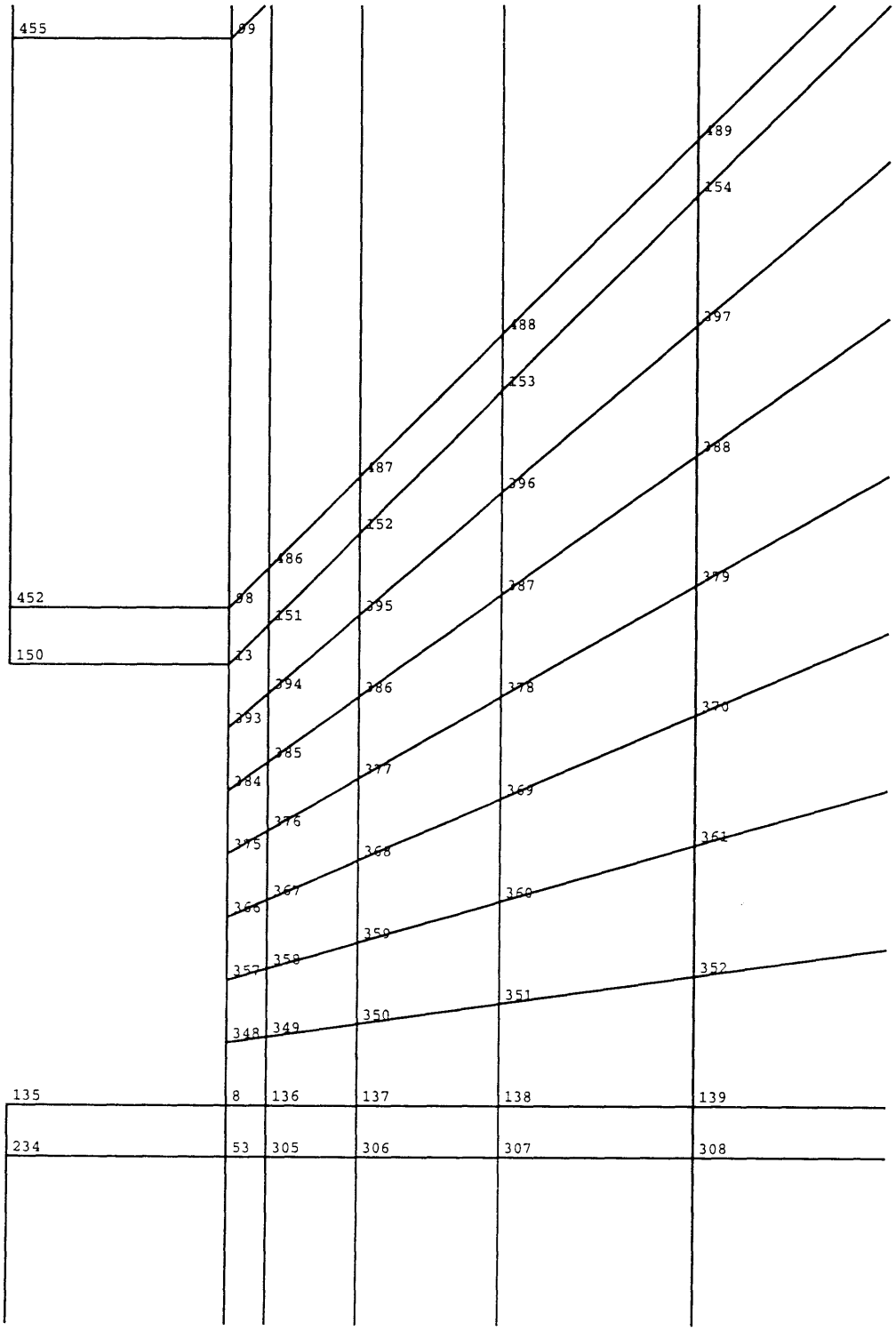

U_2 U_3
B ✓ -
C - ✓
D - -

ADINA-PLOT VERSION 6.1.4, 7 APRIL 1995
SPECIMEN GEOMETRY

ADINA ORIGINAL
LOAD_STEP
TIME 1.000 0.0004595

XVMIN 0.004500
XVMAX 0.01300
YVMIN 0.06700
YVMAX 0.08000

Z
Y

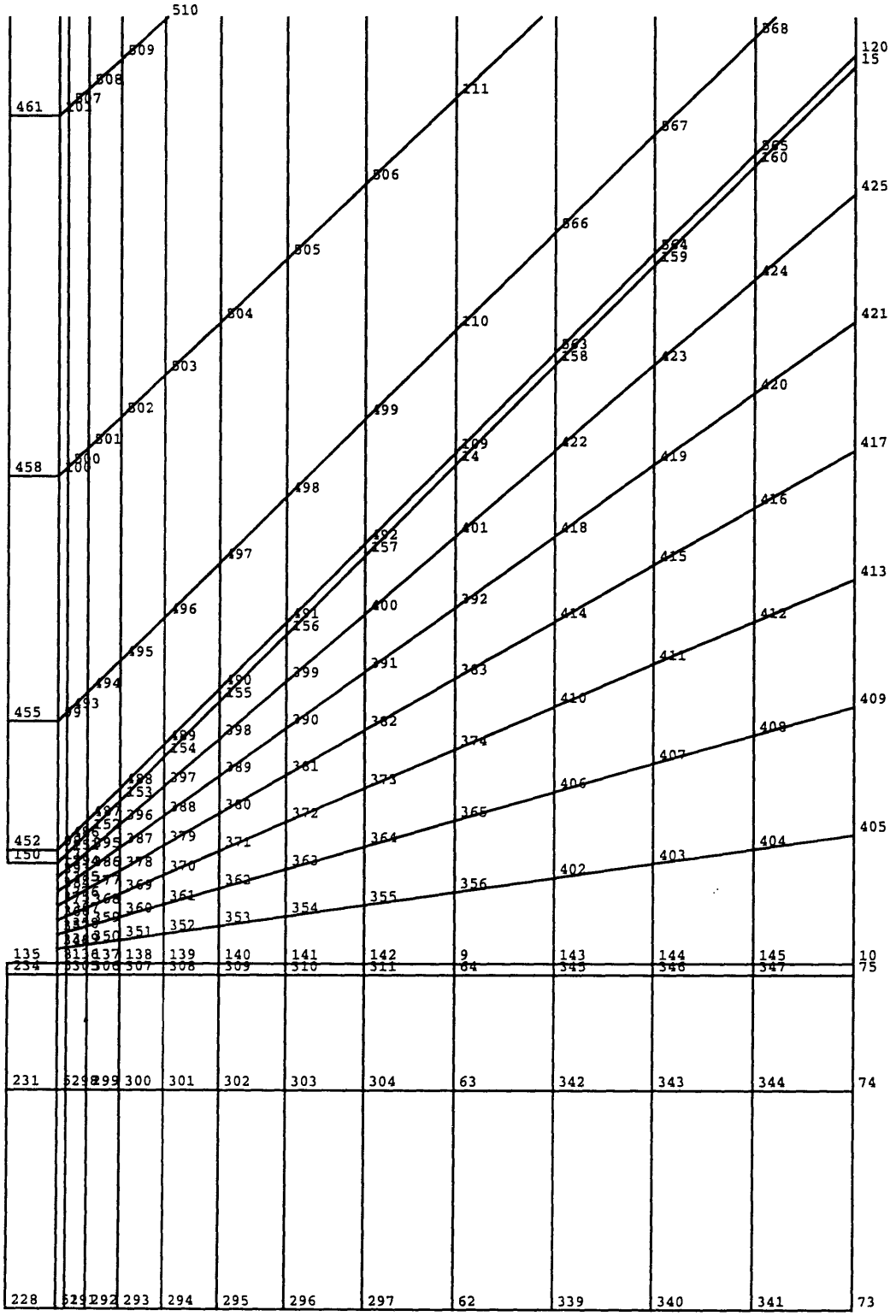

	U_2	U_3
B	✓	-
C	-	✓
D	-	-

DEGREE OF RESTRAINT OF TEST SPECIMEN

HY130

applied stress	Y-DISPLACEMENT NODE: 8	EQUIVALENT PLASTIC STRAIN AT THE NOTCH TIP
Pa	m	
1E8	5.30858E-05	
2E8	1.06172E-04	
3E8	1.59257E-04	
4E8	2.16040E-04	PLASTIC
5E8	2.74642E-04	PL:0.007
6E8	3.39646E-04	PL:0.014
7E8	4.09866E-04	PL:0.024
8E8	5.07207E-04	PL:0.035
9E8	6.54683E-04	PL:0.042
10E8	9.59142E-04	PL:0.049
11E8	1.98124E-03	PL:0.105

HY100

applied stress	Y-DISPLACEMENT NODE: 8	EQUIVALENT PLASTIC STRAIN AT THE NOTCH TIP
Pa	m	
1E8	5.30858E-05	
2E8	1.06172E-04	
3E8	1.61806E-04	PL:0.0023
4E8	2.20959E-04	PL:0.0065
5E8	2.87754E-04	PL:0.014
6E8	3.73738E-04	PL:0.021
7E8	5.18074E-04	PL:0.028
8E8	9.05962E-04	PL:0.049
9E8	2.04630E-03	PL:0.084

ADINA-PLOT VERSION 6.1.4, 7 APRIL 1995
SPECIMEN GEOMETRY

ADINA ORIGINAL XVMIN 0.000
LOAD_STEP XVMAX 0.07500
TIME 1.000 0.003797 YVMIN 0.000
YVMAX 0.1000

Z
Y

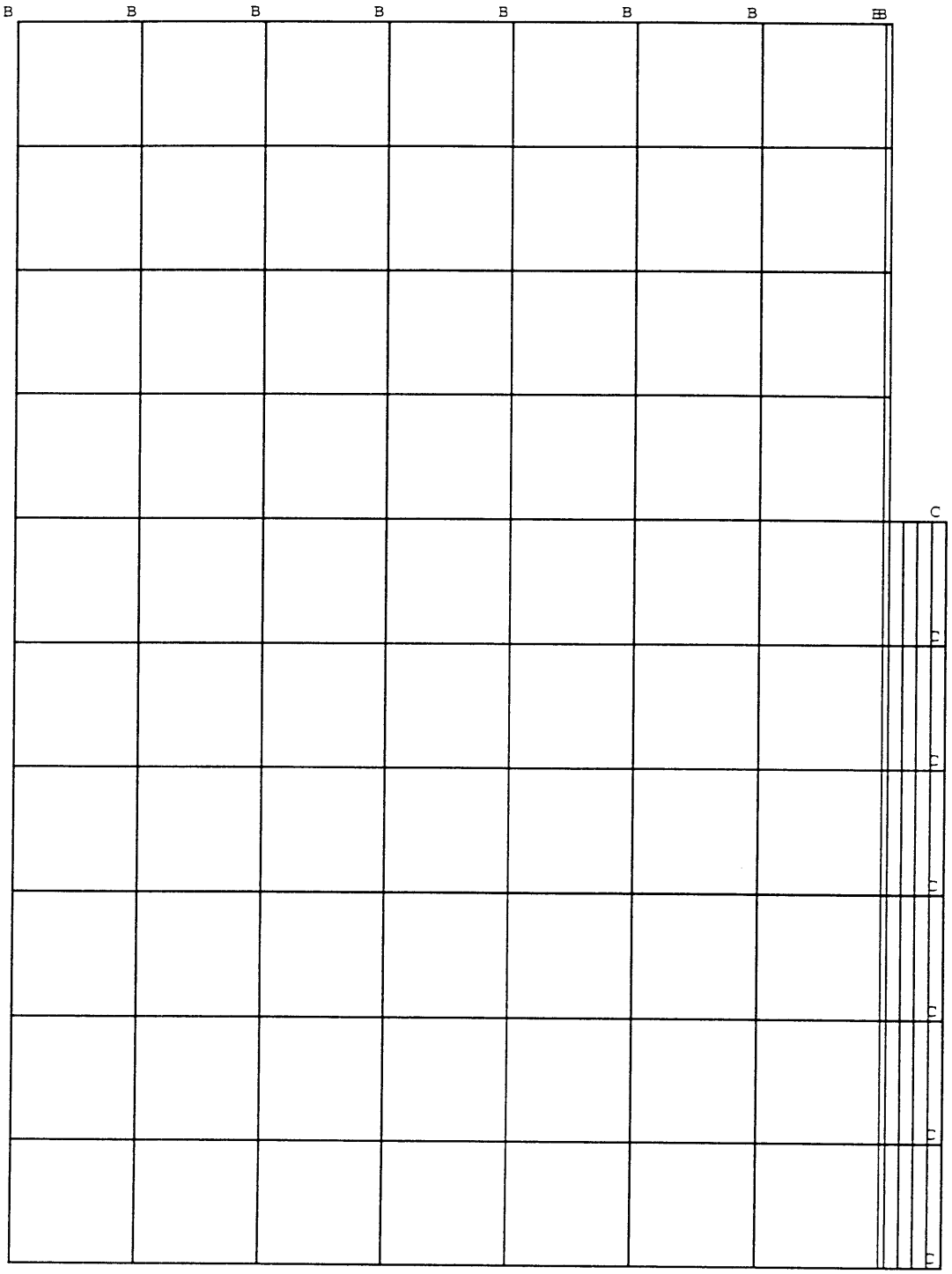

U_2 U_3
B ✓ -
C - ✓

B.3 ADINA plots

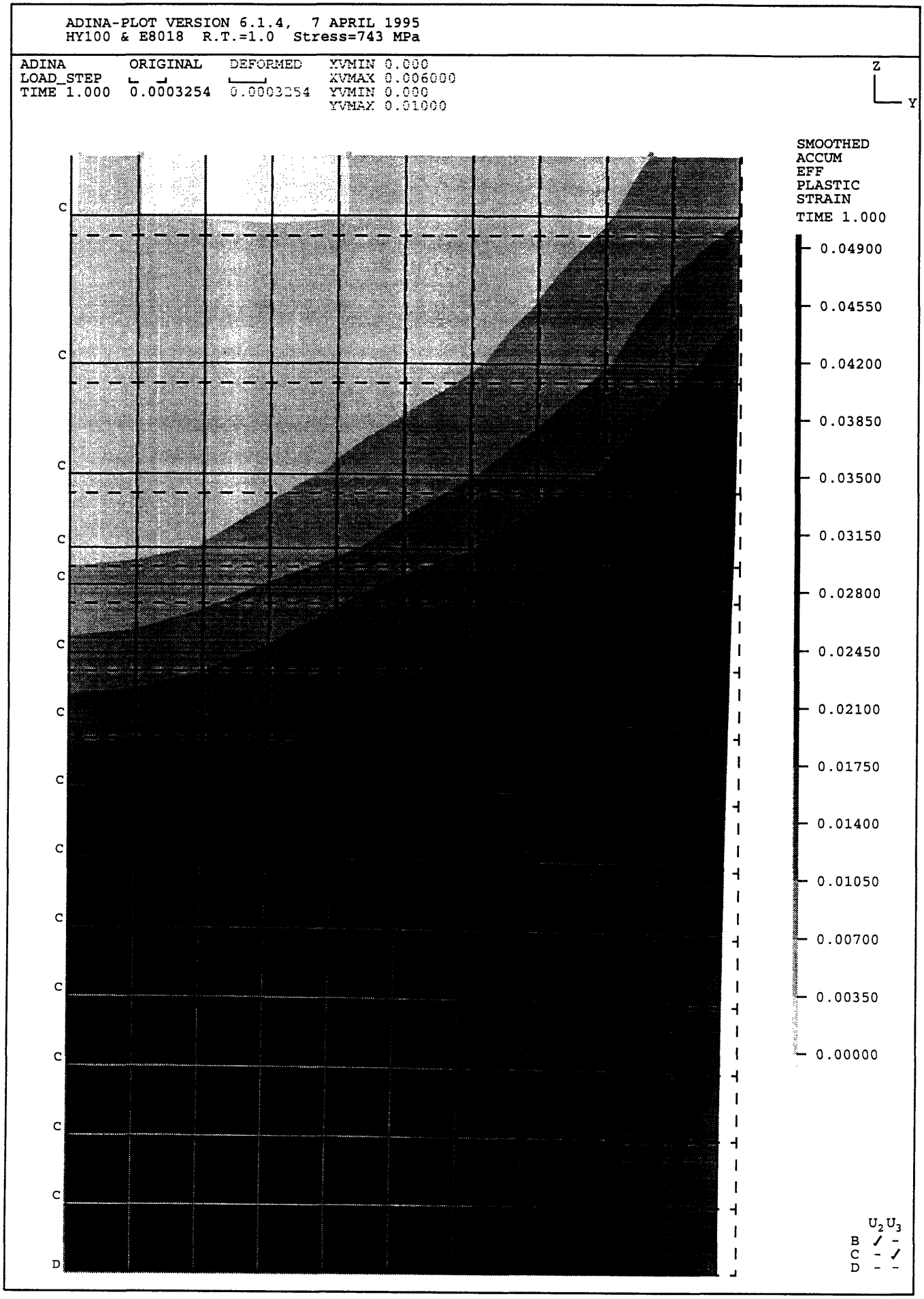
ADINA-PLOT VERSION 6.1.4, 7 APRIL 1995
HY100 & E8018 R.T.=1.0 Stress=743 MPa
ADINA
LOAD_STEP
TIME 1.000
ORIGINAL
0.0003254
DEFORMED
0.0003254
XVMIN 0.000
XVMAX 0.006000
YVMIN 0.000
YVMAX 0.01000
Z
Y
SMOOTHED
ACCUM
EFF
PLASTIC
STRAIN
TIME 1.000
0.04900
0.04550
0.04200
0.03850
0.03500
0.03150
0.02800
0.02450
0.02100
0.01750
0.01400
0.01050
0.00700
0.00350
0.00000
C
D
U2 U3
B / -
C - /
D - -

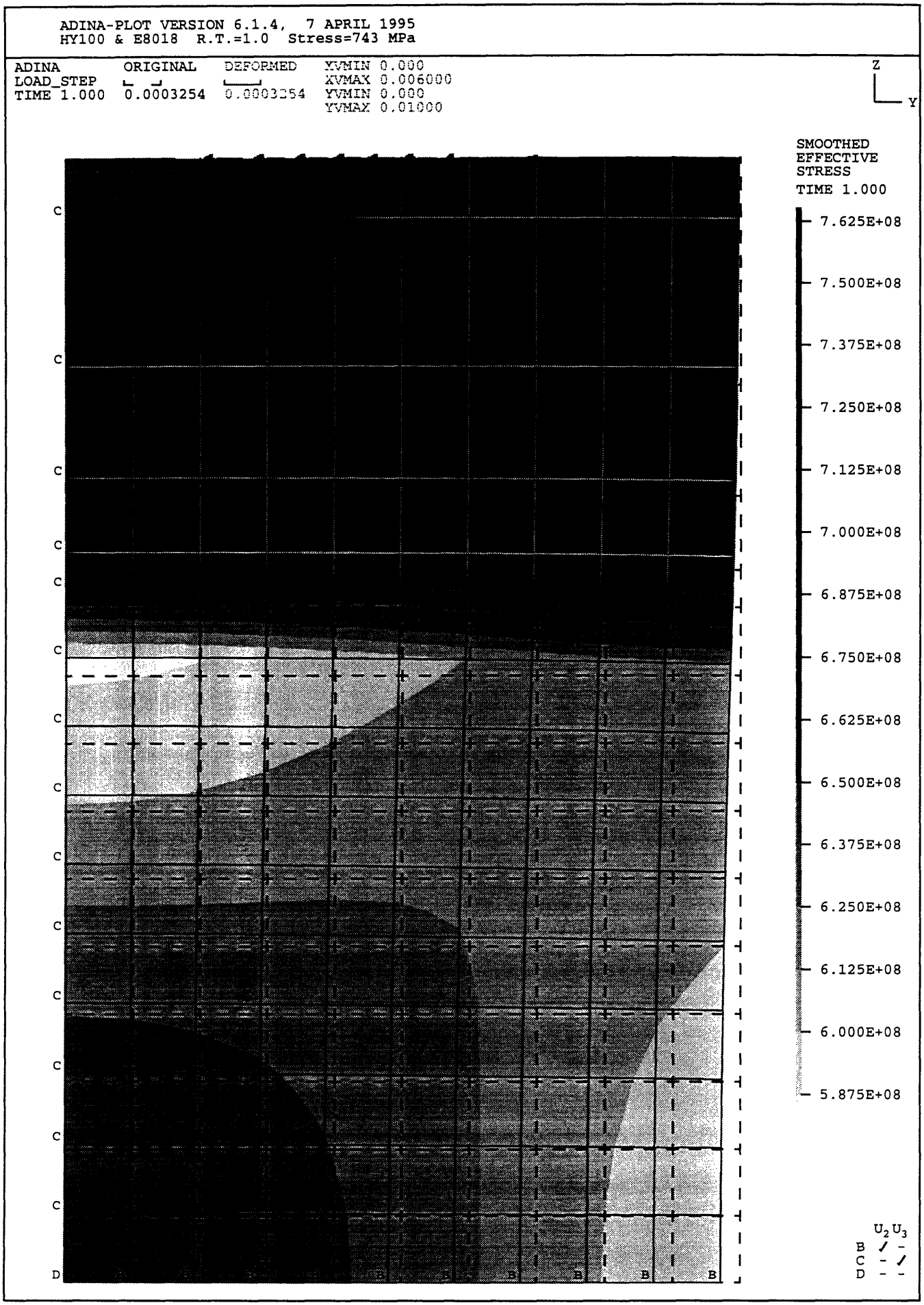
ADINA-PLOT VERSION 6.1.4, 7 APRIL 1995
HY100 & E8018 R.T.=1.0 Stress=743 MPa
ADINA
LOAD_STEP
TIME 1.000
ORIGINAL
0.0003254
DEFORMED
0.0003254
XVMIN 0.000
XVMAX 0.006000
YVMIN 0.000
YVMAX 0.01000
Z
Y
SMOOTHED
EFFECTIVE
STRESS
TIME 1.000
7.625E+08
7.500E+08
7.375E+08
7.250E+08
7.125E+08
7.000E+08
6.875E+08
6.750E+08
6.625E+08
6.500E+08
6.375E+08
6.250E+08
6.125E+08
6.000E+08
5.875E+08
U2 U3
B / -
C - /
D - -

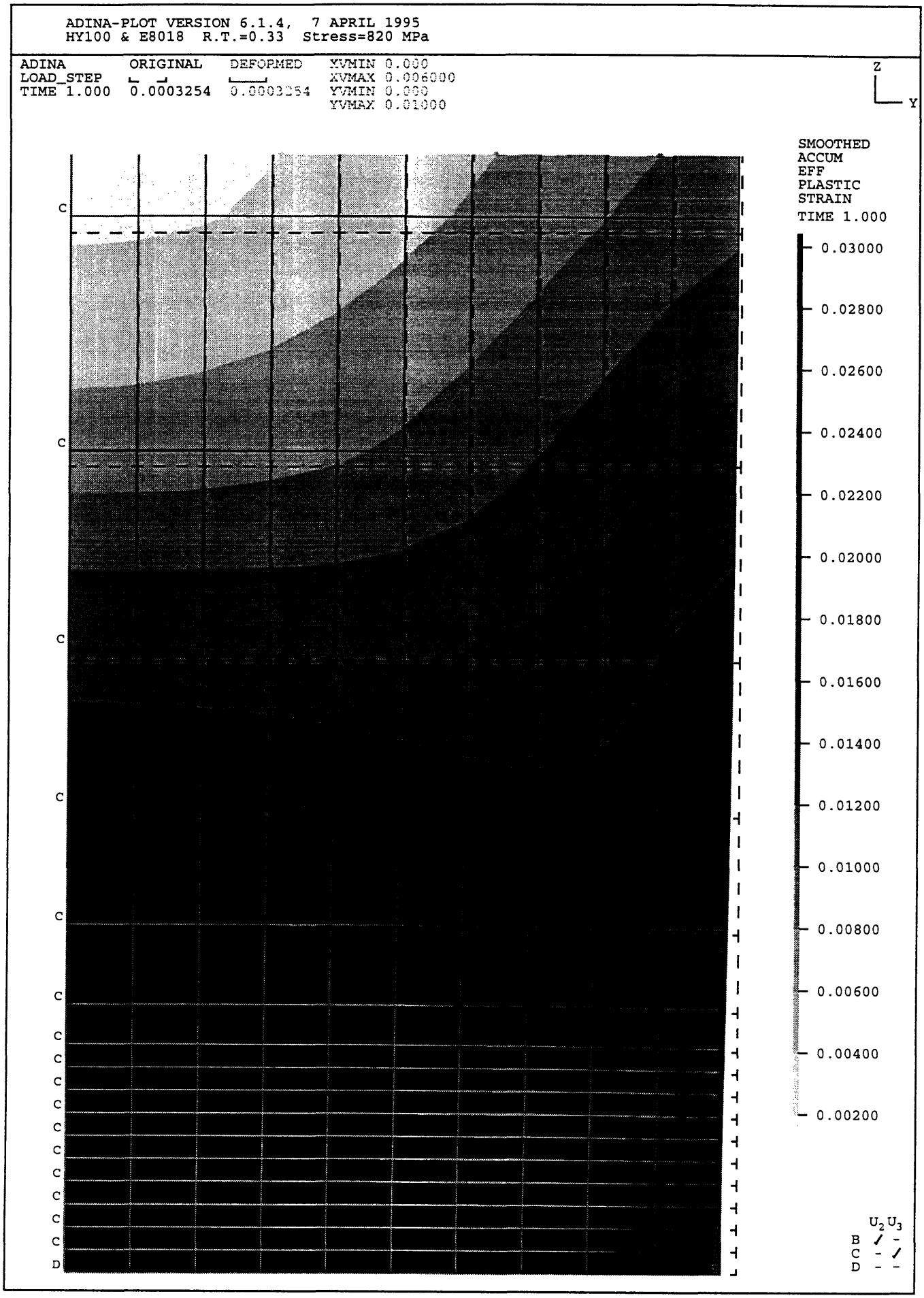
ADINA-PLOT VERSION 6.1.4, 7 APRIL 1995
HY100 & E8018 R.T.=0.33 Stress=820 MPa
ADINA
LOAD_STEP
TIME 1.000
ORIGINAL
0.0003254
DEFORMED
0.0003254
XVMIN 0.000
XVMAX 0.006000
YVMIN 0.000
YVMAX 0.01000
Z
Y
SMOOTHED
ACCUM
EFF
PLASTIC
STRAIN
TIME 1.000
0.03000
0.02800
0.02600
0.02400
0.02200
0.02000
0.01800
0.01600
0.01400
0.01200
0.01000
0.00800
0.00600
0.00400
0.00200
U2 U3
B ✓ -
C - ✓
D - -

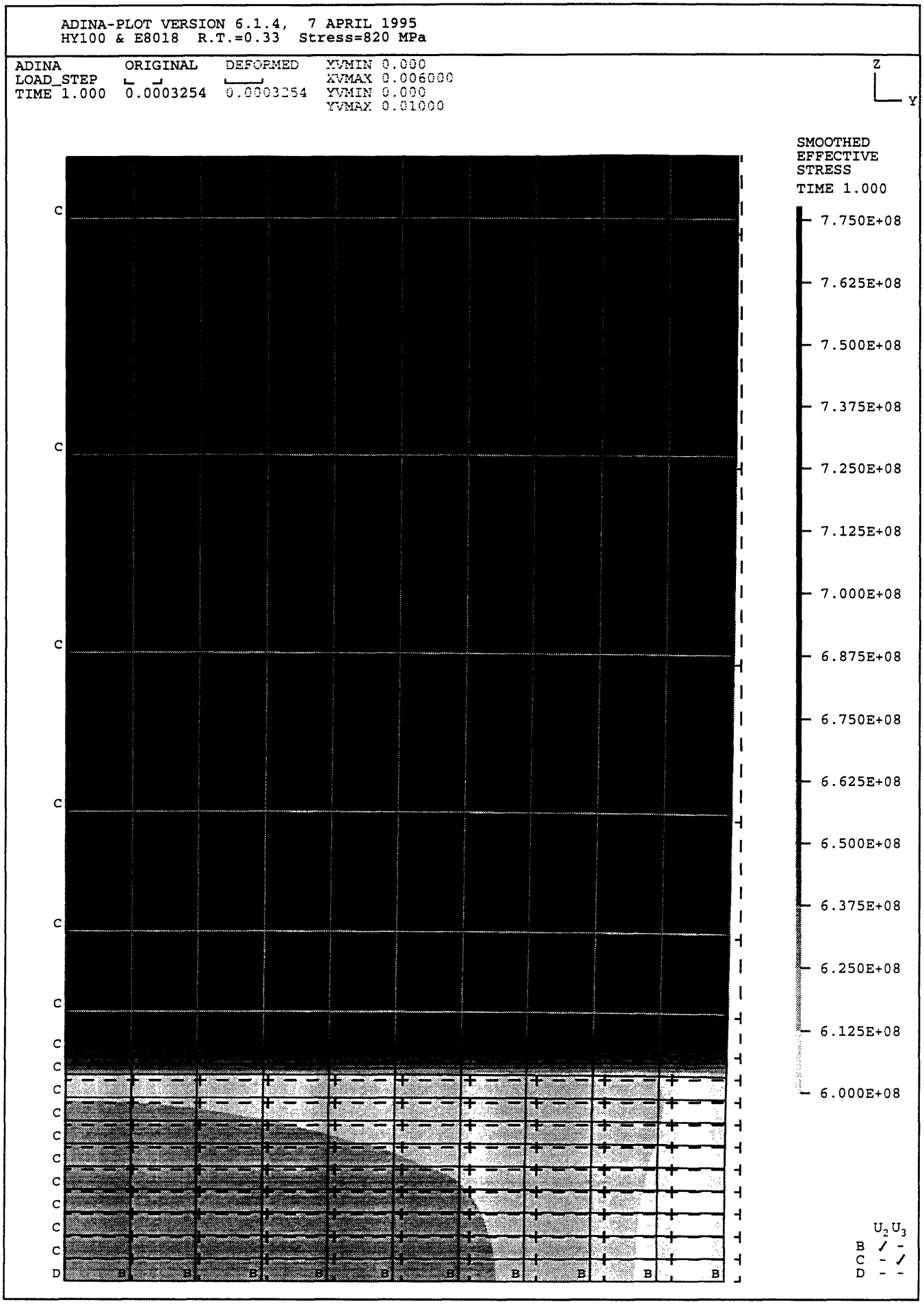
ADINA-PLOT VERSION 6.1.4, 7 APRIL 1995
HY100 & E8018 R.T.=0.33 Stress=820 MPa
ADINA ORIGINAL DEFORMED
LOAD_STEP
TIME 1.000 0.0003254 0.0003254
XVMIN 0.000
XVMAX 0.006000
YVMIN 0.000
YVMAX 0.01000
Z
Y
SMOOTHED
EFFECTIVE
STRESS
TIME 1.000
7.750E+08
7.625E+08
7.500E+08
7.375E+08
7.250E+08
7.125E+08
7.000E+08
6.875E+08
6.750E+08
6.625E+08
6.500E+08
6.375E+08
6.250E+08
6.125E+08
6.000E+08
U2 U3
B / -
C - /
D - -

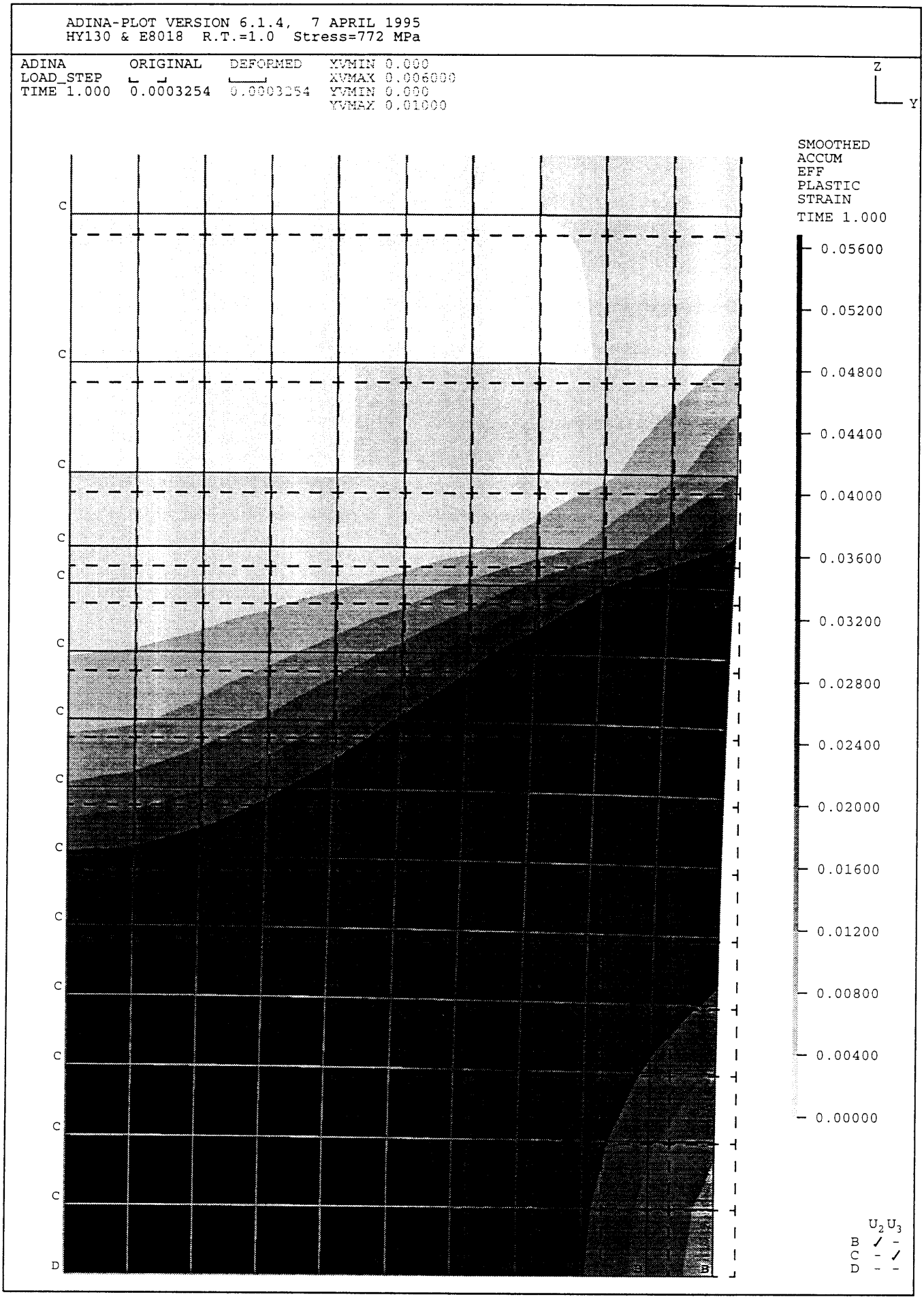
ADINA-PLOT VERSION 6.1.4, 7 APRIL 1995
HY130 & E8018 R.T.=1.0 Stress=772 MPa
ADINA ORIGINAL DEFORMED
LOAD_STEP
TIME 1.000 0.0003254 0.0003254
XVMIN 0.000
XVMAX 0.006000
YVMIN 0.000
YVMAX 0.01000
Z
Y
SMOOTHED
ACCUM
EFF
PLASTIC
STRAIN
TIME 1.000
0.05600
0.05200
0.04800
0.04400
0.04000
0.03600
0.03200
0.02800
0.02400
0.02000
0.01600
0.01200
0.00800
0.00400
0.00000
C
D
B
U2 U3
B ✓ -
C - ✓
D - -

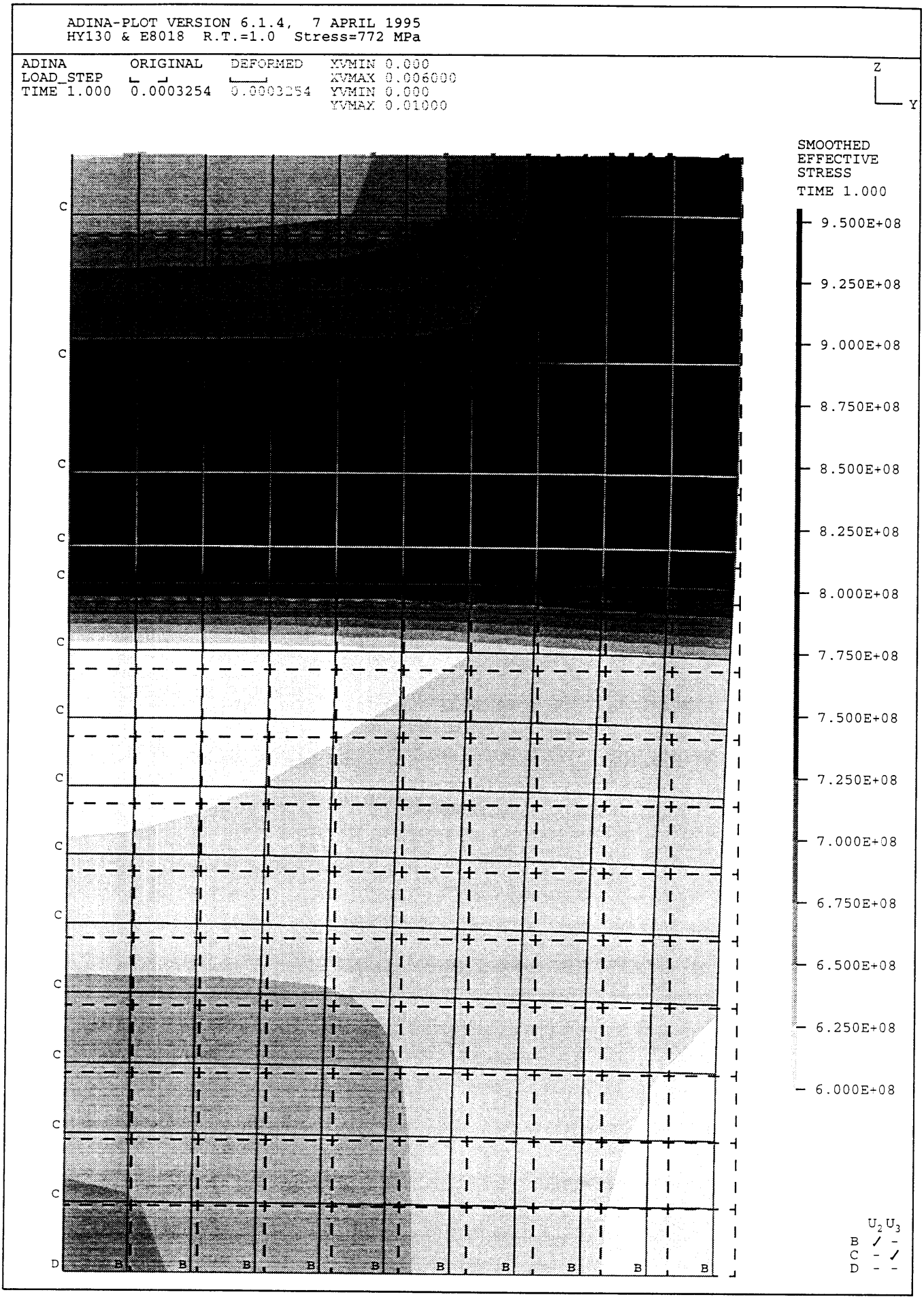
ADINA-PLOT VERSION 6.1.4, 7 APRIL 1995
HY130 & E8018 R.T.=1.0 Stress=772 MPa
ADINA ORIGINAL DEFORMED
LOAD_STEP
TIME 1.000 0.0003254 0.0003254
XVMIN 0.000
XVMAX 0.006000
YVMIN 0.000
YVMAX 0.01000
Z
Y
SMOOTHED
EFFECTIVE
STRESS
TIME 1.000
9.500E+08
9.250E+08
9.000E+08
8.750E+08
8.500E+08
8.250E+08
8.000E+08
7.750E+08
7.500E+08
7.250E+08
7.000E+08
6.750E+08
6.500E+08
6.250E+08
6.000E+08
U2 U3
B / -
C - /
D - -

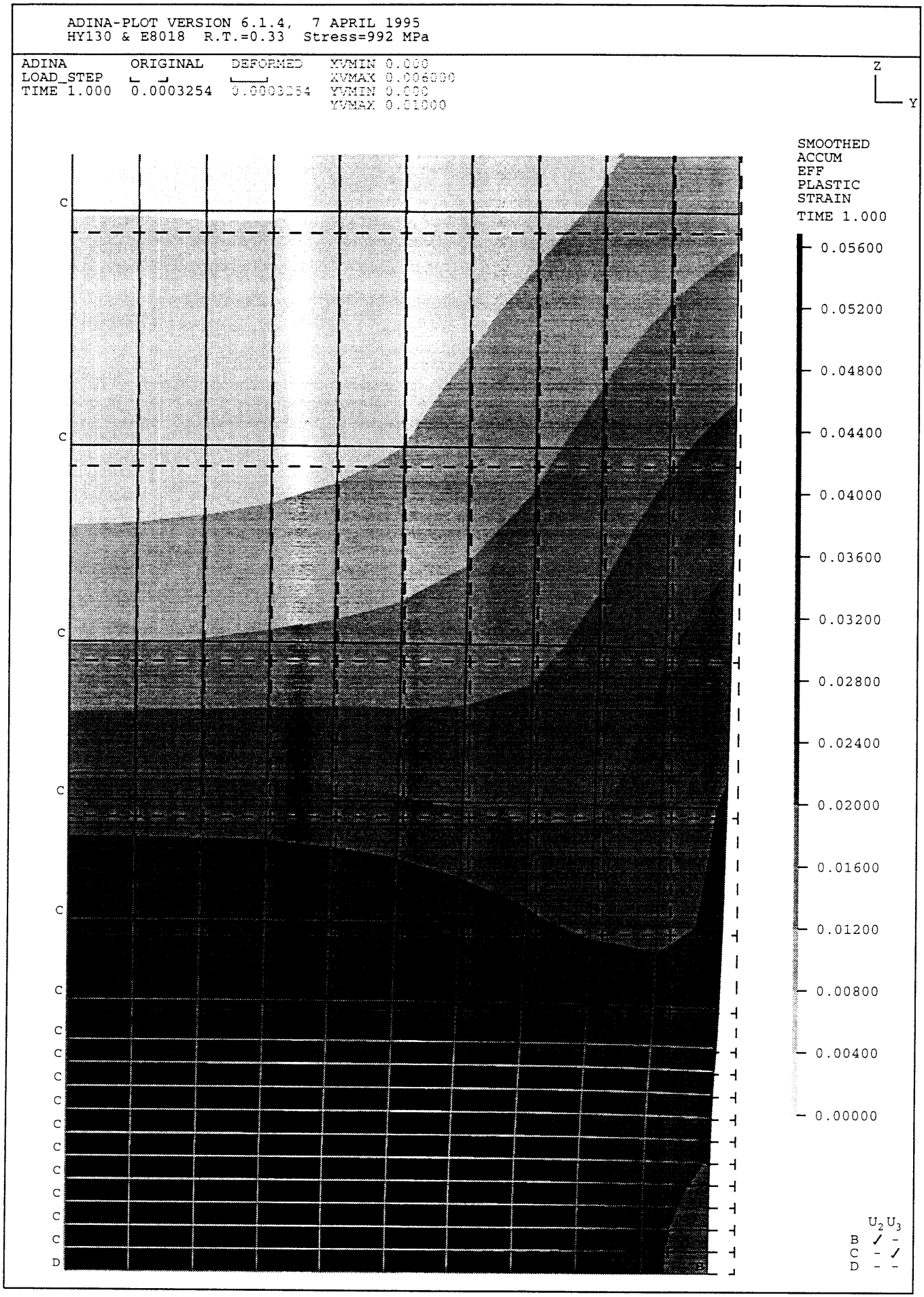
ADINA-PLOT VERSION 6.1.4, 7 APRIL 1995
HY130 & E8018 R.T.=0.33 Stress=992 MPa
ADINA ORIGINAL DEFORMED XVMIN 0.000
LOAD_STEP XVMAX 0.006000
TIME 1.000 0.0003254 0.0003354 YVMIN 0.000
YVMAX 0.01000
Z
Y
SMOOTHED
ACCUM
EFF
PLASTIC
STRAIN
TIME 1.000
0.05600
0.05200
0.04800
0.04400
0.04000
0.03600
0.03200
0.02800
0.02400
0.02000
0.01600
0.01200
0.00800
0.00400
0.00000
U2 U3
B / -
C - /
D - -

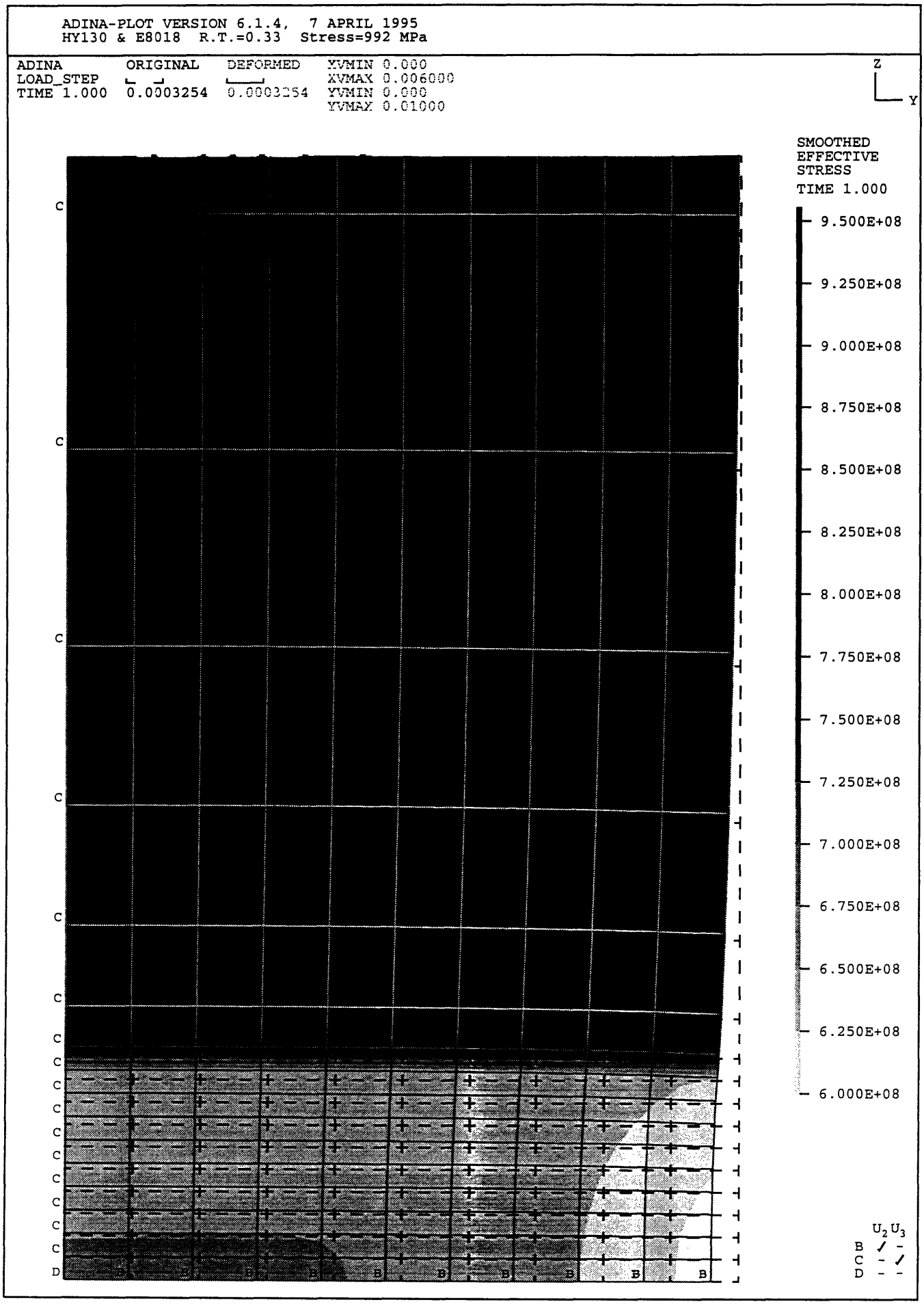
ADINA-PLOT VERSION 6.1.4, 7 APRIL 1995
HY130 & E8018 R.T.=0.33 Stress=992 MPa
ADINA ORIGINAL DEFORMED
LOAD_STEP
TIME 1.000 0.0003254 0.0003254
XVMIN 0.000
XVMAX 0.006000
YVMIN 0.000
YVMAX 0.01000
Z
Y
SMOOTHED
EFFECTIVE
STRESS
TIME 1.000
9.500E+08
9.250E+08
9.000E+08
8.750E+08
8.500E+08
8.250E+08
8.000E+08
7.750E+08
7.500E+08
7.250E+08
7.000E+08
6.750E+08
6.500E+08
6.250E+08
6.000E+08
U2 U3
B ✓ -
C - ✓
D - -

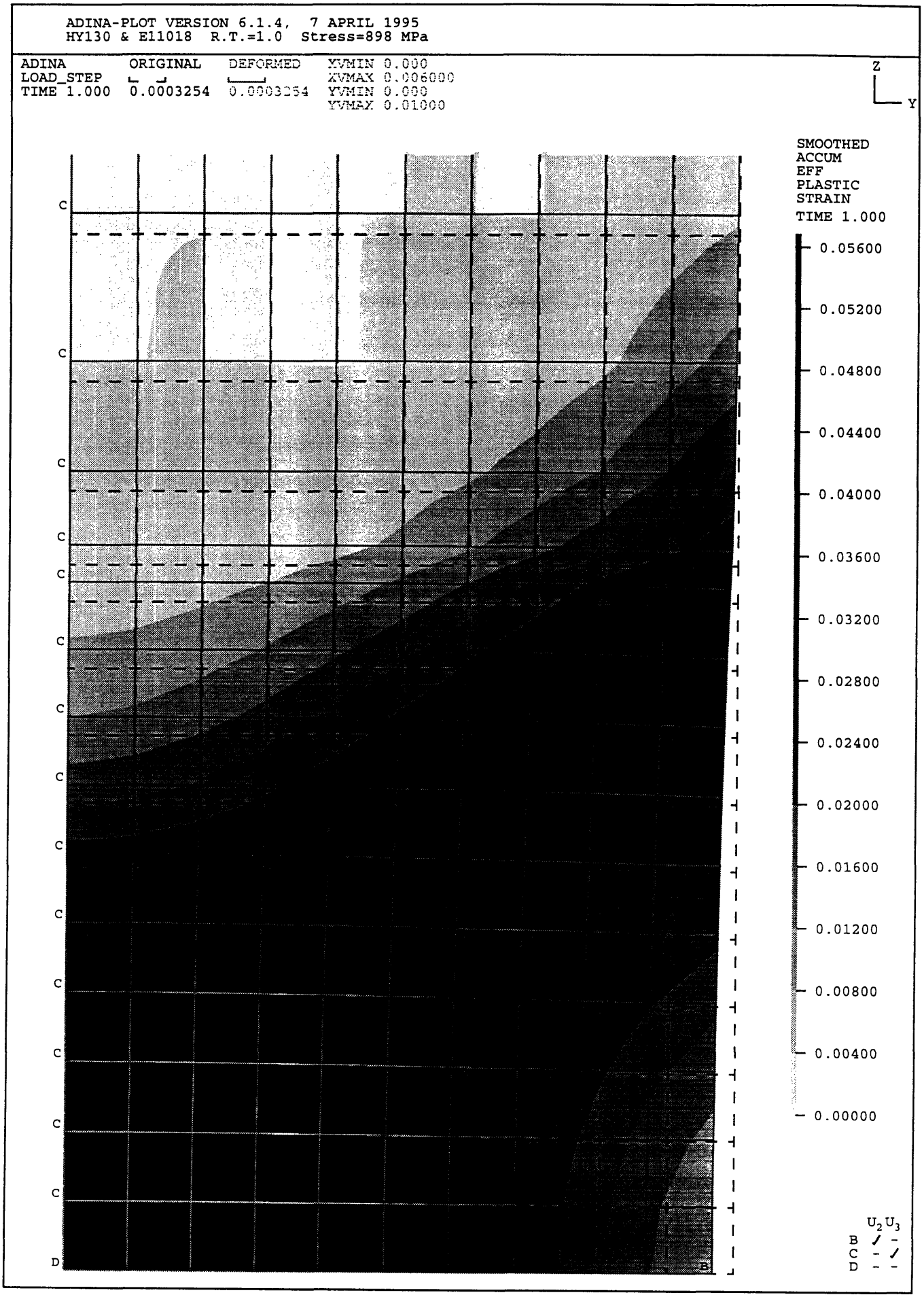
ADINA-PLOT VERSION 6.1.4, 7 APRIL 1995
HY130 & E11018 R.T.=1.0 Stress=898 MPa
ADINA ORIGINAL DEFORMED XVMIN 0.000
LOAD_STEP XVMAX 0.006000
TIME 1.000 0.0003254 0.0003254 YVMIN 0.000
YVMAX 0.01000
Z
Y
SMOOTHED
ACCUM
EFF
PLASTIC
STRAIN
TIME 1.000
0.05600
0.05200
0.04800
0.04400
0.04000
0.03600
0.03200
0.02800
0.02400
0.02000
0.01600
0.01200
0.00800
0.00400
0.00000
C
D
U2 U3
B ✓ -
C - ✓
D - -

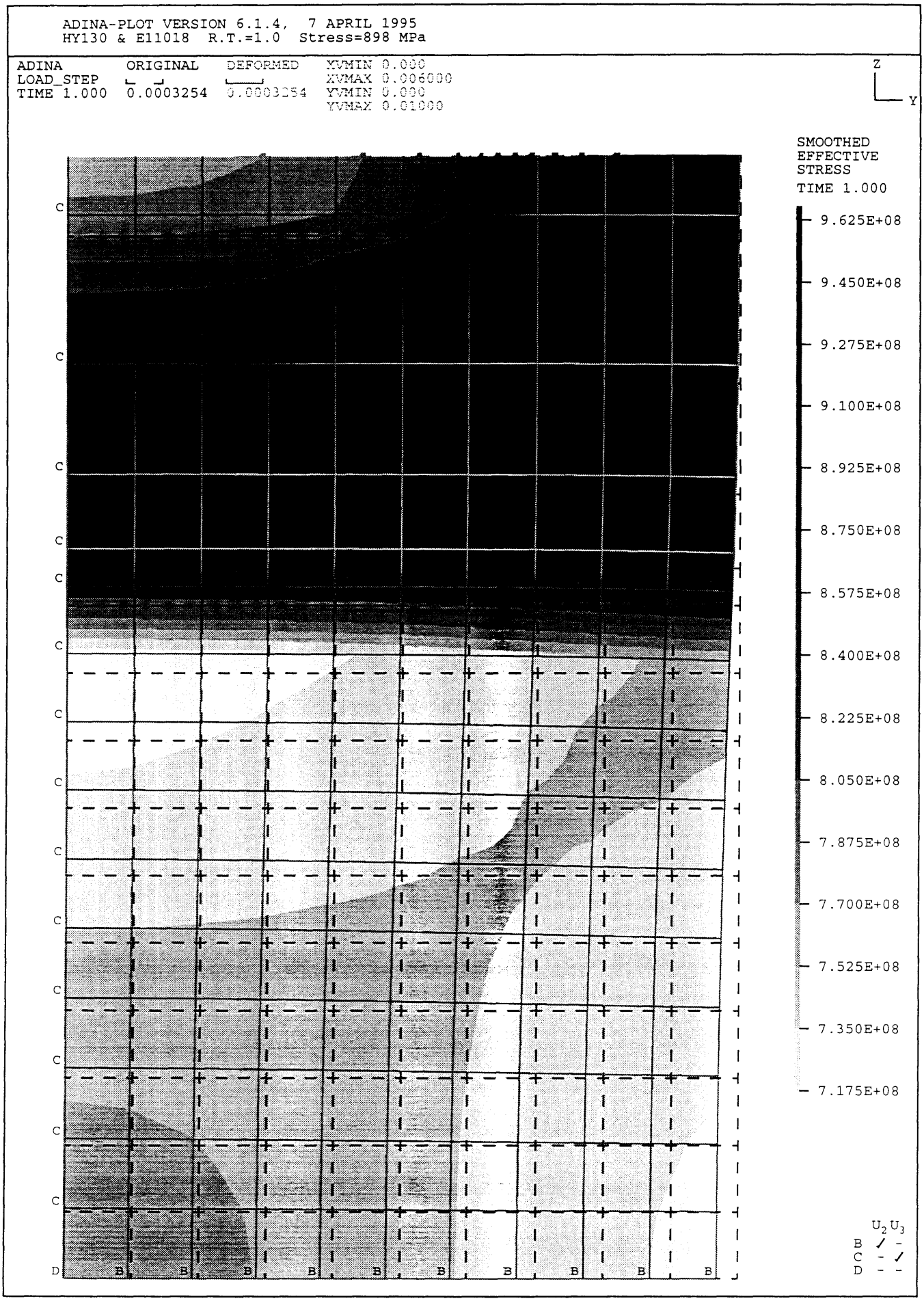
ADINA-PLOT VERSION 6.1.4, 7 APRIL 1995
HY130 & E11018 R.T.=1.0 Stress=898 MPa
ADINA ORIGINAL DEFORMED
LOAD_STEP
TIME 1.000 0.0003254 0.0003254
XVMIN 0.000
XVMAX 0.006000
YVMIN 0.000
YVMAX 0.01000
Z
Y
SMOOTHED
EFFECTIVE
STRESS
TIME 1.000
9.625E+08
9.450E+08
9.275E+08
9.100E+08
8.925E+08
8.750E+08
8.575E+08
8.400E+08
8.225E+08
8.050E+08
7.875E+08
7.700E+08
7.525E+08
7.350E+08
7.175E+08
U2 U3
B / -
C - /
D - -

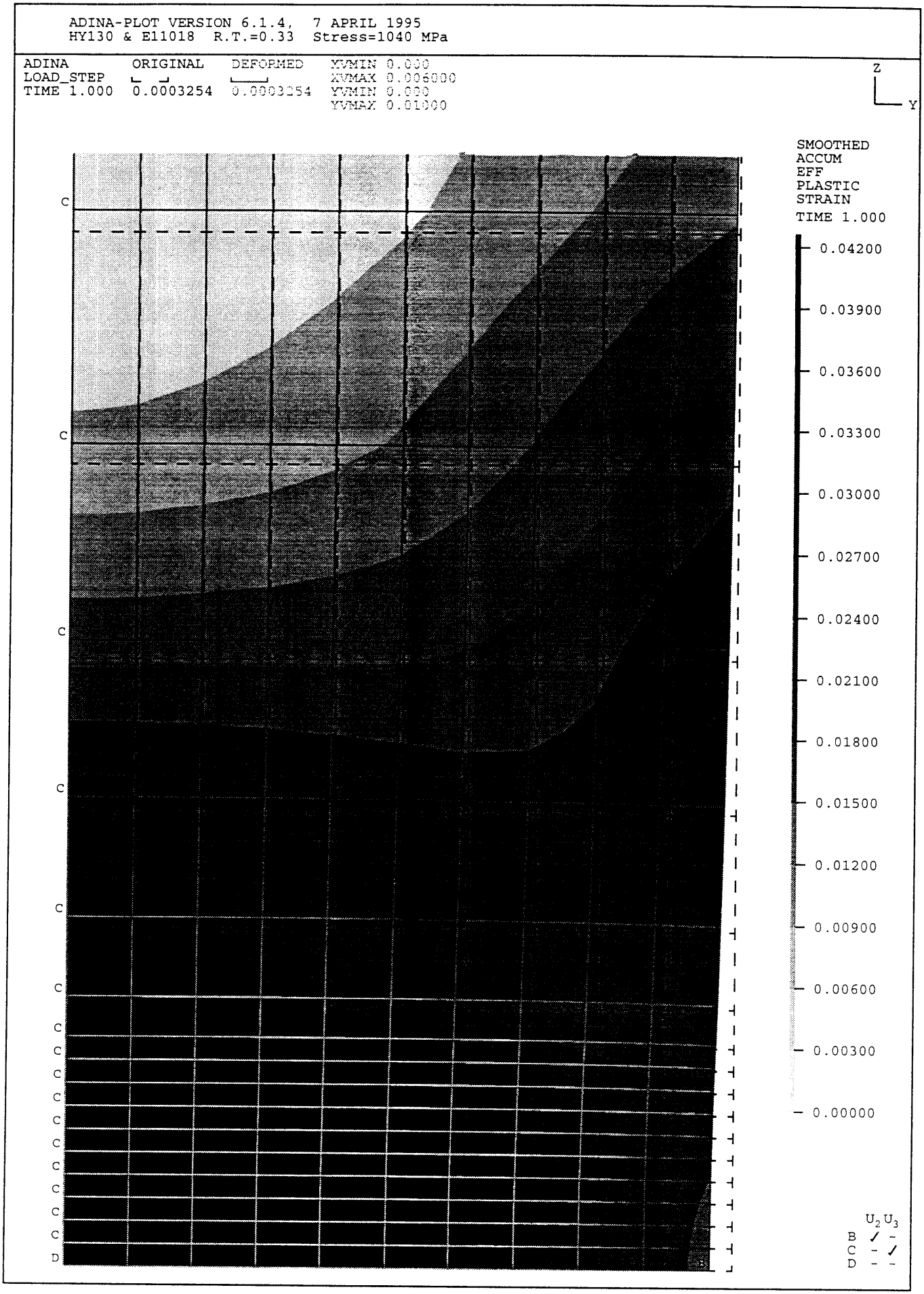
ADINA-PLOT VERSION 6.1.4, 7 APRIL 1995
HY130 & E11018 R.T.=0.33 Stress=1040 MPa
ADINA ORIGINAL DEFORMED
LOAD_STEP
TIME 1.000 0.0003254 0.0003254
YVMIN 0.000
YVMAX 0.006000
YVMIN 0.000
YVMAX 0.01000
Z
Y
SMOOTHED
ACCUM
EFF
PLASTIC
STRAIN
TIME 1.000
0.04200
0.03900
0.03600
0.03300
0.03000
0.02700
0.02400
0.02100
0.01800
0.01500
0.01200
0.00900
0.00600
0.00300
0.00000
U2 U3
B ✓ -
C - ✓
D - -

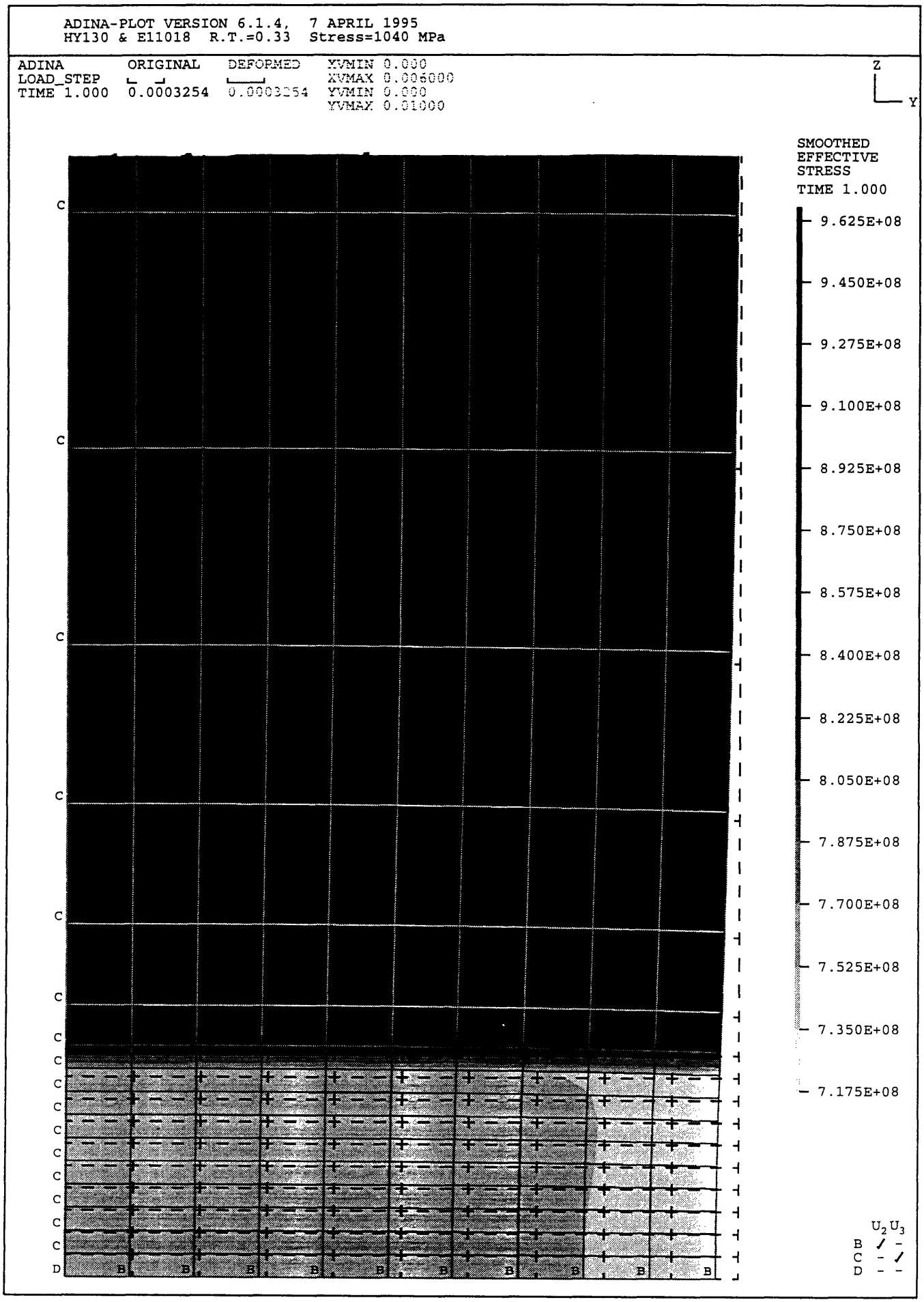
ADINA-PLOT VERSION 6.1.4, 7 APRIL 1995
HY130 & E11018 R.T.=0.33 Stress=1040 MPa
ADINA
LOAD_STEP
TIME 1.000
ORIGINAL
0.0003254
DEFORMED
0.0003254
XVMIN 0.000
XVMAX 0.006000
YVMIN 0.000
YVMAX 0.01000
Z
Y
SMOOTHED
EFFECTIVE
STRESS
TIME 1.000
9.625E+08
9.450E+08
9.275E+08
9.100E+08
8.925E+08
8.750E+08
8.575E+08
8.400E+08
8.225E+08
8.050E+08
7.875E+08
7.700E+08
7.525E+08
7.350E+08
7.175E+08
U2 U3
B / -
C - /
D - -

ADINA-PLOT VERSION 6.1.4, 7 APRIL 1995
SPECIMEN GEOMETRY

ADINA ORIGINAL XVMIN 0.000
LOAD_STEP XVMAX 0.01300
TIME 1.000 0.004881 YVMIN 0.000
YVMAX 0.1500

Z
Y

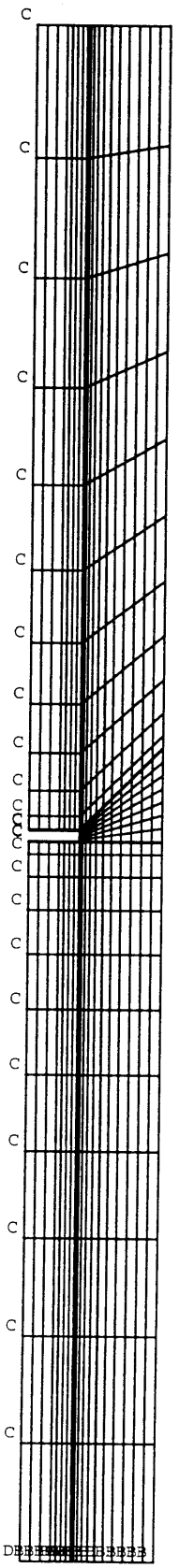

U_2 U_3
B ✓ -
C - ✓
D - -

ADINA-PLOT VERSION 6.1.4, 7 APRIL 1995
SPECIMEN GEOMETRY

ADINA ORIGINAL
LOAD_STEP
TIME 1.000 0.0006834

XVMIN 0.000
XVMAX 0.01300
YVMIN 0.06400
YVMAX 0.08500

Z
Y

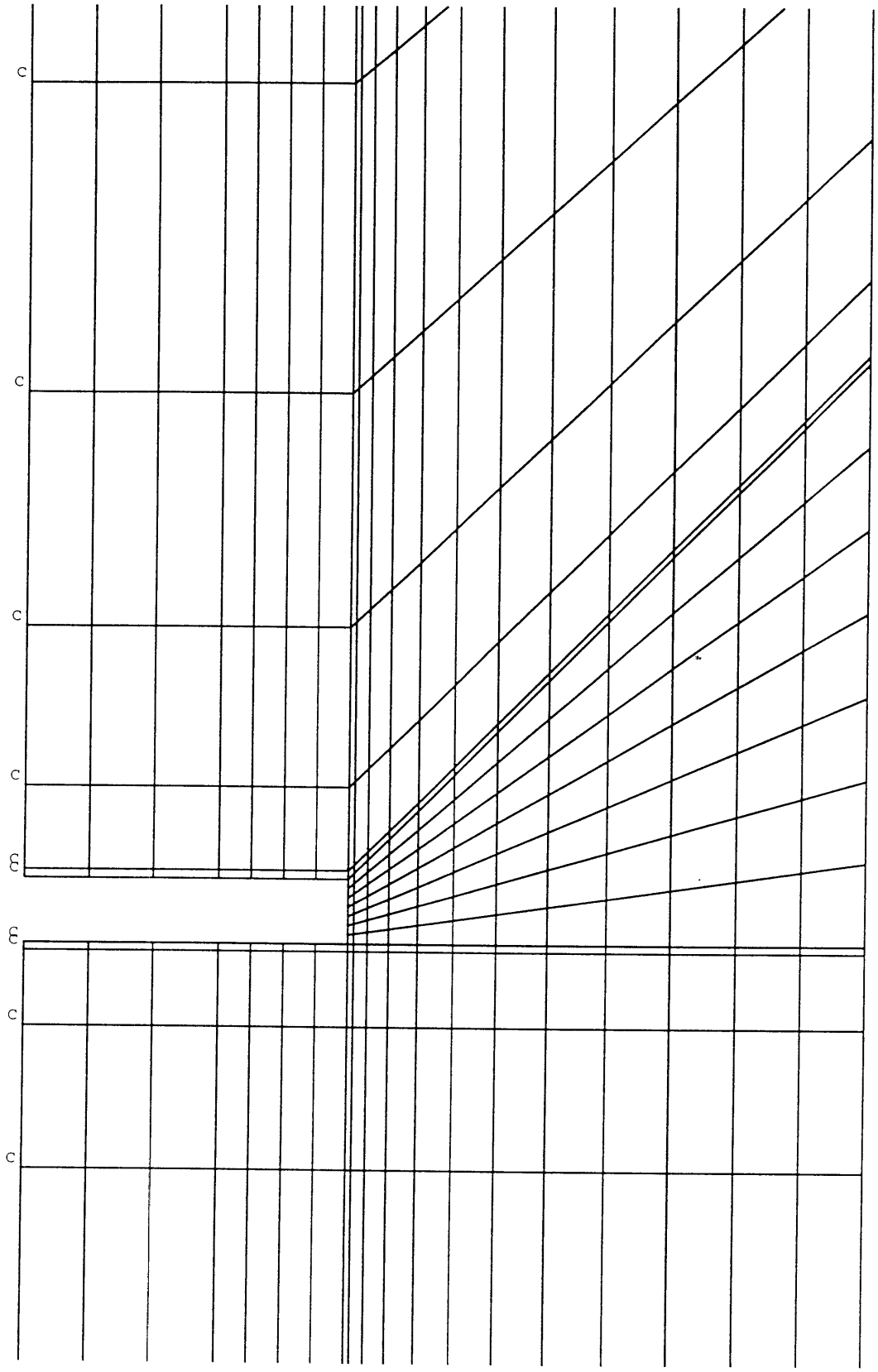

U2 U3
B / -
C - /
D - -

ADINA-PLOT VERSION 6.1.4, 7 APRIL 1995
SPECIMEN GEOMETRY

ADINA ORIGINAL
LOAD_STEP
TIME 1.000 0.0001081

XVMIN 0.004500
XVMAX 0.006500
YVMIN 0.07000
YVMAX 0.07300

Z
Y

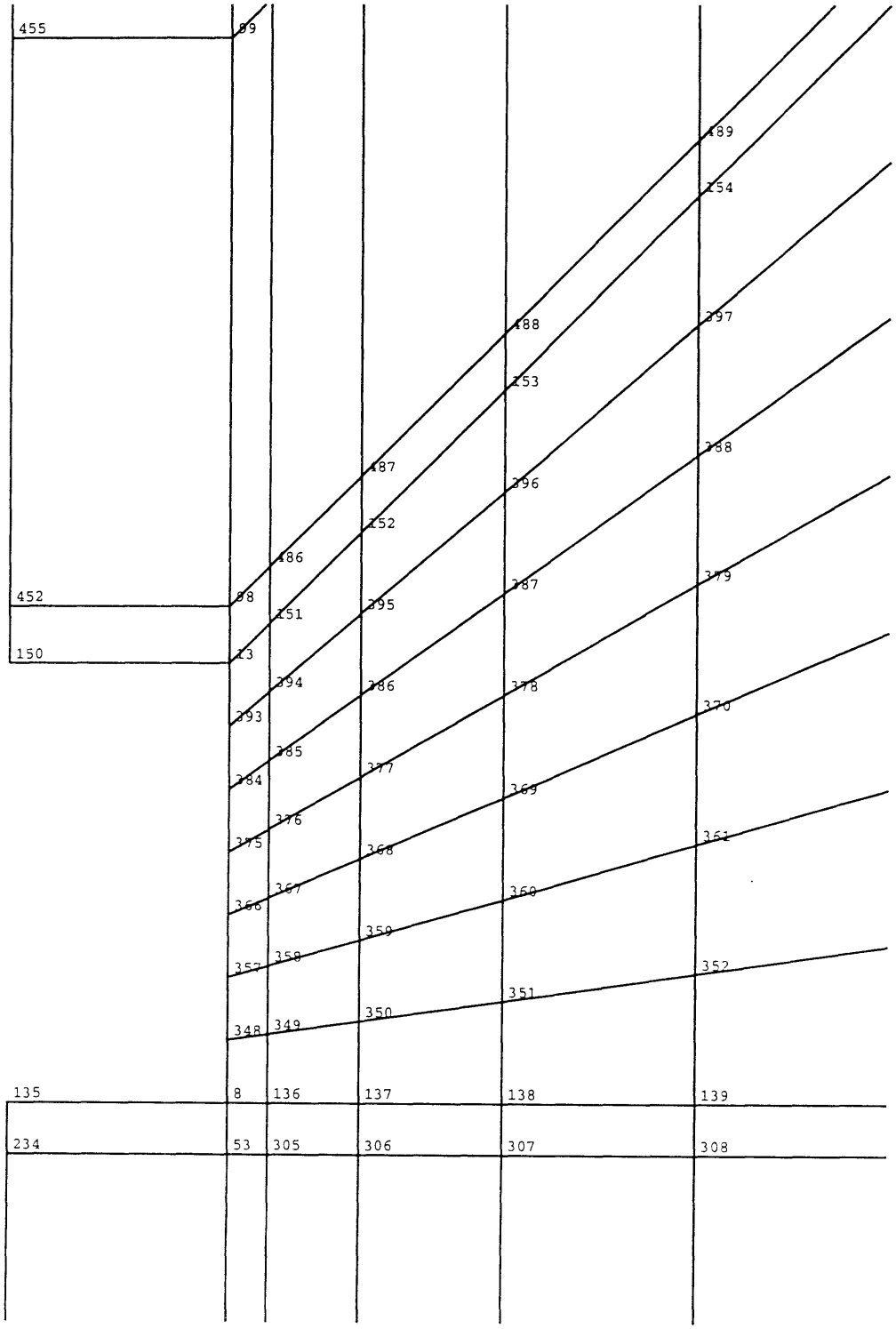

	U_2	U_3
B	✓	-
C	-	✓
D	-	-

ADINA-PLOT VERSION 6.1.4, 7 APRIL 1995
SPECIMEN GEOMETRY

ADINA ORIGINAL
LOAD_STEP
TIME 1.000 0.0004595

XVMIN 0.004500
XVMAX 0.01300
YVMIN 0.06700
YVMAX 0.08000

Z
Y

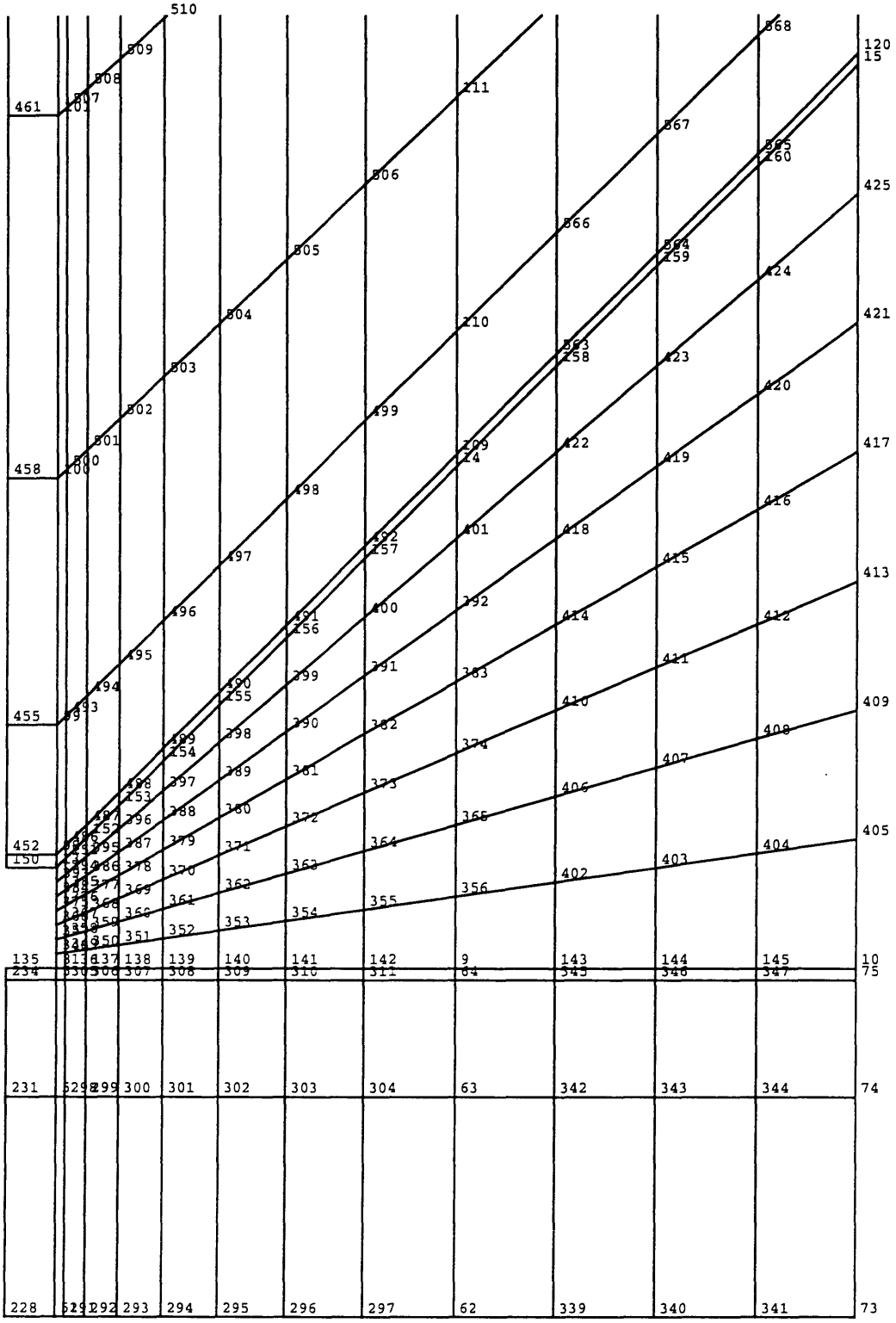

U_2 U_3
B ✓ -
C - ✓
D - -

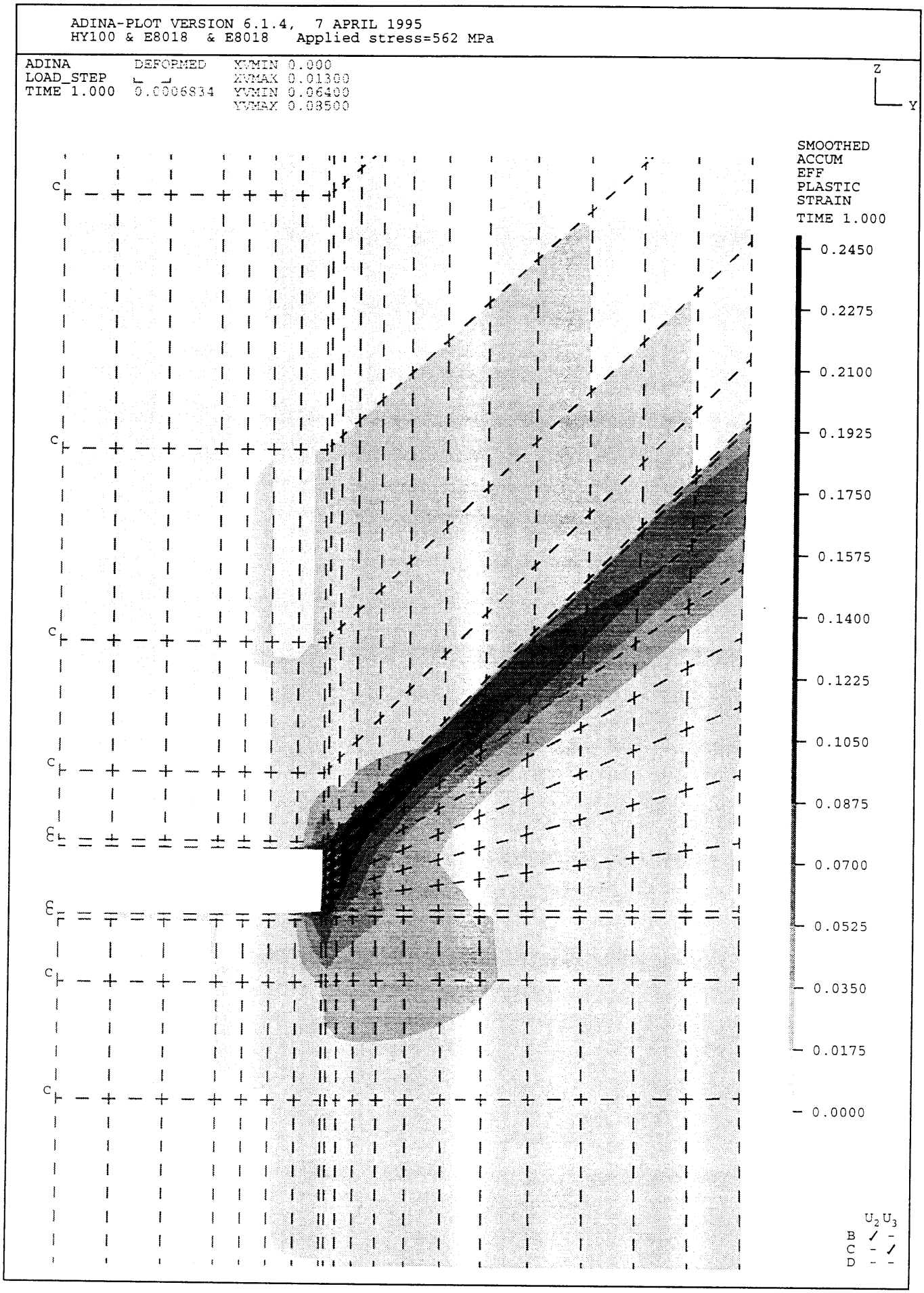
ADINA-PLOT VERSION 6.1.4, 7 APRIL 1995
HY100 & E8018 & E8018 Applied stress=562 MPa
ADINA
LOAD_STEP
TIME 1.000
DEFORMED
0.0006834
XVMIN 0.000
XVMAX 0.01300
YVMIN 0.06400
YVMAX 0.08500
Z
Y
SMOOTHED
ACCUM
EFF
PLASTIC
STRAIN
TIME 1.000
0.2450
0.2275
0.2100
0.1925
0.1750
0.1575
0.1400
0.1225
0.1050
0.0875
0.0700
0.0525
0.0350
0.0175
0.0000
U2 U3
B / -
C - /
D - -

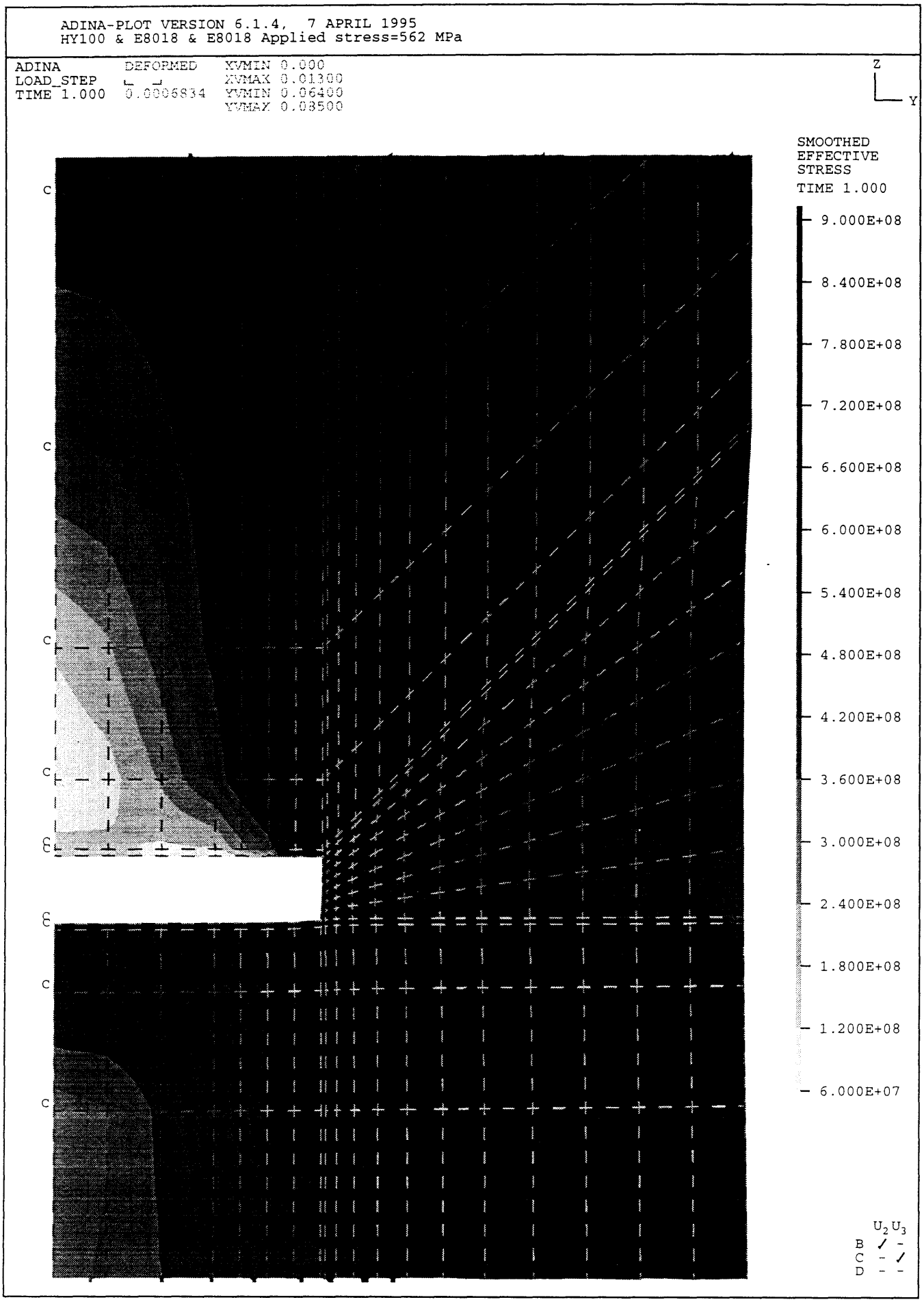
ADINA-PLOT VERSION 6.1.4, 7 APRIL 1995
HY100 & E8018 & E8018 Applied stress=562 MPa
ADINA
LOAD_STEP
TIME 1.000
DEFORMED
0.0006834
XVMIN 0.000
XVMAX 0.01300
YVMIN 0.06400
YVMAX 0.08500
Z
Y
SMOOTHED
EFFECTIVE
STRESS
TIME 1.000
9.000E+08
8.400E+08
7.800E+08
7.200E+08
6.600E+08
6.000E+08
5.400E+08
4.800E+08
4.200E+08
3.600E+08
3.000E+08
2.400E+08
1.800E+08
1.200E+08
6.000E+07
U2 U3
B ✓ -
C - ✓
D - -

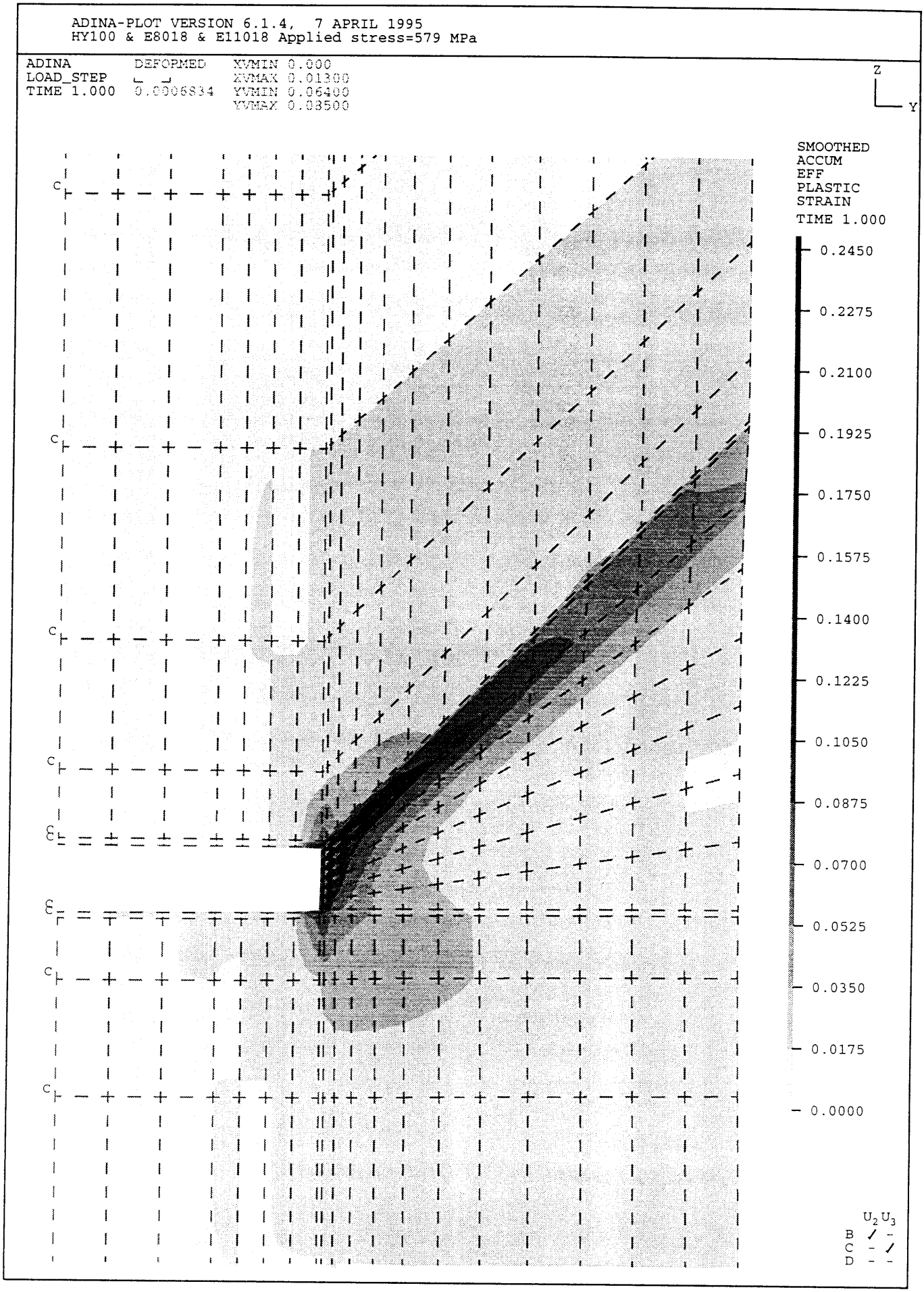
ADINA-PLOT VERSION 6.1.4, 7 APRIL 1995
HY100 & E8018 & E11018 Applied stress=579 MPa
ADINA
LOAD_STEP
TIME 1.000
DEFORMED
0.0006834
XVMIN 0.000
XVMAX 0.01300
YVMIN 0.06400
YVMAX 0.08500
Z
Y
SMOOTHED
ACCUM
EFF
PLASTIC
STRAIN
TIME 1.000
0.2450
0.2275
0.2100
0.1925
0.1750
0.1575
0.1400
0.1225
0.1050
0.0875
0.0700
0.0525
0.0350
0.0175
0.0000
U2 U3
B / -
C - /
D - -

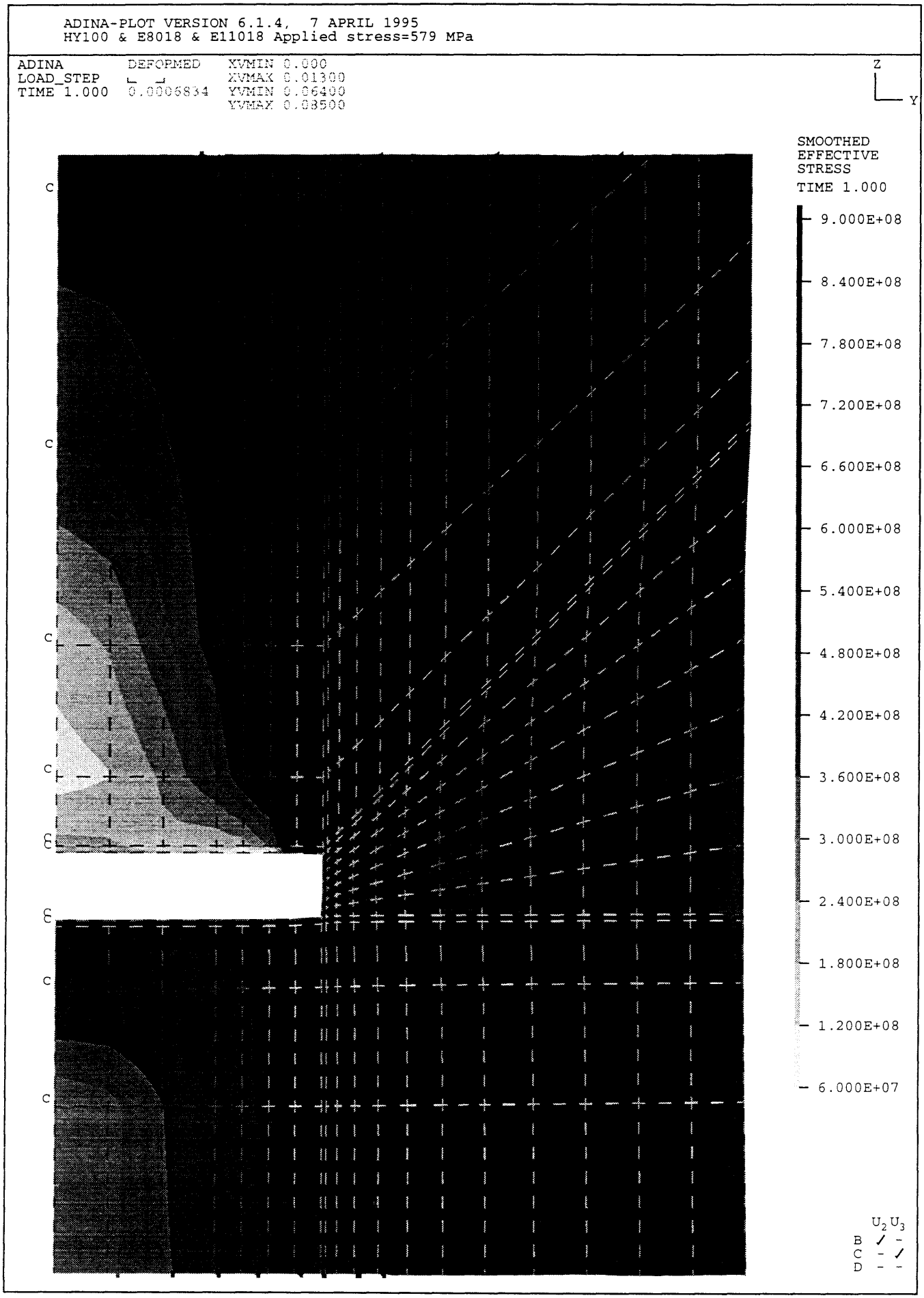
ADINA-PLOT VERSION 6.1.4, 7 APRIL 1995
HY100 & E8018 & E11018 Applied stress=579 MPa
ADINA
LOAD_STEP
TIME 1.000
DEFORMED
0.0006834
XVMIN 0.000
XVMAX 0.01300
YVMIN 0.06400
YVMAX 0.08500
Z
Y
SMOOTHED
EFFECTIVE
STRESS
TIME 1.000
9.000E+08
8.400E+08
7.800E+08
7.200E+08
6.600E+08
6.000E+08
5.400E+08
4.800E+08
4.200E+08
3.600E+08
3.000E+08
2.400E+08
1.800E+08
1.200E+08
6.000E+07
U2 U3
B ✓ -
C - ✓
D - -

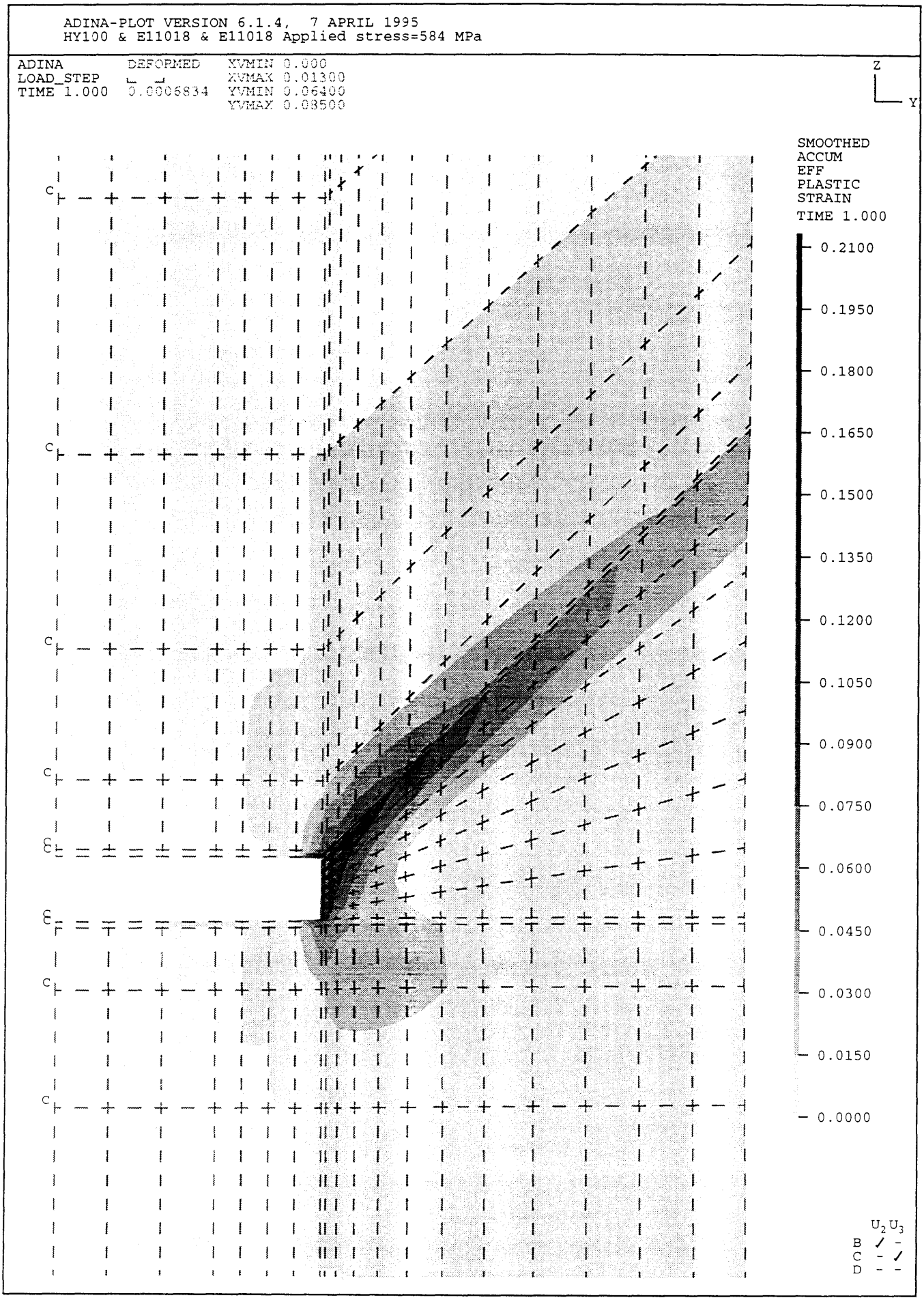
ADINA-PLOT VERSION 6.1.4, 7 APRIL 1995
HY100 & E11018 & E11018 Applied stress=584 MPa
ADINA
LOAD_STEP
TIME 1.000
DEFORMED
0.0006834
XVMIN 0.000
XVMAX 0.01300
YVMIN 0.06400
YVMAX 0.08500
Z
Y
SMOOTHED
ACCUM
EFF
PLASTIC
STRAIN
TIME 1.000
0.2100
0.1950
0.1800
0.1650
0.1500
0.1350
0.1200
0.1050
0.0900
0.0750
0.0600
0.0450
0.0300
0.0150
0.0000
U2 U3
B ✓ -
C - ✓
D - -

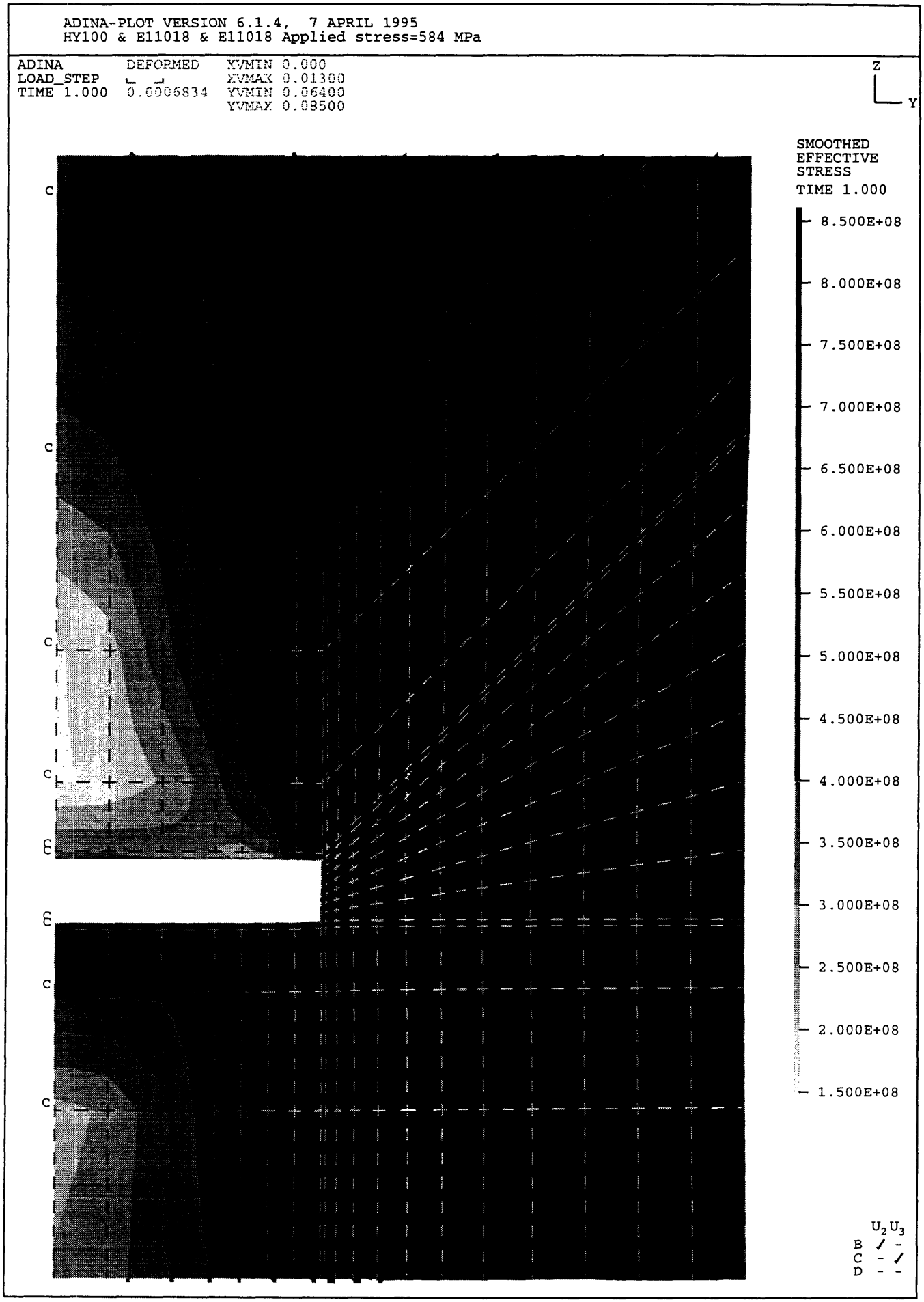
ADINA-PLOT VERSION 6.1.4, 7 APRIL 1995
HY100 & E11018 & E11018 Applied stress=584 MPa
ADINA
LOAD_STEP
TIME 1.000
DEFORMED
0.0006834
XVMIN 0.000
XVMAX 0.01300
YVMIN 0.06400
YVMAX 0.08500
Z
Y
SMOOTHED
EFFECTIVE
STRESS
TIME 1.000
8.500E+08
8.000E+08
7.500E+08
7.000E+08
6.500E+08
6.000E+08
5.500E+08
5.000E+08
4.500E+08
4.000E+08
3.500E+08
3.000E+08
2.500E+08
2.000E+08
1.500E+08
U2 U3
B / -
C - /
D - -

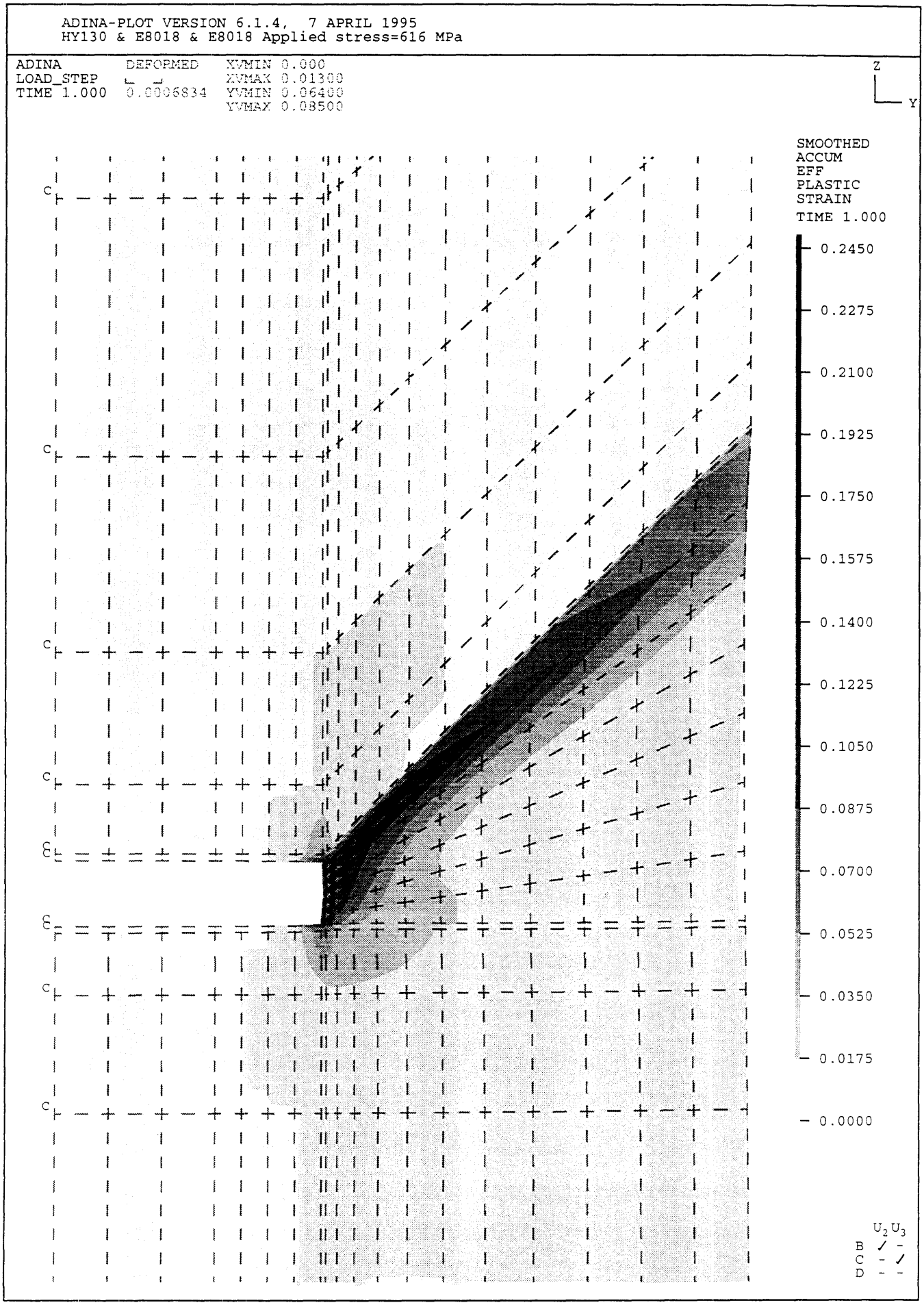
ADINA-PLOT VERSION 6.1.4, 7 APRIL 1995
HY130 & E8018 & E8018 Applied stress=616 MPa
ADINA
LOAD_STEP
TIME 1.000
DEFORMED
0.0006834
XVMIN 0.000
XVMAX 0.01300
YVMIN 0.06400
YVMAX 0.08500
Z
Y
SMOOTHED
ACCUM
EFF
PLASTIC
STRAIN
TIME 1.000
0.2450
0.2275
0.2100
0.1925
0.1750
0.1575
0.1400
0.1225
0.1050
0.0875
0.0700
0.0525
0.0350
0.0175
0.0000
U2 U3
B ✓ -
C - ✓
D - -

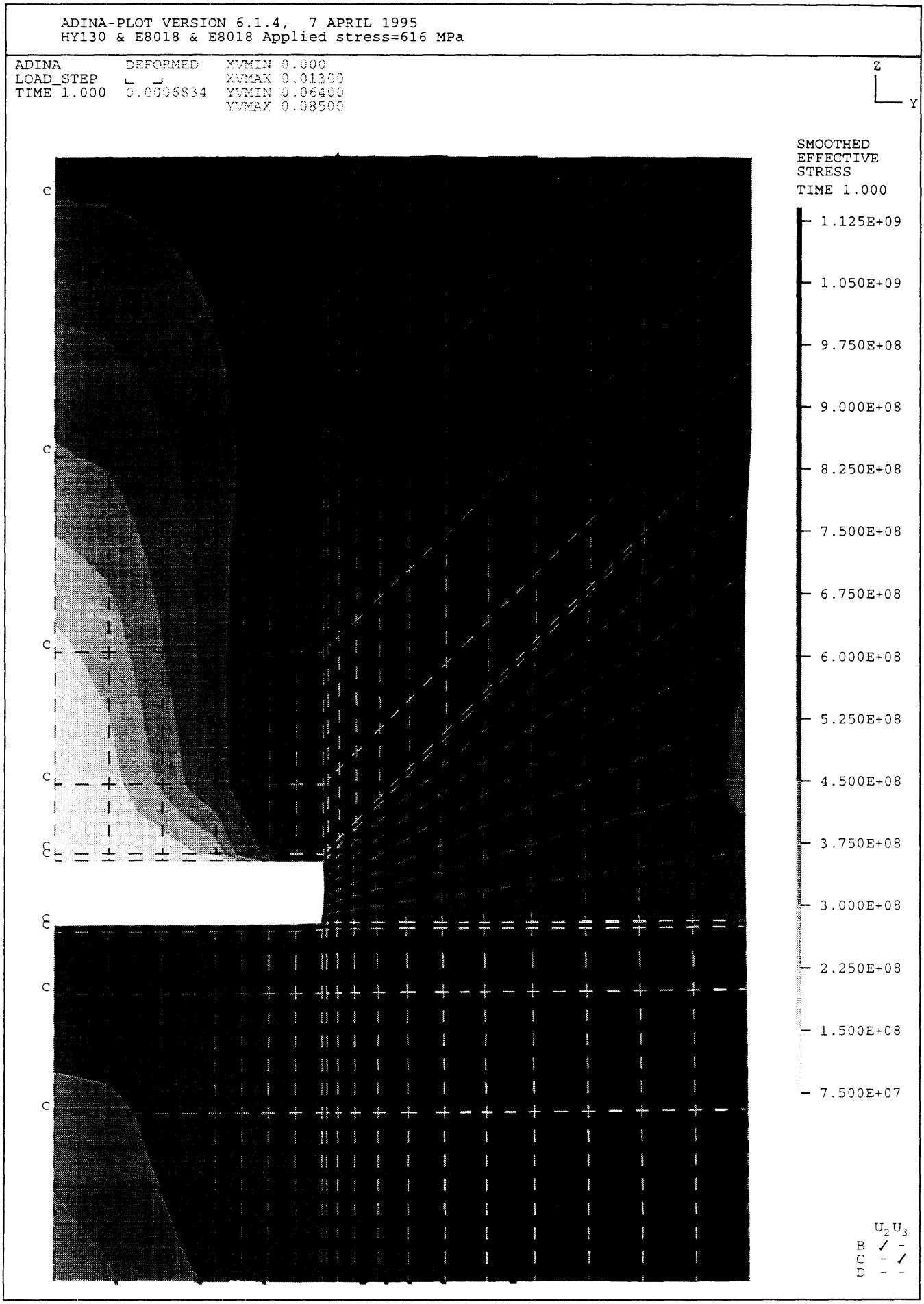
ADINA-PLOT VERSION 6.1.4, 7 APRIL 1995
HY130 & E8018 & E8018 Applied stress=616 MPa
ADINA
LOAD_STEP
TIME 1.000
DEFORMED
0.0006834
XVMIN 0.000
XVMAX 0.01300
YVMIN 0.06400
YVMAX 0.08500
Z
Y
SMOOTHED
EFFECTIVE
STRESS
TIME 1.000
1.125E+09
1.050E+09
9.750E+08
9.000E+08
8.250E+08
7.500E+08
6.750E+08
6.000E+08
5.250E+08
4.500E+08
3.750E+08
3.000E+08
2.250E+08
1.500E+08
7.500E+07
U2 U3
B ✓ -
C - ✓
D - -

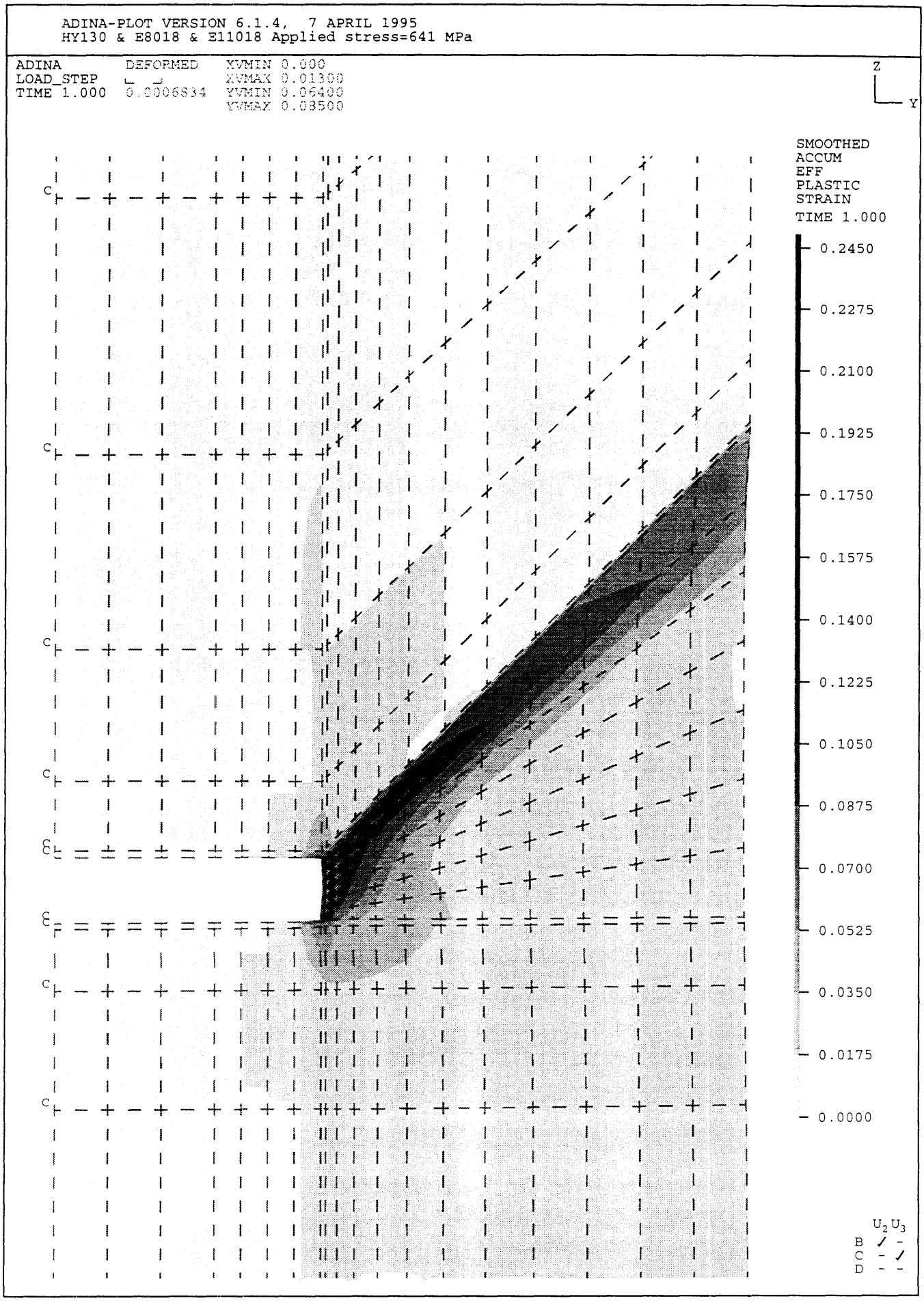
ADINA-PLOT VERSION 6.1.4, 7 APRIL 1995
HY130 & E8018 & E11018 Applied stress=641 MPa
ADINA
LOAD_STEP
TIME 1.000
DEFORMED
0.0006834
XVMIN 0.000
XVMAX 0.01300
YVMIN 0.06400
YVMAX 0.08500
Z
Y
SMOOTHED
ACCUM
EFF
PLASTIC
STRAIN
TIME 1.000
0.2450
0.2275
0.2100
0.1925
0.1750
0.1575
0.1400
0.1225
0.1050
0.0875
0.0700
0.0525
0.0350
0.0175
0.0000
U2 U3
B ✓ -
C - ✓
D - -

ADINA-PLOT VERSION 6.1.4, 7 APRIL 1995
HY130 & E8018 & E11018 Applied stress=641 MPa

ADINA
LOAD_STEP
TIME 1.000

DEFORMED
0.0006834

XVMIN 0.000
XVMAX 0.01300
YVMIN 0.06400
YVMAX 0.08500

Z
Y

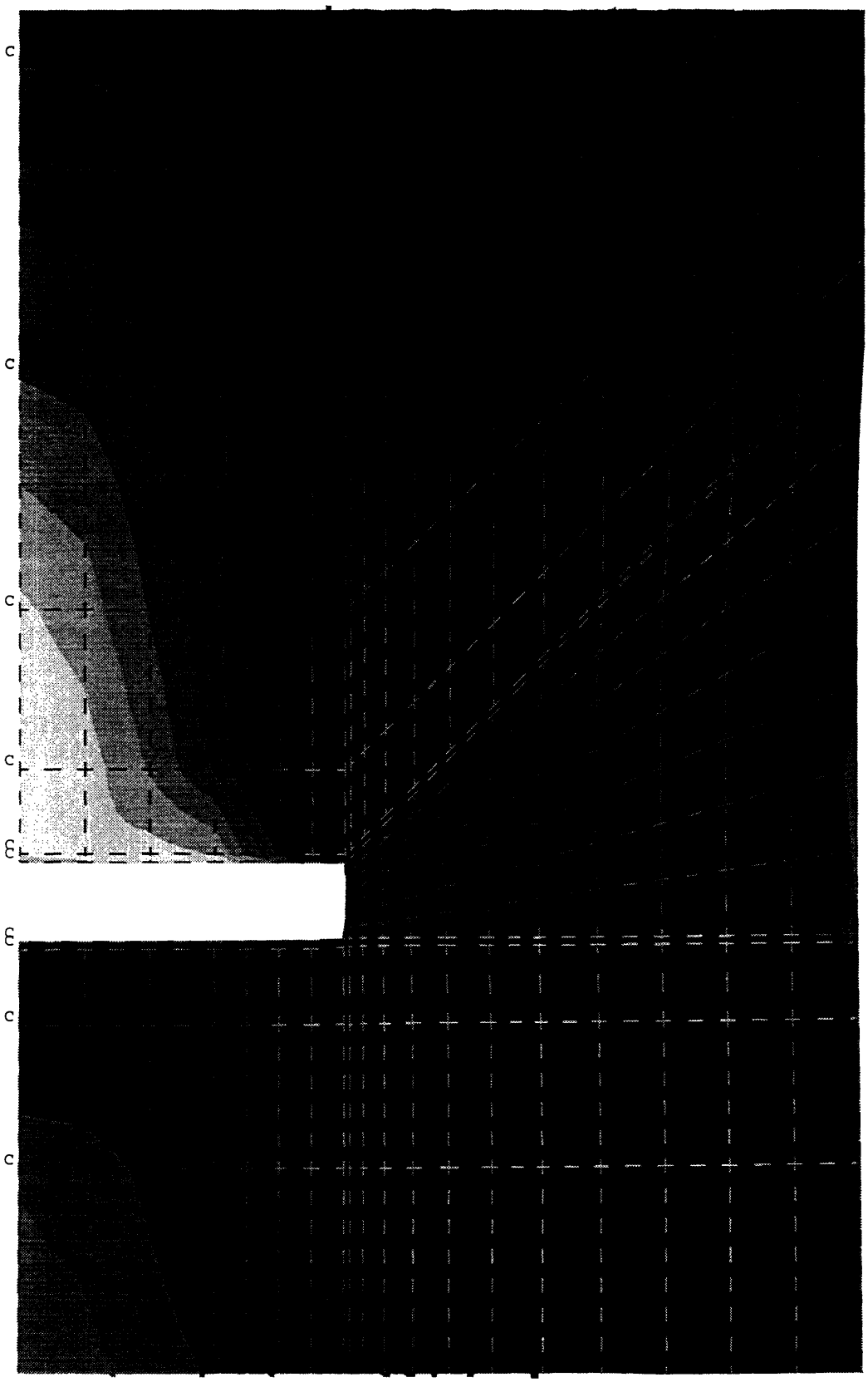

SMOOTHED
EFFECTIVE
STRESS
TIME 1.000

1.125E+09
1.050E+09
9.750E+08
9.000E+08
8.250E+08
7.500E+08
6.750E+08
6.000E+08
5.250E+08
4.500E+08
3.750E+08
3.000E+08
2.250E+08
1.500E+08
7.500E+07

	U_2	U_3
B	/	-
C	-	/
D	-	-

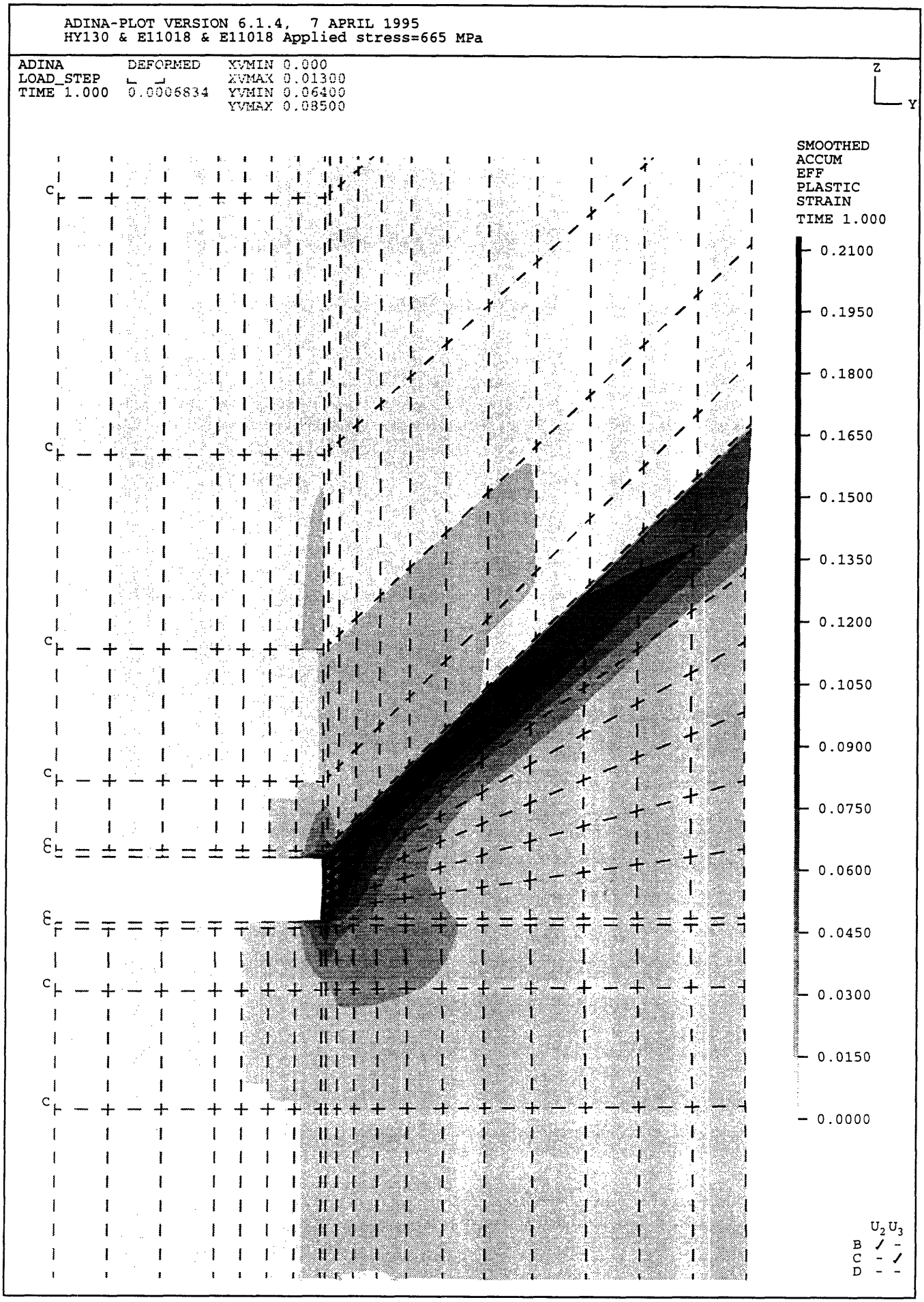
ADINA-PLOT VERSION 6.1.4, 7 APRIL 1995
HY130 & E11018 & E11018 Applied stress=665 MPa
ADINA
LOAD_STEP
TIME 1.000
DEFORMED
0.0006834
XVMIN 0.000
XVMAX 0.01300
YVMIN 0.06400
YVMAX 0.08500
Z
Y
SMOOTHED
ACCUM
EFF
PLASTIC
STRAIN
TIME 1.000
0.2100
0.1950
0.1800
0.1650
0.1500
0.1350
0.1200
0.1050
0.0900
0.0750
0.0600
0.0450
0.0300
0.0150
0.0000
U2 U3
B / -
C - /
D - -

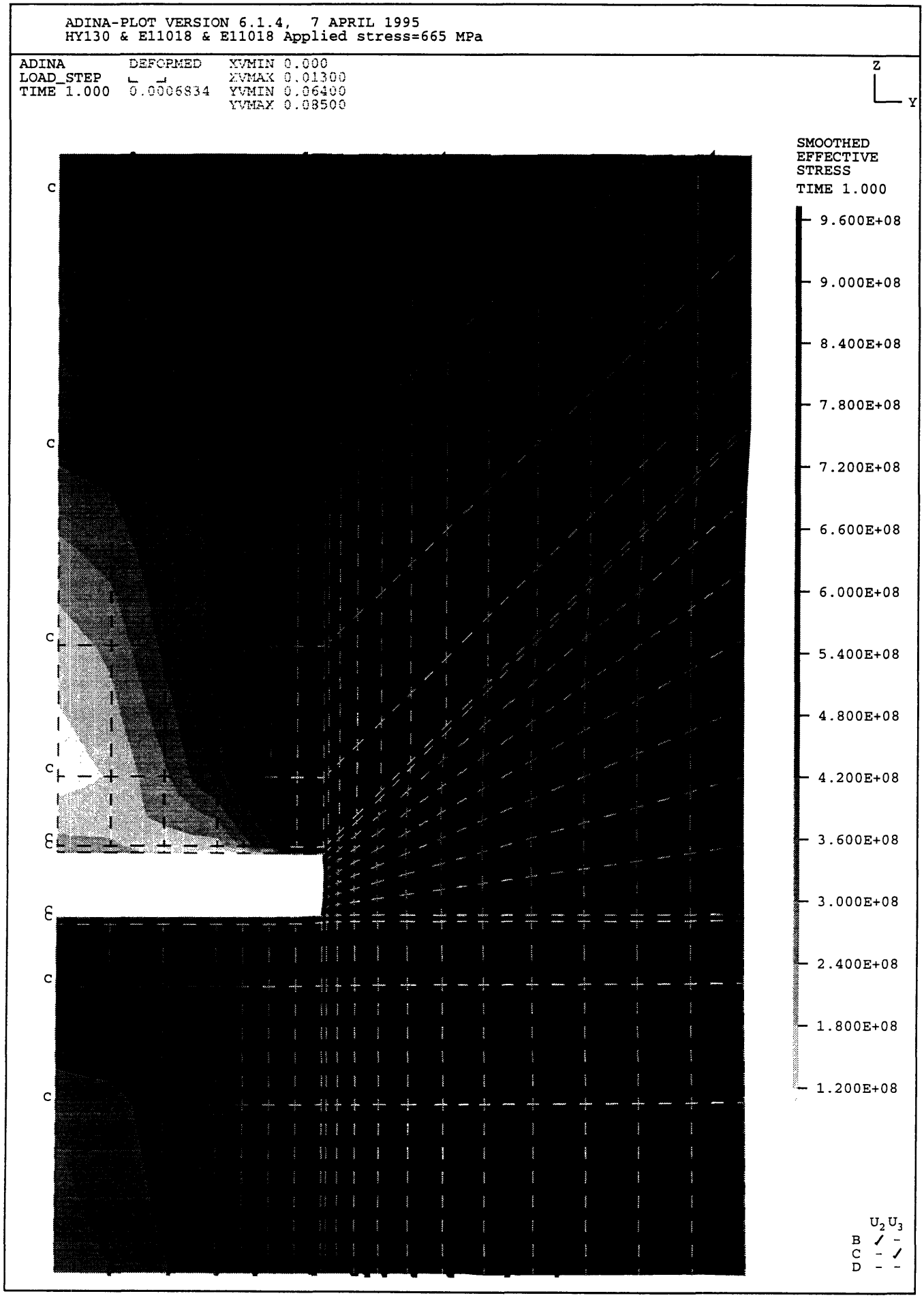
ADINA-PLOT VERSION 6.1.4, 7 APRIL 1995
HY130 & E11018 & E11018 Applied stress=665 MPa
ADINA
LOAD_STEP
TIME 1.000
DEFORMED
0.0006834
XVMIN 0.000
XVMAX 0.01300
YVMIN 0.06400
YVMAX 0.08500
Z
Y
SMOOTHED
EFFECTIVE
STRESS
TIME 1.000
9.600E+08
9.000E+08
8.400E+08
7.800E+08
7.200E+08
6.600E+08
6.000E+08
5.400E+08
4.800E+08
4.200E+08
3.600E+08
3.000E+08
2.400E+08
1.800E+08
1.200E+08
U2 U3
B / -
C - /
D - -

Bibliography

[1] Masao Toyoda. Significance of mismatching of steel welds: Over/undermatch versus evenmatch. *Materials Engineering, ASME*, 1993.

[2] M. M. Lee and A. R. Luxmoore. Effect of weld metal mismatch on fracture mechanical parameters. *Materials Engineering, ASME*, 1993.

[3] D. T. Reed and B. I. Petrovski. Elastic-plastic fracture at surface flaws in hsla steel weldments. *Transactions of the ASME*, 1992.

[4] Y. Nakano and T. Kubo. Effect of strength matching on fracture behavior of notched, high strength steel welded joint. *Materials Engineering, ASME*, 1993.

[5] B. Lianv and R. Denys. The characteristics of modern high strength steel weldments. Technical report, Statoil AC and Laboratory Soete Gent, Stavanger, Norway and Gent, Belgium.

[6] M. Kocak J. Knaack and K. H. Schwalbe. Fracture behavior of undermatched weld joints. Technical report, GKSS Research Center Geesthacht, Geesthacht, Germany.

[7] B. I. Petrovski D. T. Reed. Application of very low yield strength consumables in the root pass of weldments to avoid preheating. *Welding in the World*, 1994.

[8] K. Satoh M. Toyoda K. Ukita A. Nakamura T. Katsuura. Applicability of undermatched electrodes to circumferential welded joint of ht80 penstock. 1978.

[9] Kunihiko Satoh and Masao Toyoda. Effect of mechanical heterogeneity on the static tensile strength of welded joints. *Journal of Japan Welding Society*, 1971.

[10] The Committee on Effective Utilization of Weld Metal Yield Strength. Effective use of weld metal yield strength for hy-steels. Technical Report NMAB-380, National Materials Advisory Board, Washington, D.C., 1983.

[11] ASM International Handbook Committee. *ASM Handbook: Welding Brazing and Soldering.* ASM International, 1994.

[12] Stout and Doty. *Weldability of Steels.* Welding Research Council, 1971.

[13] Koichi Masubuchi. *Analysis of Welded Structures.* Pergamon Press, Oxford/New York, 1980.

[14] F. R. Coe. *Welding Steels Without Hydrogen Cracking.* The Welding Institute, 1973.

[15] David Broek. *Elementary Engineering Fracture Mechanics.* Kluwer Academic Publishers, 1986.

[16] A. Phillips. *Introductory Welding Metallurgy.* American Welding Society, 1973.

[17] F. A. McClintock. *Mechanical Behavior of Materials.* Addison-Wesley Publishing Company, Reading MA, 1966.

[18] John Emmanuel Agapakis. Welding of high strength and stainless steels: A study on weld metal strength and stress relieving. Master's thesis, Massachusetts Institute of Technology, May 1982.

[19] Koichi Masabuchi J. M. Cushing P. Tannery and E. Olsen. Early detection of fatigue crack initiation in a weldment by a system composed of a laser microscope and a video microscope. Technical report, Massachusetts Institute of Technology, Cambridge, MA.

[20] *Manual of Steel Construction. Allowable stress design.* American Institute of steel Construction Inc., Chicago, Illinois.

[21] C. G. Salmon R. N. White. *Building Structural Design Handbook.* A Wiley-Interscience Publication, New York.

[22] Hiroshi Tada. *The stress analysis of Crack Handbook.* Paris Production Incorporated, St. Louis, Missouri, 1985.

[23] Y. Wadayama T. Matsumoto, H. Satoh. Investigations on evaluation method for yield strength of round bar undermatched joint. 1988.

[24] *ADINA user manual.* ADINA R D Inc, 1992.

[25] J. W. Simons J. H. Giovanola, R. W. Kropp and A. H. Marchand. Investigation of the fracture behavior of scaled hy-130 weldments. Technical Report NAVSWC TR 90-360, Naval Surface Warfare Center, Dahlgren Virginia, 1990.

[26] Akira Umekuni and Koichi Masubuchi. Usefulness of undermatched weld for high-strength steels. Technical report, Massachusetts Institute of Technology, Cambridge, MA.